

Doxycycline-inducible viral vector systems for selective overexpression of supportive factors to enhance *in vitro* megakaryocyte and platelet production

Vom Fachbereich Biologie der Technischen Universität Darmstadt

Zur Erlangung des akademischen Grades

**Doctor rerum naturalium
(Dr. rer. nat.)**

Dissertation von

Katharina Cullmann, M. Sc.

aus Idar-Oberstein

1. Referentin: Prof Dr. Beatrix Süß
2. Referentin: Prof. Dr. Ulrike Nuber
3. Referentin: Prof. Dr. Dr. Ute Modlich

Darmstadt, 2019

Cullmann, Katharina: Doxycycline-inducible viral vector systems for selective overexpression of supportive factors to enhance *in vitro* megakaryocyte and platelet production

Darmstadt, Technische Universität Darmstadt

Veröffentlichungsjahr der Dissertation auf TU Prints: 2020

Tag der mündlichen Prüfung: 03.September 2019

Veröffentlicht unter CC BY-SA 4.0 International

<https://creativecommons.org/licenses/>

Die vorliegende Arbeit wurde unter der Leitung von Prof. Dr. Dr. Ute Modlich in der Arbeitsgruppe „Gene Modification in Stem Cells“ in der Abteilung Veterinärmedizin am Paul-Ehrlich-Institut in Langen angefertigt.

Die Betreuung seitens der Technischen Universität Darmstadt erfolgte durch Prof. Dr. Beatrix Süß und Prof. Dr. Ulrike Nuber aus dem Fachbereich Biologie.

Teile dieser Arbeit wurden publiziert in:

Sustained and regulated gene expression by Tet-inducible “all-in-one” retroviral vectors containing the CBX3-UCOE®

Cullmann K, Blokland KEC, Sebe A, Schenk F, Ivics Z, Heinz N, Modlich U.
Biomaterials. (2019)

<https://doi.org/10.1016/j.biomaterials.2018.11.006>

CONTENTS

CONTENTS	2
ABSTRACT (Englisch)	5
ZUSAMMENFASSUNG	7
1 INTRODUCTION	9
1.1 Megakaryopoiesis and platelet biogenesis.....	9
1.1 Platelet morphology and functionality	10
1.2 Fetal platelet biogenesis.....	14
1.3 Regulators of megakaryocyte and platelet differentiation.....	15
1.4 Gene modification with viral vectors	18
1.4.1 Self-inactivating retroviral vectors	18
1.4.2 Doxycycline inducible all-in-one retroviral vectors	22
1.5 Induced pluripotent stem cells (iPSC)	23
1.6 Ubiquitous chromatin opening elements (UCOE).....	24
1.7 <i>In vitro</i> generation of platelets	25
2 AIM OF THE STUDY	27
3 MATERIALS AND METHODS	29
3.1 Materials	29
3.1.1 Technical devices.....	29
3.1.2 Expendable items.....	30
3.1.3 Chemicals and reagents	31
3.1.4 Buffers and solutions.....	33
3.1.5 Cytokines	34
3.1.6 Antibodies	34
3.1.7 Enzymes	35
3.1.8 Kits	36
3.1.9 Plasmids.....	36
3.1.10 Oligonucleotides.....	37
3.1.11 Bacterial strains, cells and cell lines	38
3.1.12 Culture media.....	39
3.2 Methods.....	40
3.2.1 Molecular biology tools.....	40
3.2.2 Cell culture	45

3.2.3	Cytospin and cytomorphological staining.....	50
3.2.4	Electron Microscopy.....	50
3.2.5	Flow cytometry.....	50
3.2.6	Platelet activation.....	51
3.2.7	Immunocytochemistry for detection of pluripotency.....	52
3.2.8	PrestoBlue® cell viability assay.....	53
4	RESULTS.....	54
4.1	Supporting factors for increased megakaryocyte differentiation and platelet release from murine iPSC.....	54
4.1.1	Generation of R26M2 iPSC by lentiviral reprogramming and screening for hematopoietic differentiating clones.....	55
4.1.2	Characterization of pluripotency marker expression of R26M2K2 and R26M2K3 iPSC clones.....	56
4.1.3	Tet-inducible gammaretroviral vectors overexpressing supporting factors for megakaryocyte and platelet differentiation <i>in vitro</i>	59
4.1.4	Transduction of R26M2K2 iPSC with vectors supporting megakaryocyte differentiation.....	61
4.1.5	Differentiation of R26M2K2 into megakaryocyte progenitors and platelets.....	62
4.2	Generation of Tet all-in-one gammaretroviral vectors with low silencing potential.....	83
4.2.1	Influence of the insertion of the A2UCOE on the dynamic range of transcriptional activation.....	85
4.2.2	Anti-silencing potential of different A2UCOE-Tet vectors in P19 carcinoma cells.....	87
4.2.3	A2UCOE in Tet-inducible all-in-one vectors in murine iPSC.....	90
4.2.4	Vector performance after replacement of the PGK promoter by a U670s/CBX3 element.....	93
4.2.5	A2UCOE in Tet-all-in-one vectors in human induced pluripotent stem cells during differentiation.....	97
4.2.6	Expression of Mpl from the UCOE-Tet gammaretroviral vectors.....	101
5	DISCUSSION.....	104
5.1	Production of platelets and megakaryocytes <i>in vitro</i> from R26M2 iPSC.....	104
5.1.1	R26M2K2 iPSC for the generation of megakaryocytes and platelets <i>in vitro</i>	104
5.1.2	Comparison of single supportive factors during MK differentiation and terminal maturation.....	105
5.1.3	Comparison of candidate factors on platelet generation from R26R2K2 iPSC.....	110
5.1.4	Platelets differentiated from Gata1-overexpressing R26M2K2 iPSC were functional.....	112

5.1.5	Overexpression of Nfe2 during differentiation increased the platelet production per megakaryocyte.....	113
5.2	Incorporation of A2UCOE to prevent silencing of Tet-all-in-one gammaretroviral vectors.....	114
5.2.1	Incorporation of some of the A2UCOE lowers titers and interferes with regulation of Tet-all-in-one gammaretroviral vectors.....	114
5.2.2	Anti-silencing efficiency in P19 cells	115
5.2.3	Expression of Mpl from the Tet-all-in-one vectors confers growth advantage to cytokine dependent cells.....	116
5.2.4	Anti-silencing effects of A2UCOE in pluripotent stem cells.....	117
6	CONCLUSION	121
	REFERENCES	123
	ABBREVIATIONS	140
	CONTRIBUTIONS	145
	LIST OF FIGURES	146
	CURRICULUM VITAE	148
	DANKSAGUNG	149
	EHRENWÖRTLICHE ERKLÄRUNG	150

ABSTRACT (Englisch)

The generation of platelets and megakaryocytes (MK) *in vitro* provides a potent strategy to overcome the shortage of today's platelet transfusions to patients with acute needs. The amount of patients, depending on donations, and in need for transfusions are increasing while platelet donors are not more frequent. Furthermore, the risk of bacterial contamination in platelet products is high due to their storage at room temperature to prevent platelet activation. This also shortens the shelf life of platelet products. After repetitive transfusions, patients can develop refractoriness and immunity adding further complications to the use of platelet therapies. Therefore, alternative sources for platelets are sought for. Platelets can be produced *in vitro* from MK progenitors, hematopoietic stem cells or pluripotent stem cells. However, production is inefficient, particularly taking in consideration that the tremendous amount $4-5 \times 10^{11}$ platelets have to be produced for filling one transfusion unit.

In this study, we wanted to explore whether the expression of single supporting candidate factors in murine induced pluripotent stem cells (iPSC) could increase platelet production *in vitro*. We concentrated on the overexpression of major transcription factors of early-phase megakaryopoiesis (Gata1, Pbx1, and Evi1) and late phase (Nfe2) to enhance MK production platelet release. Furthermore, to support platelet release from MK, we expressed hyperactive variants of the small GTPases RhoA and Cdc42. Gene modifications in iPSC, however, experience major drawbacks because of silencing of ectopic gene expression especially during differentiation. Furthermore, expression of the supportive factors has to be tightly controlled to avoid unwanted interference of the factors with pluripotency and differentiation since the transduction has to be performed in the pluripotent state. To overcome this, a tet-inducible expression system in iPSC was developed which was based on the generation of iPSC containing the reverse tetracycline (rt) transactivator TA-M2 in the Rosa26 safe harbor locus to prevent gene silencing of the (rt)TA-M2 and thereby guaranteeing its robust expression throughout the differentiation process. After verification of pluripotency and differentiation potential of the generated iPSC, the candidate factors were introduced with gammaretroviral vectors containing the respective transgene expressed from a Tet-responsive minimal promoter. In our experiments we found that overexpression of Gata1 elevated production of megakaryocyte progenitors, however, full maturation of the cells was impaired. In contrast, overexpression of Nfe2 elevated numbers of released platelets. In a second approach, we developed a doxycycline (dox)-induced overexpression system that should be transferable to human cells. We improved Tet-inducible all-in-one gammaretroviral vectors by introducing different ubiquitous chromatin opening elements derived from the

human HNRPA2B1/CBX3 locus (A2UCOE), previously proven to prevent silencing of constitutive-expressing retroviral vectors in hiPSC. Tet-all-in-one retroviral vectors rely on a persistent expression of the transactivator and good regulation of the tet-responsive promoter. The incorporation of an additional element (with promoter activity) can interfere with the regulation. We incorporated elements of different sizes in sense and antisense transcriptional orientation into Tet-all-in-one gammaretroviral vectors and tested these for the regulation and anti-silencing capacity in different cell lines including murine and human iPSC. The U670 was identified to be the most potent element in preventing silencing which also conferred the strongest expression from the vector in the induced state. Longer fragments also sustained the gene expression but vector titers and induction efficiencies were impaired. Gammaretroviral Tet-all-in-one vectors turned out to be superior to their lentiviral counterparts due to the capability to produce higher titers. Finally, the expression and tight regulation of the thrombopoietin receptor Mpl within Tet-inducible gammaretroviral vectors after incorporation of the U670s element was confirmed by cytokine-dependent cell growth. In addition, the PGK promoter could be replaced by the 670bp elements and sustained transgene silencing without interfering with the tight regulation of the vectors. With this part of the study, we found potent gammaretroviral vector candidates which pave the way for future application of overexpression of GATA1 and NFE2 in the human system to increase MK and platelet production *in vitro*.

ZUSAMMENFASSUNG

Die Verabreichung von Thrombozyten zur Behandlung von Folgen verschiedener medizinischer Indikationen ist nicht immer komplikationslos. Zum einen steigt die Zahl der Patienten, die diese Therapien benötigen, bei gleichbleibender Zahl von Thrombozyten-Spendern, was die Knappheit der Produkte in den nächsten Jahren zur Folge haben könnte. Außerdem erhöht die Aufbewahrung der Thrombozyten-Konzentrate bei Raumtemperatur das Risiko bakterieller Kontaminationen. Somit können die Blutprodukte nur wenige Tage gelagert werden und viele Einheiten müssen unverwendet entsorgt werden. Darüber hinaus reagieren einige Spender mit Immunreaktion auf die erhaltenen Präparate, was zur Refraktärität von Thrombozyten führt. Eine mögliche Lösung hierfür ist die Produktion von patienteneigenen und HLA-kompatiblen Thrombozyten in der Zellkultur aus induzierten pluripotenten Stammzellen (iPSC). Ein großes Hindernis ist dabei die große Menge an Zellen, die hergestellt werden muss ($4-5 \times 10^{11}$) und die mindere Funktionalität der in Kultur hergestellten Thrombozyten im Vergleich zu den gespendeten. In dieser Arbeit haben wir eine Strategie entwickelt, um Ausbeute und Funktionalität der im Labor hergestellten Thrombozyten zu steigern. Dies basiert auf einem induzierbaren gammaretroviralen Vektorsystem. Im ersten Teilprojekt sollen Ausbeute und Funktionalität von *in vitro* erzeugten Thrombozyten gesteigert werden, indem spezifische Faktoren zu einem bestimmten Zeitpunkt während der Differenzierung überexprimiert werden. Im Fokus standen hierbei die Transkriptionsfaktoren Gata1, Pbx1 und Evi1 die ein frühes Stadium der Megakaryopoese kontrollieren und Nfe2, der die Freisetzung von Thrombozyten steuert. Eine besondere Herausforderung ist die Stilllegung der eingebrachten Gene, insbesondere während der Differenzierung von iPSC. Der PGK Promotor, der in vielen Systemen die Expression des Transaktivators des Tet-induzierbaren Systems steuert, ist davon ganz besonders betroffen durch seine vielen potenziellen Methylierungsstellen. Durch die Erzeugung von murinen iPSC, die den (rt)TA-M2 von einem internen Locus exprimieren, konnte dessen kontinuierliche Expression gewährleistet werden. Nach Verifizierung der Pluripotenz und des Differenzierungsmusters der generierten iPSC und deren Transduktion mit den einzelnen unterstützenden Faktoren wurde gezeigt, dass die Überexpression von Gata1 zu einem prozentualen Anstieg der Vorläuferzellen führte, die jedoch Defizite in der finalen Ausreifung aufwiesen. Im Gegensatz dazu führte die Überexpression von Nfe2 zu einer gesteigerten Anzahl von freigesetzten Thrombozyten pro Megakaryozyt. Überexpression beider Faktoren in Kombination wäre daher eine vielversprechende Kombination für künftige Studien. Um dieses System auf die Differenzierung von humanen Thrombozyten

aus iPSC übertragen zu können, haben wir gammaretrovirale All-in-one-Vektoren optimiert. Hierbei wird die Stilllegung des PGK Promotors durch das Einfügen eines Chromatin-öffnenden-elements (A2UCOE) verhindert. Dieses stammt vom humanen HNRPA2B1/CBX3 Genlocus. Da die Elemente Promotoraktivität besitzen, könnte deren Einbringen die Regulierbarkeit der Vektoren beeinträchtigen. Wir haben Elemente verschiedener Größen und Lokalisationen in jeweils zwei verschiedenen transkriptionellen Orientierungen vor den PGK Promotor eingesetzt. Dabei stellte sich heraus, dass sich das Element U670s besonders eignet, da die Regulierung nicht beeinträchtigt war und die Stilllegung des Transgens in verschiedenen Zelllinien inklusive hiPSC verzögert bzw. verhindert werden konnte. Dabei waren gammaretrovirale Vektoren den lentiviralen überlegen, aufgrund der höheren Titer, die erreicht werden konnten. Die Funktionalität des Vektors wurde durch die regulierte Expression des Thrombopoietinrezeptors Mpl und das daraus resultierende Cytokin-abhängige Wachstum von transduzierten Zellen bestätigt. Auch der Austausch des PGK Promotors durch das U670 Element konnte die Expression des Transgens weiterhin regulieren. Hiermit haben wir Vektoren hergestellt, um die Faktoren GATA1 und NFE2 auch im humanen System überexprimieren zu können und somit zur Steigerung der Ausbeute generierter Megakaryozyten und Thrombozyten in der Zellkultur auch im humanen System beitragen zu können.

1 INTRODUCTION

1.1 Megakaryopoiesis and platelet biogenesis

Adult platelet biogenesis in mammals is a multistep process that is initiated in hematopoietic stem cells (HSC) residing in the bone marrow (BM) (Figure 1). In the classical megakaryopoiesis model, MK evolve from Megakaryocyte-Erythrocyte-Progenitor cells (MEP) in a hierarchical order where high proliferative potential-colony-forming unit-megakaryocytes (HPP-CFU-MK) stem from MEPs directly. HPP-CFU-MK give rise to burst-forming unit-megakaryocytes (BFU-MK) which then produce more differentiated progenitors, colony-forming unit-megakaryocytes (CFU-MK). CFU-MKs develop into immature MKs or megakaryoblasts (Debili et al., 1996; N Debili, L Coulombel, L Croisille, A Katz, J Guichard, J Breton-Gorius and W Vainchenker, 1996; Szalai et al., 2006; Sanada et al., 2016). The megakaryoblasts proliferate and increase in size up to 100 μm during further development. They also undergo endomitosis, a process in which the DNA content is increasing while cell division does not occur, and become multilobulated with nuclei up to 64 and 128N. The formation of the demarcation membrane system (DMS) during cytoplasmic maturation of MK was shown to divide the cells into small platelet areas. These are the source for the cell membranes for future platelets and serve as membrane reservoir for platelet release at the tips of the cellular protrusions (Eckly et al., 2014). Formation of cellular elongation of the MK is initiated by microtubules migrating to the cell cortex, a network of actin filaments at the edge of the cells which is responsible for their shape. Organelles and granules are transported to the tips of the protrusions by microtubules (Patel et al., 2005). During maturation, megakaryocytic progenitors migrate from the osteoblastic niche to the vascular niche within the BM (Behrens and Alexander, 2018). Once homed to the vascular niche, MK extend their protrusions through gaps of the endothelial cells, lining of the vascular sinusoids into the blood stream. Subsequently, pro-platelets are formed which then rupture into platelets once exposed to the shear forces of the blood stream in the lumen of BM sinusoids (Italiano et al., 2007; Brown et al., 2018).

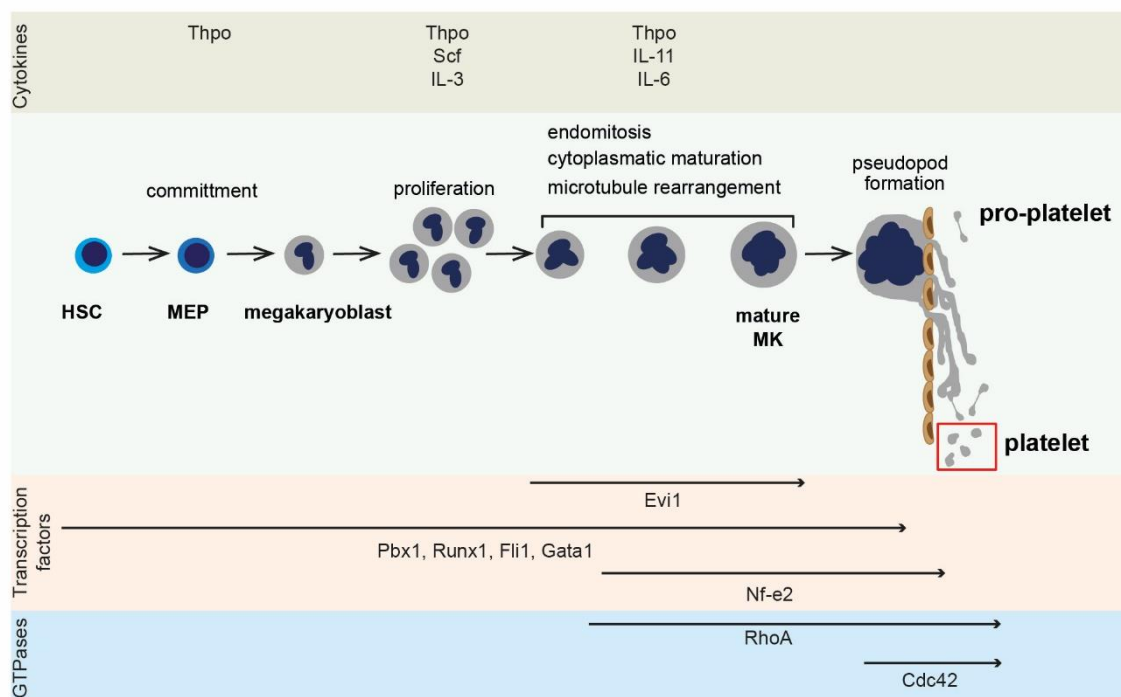


Figure 1 Mammalian megakaryopoiesis and platelet biogenesis. HSC residing in the BM undergo different intermediate maturation steps which result in the generation of a committed progenitor called MEP which then gives rise to proliferating megakaryoblasts. After proliferation, they perform endomitosis and cytoplasmic maturation forming cellular protrusions which extend through gaps of the endothelial cells lining the vascular sinusoids. Once exposed to the shear forces of the bloodstream, pro-platelets are generated which release platelets into the circulation. Since the process involves multiple intermediate steps, it is also regulated at multiple steps during differentiation by early and later transcription factors (modified after Pang et al., 2005).

1.1 Platelet morphology and functionality

There are about $1.5\text{-}4 \times 10^5$ platelets per microliter of blood circulating in the human body and about 1×10^6 per microliter in murine blood. In the non-activated state in the blood, platelets are small discoid shaped cells of about $2 \mu\text{m}$ in diameter in humans and $0.5 \mu\text{m}$ in mice. They have a very specific cellular morphology, depicted in Figure 2 without a nucleus and with different types of granules. Alpha granules (α -granules) are the most abundant type of granules in platelets and contain coagulation factors (e.g. Factor V, Factor VIII and Factor VI) as well as adhesion molecules (e.g. P-selectin, Von-Willebrand-Factor (VWF), fibrinogen and fibronectin), playing a role in adhesion and interaction between platelets with leukocytes and endothelial cells (Li et al., 2017). In addition, cytokines such as VEGF and angiogenin as well as platelet-factor 4 and antiangiogenic factors, involved in the regulation of growth and angiogenesis, are stored in α -granules (Whiteheart, 2011). They further contain chemokines (interleukin (IL)-8, RANTES) as well as immunomodulatory molecules and antibodies (Complement factors, IgG) (Burnouf et al., 2016). The cargo of dense granules (δ -granules), named as such because of their

high electron density in electron microscopy, are mainly small molecules like serotonin, histamine, ADP and polyphosphates (Ali et al., 2015; Li et al., 2017; Sharda and Flaumenhaft, 2018). The third type of granules are the lysosomes (λ -granules) which mainly store hydrolases, proteases and glycosidase for the lysis of phagocytic components. They may also have a role in degradation of extracellular matrix components (Ramadan A. Ali et al.; Ali et al., 2015; Heijnen and van der Sluijs, 2015). Another morphological structure unique to platelets is the presence of two different internal membrane structures, the open canalicular system (OCS) and the dense tubular system (DTS). The OCS is derived from the cytoplasmic membrane of MK and is therefore connected to the surface (van Nispen tot Pannerden et al., 2010). Platelets can take up plasma proteins such as fibrinogen and tissue factor (TF) via the OCS (Harrison et al., 1989; Escolar et al., 2008). α -granules and δ -granules can fuse with the OCS and release their contents during platelet activation. Furthermore, they are a reservoir for platelet surface receptors in the inactivated state and a reservoir for the membrane itself during formation of filopodia and final spreading after activation (Selvadurai and Hamilton, 2018). The DTS in contrast is not connected to the surface and is derived from the smooth endoplasmic reticulum of MK. It serves as a site of synthesis for prostaglandin and thromboxane, two major effector molecules of platelet activation, and as an internal calcium storage (Gerrard et al., 1978).

Even though the major function of platelets is in thrombosis and hemostasis, platelets critically contribute to a variety of other vascular functions. In angiogenesis, platelets release pro- and antiangiogenic factors after activation and thereby impact angiogenesis-dependent processes such as wound healing and vessel formation (Walsh et al., 2015). In immune responses, the translocation of the granules to the surface after activation leads to the release of inflammatory and bioactive molecules such as PF4 and RANTES responsible for the activation of monocytes and the differentiation of monocytes into macrophages (Ali et al., 2015). Platelets have been shown to interact as defense mechanism against bacterial invasion as they are able to directly or indirectly bind to bacteria via Low affinity immunoglobulin gamma Fc region receptor II-a (Fc γ RIIa), Toll-like-receptors (TLRs), Glycoprotein (GP) IIb-IIIa, and GPIb and bundle fibrinogen-bound bacteria. With this, they contribute to the first line of host defense by reducing bacterial growth rate and producing reactive oxygen species (ROS) with direct antimicrobial activity (Yeaman, 2014; Gaertner et al., 2017). During thrombosis and hemostasis, activation of the normally quiescent platelets by vessel injury is initiated by interaction with the subendothelial matrix such as collagen and von VWF. First, platelets become partially activated and change their shape. Degranulation releases signaling molecules and

recruits additional platelets to the site of injury. At the same time, the tissue factor (TF) clotting cascade is initiated, resulting in the full activation of platelets. TF in the vessel lumen comes into contact with Factor VIIa and Factor IXa in the blood. Factor IXa interacts with Factor Va, leading to the cleavage of small amounts of the zymogen prothrombin into thrombin. Increased thrombin production is regulated by a feedback loop mediated by Factor Xa, followed by full activation of platelets. Thrombin initiates the cleavage of fibrinogen into fibrin which then is cross-linked to fibers forming a mesh to stabilize the clot (Nieman and Schmaier, 2007; Ali et al., 2015). During platelet activation, the stimulation of rapid reorganization of the actin skeleton at the cortex of platelets results in the transformation of the discoid to fully spread shapes. Here, extension of filopodia and the generation of lamellipodia result in an increased surface area (Coughlin, 2005; Aslan et al., 2012). Furthermore, thrombin is a potent agonist for platelet activation *ex vivo* and is responsible for shape change as well as release of effector molecules (Coughlin, 2005).

On their surface, platelets are equipped with different receptors, shown in Figure 2. GPIIb/IIIa (also termed integrin α IIb β III; or CD41/ CD61) is the most abundant surface receptor (15% of the total surface proteins, 80,000 receptors per platelet) (Jennings and Phillips, 1982; Wagner et al., 1996; French and Seligsohn, 2000). It is involved in the adhesion to the endothelium as well as aggregation by crosslinking of adjacent platelets via fibronectin. In the resting state, the receptor moderately binds to VWF, but after activation, it undergoes a conformational change resulting in an increase of the binding affinity to adhesive fibrinogen and thereby participating in plug formation (Durrant et al., 2017). GPIIb/IIIa also can interact with fibrinogen and collagen (Andrews et al., 2014). The second surface receptor of the β III family is the α v β 3 which is involved in platelet adhesion to extracellular matrix proteins mainly interacting with vitronectin (Bennett, 2005). The second most abundant surface molecule is the GPIb-IX-V multiprotein complex consisting of GPIb α (CD42b), GPIb β (CD42c), GPIX (CD42a) and GPV (CD42d) which belongs to the family of the leucine-rich receptors. Its major ligand is the VWF and therefore responsible for rolling and adhesion to the subendothelium, however, it also interacts with other ligands such as thrombin and P-selectin (Li and Emsley, 2013). Under immobilization or increased shear forces, VWF undergoes morphological changes which in turn lead to the binding to the GPIb α . Subsequently, downstream signaling of GPIb α increases intracellular calcium release, expression of P-Selectin on the surface and filopodia formation resulting in platelet clearance (Deng et al., 2016). Platelets also express 3 members of the β 1 family receptors (Bennett, 2005). GPVI (α 2 β 1, CD49b/CD29) is the major receptor for collagen and is a member of the Ig receptor family

which exists in up to 10,000 copies on the platelet surface. It can exist as a dimer, whereas dimerization is enhanced by platelet activation and after ligand binding (Arthur et al., 2007; Andrews et al., 2014). The glycoprotein $\alpha 6\beta 1$ is the major receptor of laminin which is highly abundant in the basement membrane. Laminin is an important extracellular matrix protein which is exposed after vascular damage. The interaction between laminin and its receptor $\alpha 6\beta 1$ not only supports the adhesion of platelets to the site of vascular injury but also platelet spreading (Inoue et al., 2006). Another receptor involved in platelet adhesion is $\alpha 5\beta 1$ which is interacting with fibronectin to initiate the interaction of resting platelets and promoting the interaction of other receptors to amplify the platelet response (Kasirer-Friede et al., 2007). At the edge of the cells, marginal bands can be detected in resting platelets. This is a peripheral network of microtubule bundles and actin filaments maintaining the discoid shape. During activation when platelets become spherical, the interaction between actin and tubulin leads to filopodia and lamellopodia formation as well as accumulation of the granules at the center of the cells and enhanced platelet degranulation (Sadoul, 2015).

The major receptors for thrombin are protease activated receptor (PAR) 1 and PAR4 in humans. In mice, thrombin mainly interacts with PAR3 and PAR4 due to the lack of PAR1 on platelets, which get cleaved by thrombin at their extracellular N-terminus and thereby initiating downstream signaling (Coughlin, 2000). The major receptors for the interaction of platelets with ADP are the P2 receptors P2Y₁ and P2Y₁₂. However, their abundance on the surface of a platelet is much lower (150 copies). They are required for full platelet activation in response to ADP. P2Y₁ initiates weak responses to ADP and P2Y₁₂ completes the aggregation reaction (Hechler and Gachet, 2011). Another important stimulus of platelet activation is the agonist thromboxane A₂ (TxA₂) which is released after vessel injury. The interaction via the thromboxane receptor (TP) on the surface of platelets is involved in the initiation of platelet degranulation and shape change (Rucker and Dhamoon, 2019). Vascular endothelial cells produce prostaglandin I₂ (PGI₂) to prevent platelets from becoming activated in case of intact vascular integrity. The prostaglandin receptor (IP) on the platelet surface interacts with PGI₂ and thereby counteracts platelet activation. Another receptor, highly expressed on the surface of platelets is the C-type lectin receptor (Clec-2) which interacts mostly with the transmembrane protein podoplanin highly expressed in various types of malignancies such as squamous cell carcinomas, mesotheliomas, glioblastomas and osteosarcomas. Therefore, interaction of Clec-2 and podoplanin is determined to be one of the mechanisms in which platelets are involved in tumor metastasis (Lowe et al., 2012).

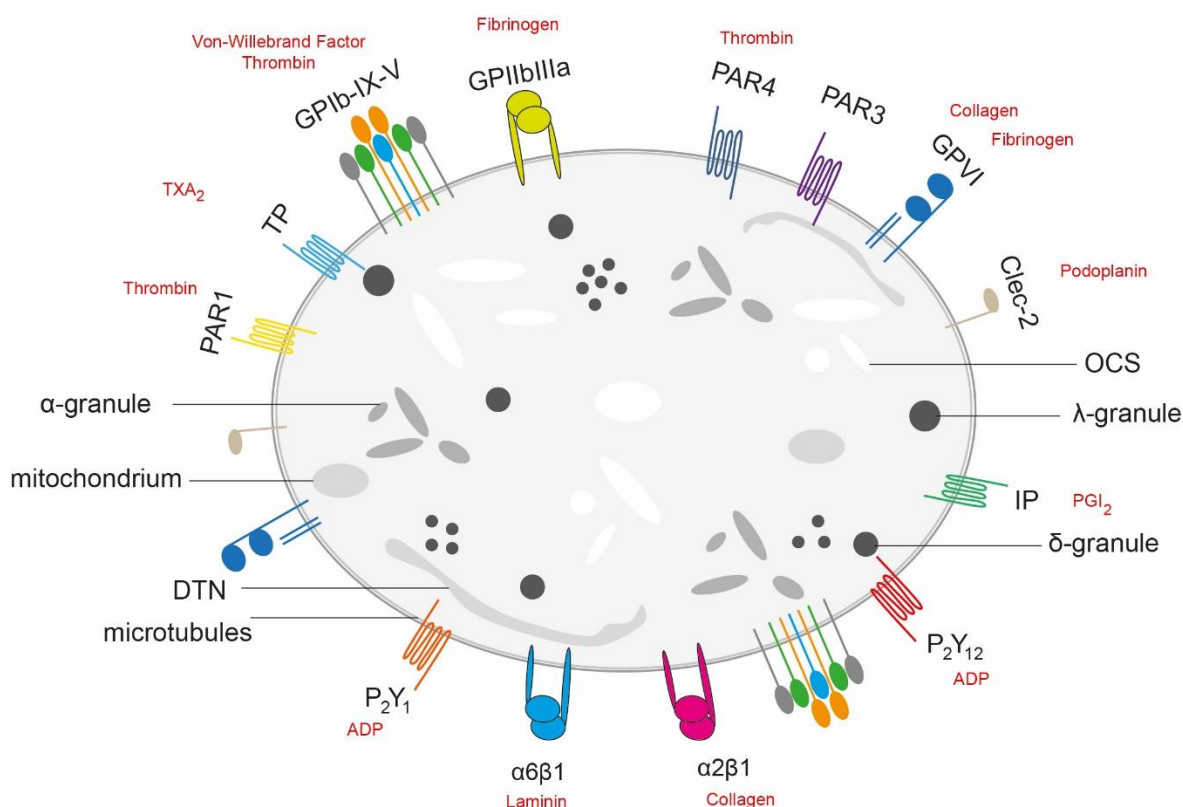


Figure 2 Schematic overview of platelet structure and surface markers. Platelets show a unique ultrastructure when imaged with transmission electron microscopy. The absence of a nucleus is a major platelet feature. After activation of platelets, the granules fuse with the plasma membrane and the granule content is released to augment signaling. They contain two different internal networks, the OCN and DTN as well as lysosomes and mitochondria. On their surface, they are equipped with platelet-specific surface receptors which also mainly interact during platelet activation and are responsible for initiating downstream signaling after binding to their appropriate effector molecules. Human and murine platelets differ in terms of the PAR receptors (PAR1: human, PAR3: murine) (adapted from Zapata et al., 2014).

1.2 Fetal platelet biogenesis

During murine embryogenesis, hematopoiesis occurs in three phases of primitive and definitive hematopoiesis (Ciau-Uitz et al., 2014). In vertebrates, primitive hematopoiesis consisting of erythro-myeloid cells is initiated in blood islands within the yolk sac on day 7 after gestation (Palis et al., 1999; Xu M et al., 2001; Ferkowicz et al., 2003). In 2001, Xu et al. showed evidence for primitive murine megakaryogenesis in the yolk sac (Xu M et al., 2001). Until day 11, the hematopoietic progenitors increase in cell numbers in the yolk sac and in the para-aortic splanchnopleura/aorta-gonad-mesonephros region (PAS/AGM). Autonomous definitive hematopoietic stem cells (HSC) were first detected within the PAS/AGM on day 10.5 after gestation in the mouse. On day 11.5, HSCs can also be detected in the yolk sac (Jaffredo et al., 2005). This stadium defines the second wave of developmental hematopoiesis. Emerging HSC start decreasing in the PAS/AGM and yolk sac and migrate to the fetal liver. Proliferation of HSC in the fetal liver can be measured until day 15 or 16 and is followed by a decrease indicating the mobilization of HSC from

the fetal liver to the BM and spleen (Christensen et al., 2004). The generation of these HSC which emerge from their original compartment and seed different sites of hematopoiesis is considered to be the third phase of embryonic hematopoiesis (Ciau-Uitz et al., 2014). MEP appear during primitive hematopoiesis in the yolk sac at embryonic day 7.5 and 9.5 (Xu M et al., 2001; Tober et al., 2007). More recent studies have discovered the presence of diploid platelet forming cells residing in the yolk sac at day 10.5 which express CD41 but lack the expression of CD45 (Potts et al., 2014). During the later stages of definitive hematopoiesis, MK are also localized in the fetal liver (FL) between embryonic day 9.5 and 10.5. Embryonic MK differ from adult ones in their response to thrombopoietin (Thpo) and in their size (Cortegano et al., 2018). However, FL-derived cells from day 10.5 and 11.5 increase in size and ploidy during MK maturation (Matsumura and Sasaki, 1988).

1.3 Regulators of megakaryocyte and platelet differentiation

During migration from the osteoblastic to the vascular niche in the BM, maturing cells are exposed to a gradient of cytokines and other environmental factors supporting maturation and platelet release. The factors are included in Figure 1. The major cytokine regulating MK differentiation and MK progenitor cell proliferation is Thpo (Kuter et al., 1994; Broudy and Kaushansky, 1995; Kato et al., 1995). The binding of Thpo to its specific cell surface receptor Mpl (homologue of the myeloproliferative leukemia virus oncogene) is followed by conformational changes of the receptor and subsequent phosphorylation, thus activating cellular downstream signaling via PI-3 kinase-Akt signaling (Pulikkan et al., 2012) MAPK (Erk1/Erk2), p38 MAPK (Drachman et al., 1997) and Stat3/Stat5 pathways (Kirito et al., 2002). *Thpo*- and *Mpl* knockout mice have decreased numbers of MK and also decreased platelet counts of more than 80% (Gurney et al., 1994; Sauvage et al., 1996). Thpo/Mpl-signaling also regulates the development of HSC by supporting their survival, proliferation and promotion of self-renewal and proliferation after BM transplantation (Kimura et al., 1998; Solar et al., 1998; Fox et al., 2002). In turn, *Thpo/Mpl*-deficient mice have reduced granulocyte-macrophage, erythroid, and multilineage progenitors (Carver-Moore et al., 1996; Kuter, 2014). *In vitro*, the addition of Thpo stimulates polyploidization of primary immature MK (Broudy et al., 1995; Debili et al., 1995).

The fact that there are residual MK and platelets present in Thpo/Mpl knockout mice leads to the suggestion that also other cytokines are involved in MK and platelet production. For example, mice with a severe reduction in the levels of SCF (Stem cell factor) also develop

severe anemia and thrombocytopenia (Ebbe et al., 1978; Kaushansky, 2009). Cytokines affecting MK growth or maturation are IL-3, IL-6, IL-11. Crossing *Mpl*-deficient mice with other cytokine-receptor-deficient mice shows that cytokines of the IL-family alone are dispensable for normal or stimulation of hematopoiesis *in vivo* (Kaushansky, 2009).

In vitro, cytokines of the IL-family alone also have little or no effect on the proliferation or maturation of MK but they are known to augment megakaryopoiesis *in vitro* (Behrens and Alexander, 2018). Supplementation with IL-3 leads to an increase in numbers of MK from MK cell lines (Avraham et al., 1992). IL-6, IL-11 and LIF interact on the increased size and ploidy of MK *in vitro* (Ishibashi et al., 1989; Burstein et al., 1992; Teramura et al., 1992). *In vivo*, application of IL-6 and IL-11 increases platelet counts in mice *in vivo* or facilitates the recovery from thrombocytopenia after chemotherapy and transplantation, indicating their supportive role for megakaryopoiesis and platelet release.

In addition to cytokines, transcription factors are essential for different maturation steps of megakaryopoiesis, pro-platelet formation and platelet release. Gata1, the most important transcription factor, is named after its DNA binding motif 5'-[AT]GATA[AG]-3'. It controls MK maturation until the state of establishment of mature MK. In mice, *Gata1* knockout is embryonal lethal at day 11.5 due to severe anemia (Fujiwara et al., 1996). Lineage-specific knockout of *Gata1* in MK results in the accumulation of late-stage MK, lacking the capacity for pro-platelet formation and thereby causing thrombocytopenia and showing its role in earlier stages of megakaryopoiesis until mature MK are generated (Shivdasani et al., 1997). *In vitro*, knockout of *Gata1* in fetal liver MK leads to the differentiation of smaller cells with lower ploidy. The cell cycle gene cyclin D1 is a direct target of Gata1, showing its influence on endomitosis and demonstrating the role of Gata1 in MK maturation (Muntean et al., 2007). Furthermore, Gata1 is also involved in granule formation since a mutation in the human *GATA1* gene is one of the mutations responsible for development of the Gray platelet syndrome, a bleeding disorder associated with markedly reduced number or absence α -granules, moderate bleeding and macrothrombocytopenia (Tubman et al., 2007). Gata1 cooperates with its co-factor friend of Gata1 (FOG1), a zinc finger protein that plays a critical role in the formation of a cell-specific transcriptional complex and bridges DNA-bound GATA-1 to distant sites along the chromatin (Tsang et al., 1997). Similar to Gata1, Runx1 (Runt-related transcription factor 1) is involved in cytoplasmic maturation and polyploidization processes (Tijssen and Ghevaert, 2013). Conditional knockout of *Runx1* in mice shows a reduction of mature multilobulated nuclei in the BM with accumulation of premature MK with a similar morphology to micromegakaryocytes, observed in human myelodysplastic syndromes with defects in polyploidization and

formation of the demarcation membrane (Ichikawa et al., 2004; Tijssen and Ghevaert, 2013). However, the conditional knockout has no impact on the HSC maintenance or survival, the mice show also other abnormalities like reduction of platelet counts, a block in lymphocyte development and development of myeloproliferative phenotype (Gronow et al., 2005). In humans, chromosomal translocations and mutations of the RUNX1 gene are associated with different types of acute myeloid leukemias (AML) and acute lymphoblastic leukemia (ALL) (Asou, 2003). Pbx1 (Pre B-cell leukemia factor 1) is a co-factor of the HOX transcription factors and is expressed during embryonic hematopoiesis. Furthermore, studies in *Pbx1*^{-/-} mice show that the lack of the transcription factor is embryonically lethal at day 16 of embryonic development due to anemia (DiMartino et al., 2001). *Pbx1* overexpression in a *Mpl* knockout background mouse model of adult hematopoiesis (performed by our own group) results in an enrichment of MK in the BM, indicating its essential role from early until final stages of MK development and maturation (Kohlscheen et al., 2019). The transcription factor Scl1 (stem cell leukemia 1), also known as Tal1 (T-cell acute lymphocytic leukemia 1), was also first described in association with the occurrence of an acute lymphoblastic leukemia and was shown to regulate yolk sac hematopoiesis in *Scl*^{-/-} in mice since the embryos were dying at embryonic day 9.5, thus indicating the role in regulation of embryonic hematopoiesis (Begley and Green, 1999). Furthermore, conditional *Scl*-null mice show an increased number of MK with higher ploidy but impaired platelet production, indicating a regulation also on the level of platelet release under thrombopoietic stress conditions (McCormack et al., 2006). Another transcription factor involved in platelet release is Nfe2 (Nuclear factor erythroid 2). Nfe2 is heterodimer of a hematopoietic restricted p45 subunit and Maf proteins (p18) such as MafK and MafG (Andrews, 1998). Knockout of the p45 subunit in mice results in increased prenatal death of animals due to hemorrhages and, in case of their survival, postnatal thrombocytopenia (Shivdasani et al., 1995). *Nfe2*^{-/-} MK entirely lack the capability of pro-platelet formation and show reduced granule formation along with reduced DMS establishment (Lecine et al., 1998). Evi1 (Ectopic viral integration site 1) is a transcription factor highly expressed in hematopoietic progenitor cells, MKs and platelets (Tozawa et al., 2014) and its overexpression is associated with the development of myeloid leukemia. However, conditional knockout in mice results in the establishment of thrombocytopenia without affecting the white blood cell counts (Goyama et al., 2008; Huang and Cantor, 2009). Whereas it negatively regulates the development from HSC into granulocytes and erythrocytes, the overexpression in a megakaryocytic cell line *in vitro* increases their polyploidy, showing that Evi1 is a further key factor for MK maturation at later stages 17 (Shimizu et al., 2002; Tozawa et al., 2014).

Despite the role of transcription factors on different levels of megakaryopoiesis, GTPases facilitate various cellular processes like cell division, exocytosis, and actin cytoskeletal dynamics (Etienne-Manneville and Hall, 2002; Aslan and McCarty, 2013). RhoA is a guanosine exchange factor which circulates between an inactive GDP-bound state and an active GTP-bound state. Conditional knockout in mice results in severe macrothrombocytopenia, indicating RhoA's essential role in platelet release from mature MK. Platelets isolated from *RhoA* knockout mice perform less spreading and clot formation, which also shows interference of RhoA in platelet functionality (Pleines et al., 2012). Another well studied GTPase, Cdc42, is also involved in generation of stress fibers as well as filopodia and lamellipodia formation (Nobes and Hall, 1995). *Cdc42* knockout in mice also showed a phenotype similar to that of *RhoA* knockout mice. They also present with macrothrombocytopenia and reduced platelet numbers. However, here, *Cdc42* knockout also results in the increased granule secretion and slightly increased activation potential (Pleines et al., 2010). Cdc42 was shown to be a main regulator of DMS during megakaryopoiesis *in vitro* and *in vivo* (Antkowiak et al., 2016).

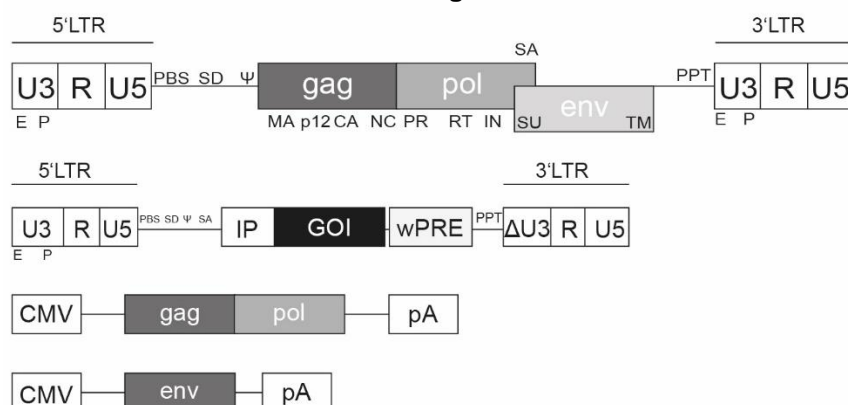
1.4 Gene modification with viral vectors

1.4.1 Self-inactivating retroviral vectors

In our study, we aimed for stable and long-term gene modification. Therefore, a retroviral vector system, derived from the murine leukemia virus (MLV) which belongs to the genus of *gammaretroviruses*, as well as lentiviral vectors, derived from human immunodeficiency virus (HIV), were employed. Viral particles of enveloped viral vector harbor capsid proteins enclosing two copies of single-stranded RNA, the viral genome. A fully functional retroviral genome carries genes for the formation of infectious particles from the infected host cells which encode gag and pol for the structural and enzymatic proteins like polymerase (pol: polymerase, reverse transcriptase, integrase) and group associated antigen (gag: matrix, capsid, nucleocapsid) which are shared by all retroviruses. The integrated provirus in return does not code for these structural proteins and therefore lacks the ability to form infectious particles. Detailed pictures of the viral genomes of gammaretroviruses and lentiviruses and the descending viral vectors are shown in Figure 3. The first retroviral vectors have already been developed more than 30 years ago from different viral origins including Moloney murine leukemia virus (MMTV) and MLV (Gilboa et al., 1982; Williams et al., 1984; Mulligan, 1993). Over the course of time, they have been engineered for a safer and more efficient transduction (Baum et al., 1995). The so-called split packaging design supplies these, together with the envelope (env) of choice on separate plasmids

during the generation of the viral vector particles (Miller, 1990). Deletion of the enhancer promoter from the LTR led to the so called self-inactivating (SIN) configuration (Yu et al., 1986). Also, pseudotyping with envelope proteins derived from other viruses has broadened the host range of the vector particles (Emi N., 1991). In contrast to gammaretroviral vectors, lentiviral vectors have the ability to transduce also non-dividing cells, which allows higher transduction efficiencies (Naldini et al., 1996; Dull et al., 1998; Schambach et al., 2013).

A Gammaretrovirus and descending viral vector



B Lentivirus and descending viral vector

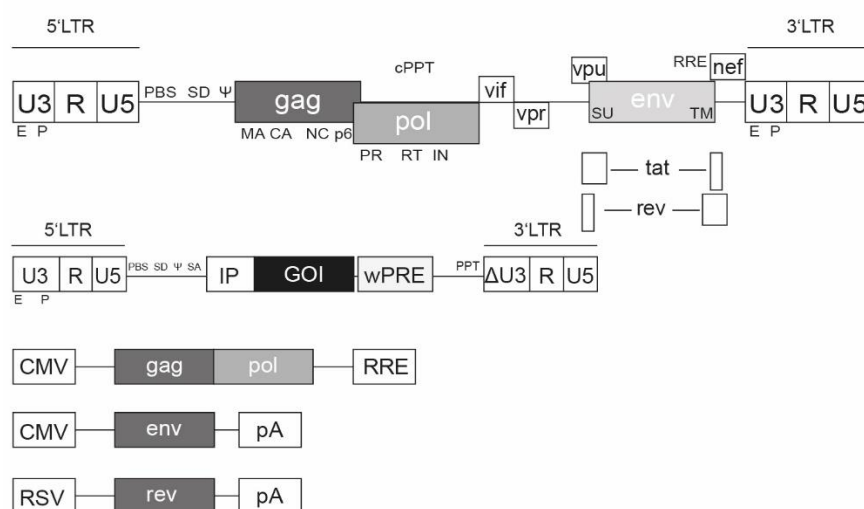


Figure 3 Genome of gammaretroviruses and lentiviruses and the corresponding designed expression vectors with helper plasmids and the split packaging design. The genomes are flanked by long terminal repeats (LTR) which can be dissected to the unique region 3 (U3), repeat region (R), and the U5 region. Further structural elements are the primer binding site (PBS), the packaging signal ψ , the splice donor (SD) and acceptor sites (SA) and the retrovirus-specific polypurine tract (PPT) initiating the DNA synthesis of the reverse transcription. For generation of retroviral vectors, the retroviral genomes have been deleted for all viral genes. The gene of interest (GOI) and an additional woodchuck posttranscriptional regulatory element (wPre) are flanked by long terminal repeats (LTR). For the 3rd generation of gammaretroviral and lentiviral vectors, the enhancer (E) and promoter (P) were deleted, resulting in a SIN configuration where the transgene is expressed from an internal promoter of choice (IP). For the production of the viral vector particles, the expression vector has to be co-transfected with the helper plasmids expressing gag/pol, env and rev genes (the latter only in the lentiviral context) from the cytomegalovirus promoter (CMV) or rous sarcoma virus promoter (RSV). (A) Gammaretrovirus and the descending viral vector. The genome of a gammaretrovirus is segmented into three main sequences: gag (encoding for Matrix protein (MP), protein p12, the capsid (CA) and the nucleocapsid (NC)); pol (encoding for the protease (PR), the reverse transcriptase (RT), the integrase (IN), and env (encoding for the surface (SU) and transmembrane (TM) domain of the envelope protein). (B) Lentivirus and the descending viral vector. In Addition to the genes shared with gammaretroviruses, the lentiviral genome encodes virulence genes vif, vpr, vpu and nef. The tat protein is important for promoter activation and the rev protein stabilizes unspliced viral mRNA and leads to its cytoplasmatic transport by binding to the rev responsive element (RRE). Lentiviruses contain a second central polypurine tract (cPPT) (modified after Maetzig et al., 2011; Schambach et al., 2013).

Generation of viral vector particles is shown in Figure 4. MLV-derived retroviral vectors can be pseudotyped by various viral envelopes such as vesicular stomatitis viral glycoprotein (VSVg) (Burns et al., 1993). Viral particles enveloped by VSVg enter the host cell via receptor-mediated endocytosis and release the virus core, containing capsid, reverse transcriptase, integrase, nuclear capsid and RNA, into the host cell cytoplasm or they enter the cell by transition through the endosome, which results in the unpacking of the viral particles (Maetzig et al., 2011). Once entered and unpacked, reverse transcriptase (RT) converts the viral RNA into double-stranded DNA, followed by the entry into the nucleus. In the case of the gammaretroviral vectors, nuclear entry occurs during the breakdown of the nuclear membrane during mitosis, which then leads to permanent integrase-mediated integration into the host cell genome (Hindmarsh and Leis, 1999).

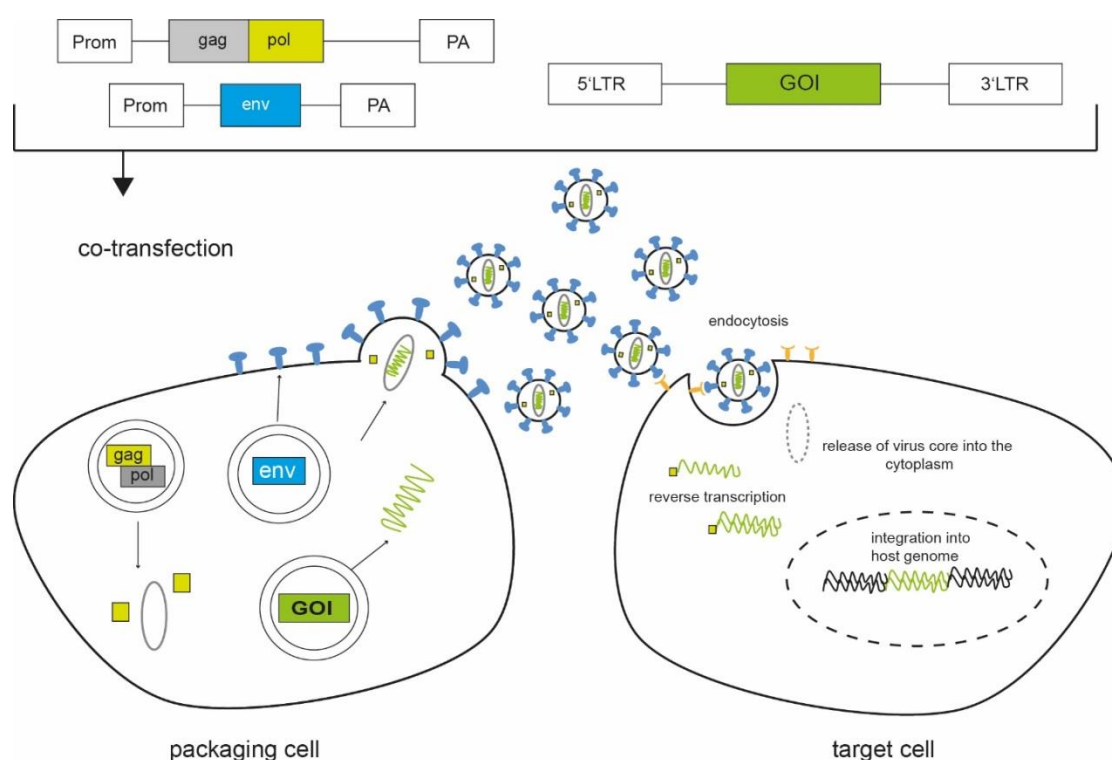


Figure 4 Generation of retroviral vectors. During the retroviral life cycle, viral particles enter their target cells via receptor-mediated endocytosis in case of a VSVg envelope and release the virus core into the cytoplasm of the cells. Reverse transcriptase converts the viral RNA into double stranded DNA which then integrates into the host cell mediated by the enzyme integrase. Information for the formation of new viral particles is encoded on the viral RNA. The proteins assemble together with viral RNA and particles released by budding of the host cell membrane. For the generation of viral vectors, the genes encoding for envelope, polymerase and integrase are split on different expression plasmids which are transfected separately into the packaging cells. Due to the lack of the packaging signal of the so-called helper plasmids, only the genetic information of the transfer plasmid is packaged into the viral particles. Hereby, formation of viral particles after integration of the viral vector of the host cell genome is prevented (Adapted and modified after Maetzig et al., 2011; Vannucci et al., 2013).

The self-inactivating (SIN) technology, developed by Gilboa and colleagues in 1986 and further modified to achieve high titers, contains a deletion of the 3'U3 region harboring the enhancer/promoter region allowing the non-viral regulation of the gene expression (Yu et al., 1986; Dull et al., 1998; Schambach et al., 2006). When the 3'UTR is copied into the 5'UTR during reverse transcription, the enhancers/promoters are deleted and the gene expression of the vector can be initiated from an internal promoter of choice (Maetzig et al., 2011) (see Fig 5).

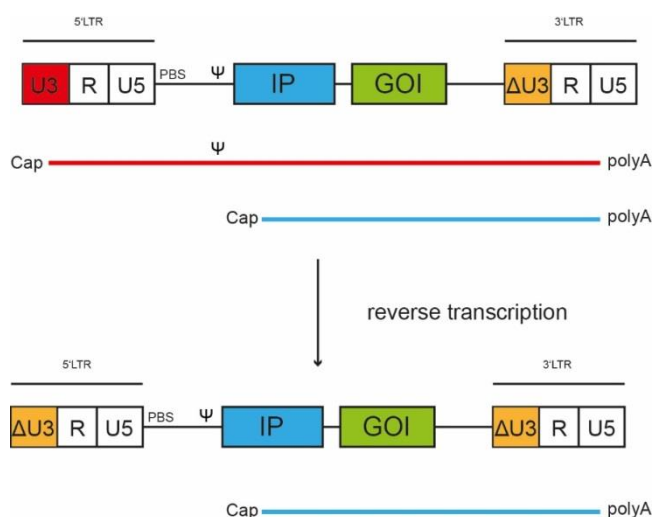


Figure 5 Self-inactivating retroviral vectors. The deletion of the U3 region of the 3'LTR (Δ U3, orange) leads to the loss of the promoter activity of the LTR. Two different mRNAs are generated from the viral vector plasmid: One originates from the original promoter in the U3 of the 5' LTR (red), the other one from the internal promoter (IP, blue). Only the full length RNA carries the packaging signal (Ψ) and is, therefore, included in the viral vector particle. During reverse transcription, the Δ U3 of the 3'LTR is copied to the 5'LTR result in its loss of promoter activity. After integration, both LTR are devoid of enhancer/promoter sequences by the deletion in the U3 and the resulting mRNA after vector integration into the host genome is initiated from the IP (blue line) (Modified after Maetzig T. et al, 2011).

1.4.2 Doxycycline inducible all-in-one retroviral vectors

In 1992, Gossen and Bujard first published a system relying on regulatory elements of the tetracycline (Tet) -resistance operon in *E.coli*. Herein, transcription of Tet-resistant genes is negatively regulated by a repressor. This system turned out to have the ability of gene regulation in mammalian cells. Gossen and Bujard generated an artificial transcription factor consisting of a Tet repressor (TetR) and the C-terminal domain of VP16 protein from herpes simplex virus (HSV) which is essential for the activation of early viral genes. This hybrid transactivator (tTA) is prone to stimulate promoters fused to the Tet operon (TetO). Within the “Tet-Off” system, application of low doses of dox prevents the transactivator to bind to the TetO and thus, transcription does not take place (Gossen and Bujard, 1992).

Random mutagenesis of the tTA led to the development of a reverse controlled transgenesis transactivator (rtTA) which interacts in an opposite way. Application of dox

leads to the inactivation of the repressor and therefore, the rtTA can bind to the TetO leading to transcriptional activation of downstream genes. This is known to be the “Tet-On” system (Benabdellah et al., 2011). The rtTA used in this case is the rtTA2^S-M2 ((rt)TA-M2) which is expressed under the control of a constitutively active phosphoglycerate kinase promoter (PGK). The Tet-operator fused to a minimal promoter (T11) and the cDNA of choice build the Tet-responsive unit. Conformational changes in M2 upon binding to dox lead to the interaction of M2 with the TetO. In turn, the T11 minimal promoter initiates transcription of the transgene of choice which is located downstream of the Ptet-T11 (Heinz et al., 2011).

Despite the all-in-one vectors, all the components of the system can also be delivered as a two-vector system for robust genetic modification (Vigna et al., 2002). In 2005, Konrad Hochedlinger and colleagues developed a knockin mouse containing the reverse transactivator (rt)TA-M2 in the Rosa26 safe harbor locus named B6.Cg-Gt(ROSA)26Sor^{tm1(rtTA^S*M2)^{Jae}/J. Here, the transactivator is constitutively expressed from the Rosa26 locus (Hochedlinger et al., 2005). In animal experiments, residual components can be delivered via retroviral vectors expressing the Tet-responsive internal promoter and the transgene of choice (Magnusson et al., 2007; Kustikova et al., 2013).}

1.5 Induced pluripotent stem cells (iPSC)

In 2006, Takahashi, Yamanaka and colleagues succeeded in the discovery of a paradigm shift, the generation of induced pluripotent stem cells that reverses somatic cells into an embryonic state (Takahashi and Yamanaka, 2006). The murine fibroblasts used in their first experiments were transduced with viral vectors overexpressing embryonic transcription factors Oct3/4 (Octamer-binding transcription factor-3/4), Klf 1 (Kruppel Like Factor-4), Sox2 (Sex-determining region Y)-box 2, and cMyc (OSKM factors). Shortly after having succeeded in reprogramming mouse fibroblasts into iPSC, the same approach could also be applied to human cells (Takahashi and Yamanaka, 2006; Takahashi et al., 2007; Yu et al., 2007). The first sign of successful reprogramming is the appearance of a cellular morphology resembling embryonic stem cells. Additionally, iPSC also show other embryonic stem cell features like self-renewing capacity and the ability of differentiation into ectoderm, endoderm and mesoderm. The discovery of the generation of iPSC is very valuable for new approaches in patient-specific cellular therapies and disease modeling as well as drug screening. Furthermore, it paves the way for wildlife and animal conservation efforts as well as reanimation of extinct species (Stanton et al., 2019). During the course of time, reprogramming methods changed from the original use of integrating viral vectors (e.g. lentiviral vectors) in which the reprogramming cassette was excisable at later stages. Non-integrating strategies were based on viral vectors derived

from sendai virus or adenoviruses (Stadtfield et al., 2008; Chen et al., 2013). Also, non-integrating non-viral based reprogramming such as the delivery of synthetic modified mRNA or proteins as well as episomal vectors can be used to deliver the reprogramming factors (Kim et al., 2009; Jia et al., 2010; Warren et al., 2010).

1.6 Ubiquitous chromatin opening elements (UCOE)

The development of retroviral vectors provides tools for a multitude of applications in gene therapy and regenerative medicine. The usage retroviral vectors for genetic modification of pluripotent stem cells can be applied in patient-specific therapies. However, one major obstacle is the variegated transgene expression depending on the integration site, called position effect variegation and silencing of the retroviral vectors (Jähner et al., 1982; Challita and Kohn, 1994). Pluripotent stem cells in particular are susceptible for silencing of retroviral vectors during differentiation into effector cells (Minoguchi and Iba, 2008). Also, after integration into the genome during generation of iPSC reprogramming, vectors get silenced by epigenetic mechanisms (Hotta and Ellis, 2008). Molecular mechanisms responsible for epigenetic silencing are DNA methylation and histone modifications.

To prevent silencing, a couple of strategies have been developed such as addition of anti-silencing sequences (McInerney et al., 2000). Insertion of insulator elements such as the chicken HS4 insulator and scaffold/matrix attachment regions (S/MAR) into retroviral vectors shield the vectors from the spread of heterochromatin into the euchromatic regions and associated gene silencing (Agarwal et al., 1998; Emery et al., 2000; Neville et al., 2017). Another strategy is the incorporation of UCOE. The best studied element is derived from an intergenic region between two ubiquitously expressed genes which are transcribed in opposite orientation (see Figure 6): the heterologous nuclear ribonucleoprotein A2B1 (*HNRA2B1*) and the chromobox homolog 3 (*CBX3*) first discovered by M. Antoniou et al. in 2003. It was discovered by integrating a 16kb region into centromeric heterochromatin (Antoniou et al., 2003). Further experiments revealed that the element can be dissected into smaller functional units, which allows their usage in retroviral vectors (Lindahl Allen et al., 2009). The intergenic region is highly enriched in unmethylated CpG, also termed CpG island (Gardiner-Garden and Frommer, 1987). Although the molecular mechanism of the functionality of the element remains still unknown, it is incorporated into retroviral vectors in a variety of applications such as the *ex vivo* bioengineering of iPSC-derived macrophages or *in vivo* chemoselection after transplantation of genetically modified cells (Pfaff et al., 2013; Phaltane et al., 2014; Ackermann et al., 2017). Further modification and thereby removal of a canonical splice donor and a cryptic splice site of the 670bp element spanning the transcriptional start site

of the CBX3 resulted in enhanced anti-silencing capacity after incorporation into constitutively expressed lentiviral vectors (Müller-Kuller et al., 2015).

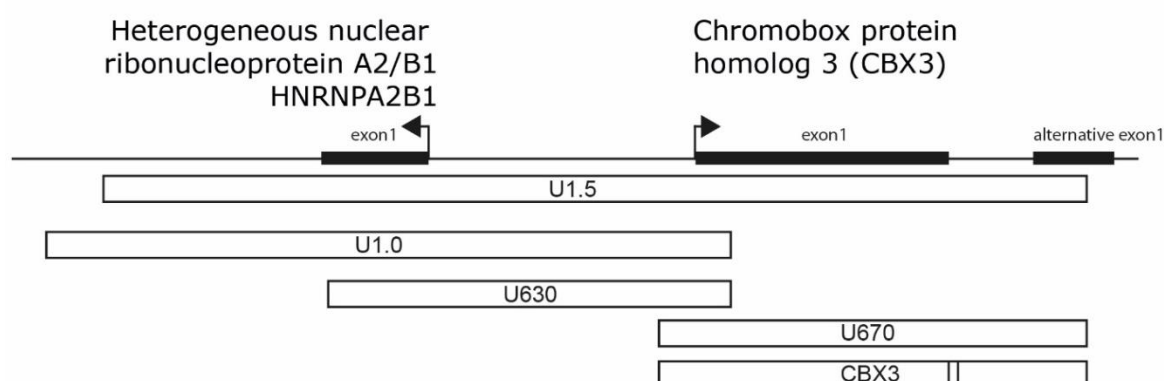


Figure 6 Ubiquitous chromatin opening elements and their location. The different A2UCOE are derived from two housekeeping genes expressed in opposite orientation. Exons are indicated by horizontal black bars, arrows indicate transcriptional start sites of the corresponding genes. Annotation of exons based on NM_007276.4 (transcriptvariant1,CBX3), NM_016587.3 (transcriptvariant2,CBX3) and NM_002137.3 (transcriptvariantA2). Mutations in cryptic splice site and canonical splice donor in the CBX3 element are indicated by vertical bars. (Modified after Cullmann et al., 2019).

1.7 *In vitro* generation of platelets

Platelet transfusion is the treatment of choice for patients suffering from thrombocytopenia caused by e.g. chemotherapy, radiation treatment, organ transplantation and inherited diseases. However, this is associated with several drawbacks such as the limited shelf life of the platelet products, the storage-related deterioration, the donor-dependency as well as patients developing allogenic antibodies against donor platelets after repetitive transfusions, a disease called platelet refractoriness. Due to this, several laboratories have made great efforts in the *in vitro* generation of platelets from different sources. Achieving the tremendous amount of $2\text{-}5 \times 10^{11}$ platelets per transfusion unit from *in vitro* sources with platelet functionality comparable to freshly isolated cells still seems to be challenging. Platelets can be differentiated *in vitro* from two major sources. 1) Hematopoietic progenitors produce fully functional MK and platelets, however, they still show limited expansion potential and there is still a risk for alloreactivity of the patients (Choi et al., 1995; Di Buduo et al., 2015; Strassel et al., 2016) 2) Pluripotent stem cells including ESC and iPSC provide a renewable and unlimited source which also paves the way for personalized medicine. Two very promising technologies using iPSC resulted in the generation of expandable MK cell lines from either overexpression of major supportive factors (GATA1, SCL1, FLI1, c-MYC, BMI1) or anti-apoptotic factors BCL-XL) from which platelets can be produced showing comparable functionality to freshly isolated platelets (Nakamura et al., 2014; Moreau et al., 2016). Efforts made by Börger et al. showed that

also HLA-universal MK and platelets can be differentiated *in vitro* by silencing HLA I, which is a step towards universal platelet transfusions (Börger et al., 2016). With regards to the increase in output of *in vitro* generated platelets, several types of bioreactors have been developed. Two systems were designed to increase the platelet release by the application of shear forces under flow conditions: static MK attach to an appropriate matrix and extend their protrusions under shear, for example through small gaps, mimicking those of the endothelial cells lining the vascular sinusoids of the BM (Thon et al., 2014). A bioreactor is based on VWF-coated micro pillars to which the MK can attach, elongate and rupture under microfluidic conditions (Blin et al., 2016). The latest approach combines usage of immortalized MK, their proliferation up to 5×10^{10} followed by exposure to turbulence in a liquid bioreactor. Shedded platelets show similar functions to freshly isolated ones whilst achieving cell counts in the range of 10^{11} . However, the underlying MK still produce only around 80 platelets per MK, which is still far less than the predicted 1000 a MK can produce *in vivo* (Ito et al., 2018).

2 AIM OF THE STUDY

Since the medical demand for blood products is increasing but blood donations will stay constant, a blood crisis in the upcoming years is very likely. Platelet products for transfusion are especially affected due to their short shelf life and special storage conditions to prevent activation and bacterial contamination. *In vitro* generated platelets and MK progenitors from iPSC are one of the earliest and most promising bioengineered blood products coming to application in human patients in the future. Furthermore, MK and platelets generated from iPSC could be utilized for disease modeling. However, there are still some hurdles to take since the production of platelets and MK from pluripotent stem cells is inefficient and also the functionality of culture-derived MK progenitors and platelets is impaired. iPSC can be modified with retroviral vectors in the pluripotent state. Overexpression of supporting factors such as major transcription factors can be beneficial for the manufacturing process and the quality of generated cells. However, their overexpression at very early stages of pluripotency might also be disadvantageous for the differentiation process. In this project, we were aiming for the overexpression of single supportive factors via a dox-inducible gammaretroviral vector to increase numbers and functionality of generated platelets and their progenitors *in vitro*. We therefore chose to overexpress the major transcription factors involved in early and late stages of megakaryopoiesis and platelet release, Gata1 and Pbx1. We also thought that overexpression of Evi1 would lead to directed proliferation of progenitors. Another very important candidate is Nfe2, a transcription factor that regulates mostly platelet release. To also enhance platelet release and functionality, we chose to overexpress hyperactive variants of the two very important GTPases RhoA and Cdc42 (RhoA^{hc} and Cdc42^{hc}, respectively) with Tet-inducible retroviral vectors.

Retroviral vectors are often susceptible to epigenetic silencing via methylation of cytosine residues of the DNA. In our system, we utilized a human phosphoglycerate kinase (PGK) promoter for ubiquitous expression of the transactivator ((rt)TA-M2) in Tet-all-in-one retroviral vector configurations. The PGK promoter is highly enriched in CpG islands and therefore the most vulnerable component of the vector concerning epigenetic silencing. To prevent silencing during pluripotency and differentiation, we were following these two different strategies.

1) Generation of murine iPSC expressing the (rt)TA-M2 from the Rosa26 locus (B6.Cg-Gt(ROSA)26Sor^{tm1(rtTA^{M2})Jae/J}) should allow a continuous expression of (rt)TA-M2 and prevent transgene silencing during differentiation. Transduction of the respective single

supportive factors should be controlled by a Tet-responsive T11 minimal promoter. Based on the transduction of the iPSC in the pluripotent state, the cells should express the transgene (Gata1, Nfe2, Pbx1, Evi1, RhoAhc, Cdc42hc) after the induction with dox during the differentiation of the iPSC into MK and platelets. Generation of MK will further be supported by co-cultivation on OP9 feeder cells and supplementation with Thpo and Scf. The supportive effect of each single factor was evaluated by MK/platelet-specific surface maker expression, MK/platelet yield and morphology.

2) Dox-inducible gammaretroviral vectors should also be applicable for usage in a human system of MK and platelet bioengineering from iPSC in the future. Epigenetic silencing especially during differentiation is comparable. We were, therefore, aiming to generate dox-inducible gammaretroviral all-in-one vectors that are less susceptible to epigenetic silencing. UCOE can be inserted upstream the PGK promoter; however, it is not clear whether they would influence the Tet-inducible system and maintain anti-silencing potential. We inserted UCOE of different sizes and locations in different orientations into the all-in-one vectors and tested their performance in terms of anti-silencing potential and regulation in various cell types including iPSC.

3 MATERIALS AND METHODS

3.1 Materials

3.1.1 Technical devices

Table 1 Technical equipment

Device	Label	Manufacturer, Headquarter
0.5-1000µl pipets	Pipetman	Gilson; Limburg Offheim (GER)
Balance	Kern ABJ 320-4NM	Kern & Sohn GmbH; Balingen (GER)
Centrifuges	Fresco 17	Thermo Fischer Scientific; Waltham (MA USA)
	Multifuge X3R	
	Cytospin 4	
Clean bench	MSC-Advantage	Thermo Fischer Scientific; Waltham (MA USA)
CO ₂ /O ₂ Incubator	Series C	Binder; Tuttlingen (GER)
Counting chamber	Neubauer	Marienfeld, Lauda Königshofen (GER)
Electrophorese power supply	EV245	neoLab; Heidelberg (GER)
Electrophorese chamber		neoLab; Heidelberg (GER)
Suction System	Aspir8 4.4 CS	CellMedia; Gutenborn (GER)
Flow cytometers	Accuri C6	BD Biosciences; Heidelberg (GER)
	LSR II SORP	
	AriaIII	
	CytoFLEX S	Beckmann Coulter; Krefeld (GER)
Fridge-Freezing combination		Liebherr; Biberach and der Riss (GER)
Gel documentation		Intas; Göttingen (GER)
Heating block	Thermomixer basic	CellMedia; Gutenborn (GER)
Incubation shaker	MaxQ 6000	Thermo Fischer Scientific; Waltham (MA USA)

Device	Label	Manufacturer, Headquarter
Incubator Microbiology	4360	Thermo Fischer Scientific; Waltham (MA USA)
Microscope	Primo Vert	Carl Zeiss; Oberkochen (GER)
	Eclipse Ti-S	Nikon GmbH; Düsseldorf (GER)
	Fluoreszenzmikroskop Observer Z1	Carl Zeiss; Oberkochen (GER)
Microwave	KMW225	Koenic; Ingolstadt (GER)
Multipipette	Multipette M4	Eppendorf; Hamburg (GER)
NanoPhotometer	P 300	Implen; München (GER)
Orbital shaker	Fisherbrand Digital	Thermo Fisher Scientific; Waltham (MA USA)
PCR devices	Tpersonal	Biometra; Göttingen (GER)
	Thermocycler	
	Tprofessional	
Pipet	accu-jet pro	Brand; Wertheim (GER)
Real-time PCR system	StepOnePlus	Applied Biosystems; Thermo Fisher Scientific Waltham (MA, USA)
Vortex	VV3	VWR; Westchester (PA USA)
Water bath	Isotemp	Thermo Fischer Scientific; Waltham (MA USA)

3.1.2 Expendable items

Table 2 Expendable items

Material	Manufacturer
Cell culture dish	Sarstedt; Nümbrecht (GER)
Reaction tubes 15ml, 50ml	Greiner Bio-One; Frickenhausen (GER)
Cell strainer (70µm, nylon)	BD Biosciences; Heidelberg (GER)
Multiwell plates (6, 12, 24 well)	Sarstedt; Nümbrecht (GER)
PCR-Reaction tubes	Nerbe plus; Winsen/Luhe (GER)
Petri dishes (Molecular Biology)	Greiner Bio-One; Frickenhausen (GER)

Material	Manufacturer
Reaction tubes 1,5ml	Sarstedt; Nümbrecht (GER)
Serological pipettes	Greiner Bio-One; Frickenhausen (GER)
Syringes	B.Braun; Melsungen (GER)
Syringe driven filter unit, Milltex, 0.2µm	Merck Millipore; Cork (IRL)

3.1.3 Chemicals and reagents

Unless otherwise stated, chemicals and reagents were obtained from the in-house facility at the Paul-Ehrlich-Institute.

Table 3 Chemicals and Reagents

Label	Manufacturer
1-Thioglycerol	Gibco; Carlsbad (CA, USA)
2-Mercaptoethanol	Gibco; Carlsbad (CA, USA)
Agarose	Thermo Fisher Scientific; Waltham, MA USA
Apyrase	Sigma Aldrich; Seelze (GER)
Ampicillin sodium salt	Sigma Aldrich; Seelze (GER)
Bovine serum albumin	Sigma Aldrich; Seelze (GER)
Calcium chloride (CaCl ₂)	Sigma Aldrich; Seelze (GER)
Chloroquine	Sigma Aldrich; Seelze (GER)
C reactive peptide (CRP)	Sigma Aldrich; Seelze (GER)
Collagenase IV	Sigma Aldrich; Seelze (GER)
4',6-Diamidin-2-phenylindol (DAPI)	Sigma-Aldrich; Seelze (GER)
Doxycycline hyclate	Sigma Aldrich; Seelze (GER)
Ethylenediaminetetraacetic acid (EDTA)	Promega BioSciences, San Luis Obispo, (CA, USA) Ethanol
Ethanol (per analysis)	Berkel AHK, Ludwigshafen (GER)
Ethanol denatured	
Fetal calf sera for cultivation of ESC	Gibco; Carlsbad (CA, USA)
Fetal calf sera, pharma grade	Biochrom; Berlin (GER)
Fibrinogen	Sigma Aldrich; Seelze (GER)
Glutamine	Biochrom; Berlin (GER)

Label	Manufacturer
Giemsa modified solution	Sigma Aldrich; Seelze (GER)
Glutamine	Biochrom; Berlin (GER)
Heparin	Sigma Aldrich; Seelze (GER)
4-(2-hydroxyethyl)-1-piperazineethanesulfonic acid4-(2-hydroxyethyl)-1-piperazineethanesulfonic acid (HEPES)	
Isopropyl β -D-1-thiogalactopyranoside (IPTG)	Carl Roth; Karlsruhe (GER)
Isofluran CP	CP Pharma, Burgdorf (GER)
Isopropyl alcohol	Berkel AHK, Ludwigshafen (GER)
Magnesium chloride ($MgCl_2$)	Ambion; Austin (TX, USA)
Matrigel	Corning; Amsterdam (NL)
May-Grünwald solution	Sigma-Aldrich; Seelze (GER)
Minimum essential medium non-essential amino acids	Gibco; Carlsbad (CA, USA)
Penicillin	Calbiochem; Darmstadt (GER)
Potassium acetate	
Potassium dihydrogen orthophosphate(KH_2PO_4)	
Potassiumchloride (KCl)	
Prostacyclin (PGI_2)	Sigma Aldrich; Seelze (GER)
Protamine sulfate	Sigma Aldrich; Seelze (GER)
Retronectin	Takara Bio; Shiga (JPN)
SDS	
Sodium azide (NaN_3)	
Sodium chloride (NaCl)	Promega BioSciences, San Luis Obispo, (CA, USA)
Sodium hydrogen phosphate (Na_2HPO_4)	
Sodium hydroxide (NaOH)	
Streptomycin sulphate	Calbiochem; Darmstadt (GER)
TrisHCl pH 7,5 ultra-pure	Gibco; Carlsbad (CA, USA)
Vectashield® Mounting Medium	Vector Laboratories, Burlingame (CA,USA)
X-Gal	CarlRoth; Karlsruhe (GER)
Prestoblu® cell viability reagent	Thermo Fischer Scientific; Waltham (MA, USA)

3.1.4 Buffers and solutions

Unless otherwise stated, buffers and solutions were manufactured in the Paul-Ehrlich-Institute in house facility. Buffers for platelet activation were obtained from the group of Dr. Markus Bender, Würzburg University.

Table 4 Buffers and solutions

Label	Composition/Concentration
2 x HeBS	280mM NaCl, 50mM HEPES, 1,5mM Na ₂ HPO ₄ , pH 7,05
20 x Tyrode's buffer (Maus)	2.73M NaCl, 53.6mM KCl, 238mM NaHCO ₃ , 8mM Na ₂ HPO ₄ , 0.5M HEPES
20x TAE buffer	0.2mM EDTA, 0.8M TRIS, 22.84ml/l glacial acetic acid,
Ampicillin	100mg/ml dissolved in ddH ₂ O
Blocking buffer for Retronectin	PBS + 2% BSA
BSA	10%
Dulbecco's PBS	136.89mM NaCl, 2.86mM KCl, 1.46mM KH ₂ PO ₄ , 8.1mM Na ₂ HPO ₄ , pH 7.1, CaCl ₂ 2 H ₂ O 0.9mM, MgCl ₂ 6H ₂ O 0.5mM
FACS-buffer	164mM NaCl, 16.55mM Na ₂ HPO ₄ , 2.7mM KCl, 1.2mM EDTA, 1.9mM KH ₂ PO ₄ , 0.1% NaN ₃
Fixation buffer platelet activation	PHEM buffer, 4% PFA, 0.033% NP40
Gelatin	0.125%
Glucose	10%
LB-Agar	LB-Medium, 1.5% Agar
MACS-buffer	137mM NaCl, ,1mM Na ₂ HPO ₄ , 2.7mM KCl, 2mM EDTA, 1.5mM KH ₂ OP ₄ , 0.07mM BSA (fraction V), pH 7.2
P2	0.2M NaOH, 1% SDS
P3	3M KaAC, pH 5.5
PBS	136.89mM NaCl, 2.86mM KCl, 1.46mM KH ₂ PO ₄ , 8.1mM Na ₂ HPO ₄ , pH 7.1
Penicillin/Streptomycin	17mM Streptomycin sulphate, 40.8mM Penicillin G potassium

Label	Composition/Concentration
PHEM buffer	100nM PIPES, 5.25nM HEPES, 10mM EGTA, 20mM MgCl ₂ , pH6.8
X-Gal	20ng/μl
Trypsin-EDTA	0.5g/l Trypsin, 0.2g/l EDTA dissolved in PBS
Washing buffer for Retronectin	PBS + 2.5% HEPES

3.1.5 Cytokines

Table 5 List of Cytokines

Cytokine	Manufacturer
mIL-3	PeptoTech; Rocky Hill (NJ, USA)
mLIF	PeptoTech; Rocky Hill (NJ, USA)
mScf	PeptoTech; Rocky Hill (NJ, USA)
mThpo	PeptoTech; Rocky Hill (NJ, USA)

3.1.6 Antibodies

All antibodies used for flow cytometry were monoclonal and of an IgG isotype except for the αCD15 which was IgM.

Flow cytometry

Table 6 Antibodies for flow cytometry

Antibody	Antigen	Manufacturer	Catalog No.
rat α-mouse CD41-PerCpCy5.5	GPIIb	Biolegend; San Diego (USA)	133918
rat α-mouse CD41-APC	GPIIb	eBioscience; San Diego (USA)	133914
hamster α-mouse CD42d-APC	GPV	eBioscience; San Diego (USA)	148506
mouse α-mouse CD15-PE	SSEA-1 (pluripotent stem cells)	Biolegend; San Diego (USA)	125606
mouse α-mouse CD62P-PE	P-selectin	eBioscience; San Diego (USA)	148306
mouse α-HA-biotin	Influenza hemagglutinin	Roche Diagnostics, Mannheim (GER)	11583816001

Visualization of the HA-Tag of the Mpl occurred via PE-conjugated streptavidin SAV-PE (BioLegend).

Immunostainings**Table 7 Antibodies for pluripotency marker immunostaining**

Antibody	Antigen	Manufacturer	Catalog No.
sc-5279 mouse α -human	hOCT3/4	Santa Cruz Biotechnology Dallas (USA)	sc-5279
sc17320 mouse α -human	hSOX2	Santa Cruz Biotechnology Dallas (USA)	sc-17320
ab80892 rabbit α -mouse	mNanog	Abcam, Cambridge (UK)	ab80892
Alexa Fluor® 488 AffiniPure goat α -mouse IgG	anti-mouse IgG IgG-Alexa 488 (secondary)	Jackson ImmunoResearch Cambridgeshire (UK)	A-11001
Cy™3 AffiniPure	donkey anti-Rabbit IgG (secondary)	Jackson ImmunoResearch Cambridgeshire (UK)	AB_2338000

Table 8 Antibodies for platelet spreading assays

Antibody	Antigen	Manufacturer	Catalog No.
14A3_Alexa488	CD41/CD61	B.Nieswandt (Würzburg University)	
GTX107175 rabbit α -mouse	β 1-tubulin (primary)	GeneTex Irvine (USA)	GTX107175
56F8-Alexa487	GPVI	B.Nieswandt (Würzburg University)	
Cy™3 AffiniPure	donkey anti-Rabbit IgG (secondary)	Jackson ImmunoResearch Cambridgeshire (UK)	AB_2338000

3.1.7 Enzymes

Restriction enzymes were purchased from Thermo Scientific (Waltham, MA, USA) unless otherwise stated. The concentration of the restriction enzymes was 10U/ μ l. For restriction digest, about 1 μ g of plasmid DNA was used.

All enzymes were used according to the instruction of the manufacturer

Taq polymerase; Thermo Scientific, 5U/ μ l (Waltham, MA, USA)

Pfu polymerase; Thermo Scientific 2.5U/ μ l (Waltham, MA, USA)

T4-DNA Ligase; Thermo Scientific 5U/ μ l (Waltham, MA, USA)

Alkaline phosphatase; Thermo Scientific 1U/ μ l (Waltham, MA, USA)

RevertAid H Minus Reverse Transcriptase Thermo Scientific 200U/ μ l (Waltham, MA, USA)

3.1.8 Kits

All kits were used according to the manufacturer's instructions.

Table 9 Kits

Name	Manufacturer
Nucleo Spin Tissue	MACHEREY-NAGEL; Düren (GER)
NucleoBond Xtra Maxi	MACHEREY-NAGEL; Düren (GER)
NucleoSpin Plasmid	MACHEREY-NAGEL; Düren (GER)
Nucleo Spin Gel and PCR clean up	MACHEREY-NAGEL; Düren (GER)
Direct-Zol RNA Kit	Zymo Research Europe; Freiburg (GER)
EZ DNA Methylation Kit	Zymo Research Europe; Freiburg (GER)
pGEM®TEasyVector Kit	Promega; Mannheim (GER)
Lineage cell depletion Kit	Miltenyi Biotech; Bergisch Gladbach (GER)
STEMdiff™ Trilineage Differentiation Kit	StemCell Technologies, Vancouver (CAN)
ReLeSR™	StemCell Technologies, Vancouver (CAN)
Stemgent™ Alkaline Phosphatase Staining Kit	ReproCell, Glasgow (UK)

3.1.9 Plasmids

pBlueScript II SK (+) (Addgene)

All gammaretroviral (GV) and lentiviral (LV) vector backbones used in these studies were kindly provided by Prof. Dr. Axel Schambach (Institute of Experimental Hematology, MHH).

Plasmids to generate gammaretroviral vectors

SERS11.T11-iGFP.pre

SERS11.T11-Gata1-iGFP.pre

SERS11.T11-Nfe2-iGFP.pre

SERS11.T11-Evi1-iGFP.pre

SERS11.T11-Pbx1-iGFP.pre

SERS11.T11-RhoAhc-iGFP.pre

SERS11.T11-Cdc42hc-iGFP.pre

SERS11.T11-eGFP-PGK-M2.pre

SERS11.T11-eGFP-U630s-PGK-M2.pre
 SERS11.T11-eGFP-U630as-PGK-M2.pre
 SERS11.T11-eGFP-U670s-PGK-M2.pre
 SERS11.T11-eGFP-U670as-PGK-M2.pre
 SERS11.T11-eGFP-U1.0s-PGK-M2.pre
 SERS11.T11-eGFP-U1.0as-PGK-M2.pre
 SERS11.T11-eGFP-U1.5s-PGK-M2.pre
 SERS11.T11-eGFP-U1.5as-PGK-M2.pre
 SERS11.T11-eGFP-CBX3-PGK-M2.pre
 SERS11.T11-eGFP-EFS-M2.pre

Plasmids for the generation of lentiviral vectors:

SIN.Lv.SFFV.OKSM.dTom
 RRL.PPT.T11-eGFP-PGK-M2.pre
 RRL.PPT.T11-eGFP-U670s-PGK-M2.pre

Helper plasmids

Table 10 Helper plasmids

Plasmid	Application
pcDNA3.MLVsyng/p	Gammaretroviral vector, gag/pol
pCDNA3.GP.CCCC	Lentiviral vector, gag/pol
pMD2.G	Envelope, vsvg
pRSV_Rev	Rev

3.1.10 Oligonucleotides

Table 11 Primers

Primer	Sequence	Dye
GFP forward	GTAACGGCCACAAGTTCAGC	
GFP reverse	TGGTGCAGATGAACTTCAGGG	
probe GFP	CTTGCCGTAGGTGGC	FAM
wPre forward	GAGGAGTTGTGGCCCGTTGT	
wPre reverse	TGACAGGTGGTGGCAATGC	
probe wPre	CTGTGTTTGCTGACGCAAC	FAM
PTBP2 forward	TCTCCATTCCCTATGTTTCATGC	
PTBP2 reverse	GTTCCCGCAGAATGGTGAGGTG	
probe PTBP2	ATGTTCTCGGACCAACTTG	JOE
Methylation PCR		

Primer	Sequence	Dye
U670 fw	TAACCGGTCGTTACCCATGGGGGAGGTGGTCCCTGCA GTTACGCC	
U670 rv	TAGCGGCCGCGGCCCTCCGCGCCTACAGCTC	
qRT PCR		
TaqMan Assay Sox2	Mm00488369_s1 (Thermo Fischer Scientific; Waltham USA)	FAM
TaqMan Assay Oct4	Mm00658129_gH (Thermo Fischer Scientific; Waltham USA)	FAM
TaqMan Assay Nanog	Mm02384862_g1 (Thermo Fischer Scientific; Waltham USA)	FAM
TaqMan Assay Actin β	Mm00607939_s1 (Thermo Fischer Scientific; Waltham USA)	VIC
Plasmid generation		
U670 fw	TAACCGGTCGTTACCCATGGGGGAGGTGGTCCCTGCA GTTACGCC	
U670 rv	TAGCGGCCGCGGCCCTCCGCGCCTACAGCTC	
Mpl fw	TAACCGGTATGCCCTCTTGGGCCCTCTTCAT	
Mpl rv	TACCATGGTCAGGGCTGCTGCCAATAGCTTAG T	
EFS fw	TAGCGGCCGCTGGCTCCGGTGCCCGTCAGTG	
EFS rv	TATCTAGACATGGTACCGGTGATGATCCCCCGCGTCA CGACACCTGTGTTCTGG	

3.1.11 Bacterial strains, cells and cell lines

The bacterial E.coli strain XL1 gold was used for amplification of plasmid DNA during cloning procedures. Cell lines and primary cells are listed below .

Table 12 Cells and cell lines

Cell line	Origin and cell type	Organism	Reference
HEK 293T	Embryonic kidney carcinoma cells	<i>Homo sapiens</i>	Xie et al., 1996
MEF (C3H)	Murine embryonic fibroblasts isolated from	<i>Mus musculus</i>	Amit et al., 2003

Cell line	Origin and cell type	Organism	Reference
	C3H/HeNRj mice		
OP9	BM stromal cells (mesenchyme) (C57BL/6 x C3H)F2 -op/op	<i>Mus musculus</i>	Nakano et al., 1994
SC1	Murine fibroblasts	<i>Mus musculus</i>	Hartley and Rowe, 1975
32D	myeloid leukemia cells	<i>Mus musculus</i>	Greenberger et al., 1983
P19	Murine embryonic carcinoma cells	<i>Mus musculus</i>	McBurney et al., 1982
primary hematopoietic stem and progenitor cells (HSPC)	B6Cg-Gr(ROSA)26 Sor ^{tm1(rtTA[*]M2)^{Jae}/J}	<i>Mus musculus</i>	Hochedlinger et al., 2005

3.1.12 Culture media

Table 13 Culture media

Strain/Cell line	Medium	Manufacturer (Medium)
XL1 gold	LB-Medium, ampicillin (1:1000)	Paul-Ehrlich-Institute; Langen (GER)
HEK 293T	DMEM (10% FCS, 1% L-glutamine)	Biowest; Nuaille (FR)
SC1	DMEM (10% FCS, 1% L-glutamine)	Biowest; Nuaille (FR)
primary bone marrow cells	StemSpan SFEM (1% L-glutamine, 1% Pen/Strep, 20ng/ml hIGF-2, 20ng/ml mThpo, 10 ng/ml mFGF-1, 10ng/ml mSCF	STEMCELL technologies; Grenoble (FR)
Murine embryonic fibroblasts (MEF)	DMEM (10% FCS, 1% L-glutamine, 1% Pen/Strep, 1% NEAA, 30 mM β -mercaptoethanol)	Biowest; Nuaille (FR)
R26M2 iPSC	DMEM (15% ES cell qualified FBS, 1% L-glutamine, 1% Pen/Strep, 1% NEAA, 30 mM β -mercaptoethanol, 1000 U/ml	Gibco; Thermo Fisher Scientific; Waltham (MA USA)

Strain/Cell line	Medium	Manufacturer (Medium)
OP9	alpha Medium (20% FCS, 1% L-glutamine)	Biochrom; Berlin (GER)
Differentiation; embryoid bodies	SF-IMDM (15% FCS, 1% Pen/Strep, 1% L-glutamine; Ascorbic Acid, MTG)	Paul-Ehrlich-Institute; Langen (GER)
Differentiation; MK	α -Medium (20% FCS, 1% L-glutamine, 1% Pen/Strep, 25 ng/mL SCF, 50 ng/mL TPO, \pm dox (1 μ g/ml))	Biochrom; Berlin (GER)
32D	RPMI (10% FCS, 1% L-glutamine, 1% sodium pyruvate, 5 ng/ml IL-3)	Biowest SAS; Nuaille (FR)
P19	α MEM (10% FCS, 2mM L-glutamine 1% Pen/Strep)	Biochrom; Berlin (GER)
mTeSR TM 1		Stem Cell Technologies; Vancouver (CAN)
Medium for Transfection	Medium for HEK293T 10% HEPES 25 μ M Protaminsulfat	

3.2 Methods

3.2.1 Molecular biology tools

3.2.1.1 Plasmids for viral vector generation

Plasmids for generation of gammaretroviral vectors for transduction of murine iPSC

The plasmids for the generation of gammaretroviral vectors overexpressing the supportive candidate factors are listed in the following. Restriction digest and ligation was performed according to the instruction of the manufacturer.

SERS11.T11-iGFP.pre

SERS11.T11-Gata1-iGFP.pre

SERS11.T11-Nfe2-iGFP.pre

SERS11.T11-Evi1-iGFP.pre

SERS11.T11-Pbx1-iGFP.pre

SERS11.T11-RhoAhc-iGFP.pre

SERS11.T11-Cdc42hc-iGFP.pre

SERS11.T11-eGFP-PGK-M2.pre

For generation of the plasmids, the T11-Nfe2-iGFP and T11-Gata1-iGFP cassettes were

liberated from the pSERS.T11-Nfe2-iGFP-PGK-M2.pre plasmid using the restriction enzymes XhoI and NotI and inserted into pSERS11.T11-eGFP.pre plasmid using the same restriction enzymes. For generation of the pSERS11.T11.iGFP, the Nfe2 cDNA was digested from the plasmid using the AgeI restriction enzyme and the remaining backbone was re-ligated. The plasmids SERS11.T11-RhoAhc-iGFP.pre and SERS11.T11-Cdc42hc-iGFP.pre were generated by isolation of the respective factor (RhoAhc, Cdc42hc) with AgeI from the pRRL.PPT.mPf4-RhoAhc-i-GFP.pre and pRRL.PPT.mPf4-Cdc42hc-i-GFP.pre backbone and replacement of the Nfe2 of the pSERS.T11-Nfe2-iGFP-PGK-M2.pre which could also be removed by AgeI. Furthermore, generation of the vectors SERS11.T11-Evi1-iGFP.pre was performed by isolation of the Evi1 gene from the pSERS11.SF-Evi1-i-GFP.pre template using the restriction enzyme BamHI. After digesting the SERS11.T11-Nfe2-iGFP.pre backbone, the Evi1 was inserted and replaced the Nfe2. The plasmid SERS11.T11-Pbx1-iGFP.pre was generated using the same strategy, and also the BamHI restriction enzyme. The template for isolation of the Pbx1 was the plasmid pRRL.PPT.SFFV.Pbx1.iGFP.pre. The orientation of the respective genes was verified using by an appropriate restriction digest.

Gammaretroviral vectors SERS11.T11-iGFP-RhoAhc-iGFP.pre and SERS11.T11-iGFP-Cdc42hc-iGFP.pre were generated by F. Schenk, SERS11.T11-iGFP-Pbx1-iGFP.pre was generated by S. Lorke.

Construction of plasmids to generate retroviral Tet-all-in-one vectors containing different A2UCOE

Multiple restriction digests of the 4kb original DNA sequence (kindly provided by Prof. Dr. A. Thrasher and Dr. M. Antoniou, King's College, London) were performed to obtain the different sized A2UCOE. The resulting A2UCOE were in the sizes of 437bp, 637bp, 672bp, 1073bp and 1551 bp. The CBX2-A2UCOE contains mutations in the canonical donor splice site and potential cryptic splice acceptor site at the first exon-intron boundary and the following intron. All A2UCOE were blunt-end ligated upstream of the human PGK promoter into the gammaretroviral Tet-inducible, all-in-one vector pSERS11.T11-eGFP-PGK-M2.pre. The orientation of the A2UCOE was verified by restriction digests and sequencing. To generate the promoter-replaced variants, the gammaretroviral vector pSERS11.T11-eGFP-M2.pre was generated by liberation of the PGK.M2 from the pSERS11.T11-eGFP-PGK-M2 followed by PCR amplification of a donor M2 into the pBluescript II SK(+) (Stratagene, Amsterdam). Then, the PCR amplified M2 was digested by restriction enzymes BamHI and BspEI and subsequent ligation. Next, the A2UCOE

U670s and CBX3 were generated as described above and blunt-end ligated into the gammaretroviral vector pSERS11.T11-eGFP-M2.pre resulting in pSERS11.T11-eGFP-U670s-M2.pre and pSERS11.T11-eGFP-CBX3-M2.pre. The plasmid for the gammaretroviral vector pSERS11.T11-eGFP-EFS-M2.pre was generated by PCR amplification of the EFS promoter with the restriction sites for XbaI and NotI and inserted into the vector backbone using the respective enzymes. The lentiviral vector containing the U670s as promoter pRRL.PPT.T11-eGFP-U670s-M2 was generated by restriction enzyme digest of the T11-eGFP-U670s-M2 cassette from the corresponding gammaretroviral construct pSERS11.T11-eGFP-U670s-M2.pre using XhoI and BstZ17 and inserting into the lentiviral backbone using the same enzymes. The plasmid for the generation of the gammaretroviral vector expressing the HA-Mpl receptor was generated by PCR amplification of the U670s. Restriction sites for NcoI and AgeI were added upstream the U670s element to the forward primer. Downstream of the U670s element, a restriction site for NotI was added to the reverse primer. After PCR amplification, the U670s element was inserted into the pSERS11.T11-eGFP-PGK-M2.pre backbone by replacing the eGFP via insertion with NcoI and NotI resulting in pSERS11.T11-U670s-PGK-M2.pre.2. HA-Mpl was PCR-amplified and AgeI sites added to the appropriate primers. After restriction of the pSERS11.T11-U670s-PGK-M2.pre.2 with AgeI, amplified HA-Mpl was inserted with the corresponding restriction site resulting in pSERS11.T11-HA-Mpl-U670s-PGK-M2.pre. The resulting vectors are listed in the following.

N. Heinz and K. Blokland generated the gammaretroviral Tet-all-in-one vectors containing the different A2UCOE elements. F. Schenk generated the SERS11.T11-HA-Mpl-U670s-PGK-M2.pre vector.

Gammaretroviral vectors:

SERS11.T11-eGFP-U630s-PGK-M2.pre
SERS11.T11-eGFP-U630as-PGK-M2.pre
SERS11.T11-eGFP-U670s-PGK-M2.pre
SERS11.T11-eGFP-U670as-PGK-M2.pre
SERS11.T11-eGFP-U1.0s-PGK-M2.pre
SERS11.T11-eGFP-U1.0as-PGK-M2.pre
SERS11.T11-eGFP-U1.5s-PGK-M2.pre
SERS11.T11-eGFP-U1.5as-PGK-M2.pre
SERS11.T11-eGFP-CBX3-PGK-M2.pre
SERS11.T11-eGFP-EFS-M2.pre
SERS11.T11-HA-Mpl-U670s-PGK-M2.pre

Lentiviral vectors:

RRL.PPT.T11-eGFP-PGK-M2.pre

RRL.PPT.T11-eGFP-U670s-PGK-M2.pre

3.2.1.2 Bacteria transformation and cultivation

100µl of chemically competent *E. coli* XL 10 Gold were thawed on ice and mixed with either 1µl of plasmid DNA or 10µl of ligation sample. Transformation was performed by heat shock at 42°C for 2min followed by incubation in 1ml LB medium for 30min (37°C). Bacteria were either inoculated onto LB-agar plates (100mg/ml ampicillin) for selection or inoculated into liquid LB medium (100mg/ml ampicillin, 200rpm).

3.2.1.3 Blue-white screen

Bisulfite-converted PCR products (see Chapter 3.2.1.6) for the determination of the methylation state of the PGK promoter were inserted into pGEM[®]™ plasmid. Positive colonies were selected via blue-white -screening. Therefore, IPTG and X-Gal were additionally applied on ampicillin LB-agar plates before the transformed bacteria were plated. Due to the inactivation of the β-galactosidase in the plasmid after insertion of the PCR product, the positive colonies were identified by their white color.

3.2.1.4 Isolation of plasmid DNA from bacteria

Plasmid DNA from bacteria was isolated by the NucleoSpin[®] Plasmid Kit, NucleoBond Xtra[®] Midi/Maxi Kit (MACHERY-NAGEL) according to the manufacturer's instruction. For low amounts of plasmid DNA (1-3µg), transformed bacteria were grown in 5ml of ampicillin (100mg/l) containing LB medium at 37°C overnight. For higher amounts (>400µg), transformed bacteria were inoculated in 150-250ml LB medium (100mg/l) overnight (37°C, in a shaker 200rpm). After isolation, plasmid concentration was determined using the Nano Photometer (IMPLEN).

3.2.1.5 Real-time PCRs

All TaqMan[™] real-time PCR experiments were performed with the TaqMan[™] Fast Advanced Master Mix (Thermo Fischer Scientific, Waltham, MA, USA) according to the manufacturer's instructions. Genomic DNA was isolated using the NucleoSpin[®] Tissue kit (MACHERY-NAGEL, Düren, Germany).

Vector copy number detection

Specific primers and TaqMan probes were complementary to the PTBP2 (housekeeping gene) and the wPre element or the GFP. The average VCN was calculated by normalization to the housekeeping gene PTBP2 and the vector elements wPre or GFP and correlated to a plasmid standard as reference. The plasmid standard was kindly provided by Dr. Tobias Mätzig (Experimental Hematology, MHH). PCRs were run on the StepONEPlus Real-Time PCR System (Applied Biosystems; Thermo Scientific; Waltham; MA, USA).

Table 14: Program VCN

Step	Temperature [°C]	time [min]
1	95	05:00
2	94	00:15
3	60	00:30
4	68	01:00
Step 1-4	34 cycles	
5	68	10:00
6	4	∞

Gene expression analysis by real-time PCR

For determination of the pluripotency status of generated iPSC, the cells were depleted from the feeder cells and RNA was isolated with the Direct-Zol RNA Kit (Zymo Research). After reverse transcription of the RNA into cDNA using Random Hexamer Primers and RevertAid H Minus Reverse Transcriptase (Thermo Fischer Scientific, Waltham, MA, USA) according to the manufacturer's instructions, gene expression of Oct4, Nanog and Sox2 was determined and compared to expression in MEF and OG2 embryonic stem cells. Gene expression analysis was calculated by the delta-delta CT method and the β -actin expression was used as for normalization of the gene expression.

Table 15: PCR program gene expression analysis

Step	Temperature [°C]	time [min]
1	50	02:00
2	95	02:00
3	95	00:01
4	60	00:20
Step 3-4	40 cycles	

3.2.1.6 Promoter methylation analysis

For determination of changes in the methylation status of the PGK promoter during differentiation, genomic DNA (gDNA) from undifferentiated KOLF2 hiPSC (kindly provided from Dr. Bill Skarnes (Sanger Institute's Human Induced Pluripotent Stem Cells Initiative (Hip-Sci) project) as well as differentiated KOLF2 cells transduced with the U670s element and differentiated into the mesodermal germ layer was isolated. To test for methylated vs. non-methylated CpG residues within the promoter, a bisulfite conversion was performed. The gDNA of the transduced and differentiated/un-differentiated KOLF2 cells was isolated. The treatment of the DNA with sodium bisulfite converts non-methylated cytosine residues into uracil by a chemical reaction. Methylated cytosine residues remain unaffected. After bisulfite conversion of 600ng gDNA with the EZ DNA Methylation-Gold™ Kit (Zymo Research, Irvine CA, USA) according to the manufacturer's instructions, the PGK promoter was amplified using the appropriate primers. Design of the primers was done by Dr. Mania Ackermann (Experimental Hematology, MHH) using the MethPrimer program (<https://www.urogene.org/methprimer/>). Sequences of the primers are included in Table 11. After PCR amplification, the PGK promoter fragment was subcloned into the pGEM®™ plasmid (Promega, Mannheim, GER). Positive colonies were identified by blue-white screening, isolated and subjected to sequencing with the supreme run sequencing technology (GATC biotech (Eurofins), Ebersberg, GER) according to the manufacturer's instructions. Data were analyzed using the BiQ Analyzer software.

3.2.2 Cell culture

All cell lines, primary cells and differentiation cell cultures, were grown in the appropriate culture medium (Table 10) and incubated at 37°C and 5% CO₂ and 90% humidity. HEK293T, SC1, MEF and OP9 and R26M2 iPSC were split every 2-3 days to 80% confluency. Prior to splitting, the cells were detached with Trypsin-EDTA (0.5 g/l Trypsin,

0.2g/l EDTA dissolved in PBS). 32D cells were grown in suspension to 80% confluency and split every 2-3 days.

3.2.2.1 Production of viral particles and determination of the infectious particle titer

Infectious viral vectors were produced in human HEK 293T packaging cells by transient transduction of the respective plasmids for the split packaging by calcium-phosphate transduction. All vectors were pseudotyped with VSVg glycoprotein (Naldini et al., 1996). Concentrations of the respective plasmids and chemicals for the production of gammaretro- and lentiviral vectors are listed in Table 16. One day prior to transfection, HEK 293T cells were plated at a density of 10^6 cells per 10cm culture dish. For transfection, culture medium was aspirated and 8ml of transfection medium containing chloroquine (25 μ M) was added (Table 13).

Table 16: Concentration transfection gammaretroviral and lentiviral vectors

Gammaretroviral vector		Lentiviral vector	
Transfer vector plasmid	10 μ g	Transfer vector plasmid	10 μ g
Syngagpol plasmid	10 μ g	Gag/pol plasmid	10 μ g
Envelope plasmid	1.5 μ g	Envelope plasmid	1.5 μ g
CaCl ₂ (5M)	25 μ l	Rev plasmid	5 μ g
H ₂ O	add to 500 μ l	CaCl ₂ (5M)	25 μ l
		H ₂ O	add to 500 μ l

After mixing the plasmids with CaCl₂, the mixture was dropped to 500 μ l HEPES buffered saline (HeBS) using the “bubbling technique”. Hereby, DNA mixture was added to the HeBS buffer under constant mixing by air bubbling to improve precipitation. After 10min, incubation solution was added dropwise to the cell culture plate with transfection medium. Transfection medium was changed after 12h of incubation into DMEM containing HEPES (20mM) and 1% Penicillin/Streptomycin. The first supernatant was harvested 36h after transfection and filtrated though 22 μ m syringe filters. Supernatants were stored at 4°C until the second harvest after 48h. After pooling first and second harvest, supernatants were concentrated by centrifugation at 50.000x g for 1.5h, re-suspended in Stem Span and stored at -80°C.

The amount of infectious particles of the viral vector was determined with the help of SC1 fibroblast cells. 6×10^4 to 1×10^5 SC1 cells were seeded per well of a 12-well plate. The plates were incubated until attachment of the SC1 cells to the cell culture dish was completed. Before transfection of SC1 cells with viral supernatants, the medium was changed to culture medium containing protamine sulfate (Sigma Aldrich) ($4\mu\text{g/ml}$). Medium containing dox ($1\mu\text{g/ml}$) was used to induce gene expression when testing the Tet-all-in-one vector system. Viral supernatants were applied to the cells in different volumes to a volume of 1ml per well. After culture overnight, the medium was changed to medium without protamine sulfate. After 72 h of culture, cells were detached using PBS without Ca^{2+} containing EDTA (1 M) and gentle pipetting. The number and percentage of transduced cells was then determined by flow cytometry. Viral titers can be calculated by using the following formula:

$$\text{Titer} = \frac{\% \text{pos cells} \times \text{no. cell seeded}}{\text{vol of supernatant} [\text{ml}]} \left[\frac{\text{IP}}{\text{ml}} \right]$$

3.2.2.2 Transduction of cell lines

All cell lines were transduced in appropriate medium containing $4\mu\text{g/ml}$ of protamine sulfate (Sigma Aldrich). Prior to transduction, a defined cell number was seeded to allow the application of a defined MOI. Murine iPSC, 32D and P19 cells were transduced in suspension.

3.2.2.3 Reprogramming of murine primary HSPC into induced pluripotent stem cells

After isolation of lineage-negative (Lin⁻) cells from B6.Cg-Gt(ROSA)26Sor^{tm1(rtTA^{*}M2)Jae/J} mice cells were cultured in StemSpan-STIF medium for 24h prior transduction. Cells were grown on multi-well suspension plates and transduced with an appropriate volume of viral supernatant (SIN.Lv.OSKM.dTom) to achieve an MOI of 10 and a VCN of 1. The wells were pre-coated with RetroNectin ($3.6\mu\text{g/mm}^2$) (Takara BIO Inc.; Otsu, Japan). Viral particles were loaded to the RetroNectin by centrifugation at 2000xg for 30min at 4°C before the respective cell number was added. One week after transduction, transduced cells were transferred onto mitomycin C ($20\mu\text{g/ml}$) treated MEF feeder cells. The first iPSC colonies were isolated approximately 4 weeks after transferring the cells onto the MEF. Colonies were harvested by scratching with a 27G needle and aspirated with a pipette before transferring into Trypsin-EDTA (0.5g/l Trypsin, 0.2g/l EDTA dissolved in PBS) to generate single cells. Single cells were transferred into one well of mitomycin C treated MEF feeder cells (24-well cell culture plate) and expanded. Early passages were frozen in FCS (10% DMSO) and stored in liquid nitrogen (-180°C).

3.2.2.4 Culture of murine iPSC

Murine iPSC were cultivated on mitomycin C (20µg/ml) treated MEF feeder cells. MEF cells were seeded (40.000/well of a 6-well cell culture dish) onto gelatin-coated (0.125%) cell culture dishes and incubated for 2 days. MEF were incubated with mitomycin C for 45min before washing 3 times with PBS. MEF were plated and cultured up to 4 days before iPSC were seeded. For splitting the iPSC, they were incubated with Trypsin-EDTA (0.5g/l Trypsin, 0.2g/l EDTA dissolved in PBS). Single cells were re-suspended in KO DMEM with 10% FCS. For transduction, single cell suspension of iPSC were transferred onto gelatin-coated cell culture dishes for 40min to deplete the MEF feeder cells. After harvesting the supernatant containing iPSC and washing with 10ml PBS (300x g), cells were re-suspended, counted and seeded in the appropriate medium (see Table 13) containing protamine sulfate (4mg/ml) before addition of the viral supernatant. 2-3 days after transduction, iPSC were transferred onto mitomycin C (20µg/ml) treated feeder cells.

3.2.2.5 Culture and differentiation of human iPSC

Human KOLF2 iPSC were cultivated under feeder-free conditions on Matrigel (Corning, Amsterdam, NL)-coated cell-culture dishes in mTesR™¹ medium (Stem Cell Technologies, Vancouver, CAN) according to the instruction of the manufacturer. The cells were grown to 80% confluency and passaged in aggregates using ReLeSR™ (Stem Cell Technologies, Vancouver, CAN). Prior to transduction, cells were grown to 60% confluency. Transduction occurred once with an MOI of 5 under supplementation with protamine sulfate (4µg/ml). Differentiation was initiated 2 days after transduction. To generate embryoid bodies (EB), AggreWell plates and AggreWell EB Formation Medium (Stem Cell Technologies, Vancouver, CAN) were used according to the instructions of the manufacturer. Following 2h of incubation in the AggreWell plates to allow forming of the EB, these were then plated onto poly-HEMA (Poly(2-hydroxyethyl methacrylate), Sigma-Aldrich) coated plates in the presence of dox for three days. Fluorescence microscopy was carried out using a Nikon Eclipse Ti-S microscope (Nikon GmbH, Düsseldorf, Germany). To induce differentiation into three germ layers, the STEMdiff™ Trilineage Differentiation Kit (Stem Cell Technologies) was used according to the instructions of the manufacturer. Briefly, cells were seeded onto Matrigel (Corning)-coated plates and incubated for the indicated times in differentiation media with or without dox. Cells were then harvested and analyzed by flow cytometry.

3.2.2.6 Differentiation of murine iPSC into megakaryocytes and platelets

R26M2 iPSC were differentiated into EB. Therefore, cells were depleted from their feeder cells for 45min on 6-well gelatin-coated cell culture dishes and cultivated without feeders for 2 days on 6-well gelatin-coated cell culture dishes in differentiation medium (see Table 13). For the EB formation, 45.000 cells/ml were seeded into 6-well suspension cell culture dishes in differentiation medium (see Table 13) and subjected to orbital shaking (0.2x g) for 7 days in total. At day 5 of differentiation, the medium was supplemented with 30ng/mL murine stem cell factor (SCF), 10ng/mL murine IL-3 to support hematopoietic differentiation. At day 7 of differentiation, EB were dissociated with collagenase IV (250U/ml) and CD41⁺ early hematopoietic progenitors were enriched either by fluorescence-activated cell sorting (FACS) or magnetic activated cell sorting (MACS). For MACS, the cells were incubated with the biotinylated anti-CD41 antibody (1:100) (eBioscience; San Diego, USA) (30min, 4°C). Enrichment of the CD41-expressing hematopoietic progenitors occurred using the Anti-BiotinMicro Beads (Miltenyi Biotec, Bergisch Gladbach) according to the manufacturer's instruction. For FACS, cells were incubated with an APC-conjugated antibody against CD41 (Table 5). Further MK differentiation was performed by co-cultivation of CD41⁺ hematopoietic precursors on OP-9 feeder cells. OP-9 cells were seeded (1 x 10⁵/well) onto 6-well gelatin-coated cell culture dishes one day prior to EB dissociation and incubated overnight. To inactivate their proliferation, OP-9 were treated with mitomycin C (10µg/ml, 90min) and washed as described for MEF. After inactivation of the OP-9 and dissociation of the EB, 1 x 10⁵ CD41⁺ progenitors were seeded onto the feeder cells in MK differentiation medium (see Table 13). MK progenitor cells were harvested and analyzed earliest after 2 weeks of co-cultivation (d21 of differentiation). Cell culture supernatant was harvested into cell culture reaction tubes. Residual cells were detached from the cell culture plates using Trypsin-EDTA. OP-9 feeders were depleted by incubation on gelatin coated cell culture-dishes for 40min and residual cells were pooled to the first harvest. The cells were washed (250x g, 7min, RT) and re-suspended, counted and either re-seeded or analyzed according to their morphology or cell surface receptor expression. For further cultivation and differentiation 1 x 10⁵ total cells were seeded either on mitomycin C treated feeder cells as already described or on 6-well suspension cell culture plates. *In vitro* differentiated platelets were harvested from the supernatant of the pooled harvest of the MK. After centrifugation of the differentiated MK (250x g, 7min, RT), the supernatant was transferred into a fresh reaction tube and the platelets were pelleted at 900xg, 10min, RT and subjected to further analysis.

3.2.3 Cytospin and cytomorphological staining

For the morphological analysis of the cells and the differentiation of the cell types, cytological analysis was performed by staining of the cytoplasm and the nuclei. 10^5 cells were spun on microscope slides by centrifugation (300xg, 5min, RT) and air dried. For staining, the slides were incubated in May-Grünwald staining solution for 5min and subsequently washed with ddH₂O. Giemsa staining solution was applied for 20min, followed by another washing step, and finally air dried overnight. Slides were analyzed with the Leica DMRBE microscope (Leitz).

3.2.4 Electron Microscopy

Culture-derived platelets were harvested as described above. Cells were pelleted (900xg, 10min, RT, without break) and re-suspended in PBS, before 2.5% glutaraldehyde was added and incubated for 20min at room temperature, followed by 40min incubation at 4°C. Cells were washed twice with PBS (900xg, 10min, RT) and stored at 4°C until further processing which was performed by the Division of Immunology at the Paul-Ehrlich-Institute.

3.2.5 Flow cytometry

Characterization of the surface receptor expression of *in vitro* differentiated MK and platelets was analyzed by flow cytometry, using the BD Accuri C6 cytometer and the CytoFLEX (Beckman Coulter Krefeld, GER). Antibodies for characterization of the surface receptors for differentiated MK (CD41, CD42d) are listed in Table 6. The cells were incubated with the antibodies for 30min in the dark (4°C) in a 1:100 dilution. Differentiated MK were washed with PBS to remove unbound antibodies (300xg, 5min, RT) and re-suspended in appropriate amount of FACS buffer for analysis. For the analysis of *in vitro* generated platelets, respective amounts of antibodies were incubated with the platelets in a similar manner, but platelets were pelleted with 900xg, 5min at RT during the washing steps. For determination of the GFP expression in murine iPSC, the cells were depleted from the feeder cells as described above. The anti HA-antibody used for the detection of the Mpl transgene in 32D cells after transduction with the UCOE-Tet vectors was incubated as described above. The respective PE-conjugated secondary antibody was incubated for 10min in the dark.

3.2.6 Platelet activation

Platelet spreading and immunostainings were performed by M. Bender and M. Spindler (Würzburg University). Antibodies were kindly provided by B. Nieswand (Würzburg University)

Platelet sample preparation

For determination of the platelet activation, platelet spreading assays were performed. *In vitro* differentiated platelets were isolated as described in 3.2.2.5 and resuspended in Tyrode's buffer. As positive control washed platelets were isolated from murine whole blood. About 1ml of blood was withdrawn from one mouse by bleeding from the retro orbital plexus into reaction tubes containing 300µl of heparin (20U/ml). The mouse was subsequently euthanized. Platelet rich plasma (PRP) was obtained by centrifugation (300x g, 6min, RT, without break) and transferred together with some red blood cells into a fresh reaction tube containing 200µl of heparin (20U/ml) and spinning was repeated (300x g, 6min, RT, without break). PRP was transferred into a fresh reaction tube. To prevent activation of platelets, prostaglandin (PGI₂, final concentration 50nM) and apyrase (final concentration 0.02U/ml) were added. Platelets were pelleted at 800xg and resuspended in Tyrode's containing apyrase (final concentration 0.02U/ml) until spreading assay was performed (incubate at 37°C, at least 30min).

Spreading assay

For performance of the spreading assay, 24x60 mm cover slips were prepared in a humid chamber one day prior to the experiment. The covered area was labelled from the back. Cover slips were coated with 100µl fibrinogen (100µg/ml in sterile PBS, pH 7.14) or collagen recombinant peptide (CRP) (10µg/ml in sterile PBS, pH 7.14) and incubated overnight. The cover slips were blocked with 300µl BSA/PBS (1%, pH 7.14, 1h, RT). Before starting, the platelet spreading assays the cover slips were washed with 300µl PBS for several times to remove the remaining BSA. Reaction tubes were prepared for platelet spreading by adding 75µl of Tyrode's buffer before 30µl of washed platelets or *in vitro* differentiated platelets were added. For platelet activation, 10µl Thrombin (0.01U/ml for fibrinogen coating) and ADP (10µM) and U46 (3µM) (for CRP coating) were added. Platelet suspension was immediately transferred onto the cover slips and incubated in the humid chamber (1h, 37°C). Spreading reaction was stopped by the addition of 300µl PFA/PHEM-buffer (4%) (20min, 4°C).

Fixation and immunostaining

The microscope slides were washed 3 times with 300µl PBS and blocked with BSA (2% in PBS, 2h, 37°C or overnight, 4°C). BSA was removed by washing 3 times with 300ml PBS. Primary antibodies were incubated for 2-3h at 37°C or overnight at 4°C. Antibodies that did not bind were removed by washing of the slides 3 times with PBS. The secondary antibody was incubated for 45min at RT and the non-bound antibodies were again washed 3 times with PBS before the slides were mounted with Vectashield® Mounting Medium (Vector Laboratories, Burlingame, USA). Cover slips were dried overnight and stored at 4° until analysis.

3.2.7 Immunocytochemistry for detection of pluripotency

Murine iPSC were plated onto mitomycin C treated feeder cells into a 12-well cell culture plate as described above. For immunostainings, the medium was removed and the wells were washed twice with Dulbecco's PBS and fixed in Dulbecco's containing PFA (4%, 15min, RT). Fixation reaction was stopped by washing twice with Dulbecco's PBS. Permeabilization of the cells occurred with TritonX100 (0.2%, 15min, RT) followed by washing 3 times with Dulbecco's PBS and subsequent blocking (Dulbecco's PBS, 20% FCS, 20min, RT). Primary antibodies were incubated overnight (4°C). Antibodies that were not bound were removed by washing 3 times with Dulbecco's PBS containing 1% FCS. Secondary antibodies were diluted in Dulbecco's PBS (containing 1% FCS) and incubated for 1h (RT). Cells were washed 2 times with Dulbecco's PBS (1% FCS), covered with Dulbecco's PBS and stored until analysis (4°C, dark).

Table 17: Antibody concentrations for pluripotency markers

Antibody	Concentration
Oct3/4 (Santa Cruz)	0.8µg/µl
Sox2 (Santa Cruz)	0.3µg/µl
Nanog (Abcam)	2µg/µl
donkey anti-mouse IgG-Alexa 488 (Jackson)	1:400 dilution
rabbit anti-mouse IgG-Alexa 546 (Jackson)	1:400 dilution
goat anti-rabbit IgG-Alexa 488 (Jackson)	1:400 dilution

3.2.8 PrestoBlue® cell viability assay

The functionality of the Tet-all-in one vector Tet-U670s.Mpl was investigated in 32D cells which were transduced with the Tet.U670s.Mpl using two different MOIs (MOI 10, 20). As control, 32D cells were transduced with the U670s.GFP vector (MOI: 5, 10). 32D cells were serum starved with RPMI medium supplemented with 0.5% FCS for 16h prior starting the stimulation with Thpo. For detection of cell viability, 2×10^4 cells/well were seeded in a 96-well plate. Cells were supplemented with dox (1 μ g/ml) or left non-induced and stimulated with 5ng/ml of murine Thpo or 2ng/ml murine IL-3. After cultivation for 24h, PrestoBlue® reagent was added according to the manufacturer's instructions. OD₅₇₀ and OD₆₀₀ were detected after incubation of additional 16h (total 40h) (37°C and 5%CO₂).

4 RESULTS

4.1 Supporting factors for increased megakaryocyte differentiation and platelet release from murine iPSC

The aim of the first part of my thesis was to optimize *in vitro* production of platelets and MK from pluripotent stem cells. Since this process is still inefficient *in vitro*, overexpression of single factors influencing megakaryopoiesis and platelet release at different stages throughout the differentiation process could enhance the output of generated MK and platelets and could also lead to better functionality of the differentiated cells. We chose to overexpress Gata1, Nfe2, Pbx1, Evi1 and two hyperactive variants of the GTPases RhoAhc, and Cdc42hc (Ebbe et al., 1978; Dütting et al., 2017). The GTPases cycle between inactive (GDP-bound) and active (GTP-bound) state. In order to achieve a constitutive activation via achieving a GTP-bound state, point mutations in RhoA (F30L) and Cdc42 (F28L) were introduced (Lin et al., 1999). In our study, overexpression of single supporting factors, delivered by gammaretroviral vectors, was studied. To avoid off-target effects during pluripotency and differentiation, overexpression should be restricted to specific time points during the differentiation. This was achieved by using a Tet-inducible gammaretroviral vector system transducing the iPSC in the pluripotent state. Induction of gene expression occurred at later stages during differentiation. For this purpose, Tet-all-in-one vectors can be used. In the Tet-inducible vector used in the study, a PGK promoter initiates expression of the reverse transactivator (rt)TA-M2. This transactivator undergoes conformational changes after addition of dox, which allows its binding to the operator sequence fused to a minimal promoter (T11), thus initiating the expression of the transgene of choice. One major drawback of this system is silencing of the gammaretroviral all-in-one vectors, especially when used in iPSC and their differentiated progenies. Silencing of the PGK promoter, needed for the expression of sufficient amounts of the (rt)TA-M2 and thereby for tight regulation of the system, is one possible explanation. The PGK is highly enriched in CpG sites which are the sites prone to be methylated. In the first part of the project, we were following the strategy to become independent from the PGK promoter by generation of miPSC containing the (rt)TA-M2 in the Rosa26 safe harbor locus. Therefore, miPSC were reprogrammed from B6.Cg-Gt(ROSA)26Sor^{tm1(rtTA^{*}M2)Jae/J} mice which are genetically engineered to carry and express the (rt)TA-M2 in the Rosa26 safe harbor locus. After successful generation and characterization of the miPSC, they were transduced with the Gata1, Nfe2, Pbx1, Evi1, RhoAhc, and Cdc42hc factors in the pluripotent states using gammaretroviral vectors (details of the gammaretroviral vectors see below). Afterwards, supporting effects during MK differentiation of the murine iPSC cells of each single candidate

factor was evaluated by cell surface receptor expression, morphology and quantification of the differentiated MK.

4.1.1 Generation of R26M2 iPSC by lentiviral reprogramming and screening for hematopoietic differentiating clones

For reprogramming, as depicted in Figure 7A, lineage marker-negative cells from BM of B6.Cg-Gt(ROSA)26Sor^{tm1(rtTA^{*}M2)Jae/J} mice were isolated and transduced on retronectin-coated cell culture plates with a lentiviral vector expressing the Yamanaka factors *OCT4*, *KLF4*, *SOX2*, and *MYC* (SIN.Lv.SFFV.OKSM.dTom). After transduction, the cells were transferred onto mitomycin C-treated MEF feeder cells. Formation of typical miPSC colonies with morphological feature of embryonic stem cells (ESC) occurred 3-4 weeks after transduction, a first sign of reprogramming into the pluripotent state. The colonies were isolated and expanded. Out of the 56 isolated colonies, 31 were screened for hematopoietic differentiation potential. For this purpose, the iPSC cells were seeded as single cells into suspension cultures and subjected to orbital rotation, leading to the formation of 3-dimensional aggregates named EB. EB cultures were kept for 7 days in total. Hematopoietic differentiation was further supported by the addition of mSCF and mIL-3 at day 5 of differentiation. On day 7 of differentiation, when the EB were dissociated, the cells should express CD41 on the surface, in this case a marker for early hematopoietic progenitors which can be detected by flow cytometry (Mitjavila-Garcia et al., 2002). Only 6 of the 31 clones showed CD41 expression after 7 days of EB formation. Two of the 6 clones were further analyzed. Around 40% of the cells differentiated from R26rtTAM2_K2 (R26M2K2) and clone R26rtTAM2_K3 (R26M2K3) expressed the CD41 hematopoietic marker (Figure 7C). Since this expression was in the range of OG2 murine ESC, clones R26M2K2 and R26M2K3 were further characterized for pluripotency and utilized for the differentiation studies of miPSC.

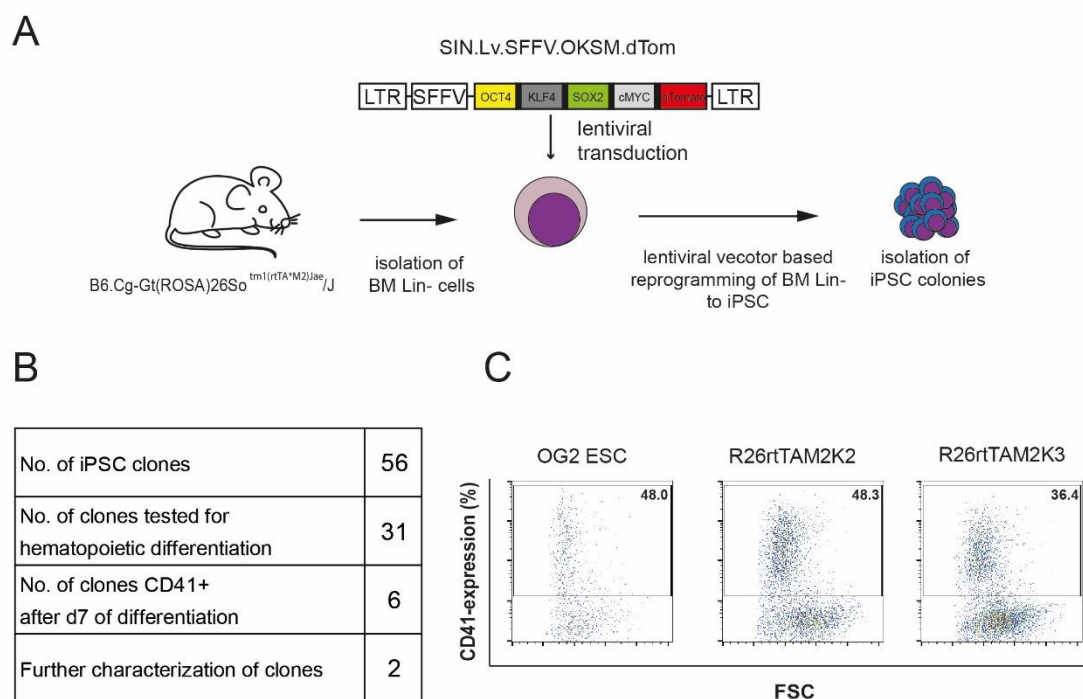


Figure 7 Generation of R26M2 iPSC. (A) Schematic overview over the generation of iPSC from of B6Cg-Gr(ROSA)36Sor^{tm1(rtTA⁺M2)Jae/J} mice. Lin- BM cells were isolated and transduced with the lentiviral vector expressing the reprogramming cassette (*OCT4*, *KLF4*, *SOX2* and *MYC*). After cultivation of the transduced cells and transfer onto MEF feeder cells, iPSC colonies were isolated 4-5 weeks after transduction. (B) Table of isolated iPSC colonies and their differentiation potential. After isolation, the clones were screened for their potential to express CD41 after hematopoietic differentiation. Two of the clones were selected for further experiments (protocol see Chapter 3.2.2.3). (C) Representative flow cytometry plots of CD41 expression at day 7 of EB differentiation and subsequent dissociation. CD41⁺ gate was set based on an unstained negative control. The percentage of CD41 expression is indicated by the numbers in the plots, respectively.

4.1.2 Characterization of pluripotency marker expression of R26M2K2 and R26M2K3 iPSC clones

Characterization of pluripotency of miPSC clones R26M2K2 and R26M2K3 was performed on the basis of the classical pluripotency features as follows: Undifferentiated murine pluripotent stem cells including iPSC express the surface marker stage specific embryonic antigen-1 (SSEA-1) (Buecker et al., 2010). As shown in Figure 8A, flow cytometry experiments of feeder-depleted R26M2K2 and R26M2K3 showed similar SSEA-1 expression as the undifferentiated murine embryonic stem cell line OG2 and murine CD45.1 iPSC generated by A. Mucci and colleagues (Mucci et al., 2018). Alkaline phosphatase (AP) is an enzyme that is highly active in the inner cell mass of preimplantation embryos in mice. It is therefore often used as a marker for assessment of the pluripotency in newly generated iPSC (Štefková et al., 2015). Active AP in cells will lead to the development of a red/purple end product (Nitroblue Tetrazolium (NBT)) when incubated with BICP (5-Bromo-4-Chloro-3-

Indolyl Phosphate) (Stemgent™ Alkaline Phosphatase Staining Kit, ReproCell, UK). R26M2K2 and R26M2K3 both show the typical color for highly active AP showing the pluripotent state, whereas the mouse embryonic fibroblast feeders remain colorless (Figure 8B). In addition, key transcription factors associated with pluripotency are sex determining region Y-box 2 (Sox2), octamer-binding transcription factor 4 (Oct4) and Nanog. In our pluripotency analysis, we determined the mRNA levels of Sox2, Oct4 and Nanog in the R26M2K2 and R26M2K3 iPSC clones by qRT-PCR and compared them to the expression in OG2 ESC control cells. mRNA expression of R26M2K2 and R26M2K3 was in a similar range and even slightly higher compared to the OG2 ESC control (Figure 8C). To verify these data, also on the protein level, immunofluorescent staining of SOX2, NANOG and OCT4 was performed on single colonies of R26M2K2 and R26M2K3. The results are shown in Figure 8D. SOX2, NANOG and OCT4 proteins were detected in the nuclei of single colonies of R26M2K2 and R26M2K3 as detected by the overlay with DAPI staining.

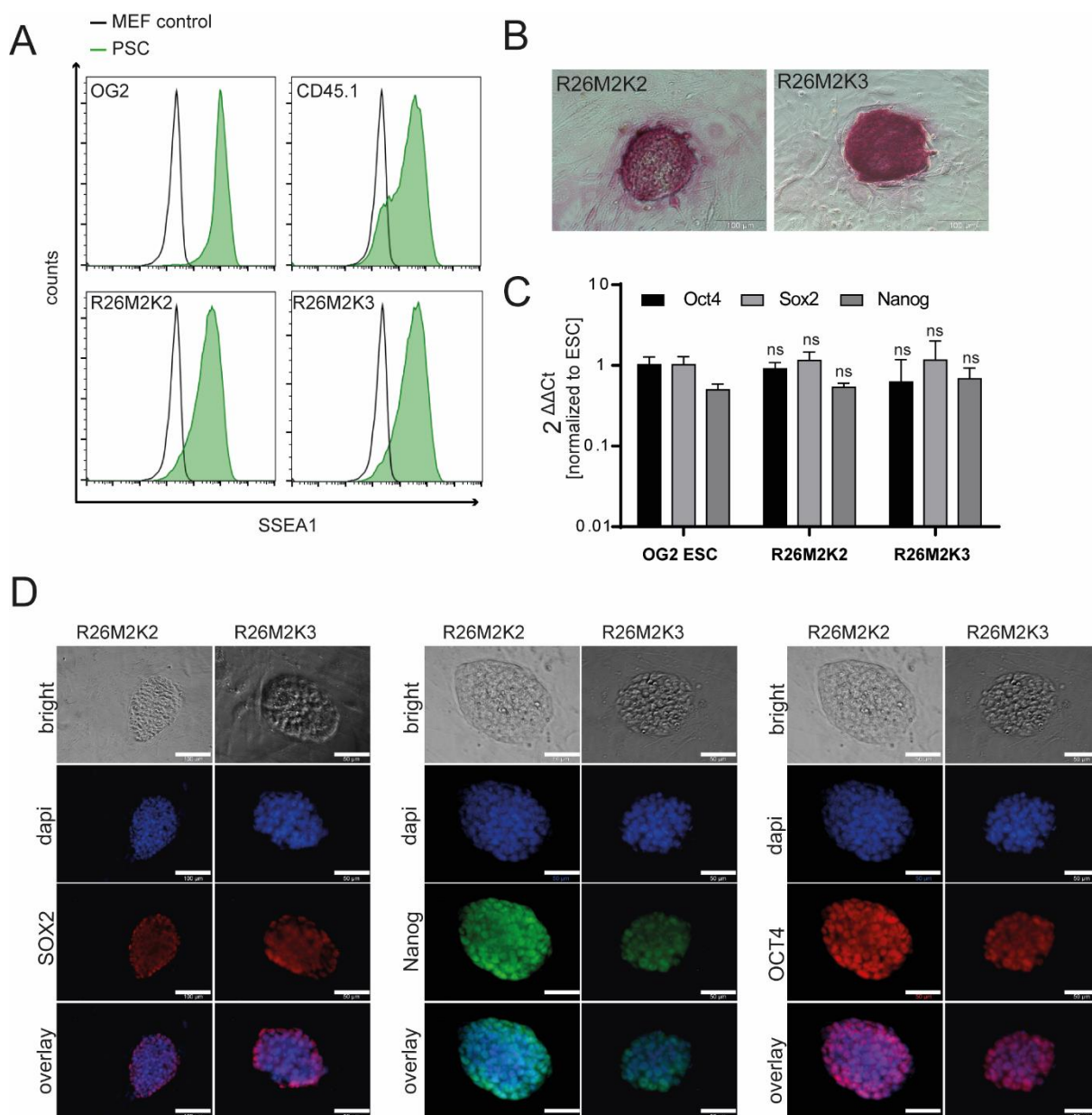


Figure 8 Characterization of pluripotency of R26M2K2 and R26M2K3. (A) Representative flow cytometry plot of the expression of SSEA1 (green histogram) of R26M2K2 and R26M2K3 in comparison to the OG2 ESC and well characterized CD45.1 murine iPSC control in the pluripotent state. As a control, MEF feeder cells were stained with the SSEA1 marker (black line). SSEA-1 expression is detected by a PE labelled anti SSEA-1 antibody. (B) Alkaline phosphatase staining of the R26M2K2 and R26M2K3 iPSC pluripotent stem cells, the scale bar indicates 100 μ m. (C) Expression of murine pluripotency markers Oct4, Nanog, Sox2 by qRT PCR (n=3, (performed in triplicates, each)), mean \pm SD, 1-way ANOVA, ns: not significant). (D) Immunofluorescence staining of R26M2K2 and R26M2K3 pluripotency markers SOX2, NANOG and OCT4.

Additionally, the integration of the reprogramming vectors was detected by vector copy number (VCN) using qPCR. The results showed that R26M2K2 had a VCN of 1 and R26M2K3 of 3. Ideally, the reprogramming cassette consisting of the transcription factors OCT4, KLF4, SOX2 and cMyc can be excised from the integration by FRT sites flanking the cassette. For the reason that the reprogramming vectors get silenced by epigenetic remodeling during transition to pluripotency (Ho et al., 2011), it is not absolutely necessary to excise the cassette, although in some cases silencing may be incomplete. The vector copy

number (VCN) detection revealed 1 integration of the reprogramming vector in R26M2K2, whereas in the R26M2K3, 3 integrations were detected. Further experiments were performed with the R26M2K2 because of the lower VCN.

4.1.3 Tet-inducible gammaretroviral vectors overexpressing supporting factors for megakaryocyte and platelet differentiation *in vitro*

To express the candidate factors to support megakaryopoiesis, the residual components necessary for the expression of the transgene of choice were delivered by retroviral vectors (Figure 9B). Therefore, gammaretroviral vectors were generated, containing the dox-inducible minimal promoter T11 which was fused to the operator sequence TetO7 followed by the coding sequence of Gata1, Nfe2, Pbx1, Evi1, RhoAhc and Cdc42hc, respectively, as functional transgenes to improve MK and platelet generation from the R26M2K2 iPSC *in vitro*. To track transgene expression during pluripotent state and differentiation, the transgenes were coupled to an eGFP (GFP) reporter via an internal ribosomal entry site (IRES). As a control, a vector encoding only for GFP was generated. The respective vectors are named as indicated in Table 18.

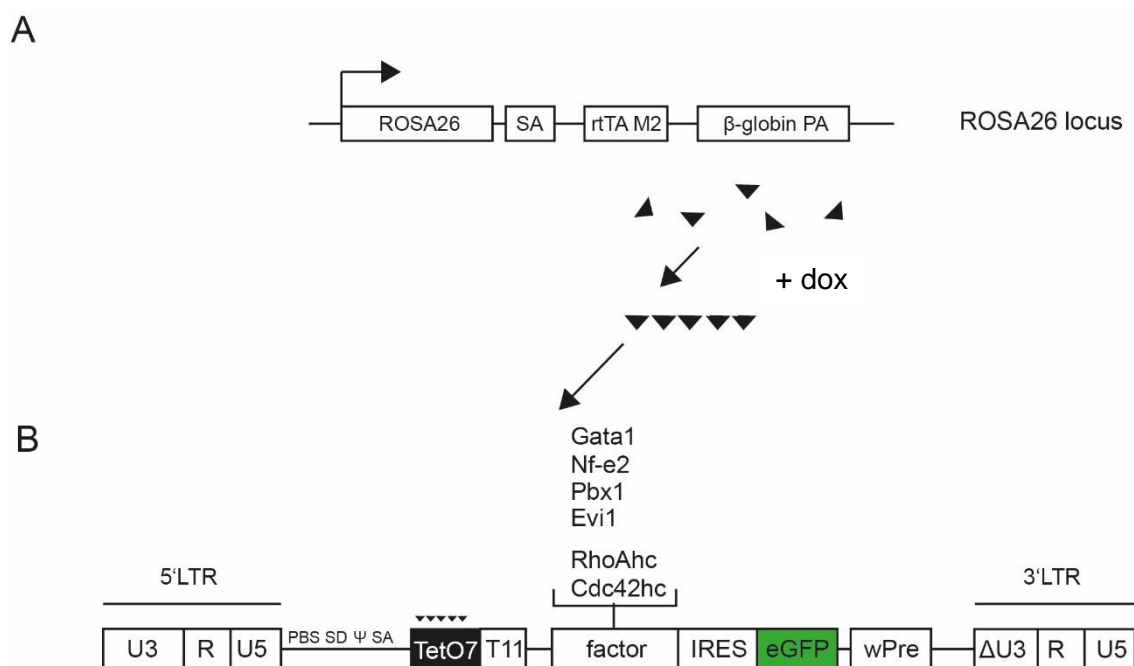


Figure 9 Rosa26 locus expressing (rt)TA-M2 and the design of the SIN gammaretroviral vector expressing the supporting factors to support megakaryopoiesis and platelet generation. (A) Schematic representation of the Rosa26 locus of the B6Cg-Gr(ROSA)36Sor^{tm1(rtTA^{M2})Jae/J} mouse and descendent iPSC. The (rt)TA-M2 gene was targeted into the Rosa26 locus and is ubiquitously expressed from the ROSA promoter. Conformational changes after exposure of the (rt)TA-M2 (depicted as triangles) to dox allow the interaction with the operator sequence fused to the minimal promoter of the gammaretroviral vectors. (B) Shown is the plasmid. The SIN deletion (Δ U3) is introduced in the 3'LTR. The LTR can be further dissected into the unique region 3 (U3), repeat region (R) and U5 region. The R region contains the polyA signal for the mRNA. The U3 region originally contains the enhancer and promoter activity which is deleted in the 3'LTR. The gene expression is initiated by an internal Tet-responsive minimal promoter (T11) which is fused to a TetO7 operator sequence. Each of the respective transgenes was incorporated downstream of the T11 separately and coupled to GFP by an internal ribosomal entry site (IRES) to visualize transgene expression in the transduced cells.

Table 18 List of gammaretroviral vectors used for transduction of miPSC R26M2K2

Transgene	Name of the vector
Gata1	Gata1.iGFP
Nfe2	Nfe2.iGFP
Evi1	Evi1.iGFP
Pbx1	Pbx1.iGFP
RhoAhc	RhoAhc.iGFP
Cdc42hc	Cdc42hc.iGFP
GFP control	iGFP.control

After production of retroviral particles of the respective vectors, supernatants were harvested and concentrated by highspeed centrifugation. The transducing units of the viral vectors were titered by transduction of a murine SC1 fibroblasts cell line. Transducing units were determined as described in Chapter 3.2.2.1. All vectors reached titers similar to that of the

GFP control vector (3×10^8 IP/ml) except for the Evi1.iGFP vector which only produced 5×10^4 IP/ml using the same conditions as for the other vector productions (Figure 10).

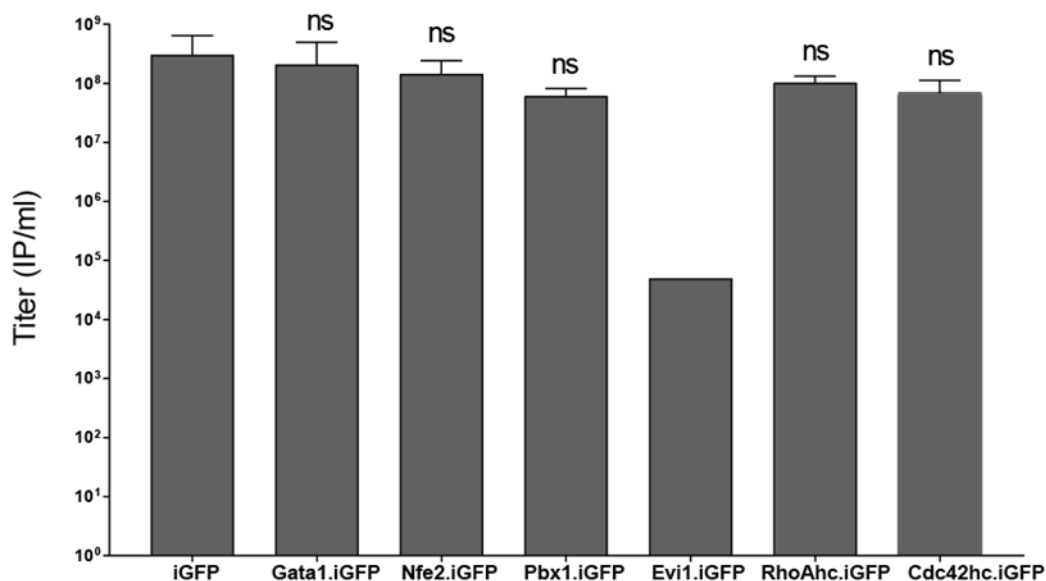


Figure 10 Titration of the Tet-inducible gammaretroviral vectors expressing the MK supporting genes. After production, the amount of infectious particles was evaluated by transducing the murine fibroblast cell line SC1. After transducing the cells with different volumes of the respective supernatants, GFP expression was determined by flow cytometry 4 days after transduction. IP/ml was determined as shown in Chapter 3.2.2.1 (n=3-6, Evi1:n=2, mean +/- SD1, way ANOVA with Dunnett's multiple comparison, ns= not significant).

4.1.4 Transduction of R26M2K2 iPSC with vectors supporting megakaryocyte differentiation

Pluripotent R26M2K2 iPSC were transduced with the viral vectors in the pluripotent state of the cells. For this purpose, they were depleted from their feeders and seeded onto gelatin-coated cell culture plates. After transduction of 10^5 cells with an MOI of 10 each in suspension and re-plating on the MEF feeder cells, iPSC were split in 2 fractions respectively. One fraction was induced with dox to evaluate transduction efficiency, whereas the other fraction remained non-induced for differentiation experiments. After 3-4 days, GFP expression was evaluated by flow cytometry. As shown in Figure 11, iPSC were transduced with levels of GFP expression between 49% (Pbx1.iGFP) and 71% (Gata1.iGFP). Transduction with Evi1.iGFP vectors resulted in very low transduction efficiency and was, therefore, not followed up in further differentiation experiments.

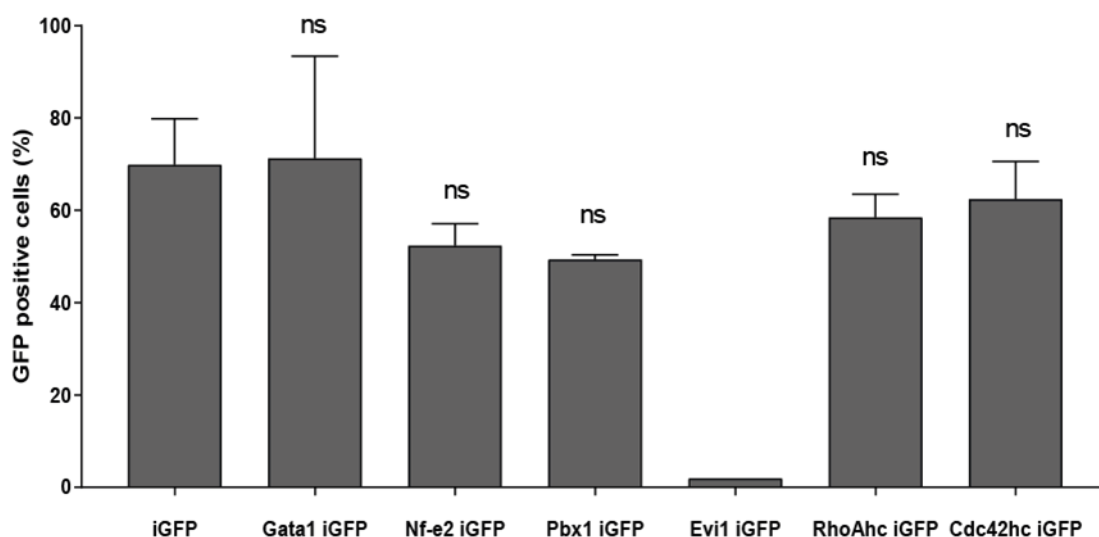


Figure 11 Transduction of R26 rtTAM2 iPSC with candidate vectors and induction of transgene expression in the pluripotent state. The iPSC were feeder-depleted and seeded onto gelatin-coated 6-well cell culture dishes. Cells were transduced in suspension with a MOI between 10 and 20. 3-4 days after transduction, iPSC were transferred onto fresh feeder cells to recover from the transduction. Expression of GFP was evaluated by flow cytometry 7 days after transduction (n=3, Evi1:n=1, mean +/- SD, 1-way ANOVA with Dunnett's multiple comparison, ns=not significant).

4.1.5 Differentiation of R26M2K2 into megakaryocyte progenitors and platelets

The transduced but non-induced iPSC were differentiated as shown in Figure 12. The experimental procedure was divided into 3 steps: in the pre-differentiation culture, the cells were depleted from their feeder cells for 2 to 3 days on a gelatin-coated matrix; next, the cells were processed into a single cell suspension culture and EB generation was initiated by rotation on an orbital shaker. Five days after the differentiation was initiated, hematopoietic differentiation was induced by supplementation with mSCF and mIL-3. Seven days after the start of the EB formation, they were dissociated with collagenase IV and the cells which express the early hematopoietic marker CD41 in the experimental procedures were enriched either by FACS or magnetic activated cell sorting (MACS). CD41+ cells were then co-cultivated on mitomycin C treated OP-9 feeder cells to further support MK differentiation. For this purpose, the culture medium was also supplemented with 25ng/ml mScf and 50ng/ml mThpo. MK, progenitors as well as platelets were analyzed first between d21 and d28 of differentiation. In case the differentiation produced a sufficient amount of cells, they were re-plated onto gelatin-coated cell culture dishes for further differentiation and analysis.

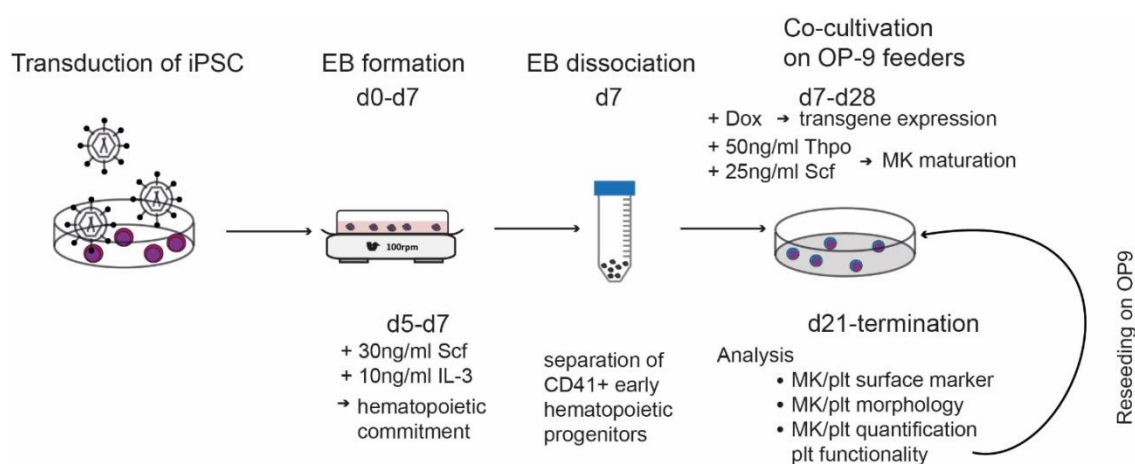


Figure 12 Differentiation scheme and workflow for transduction of R26M2K2 iPSC and differentiation into MK and platelets. After transduction of the R26M2 iPSC with the different candidate gene vectors, transduced cells were differentiated into EB by rotation on an orbital shaker for 7 days. Hematopoietic differentiation was supported by addition of mScf and mIL-3 for 2 days starting at day 5. After EB dissociation at day 7, R26M2K2 iPSC were seeded onto mitomycin C treated OP9 feeder cells. Gene expression was induced by the addition of dox. Supplementation with Thpo further supported MK differentiation. After 2-3 weeks (d21-d28 of differentiation) first MK could be detected by microscopy in the supernatant or attaching to the feeder cells which were analyzed according to their surface receptor expression pattern and morphology. Since also enlarged cells with long cellular protrusions were detected in the cultures at that time points, platelets were harvested by different centrifugation speeds (see Chapter 3.2.2.6) and analyzed also according to their surface receptor expression pattern and morphology. MK and platelets were quantified. For some experiments, MK were seeded again on mitomycin C treated OP9 cells or gelatin-coated cell culture plates for further differentiation and analysis.

4.1.5.1 Characterization of MK differentiation of R26M2K2 iPSC

Between d21 and d28 of differentiation, MK were detected by microscopy as suspension cells of increased sizes as well as adherent cells growing in clusters on the feeder layer. The differentiated MK were harvested by collecting the culture supernatant as well as by detaching them from the culture plate.

To verify the expression and induction of each transgene, GFP expression was analyzed in the differentiated MK. A representative example of the GFP expression in MK at d21 of differentiation is shown in Figure 13.

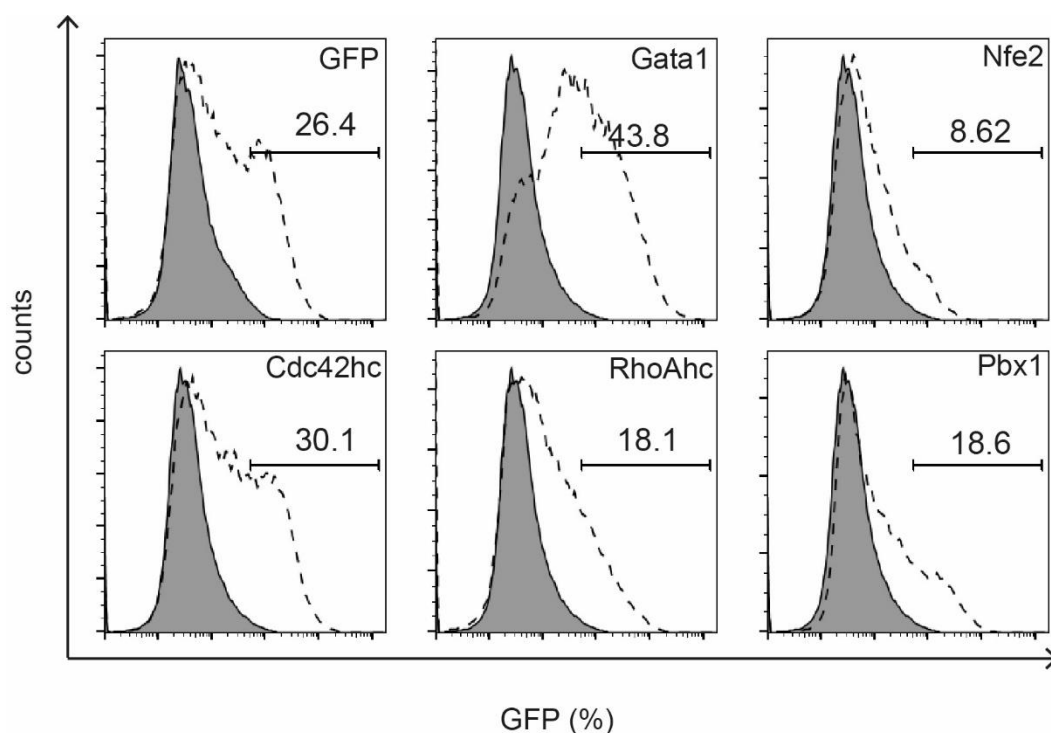


Figure 13 Detection of GFP reporter gene expression of the candidate factors at day 21 of differentiation in the MK. Representative histogram blot of GFP expression of transduced iPSC differentiated into MK analyzed by flow cytometry. Gates for GFP expression were set according to the untransduced negative control. The number in the gate indicates the respective percentage of GFP⁺ cells.

The GFP reporter signal was detectable after differentiation; however, expression was highest (43.8%) in MK derived from Gata1.iGFP-transduced cells followed by Cdc42hc.iGFP transduced cells (30.1%). GFP expression from Nfe2.iGFP, RhoAhc.iGFP and Pbx1.iGFP transduced cells was less distinct and the percentages of GFP⁺ cells reached only 18.1% of GFP expression (Pbx1.iGFP). Nfe2.iGFP-transduced and differentiated MK reached only 8.6% GFP expression after differentiation. Also, the spread of the GFP signal in all the samples was high as indicated by the high peak width. MK differentiated from R26M2K2 iPSC transduced with iGFP.control, Gata1.iGFP, and Cdc42hc.iGFP showed a clear shift in GFP expression. This could not be achieved when differentiating R26M2K2 iPSC transduced with Nfe2.iGFP, RhoAhc.iGFP, and Pbx1.iGFP transduced cells.

To evaluate whether the differentiated cells were MK or their respective progenitors or whether cells of other lineages were also generated during the differentiation process, a May-Grünwald-Giemsa staining on cytopspins was applied. After collecting the differentiated cells and depleting them from their feeders, cells were spun onto glass microscope slides and subsequently stained (see Chapter 3.2.3). In this analysis, different cell types could be distinguished according to their color, size and morphological features. Representative images of differentiated MK after 3 weeks of differentiation are depicted in Figure 14.

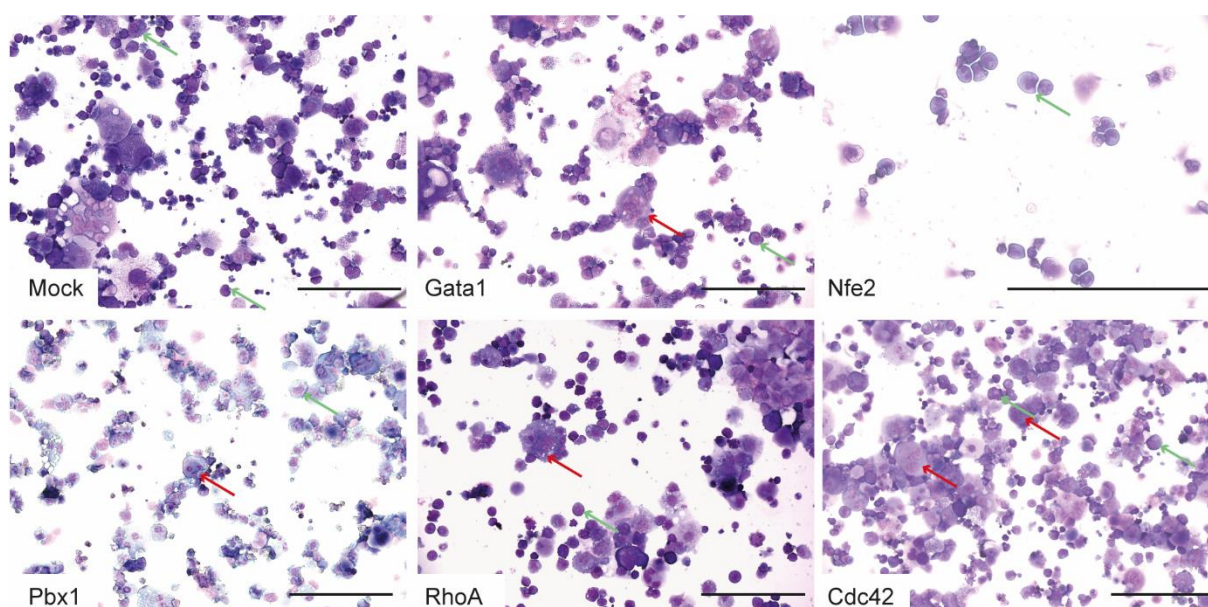


Figure 14 Differentiation of transduced R26M2K2 iPSC produced progenitors from the MK/erythrocyte lineage. May-Grünwald-Giemsa staining was performed to determine the morphology of cells at day 21-28 of differentiation. Nuclei appear in pink color. Staining of the cytoplasm in dark purple color is characteristic for cells from the MK/erythrocyte lineage. Scale bars indicate a size of 250 μ m, red arrows indicate mature MK, green arrows indicate blast cells.

The majority of the differentiated cells were of the MK/erythrocyte lineage according to their dark stained cytoplasm and to the appearance of a multilobulated nucleus. No other lineages like granulocyte/macrophage or granulocytes were detected. In the example of Gata1.iGFP overexpressing MK, enlarged cells with multilobulated nuclei as well as smaller megakaryoblast-like progenitors could be detected.

During the course of differentiation, MK undergo cytoplasmic reorganization accompanied by the formation of cellular protrusions and the development of a widely branched network of those cellular elongations. Cellular organelles are transported along the microtubule network of the protrusions to the tips. Hereby, the subcellular components of a platelet are provided at the tips and the platelets are ready to be released. MK differentiated from Gata1.iGFP transduced and induced R26M2K2 iPSC cellular elongations were detected. In Figure 15, two examples for cellular elongations from MK on day 21 of differentiation are depicted. Taking a closer look on the elongations the typical shapes with branching shafts, intermediate swellings and swellings at the tips of the protrusions were detected by microscopy (grey arrows). This indicated the generation of mature MK from iPSC overexpressing Gata1.iGFP.

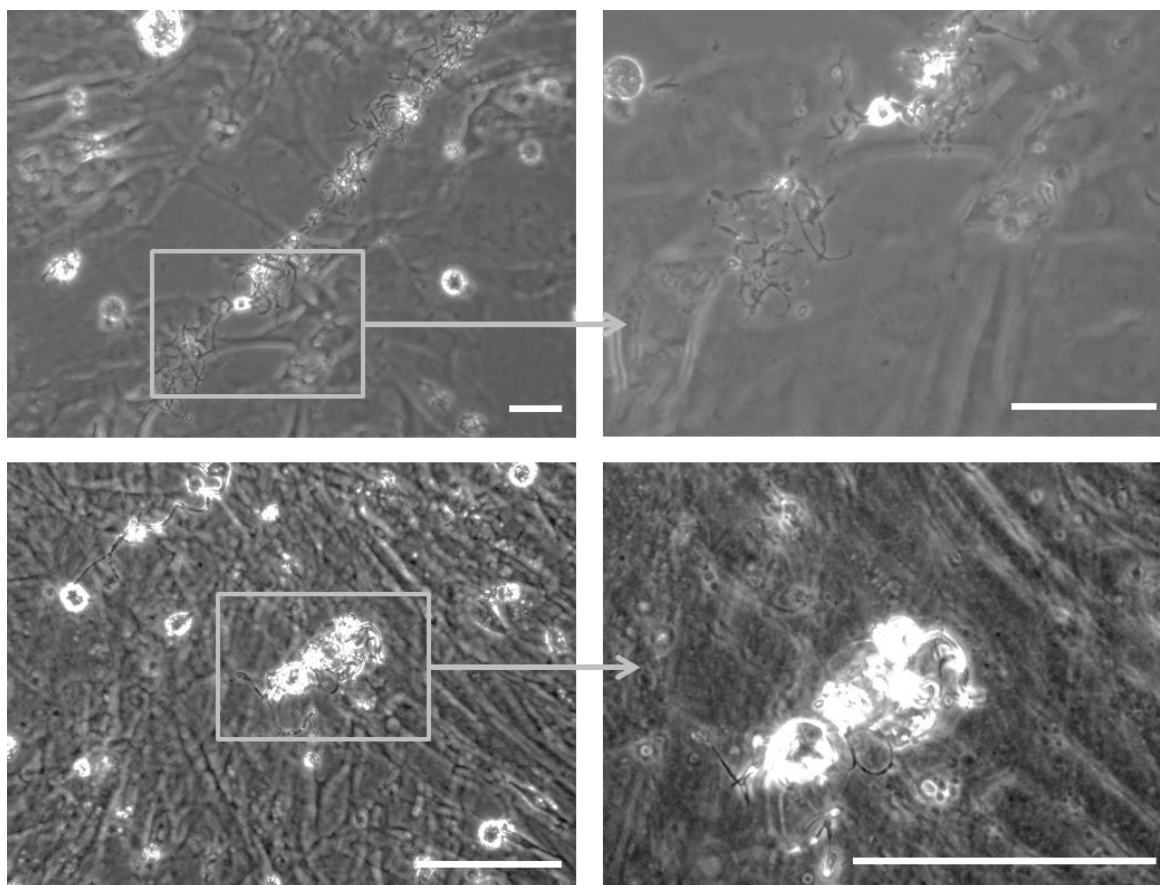


Figure 15 Gata1.iGFP overexpressing MK extending cellular protrusions. Representative images of MK from Gata1.iGFP-overexpressing cultures, at day 21 of differentiation are shown. The right panel shows the highlighted area of the left panel in higher magnification. Scale bars indicate 250 μ m.

4.1.5.2 Comparison of different candidate factors for their supportive effect to differentiate MK

To evaluate the effect of the overexpressed factors on MK differentiation from R26M2K2 iPSC, GFP⁺ versus GFP⁻ populations were analyzed and compared for each of the tested factors. CD41, the most abundant integrin on the surface of MK and platelets, was used as MK marker. Differences in MK differentiation, due to the overexpression of the different factors, was analyzed and compared according to the CD41 expression. For this purpose, CD41 expression was analyzed for the GFP⁺ and GFP⁻ populations separately. Figure 16 shows an example for the iGFP.control and Gata1.iGFP (GFP) transduced cells as histogram blots to demonstrate the gating strategy. In a first step, GFP⁺ (green line) and GFP⁻ (black line) populations were defined based on the untransduced negative control (Mock) (Figure 16A). The cut-off in CD41 expression in the GFP⁺ and GFP⁻ population was set based on FMO (fluorescence minus one) samples. FMO controls contain all of the fluorochromes (or GFP) except one. Overexpression of Gata1 in MK progenitors differentiated from R26M2K2 iPSC resulted in a shift towards higher CD41 expression on the surface of the cells and in a higher percentage of CD41-expressing cells (Gata1.iGFP, 82.2%) compared to MK progenitors differentiated from iGFP.control-transduced cells

(iGFP.control, 7.0%) in the GFP⁺ population, indicating an up to 75-fold increase by the overexpression of Gata1 (Figure 16B). This shift towards higher mean fluorescent intensities (MFI) and increased percentages in CD41 expression on the surface of differentiated progenitors was also detected within the GFP⁻ population, but not as pronounced as within the GFP⁺ population. Gata1.iGFP overexpression resulted in an about 20-fold increase in CD41 expression on the surface of GFP⁻ differentiated MK progenitors (Figure 16C).

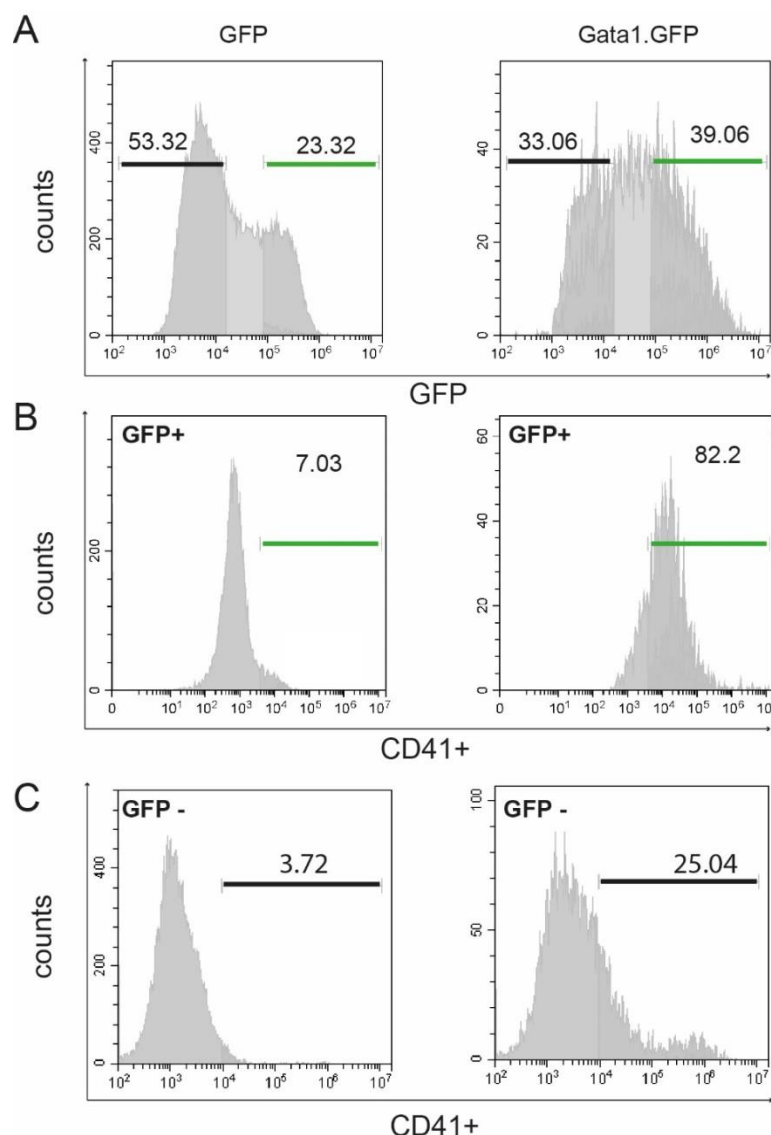


Figure 16 Expression of CD41 on the surface of MK differentiated from iGFP.control and Gata1.iGFP overexpressing cells in the GFP⁺ versus GFP⁻ populations. Representative histogram blot: Cells were differentiated as depicted in Figure 11. After seeding on OP9 feeder cells, differentiated MK were harvested at day 21 of differentiation. (A) GFP⁻ (black gate) and GFP⁺ populations (green gate) were determined according to the untransduced control (Mock). (B) GFP⁺ CD41⁺ population is shown. Gates were set according to the appropriate fluorescence-minus-one (FMO) control. (C) GFP⁻CD41⁺ population. Gates were set according to the appropriate FMO control and the numbers in the gates represent the percentages of positive cells.

The CD41 expression on the surface of MK differentiated from R26M2K2 iPSC is summarized in Figure 17. CD41 expression for each of the factors tested was compared between the GFP⁺ and GFP⁻ populations. In general, CD41 expression within the GFP⁺ population was increased compared to the GFP⁻ population for all factors tested. The

overexpression of Gata1 resulted in significantly elevated percentages of CD41 expressing MK (69%) compared to the iGFP.control (9.7%, **** $p < 0.0001$). Furthermore, the percentage of CD41⁺ cells was also enhanced to almost 39% by overexpression of Pbx1. Also, Nfe2 as well as RhoAhc and Cdc42hc overexpression increased the percentage of CD41⁺ cells after 3 weeks of differentiation, however not to a significant level.

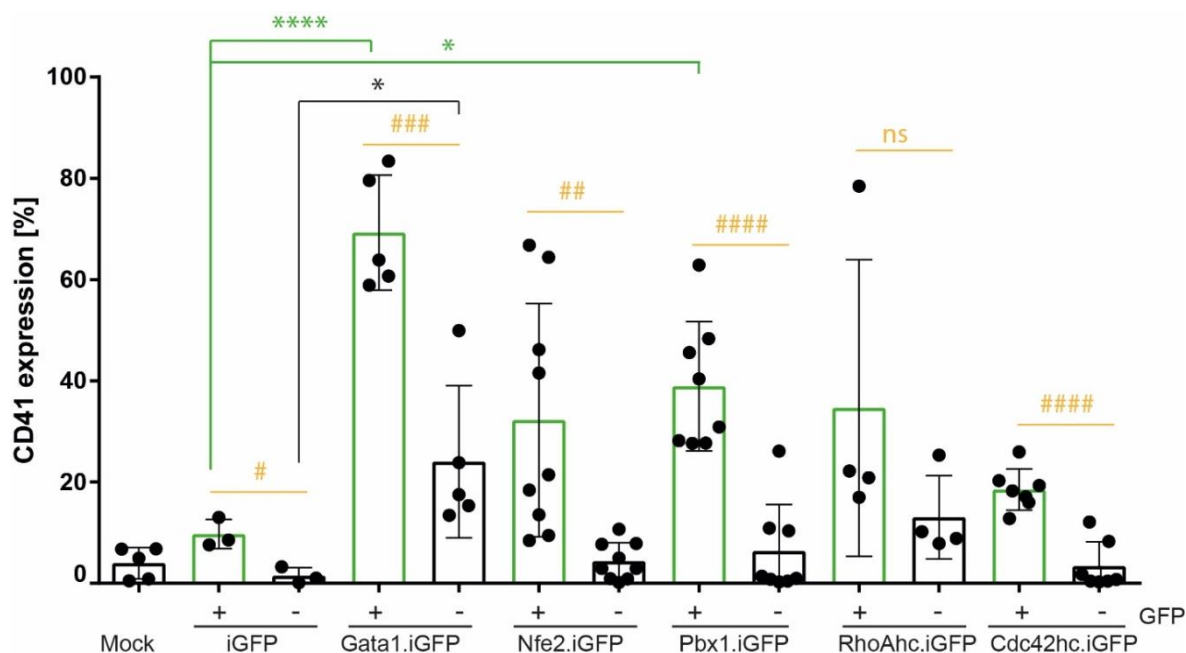


Figure 17 Summary of CD41 expression on differentiated MK at day 21 of differentiation. The integrin α IIb (CD41) on the surface MK differentiated from R26M2 iPSC transduced with the different candidates to support megakaryopoiesis was measured by flow cytometry. CD41 served as MK marker. To evaluate differences in CD41 expression between transduced and untransduced MK populations, expression was evaluated for GFP⁺ and GFP⁻ populations separately (n=3-9, mean \pm SD, **** $p < 0.0001$, * $p = 0.05$, 1-way ANOVA with Dunnett's multiple comparison of different factors (green) and student's t-test for comparison of GFP⁺ vs. GFP⁻ population (orange) # $p = 0.124$, ### $p = 0.0007$, ## $p = 0.0025$, #### $p < 0.0001$).

The second receptor detected on the surface of MK progenitors differentiated from R26M2K2 iPSC was the MK-specific marker CD42d (GPV). In *in vitro* differentiation of human CD34⁺ cord blood cells into MK, this marker only appears at later stages of differentiation and is associated with higher ploidy (Lepage et al., 2000). In our study, CD42d was therefore utilized to detect MK at later maturation stages. CD42d expression within the CD41⁺ population of the MK differentiated from the transduced R26M2K2 iPSC was analyzed. Representative histogram blots of flow cytometry experiments of differentiated MK from R26M2K2 iPSC transduced with iGFP.control and Gata1.iGFP at day 21 of differentiation are shown in Figure 18. After dividing the GFP⁺ (green line) and GFP⁻ (black line), equally to what is shown in Figure 16A (Figure 18A), and gating on CD41⁺, the CD42d expression within the CD41⁺ population was evaluated. The cut-off for CD42d positive cells was set according to the respective FMO control. In Figure 18B, the CD42d expression of the GFP⁺CD41⁺ (GFP⁺CD41⁺CD42d⁺ MK) of iGFP.control and Gata1.iGFP transduced and differentiated MK is plotted. The cell counts for GFP⁺CD41⁺CD42d⁺ were in general very low,

but according to the control, GFP⁺CD41⁺CD42d⁺ population of the differentiated MK from iGFP.control and Gata1.iGFP transduced cells were detected. The percentage of GFP⁺CD41⁺CD42d⁺ (green line) cells was about 2-fold higher in MK differentiated from Gata1.iGFP transduced R26M2K2 iPSC (42.63% GFP⁺CD41⁺CD42d⁺) compared to the iGFP.control transduced and differentiated MK on day 21 of differentiation (Figure 18B). In contrast, the GFP⁺CD41⁺CD42d⁺ population (black line) in iGFP.control transduced differentiated MK (Figure 18B) only reached 13.6%, which was about the half of the GFP-expressing counterparts, whereas the transduction with the Gata1.iGFP vector showed lower levels of CD41⁺CD42d⁺ within the GFP⁻ population (Figure 18B). Overall, this indicated a beneficial effect of Gata1 on the differentiation of CD41⁺MK progenitors, whereas the terminal maturation and expression of CD42d seemed to be inhibited.

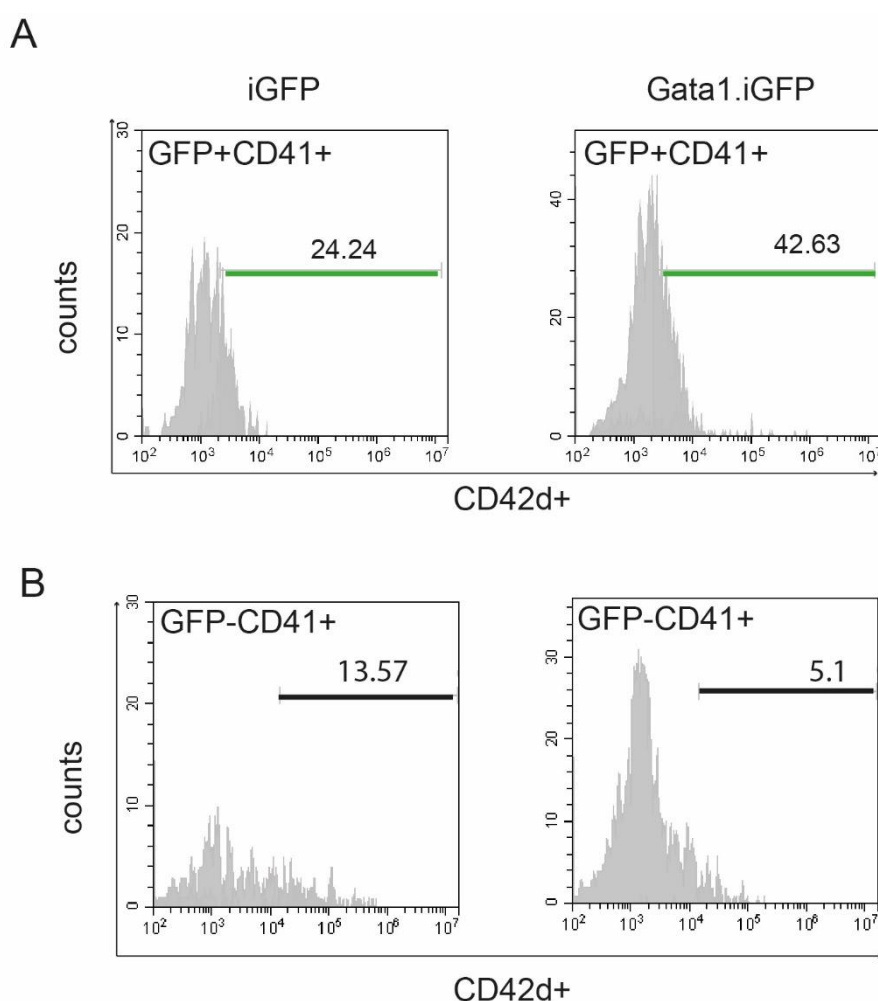


Figure 18 Expression of the surface marker CD42d within CD41⁺ for GFP⁺ and GFP⁻ populations of differentiated MK. CD42d (GPV) is a surface membrane protein specifically expressed in MK and platelets. To evaluate differences in the expression of CD42 MK differentiated from transduced R26rtTAM2, iPSC were analyzed by flow cytometry. The expression is restricted to later stages of MK differentiation, whereas expression of CD41 also appears during early stages of MK differentiation. The CD42d expressing MK within the CD41⁺ population was determined. The figure shows a representative histogram blot of the gating into GFP⁻ (black line) and GFP⁺ (green line) population as described above to verify the effect of transduced candidate factors. (A) GFP⁺CD41⁺CD42d⁺ for iGFP.control Gata1.iGFP-transduced and differentiated MK (green line) (B) GFP⁻CD41⁺CD42d⁺ for iGFP.control and Gata1.iGFP-transduced and differentiated MK (black line). The numbers in the gate represent the percentages of positive cells.

To summarize the data and further compare between GFP-expressing versus non-expressing populations as well as to compare the generation of mature MK between all factors tested, the results for the expression of CD42d within the CD41⁺ population of GFP⁺ and GFP⁻ population is plotted as a bar chart in Figure 19. Similar to the CD41 expression on the surface of the differentiated MK, the CD42d expression within the CD41 expressing cells was generally higher in the GFP⁺ population compared to the GFP⁻ population for each of the factors tested. This increase in the percentage of GFP⁺CD41⁺CD42d⁺ cells was most profound in MK differentiated from Nfe2.iGFP-transduced R26M2K2 iPSC (****p<0.0001). The CD42d expression on the surface of the differentiated MK did not significantly differ between the factors tested. The percentage of CD42d expressing MK within the GFP⁺CD41⁺ population ranged from 34% (Gata1.iGFP) to 78% (Nfe2.iGFP) within the GFP⁺ population. Interestingly, in contrast to the GFP⁺CD41⁺ population, MK differentiated from iPSC transduced with Gata1.iGFP showed the lowest percentage of CD42d expression within the CD41⁺ population for GFP⁻ and GFP⁺ population. In general, MK differentiated after all modifications, except for RhoAhc.iGFP overexpression, showed an increase in the percentage of GFP⁺CD41⁺CD42d⁺ MK differentiated from R26M2K2 iPSC compared to the untransduced control R26M2K2 (Mock), indicating a supportive effect of the factors.

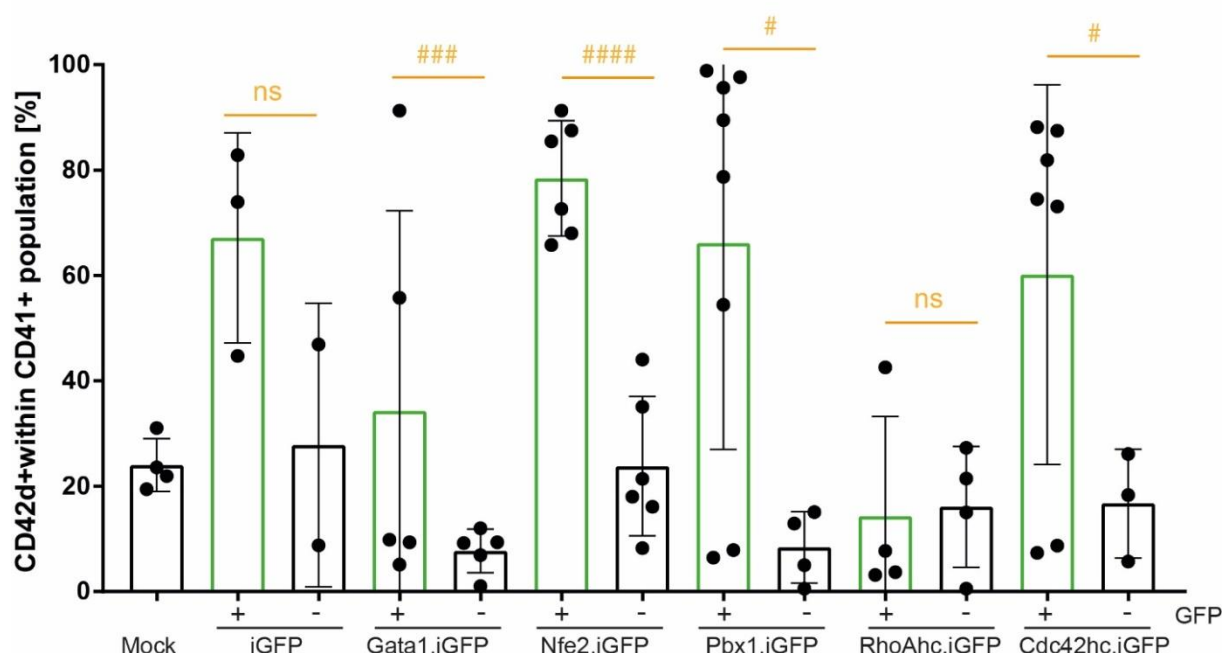


Figure 19 Summary of CD42d expression on differentiated MK at day 21 of differentiation. After transduction of the R26M2K2, iPSC and subsequent differentiation into MK expression of the CD42d surface marker within the CD41⁺ population was determined (Figure17A). To evaluate the effects of transduced and non-transduced candidate factors, GFP⁺ and GFP⁻ populations were analyzed separately. Significant differences in CD41⁺CD42d⁺ populations between GFP⁺ and GFP⁻ population were determined by Student's t-test (n=3-9, mean +/- SD, ####p<0.0001, ###p=0.0008, #p=0.017 (Pbx1,iGFP), #p=0.206 (Cdc42hc.iGFP), ns: not significant.

In addition to the percentages of the surface marker expression, it was of interest how many cells were generated in total. To evaluate the beneficial effect of each single factor on the amount of differentiated MK from R26M2K2 iPSC on day 21 of differentiation, MK cell numbers were determined. The cell numbers of GFP⁺CD41⁺ and GFP⁺CD41⁺CD42d⁺ MK were calculated from the flow cytometry data and plotted as a bar chart in Figure 20. Since 1×10^5 CD41⁺ early hematopoietic progenitors were seeded per well of a 6-well cell culture dish after dissociation of the EB, the amount of the MK/ 10^5 cells is shown. In Figure 20A, the GFP⁺CD41⁺ differentiated MK were calculated. However, the yield of GFP⁺CD41⁺ in general was very low. Numbers of MK differentiated from Gata1.iGFP transduced R26M2K2 iPSC were highest (1.5×10^4 MK) and significantly increased compared to the iGFP.control (2×10^3 MK), which is a 7.5-fold increase (**** $p < 0.0001$). Dox-induced overexpression of Cdc42hc.iGFP during the differentiation also resulted in a 6-fold increase in the generation of GFP⁺CD41⁺ MK at day 21 of differentiation (1.2×10^4 MK, ** $p = 0.0023$). Similarly, the amount of GFP⁺CD41⁺CD42d⁺ MK generated at day 21 of differentiation was highest from Gata1.iGFP transduced R26M2K2 iPSC (1.4×10^3) and also significantly increased compared to the iGFP.control transduced MK (** $p = 0.0094$) and overexpression of Cdc42hc.iGFP during MK differentiation resulted in an increase in MK numbers to 1.3×10^3 (* $p = 0.0199$) (Figure 20B).

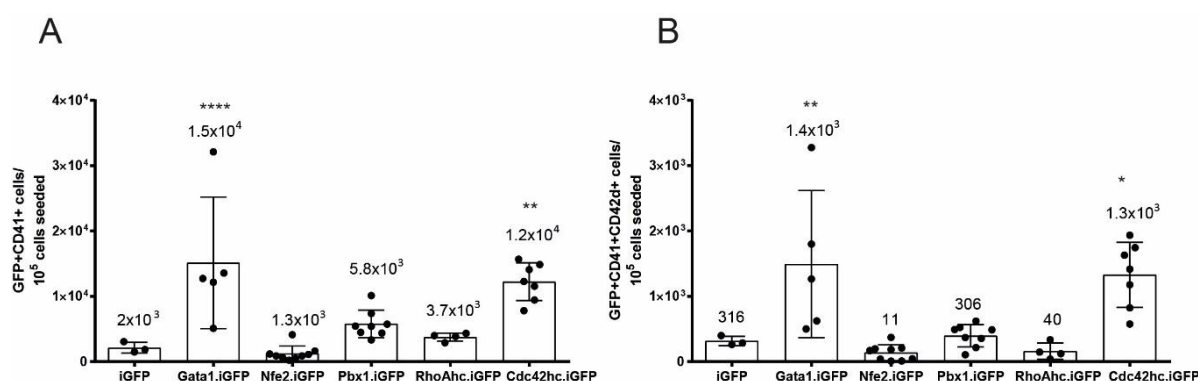


Figure 20 Quantification of MK differentiated from R26M2K2 iPSC at day 21 of differentiation. Cells were transduced with the respective candidate genes in the pluripotent state and differentiated into MK as explained above. MK surface marker expression was analyzed at day 21 of differentiation. (A) Amount of GFP⁺CD41⁺ MK is plotted. Quantification of surface receptor CD41⁺ cells in the GFP⁺ population (B) Amount of GFP⁺CD41⁺CD42d⁺ MK is plotted. Quantification occurred according to the expression of the surface receptor CD41 in the GFP⁺ population (n=3-9, mean \pm SD, 1-way ANOVA with Dunnett's multiple comparison, **** $p < 0.0001$, ** $p = 0.0023$ (GFP⁺CD41⁺ MK differentiated from Cdc42hc.iGFP), ** $p = 0.0094$ (GFP⁺CD41⁺CD42d⁺ MK differentiated from Gata1.iGFP), * $p = 0.0199$).

4.1.5.3 Effects of the overexpression of different factors on *in vitro* platelet production

Similar to the *in vitro* differentiated MK, the platelets generated from the same *in vitro* cultures after 21 days of differentiation were characterized via flow cytometry. Platelets were harvested and separated from the MK by centrifugation. Subsequently, platelets were stained for expression of the surface receptors CD41 and CD42d. Since the expression level of GFP in the harvested platelets was not detectable, GFP⁺ versus GFP⁻ populations were not analyzed separately. Representative examples for flow cytometry histogram blots of platelets differentiated from R26M2K2 iPSC either from dox-induced overexpression of Gata1.iGFP or untransduced control platelets are shown in Figure 21. For the culture-derived platelets, the life-cell gate was set according to a murine whole blood control (Figure 21A, left panel). Furthermore, the platelets generated from *in vitro* cultures are expected to be of larger size. The reason for this may lay in the lack of shear forces during their release, which are important for platelet release *in vivo*. Additionally, beads of defined sizes were used to better define the life-cell gate (Figure 21B middle panel). The resulting life-cell gate is indicated in Figure 21A (right panel). The cut-off for CD41 and CD42d expression was set according to their respective FMO control. In general, a distinct population of CD41 or CD42d expression was not detected. Gata1.iGFP overexpression in platelets lead to an increase in the percentage of CD41-expressing platelets compared to the untransduced control, as indicated by the shift towards higher CD41 expression in Figure 21B, left panel. In contrast, the percentage of CD42d expression was around 30% in both Gata1.iGFP-platelets and untransduced control.

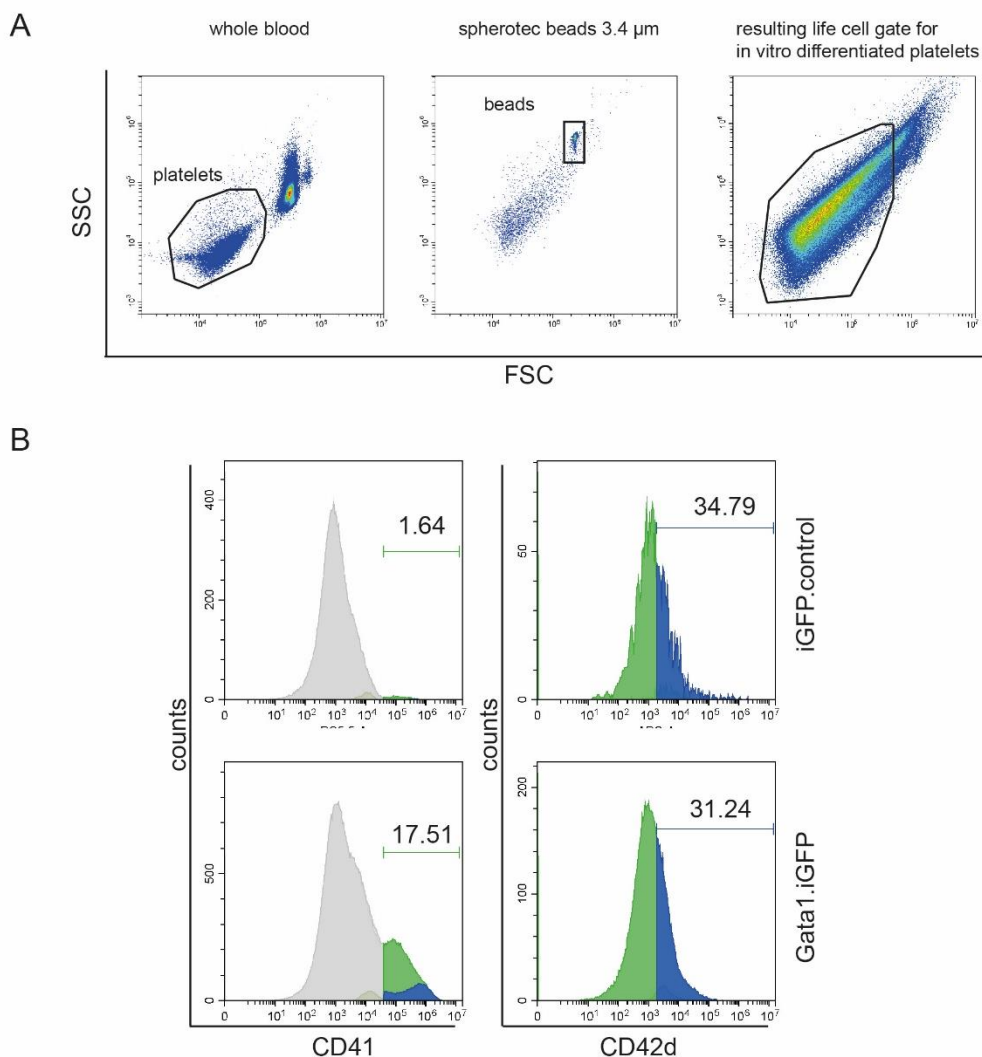


Figure 21 Expression of CD41 and CD42d on the surface of differentiated platelets. Representative histogram blots of the surface receptor expression of the differentiated platelets for their characterization. Platelets were harvested on d21 of differentiation together with the respective MK. (A) Left panel: platelet population gated from murine whole blood. Middle panel: spherotec accu count blank particles with a nominal size of 3.0-3.9 μm gated. Right panel: resulting life cell gate from blood platelets and spherotec beads. (B) Representative example for differentiated platelets isolated from iGFP.control transduced (upper panels) and Gata1.iGFP transduced (lower panels) and differentiated R26M2K2 iPSC. CD41 (green histogram) and CD42 within CD41⁺ populations (blue histogram) were gated according to the appropriate FMO control (the CD41⁻ population is depicted in grey).

The output of *in vitro* generated platelets from R26M2K2 iPSC transduced with the transcription factors Gata1, Nfe2, Pbx1 and the GTPases RhoAhc and Cdc42hc and surface CD41 and CD42d expression are summarized in Figure 22.

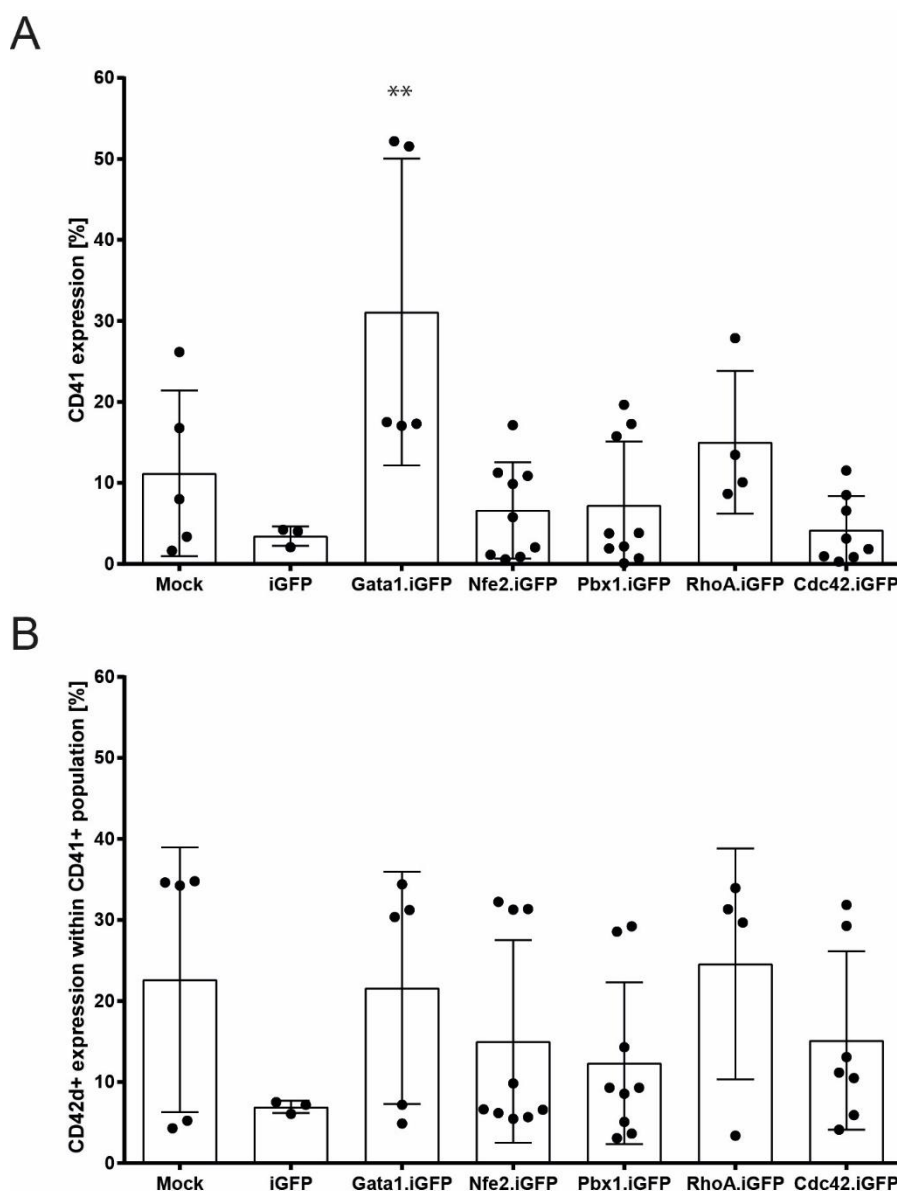


Figure 22 Summary of CD41 and CD42d surface marker expression on *in vitro* differentiated platelets.

Flow cytometry analysis of platelets differentiated from R26M2K2 iPSC and overexpression of respective candidate genes at day 21. Gene expression was initiated by the supplementation of dox at day 7 of differentiation when the EB were dissociated (see Chapter 3.2.2.6) (A) Expression of the major integrin CD41 (α IIb) on the surface of the platelets. Gating occurred as described in Figure 20. (B) Expression of CD42d within the CD41+ population. Gating occurred as described in Figure 20 (n=3-9, mean \pm SD, 1-way ANOVA with Dunnett's multiple comparison, **p=0.0029).

Similar to what has already been shown for the MK differentiated from R26M2K2 iPSC, dox-induced overexpression of Gata1.iGFP lead to an about 10-fold increase in the percentage of CD41-expressing cells (31% of Gata1.iGFP platelets express CD41, **p=0.0029) at day 21 of differentiation. The expression of the MK/platelet-specific marker CD41 on the surface of the platelets from iGFP.control differentiated cells was lowest (3.5% iGFP.control differentiated platelets express CD41 on the surface) (Figure 22A). In contrast, expression of Gata1 increased CD41+ platelets. The overexpression of the other factors generated lower percentages of CD41+ platelets which were not significantly different to the iGFP.control. There is the trend detectable that the percentage of platelets expressing CD42d within the

CD41⁺ population was slightly increased after dox-induced overexpression of all factors compared to the iGFP.control.

In addition to the expression of MK- and platelet-specific surface markers, platelets also show a very specific cellular morphology. First of all, the absence of a nucleus is one of their major hallmarks. Furthermore, they also contain different types of granules which can be distinguished by their electron density in transmission electron micrographs (TEM). Also, the different intramembrane structures like the OCN and dense tubular networks are structures unique to platelets. Platelets differentiated from R26M2K2 iPSC in which the Gata1.iGFP overexpression was induced were subjected to TEM imaging. Representative examples of platelets differentiated from Gata1.iGFP overexpressing R26M2K2 iPSC 3 weeks after differentiation are depicted in Figure 23.

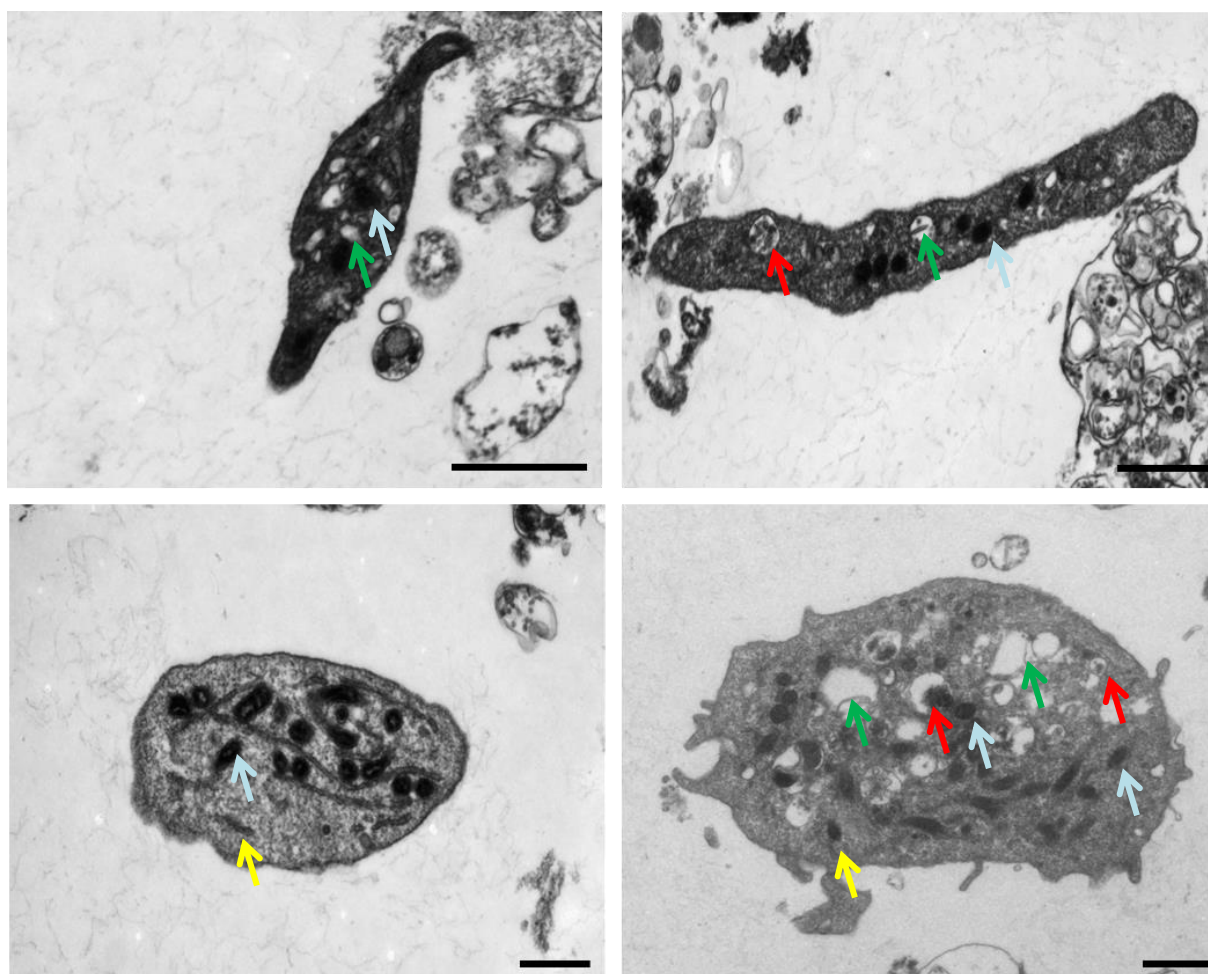


Figure 23 Transmission electron microscopy of platelets. Platelets differentiated from R26M2K2 iPSC expressing Gata1.iGFP were differentiated as described in Chapter 3.2.2.6 and harvested at d21 of differentiation for TEM imaging. Typical platelet morphological features are highlighted in different colored arrows. Yellow arrows: mitochondria, red arrows: dense granules, blue arrows: alpha granules, green arrows: OCS. Black bar indicates the size of 1 μ m.

The platelets isolated from the cultures after differentiation of R26M2K2 iPSC and dox-induced overexpression of Gata1.iGFP were increased in size compared to those isolated from murine blood but showed the typical platelet morphology with first of all the absence of

the nucleus. They contained mitochondria (light blue arrow) depicted as electron-dense structures with internal membranes. Another typical ultrastructure of platelets is the presence of the OCN which was also detected in high abundances in the differentiated platelet (green arrow). The presence of two different types of granules in which important cytokines and coagulation factors are stored was another major hallmark of platelets. Dense granules named after the high electron density from electron micrographs were also developed in *in vitro* generated Gata1.iGFP platelets, as indicated by the red arrows. The granules with lighter electron-density structures, alpha granules, which are the most abundant type of granules in platelets, are shown in yellow.

Platelets isolated from *in vitro* differentiated cultures of R26M2K2 iPSC and identified by their CD41 expression can be quantified similar to the quantification of the MK. To assess the supporting effects of the different factors tested, the output of the amount of platelets differentiated in culture was calculated. The gating strategy is depicted in Figure 21 and the numbers of CD41-expressing and CD41/CD42d double positive platelets plotted per 10^5 CD41⁺ early progenitors seeded after EB dissociation were determined (Figure 24).

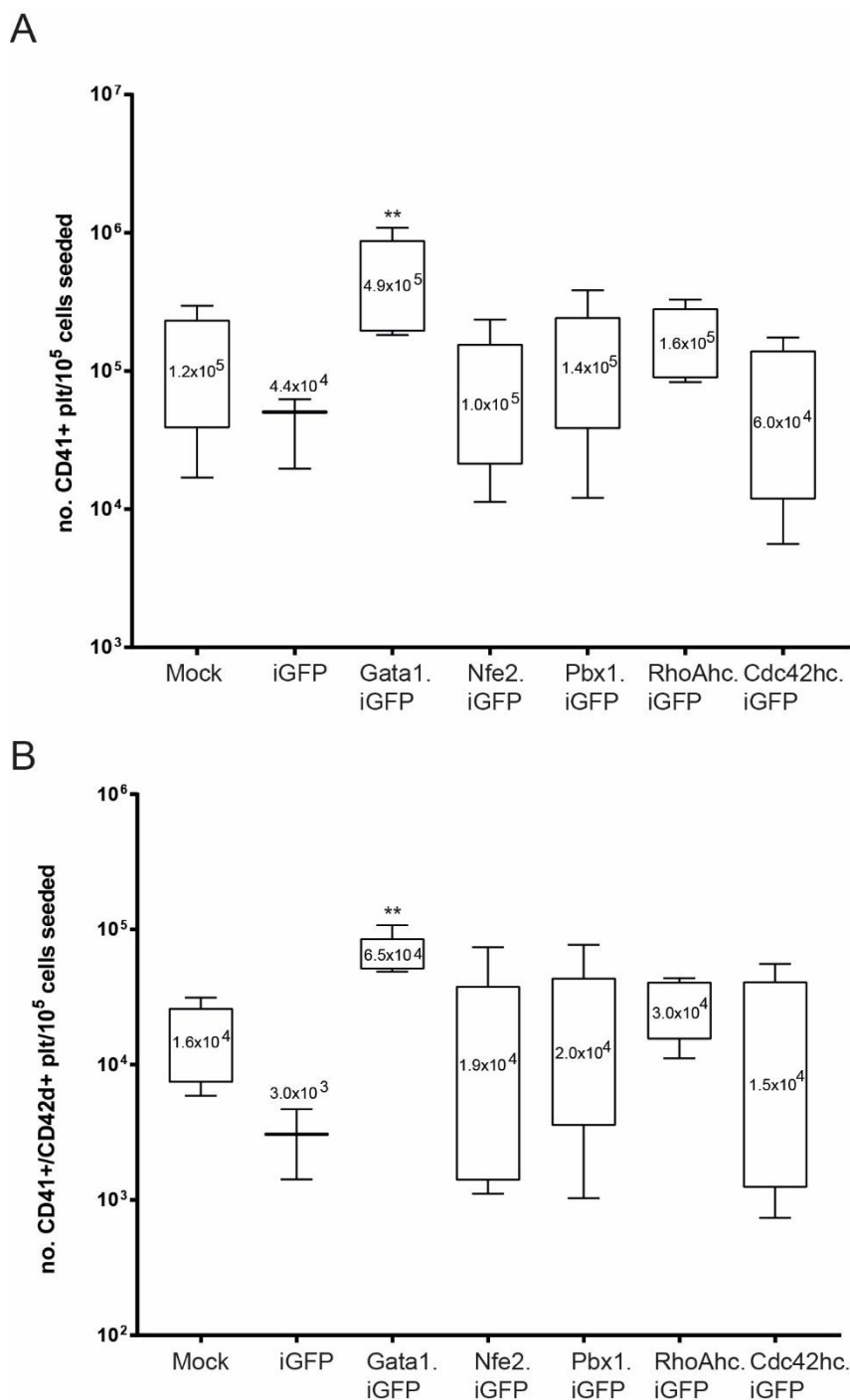
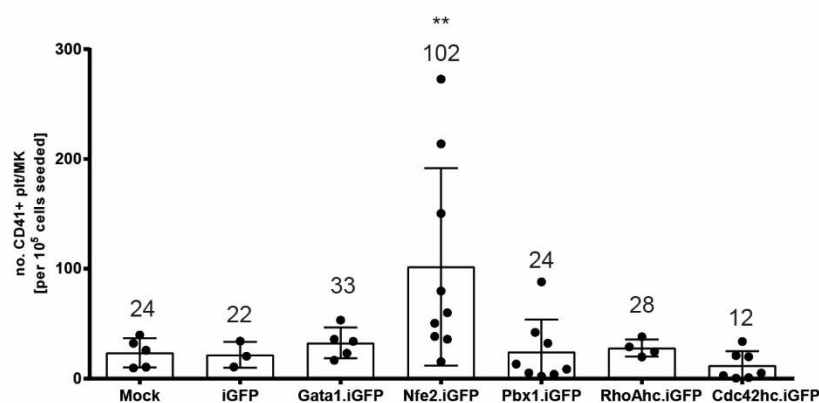


Figure 24 Quantification of platelets differentiated from R26M2K2 iPSC. Platelets isolated at d21 of differentiation were quantified according to their surface receptor expression pattern by flow cytometry. Different candidate factors induced during differentiation were compared. (A) No. of CD41+ platelets harvested per 10⁵ initial progenitors seeded. (B) Number of CD42d+ platelets within the CD41+ population per 10⁵ cells initially seeded. Numbers indicate the mean. (n=3-9, mean +/- SD, 1-way ANOVA with Dunnett's multiple comparison, **p=0.0029 (A), **p=0.0032 (B)).

Overexpression of Gata1.iGFP resulted in about 10-fold increase (4.9×10^5 CD41-expressing platelets) compared to the iGFP.control (4.4×10^4 CD41+ *in vitro* platelets **p=0.0029). The amount of CD41+ *in vitro* platelets generated from the other factors was in the same range of around 1.0×10^5 CD41 positive *in vitro* platelets. Calculation of the CD41+CD42d+ *in vitro* platelets differentiated from R26M2K2 iPSC and dox-induced

overexpression of candidate factors was again relatively equal and within the range of 1.5×10^4 (Cdc42hc.iGFP) to 3×10^4 CD41+CD42d+ (RhoAhc.iGFP) *in vitro* platelets (Figure 24B). Only dox-induced overexpression of Gata1 resulted in a significant increase in the amount of CD41+CD42d+ *in vitro* platelets (6.5×10^4 , **p=0.0032) at d21 of differentiation. It is also important to consider the number of platelets released per MK. *In vivo*, one MK releases about 1000 platelets (Sim et al., 2016). To determine how many platelets were released from a CD41+ MK differentiated from R26M2K2 iPSC and transduced with the different candidate factors, the numbers of released platelets were set into relation to the amount of CD41+ MK differentiated from the same culture at the same day. Interestingly, overexpression of Nfe2 resulted in an increase in the amount of CD41+ *in vitro* platelets released per CD41+ MK (102 CD41+ platelets/MK), which is significantly different from the iGFP.control transduced and differentiated R26M2K2 iPSC shown in Figure 25A. The overexpression of the other candidate factors released similar amounts of CD41+ *in vitro* platelets per CD41+ MK. Similar to these results, also Nfe2 resulted in increased amounts of CD41+CD42d+ *in vitro* platelets per CD41+ MK (Figure 25B), however, this was not significantly different from the iGFP.control transduced and differentiated R26M2K2 iPSC.

A



B

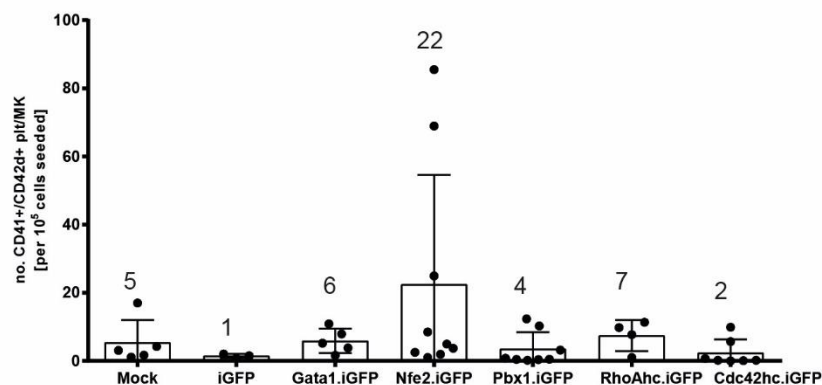


Figure 25 Quantification of platelets released per MK during *in vitro* differentiations. The amount of platelets released per MK at day 21 of differentiation was quantified by flow cytometry. Different candidate factors were transduced in the pluripotent state. Gene expression was initiated by the application of dox at day 7 of differentiation. (A) Amount of CD41+ platelets released per CD41+ MK. (B) Amount of CD41+CD42d+ platelets released per CD41+ MK (n=3-9, mean +/- SD).

4.1.5.4 Functionality of *in vitro* differentiated platelets

After the occurrence of a vascular trauma, platelets undergo sequential adhesion, activation and aggregation, which results in their spreading to increase their contact area, finally leading to plug formation which is accompanied with the flattening of the cells and the deformation of the plasma membrane (Lee et al., 2012). This can be mimicked *in vitro* in so-called platelet spreading assays. In the next step, we wanted to prove whether the *in vitro* differentiated platelets from R26M2K2 iPSC were functional *in vitro* and performed platelet spreading assays on either fibrinogen or CRP-coated cover slips in collaboration with Dr. Markus Bender from the University of Würzburg. *In vitro* generated platelets from R26M2K2 iPSC transduced with Gata1.iGFP were investigated. Gata1.iGFP overexpression was induced at day 7 of differentiation when co-cultivation on OP-9 feeder cells started. The cells were cultivated on OP-9 feeder cells for 2 weeks before MK were harvested and re-plated on suspension cell culture dishes. *In vitro* differentiated platelets were harvested by centrifugation (see Chapter 3.2.2.6). For comparison, freshly isolated, washed platelets from about 1ml of whole blood of a C57BL/6 wildtype (wt) mouse were prepared. Platelets isolated from whole blood as well as *in vitro* differentiated platelets were spread on either fibrinogen or CRP-coated cover slips and subsequently stained with antibodies against the CD41/CD61 integrin and CD42a glycoprotein (GPIX). In addition, especially for visualization of the platelet spreading, an antibody against the MK/platelet-specific tubulin (β 1-tubulin) was used. To compare the resting versus the activated state of the platelets, in some of the samples, the cells were applied to poly-L-Lysine-coated cover slips and remained non-activated as a control. Platelets isolated from wt murine whole blood showed a typical circular-shaped morphology where the CD41/CD61 and CD42a were distributed throughout the surface of the resting platelets. The β 1-tubulin could be visualized as a distinct ring at the edge of the cells. Figure 26 shows the presence of a representative example of a pro-platelet (middle panels) and platelets (lower panels) harvested from the *in vitro* cultures. Similar to platelets isolated from whole blood, *in vitro* differentiated platelets expressed CD41/CD61 throughout their surface. Also, the presence of the GPIX could be visualized by confocal microscopy. The β 1-tubulin distribution showed the same ring-like structure at the edge of the cell of the differentiated platelets which was comparable to the wt-isolated platelets.

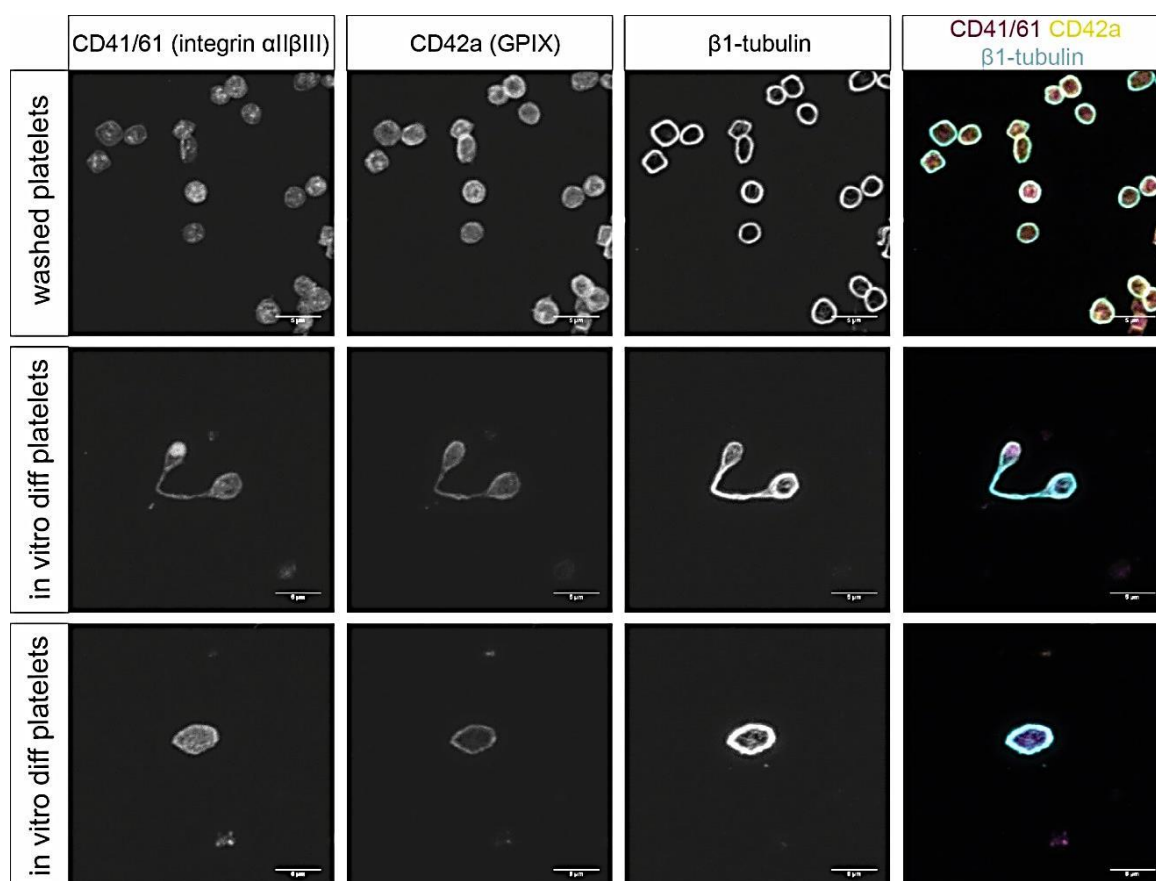


Figure 26 Resting platelets on poly-L-lysine-coated cover slips. Cells were incubated in the resting state on poly-L-lysine-coated cover slips and remained non-activated. Washed platelets isolated from murine whole blood (upper panels) were compared to *in vitro* differentiated pro-platelets (middle panels) and platelets (lower panels). In the non-activated state, platelets showed the typical circular-shaped morphology. For identification of the platelets, the integrin $\alpha\text{IIb}\beta\text{3}$ (magenta) and GPIX (yellow) were marked with primary antibodies and then incubated with fluorescent labelled antibodies for visualization via confocal microscopy. Additionally, the platelet/MK-specific $\beta\text{1-tubulin}$ was labelled with appropriate primary and secondary antibodies. Merged images are shown in the right column. Scale bars indicate a size of $5\mu\text{m}$.

In platelets, the $\beta\text{1-tubulin}$ forms monomers together with $\alpha\text{-tubulin}$ beneath the cell membrane of the cells, maintaining their discoid shape, a feature called marginal bands (Patel-Hett et al., 2008; Shin et al., 2017). When platelets get activated by various biological stimuli and agonists including ADP, thromboxane receptor agonist U46 and thrombin, this leads to cytoskeletal reorganization resulting in the formation of filopodia and lamellipodia. In this experiment, we triggered platelet activation in two different approaches. After their addition to fibrinogen in the first example, they were stimulated with thrombin to induce shape changes leading to the formation of filopodia and lamellipodia, which can be visualized by confocal microscopy using the same primary and secondary antibodies as mentioned above. Results of wt-isolated platelets and *in vitro* differentiated platelets differentiated from Gata1-overexpressing R26M2 iPSC spread on fibrinogen and activated with thrombin are included in Figure 27. During platelet activation of wt-platelets with thrombin, the ring structure of the $\beta\text{-tubulin}$ became less distinct whereas the CD41/CD61 was still distributed over the entire surface. Filopodia and lamellipodia formation was detected (upper panel Figure 27). Similar to platelets isolated from blood, the *in vitro* differentiated platelets

attached to the surface by interaction between the GPIIb/IIIa and the fibrinogen (Figure 27 middle panel, lower panel), however, distinct ring structures of β 1-tubulin were reduced. In the lower panels, filopodia formation was detected as indicated by the β 1-tubulin signal and the expression of the CD41/CD61 distribution (Figure 27, lower panel). In contrast to the blood-derived platelets, lamellipodia formation was not detected.

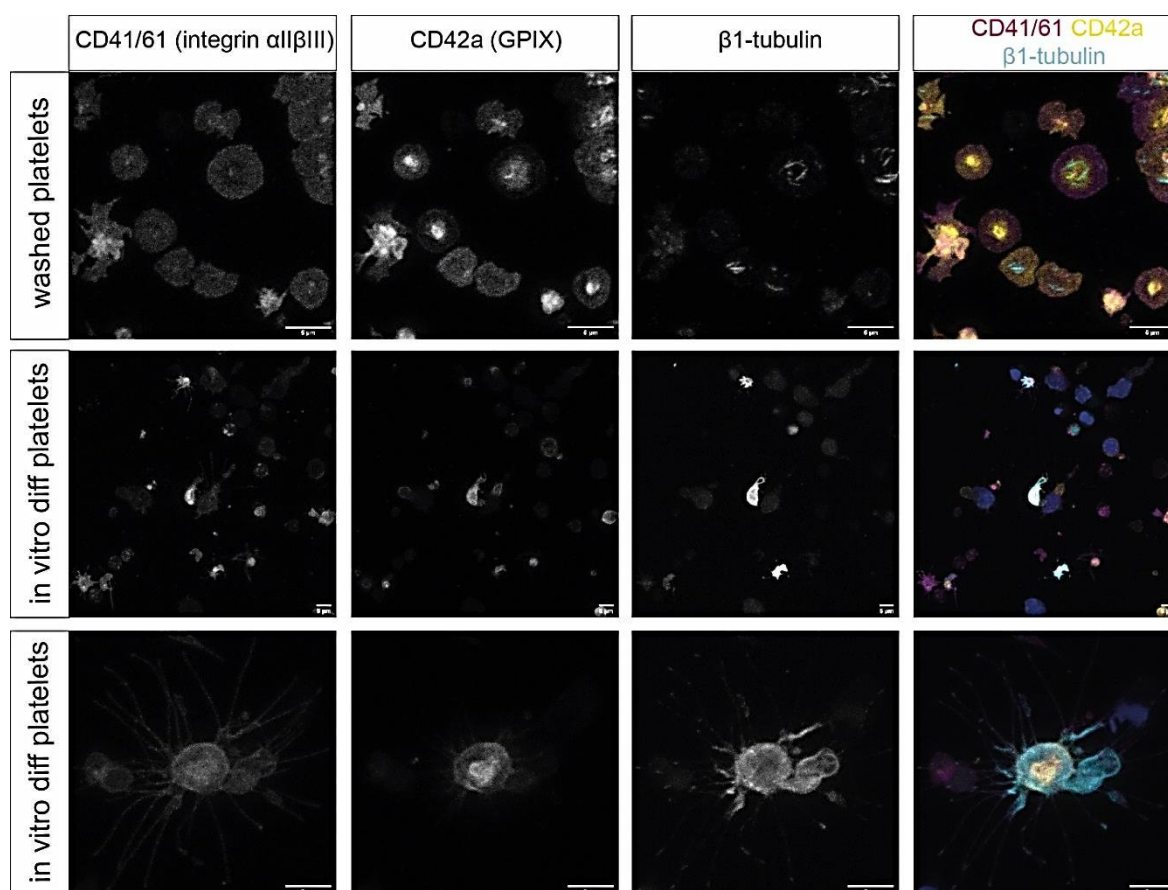


Figure 27 Platelets spread on fibrinogen-coated cover slips. Platelets isolated from blood of wt mice (as control) and *in vitro* differentiated platelets were incubated on fibrinogen-coated cover slips and activated with 0.01U/ml thrombin for 60min. For identification of the platelets, the integrin α IIb β 3 (magenta) and GPIX (yellow) were marked with primary antibodies and then incubated with fluorescent labelled antibodies for visualization via confocal microscopy. Additionally, the platelet/MK-specific β 1-tubulin was labelled with appropriate primary and secondary antibody. Merged images are shown in the right column. Scale bars indicate a size of 5 μ m. In comparison to the platelets isolated from whole blood, spreading of culture-derived platelets resulted in the formation of filopodia. Lamellipodia formation was absent in culture-derived platelets.

In addition to the spreading on fibrinogen, a second spreading assay on collagen-related peptide (CRP) was performed. The major receptors for adhesion to collagen are the glycoprotein GPVI and α 2 β 1 (Varga-Szabo et al., 2008; Lee et al., 2012). Platelets isolated from wt murine whole blood adhered to collagen and were stimulated in this case with ADP and the thromboxane receptor agonist U46. The results are included in Figure 28. Similar to fibrinogen-coated cover slips, platelet spreading occurred by the formation of filopodia and lamellipodia, however, this occurred only to a lower extent compared to the spreading on fibrinogen with thrombin stimulation (Figure 28, upper panels). Filopodia formation was also detected in case of platelets differentiated from Gata1-overexpressing R26M2K2 iPSC as

indicated by the cellular protrusions detected by the immunostaining of CD41/CD61 and β 1-tubulin. Similar to what has been observed on fibrinogen-coated cover slips, lamellipodia formation was also absent in culture-derived platelets (Figure 28, middle panels, lower panels).

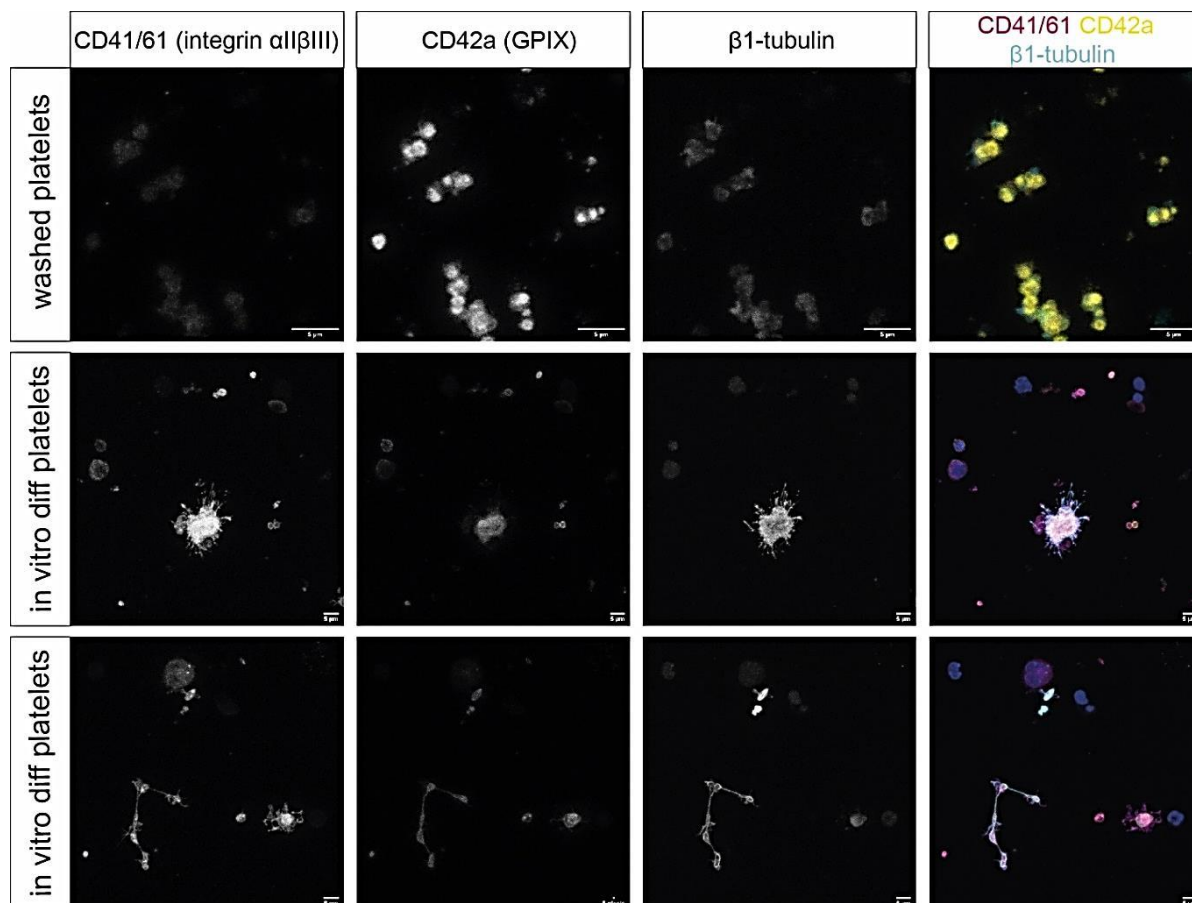


Figure 28 Platelets spread on CRP-coated cover slips. For the performance of platelet spreading assays platelets isolated from wt-mice and *in vitro* differentiated platelets were incubated on collagen-related-peptide (CRP)-coated cover slips and activated with 10 μ M ADP and 3 μ M U46 thrombin for 60min. For identification of the platelets, the integrin α II β III (magenta) and GPIX (yellow) were marked with primary antibodies and then incubated with fluorescent labelled antibodies for visualization via confocal microscopy. Additionally, the platelet/MK-specific β 1-tubulin was labelled with appropriate primary and secondary antibody. Merged images are shown in the right column. Scale bars indicate a size of 5 μ m. In comparison to the platelets isolated from whole blood, spreading of culture-derived platelets resulted in the formation of filopodia. Lamellipodia formation was absent in culture-derived platelets.

4.2 Generation of Tet all-in-one gammaretroviral vectors with low silencing potential

We have shown that tetracycline-inducible retroviral vectors represent powerful tools for time-controlled transgene expression during differentiation of iPSC, however, silencing of expression from the vectors is a drawback. In the well-studied gammaretroviral Tet-all-in-one vectors initially used in this study and published by Heinz et al., the PGK promoter initiates constitutive expression of the reverse transactivator (rt)TA-M2 (Heinz et al., 2011). This promoter fragment is highly enriched in CpG sites (63 in total) which are often responsible for gene silencing because they can be methylated. We investigated in the second part of the project whether the insertion of different UCOE derived from the HNRPA2B1-CBX3 locus (A2UCOE) can sustain transgene expression in Tet-all-in-one retroviral vectors especially for their use in iPSC. The A2UCOE is well-studied and widely used in constitutive lentiviral vectors as indicated in Chapter 1.7. The A2UCOE elements U1.5, U1.0, U670 and U630 are derived from different regions of the HNRPA2B1-CBX3 locus and were inserted in sense (s) or antisense (as) orientation in respect to the transcriptional orientation of the expression cassette in the vector upstream of the PGK promoter as shown in Figure 29. The different orientations of the respective elements and the corresponding nomenclature are listed in Figure 30. Additionally, the CBX3 element developed by Mueller-Kuller and colleagues containing mutations in a canonical splice donor and cryptic splice site was inserted. The control (PGK.Tet-control) does not have an A2UCOE incorporated.

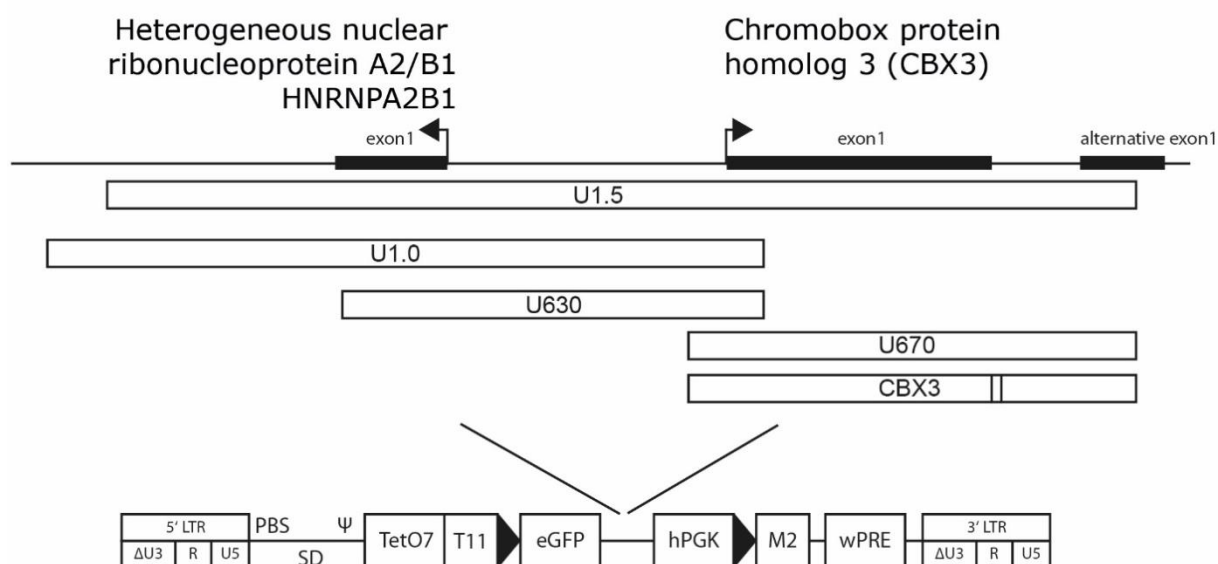


Figure 29 Tet-inducible all in one gammaretroviral vectors containing A2UCOE of different sizes. Different A2UCOE spanning the first exons of the HNRPA2B1 and the CBX3. Exons are indicated by the filled squares. Annotation of the exons is based on NM_007276.3 (transcript variant 1, CBX3), NM_016587.3 (transcript variant 2, CBX3), NM_002137.3 (transcript variant A2, HNRPA2B1). Mutations of the splice sites in the CBX1 element are indicated by vertical bars. The different A2UCOEs were inserted into a Tet-regulated, all-in-one gammaretroviral vector upstream of the PGK promoter.

element	orientation with respect to	
	HNRNP transcription	CBX3 transcription
UCOE 630s	antisense	sense
UCOE 630as	sense	antisense
UCOE 670s		sense
UCOE 670as		antisense
UCOE 1.0s	antisense	sense
UCOE 1.0	sense	antisense
UCOE 1.5s	antisense	sense
UCOE 1.5as	sense	antisense
CBX3		sense

Figure 30 Different A2UCOES are inserted into the Tet-all-in-one gammaretroviral vector in different orientations. Orientation is named sense (s) or antisense (as) according to the transcriptional orientation of the CBX3 promoter.

Tet-all-in-one vectors are tightly regulated systems and insertion of additional components, especially if they potentially have promoter activity like some of the A2UCOE, may interfere with regulation and titers. After production of gammaretroviral vector particles in HEK 293T, packaging cell lines titers were evaluated in SC1 fibroblast cell lines and are shown in Figure 31.

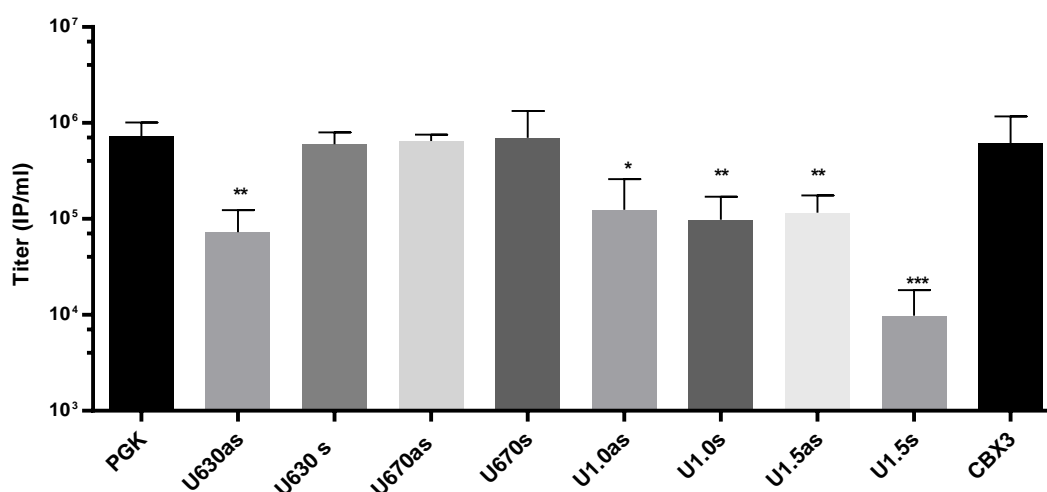


Figure 31 Titers of non-concentrated viral vector preparations. Determination occurred on mouse SC1 fibroblasts (mean ± SD, n=4, * p<0.05, ** p<0.01, *** p<0.001 compared to the PGK.Tet-control vector, Student's t-test).

The incorporation of A2UCOE elements with sizes larger than 1kb decreased the titers sevenfold (U1.0as, U1.0s, U1.5as). The drop in viral titer was most profound after incorporation of the U1.5s A2UCOE. Also, the incorporation of the U630as element decreased the titer for about two decades to 9800 +/- 3700IP/ml. Incorporation of the elements U630s, U670as, U670s and CBX3 did not alter the viral vector titers and reached the same level like the PGK.Tet-control (7.3 +/- 2.8 x 10⁵IP/ml) in un-concentrated supernatants. In the following, the vectors were further characterized in terms of regulation of gene expression and anti-silencing capacity.

4.2.1 Influence of the insertion of the A2UCOE on the dynamic range of transcriptional activation

Tet-on vectors have to be tightly regulated. After induction with dox they should express GFP at high levels and the expression should be completely turned off after dox withdrawal, a feature called dynamic range. The dynamic range measures the ratio of the transgene expression at the induced and non-induced state. To assess the influence of the different incorporated elements on the dynamic range, SC1 mouse fibroblast cells were transduced with an efficiency of 30% to 50% GFP expression with the different vectors. Histogram plots of representative examples of the flow cytometric analysis are shown in Figure 32.

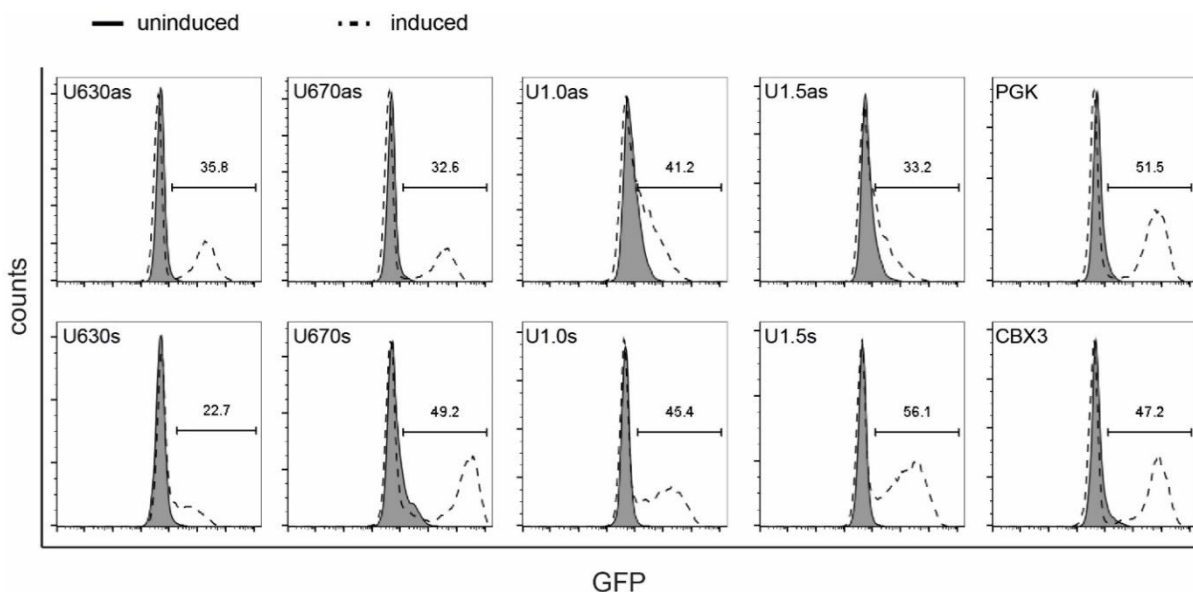
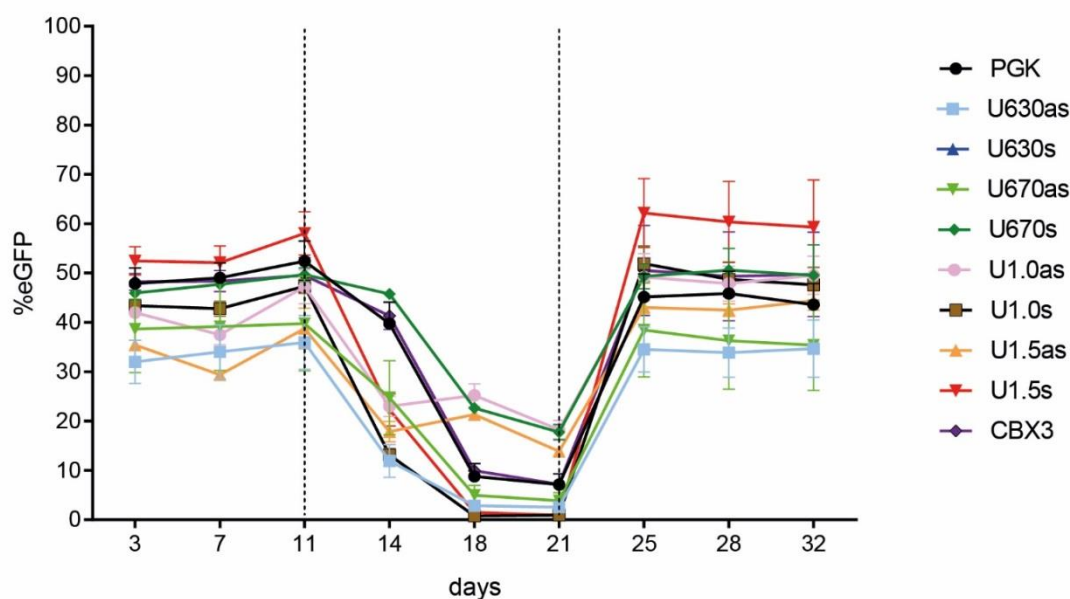


Figure 32 Regulation of A2UCOE-containing Tet-vectors by dox in SC1 fibroblasts. Representative flow cytometry plots of GFP expression after transduction of SC1 with different A2UCOE vectors. Induced: dashed line; non-induced: black line, grey filled area. Percentages of GFP⁺ cells are indicated by the respective number in the plot.

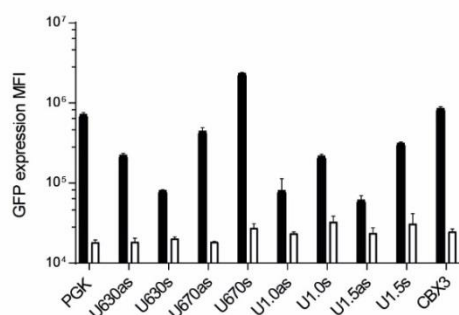
Transduction with the Tet-vectors containing the elements U630as, U670as, U670s and CBX3 showed distinct GFP⁺ populations which were very similar to the PGK-Tet.control. In contrast, GFP⁺ peaks, especially after incorporation of the elements U1.0as and U1.5, were less prominent and the spread of the GFP expression from the vectors U1.0s and U1.5s

showed a wider range of GFP expression, indicating a high variegation of the expression after transduction.

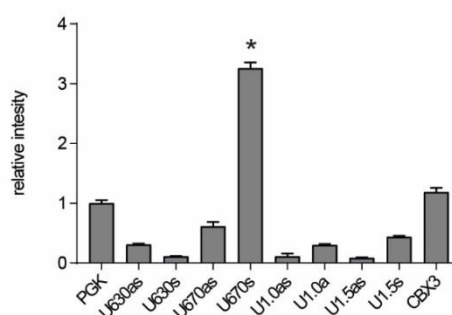
A



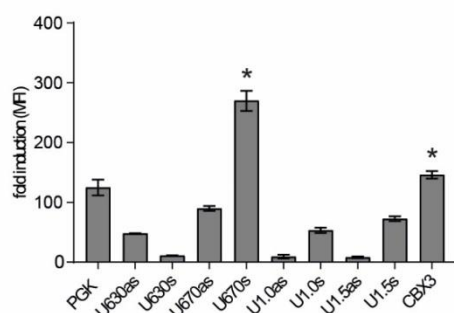
B



D



C



E

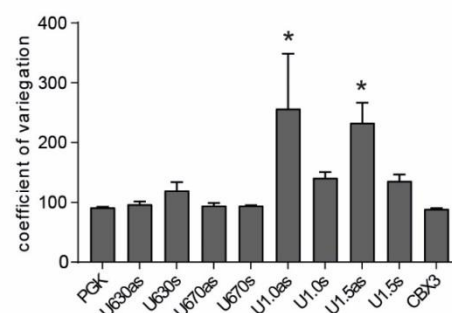


Figure 33 Regulation of A2UCOE-containing Tet-vectors by dox in SC1 fibroblasts. (A) Percentage of GFP expression was monitored by flow cytometry in transduced SC1 cells cultured in the presence of dox (days 3-11 and days 25-32) and without dox (days 14-21). (B) Intensity of GFP expression (MFI) in induced (black bars) and non-induced cells (white bars). (C) Fold induction of expression (MFI) from non-induced to induced state. (D) Relative intensity of expression (MFI) normalized to the Tet-control vector (set to 1). (E) Coefficient of variegation (CV) of expression of the GFP positive population (n=3, mean +/- SD, 1-way ANOVA with Dunnett's multiple comparison test, *p<0.05).

For a better comparison between the tested elements, GFP expression in the induced and non-induced states are shown in Figure 33. The difference in GFP expression between induced and non-induced state is depicted in Figure 33A. After dox withdrawal, GFP expression declined to background levels after 7 days. Expression reached the same levels after re-induction in all of the vectors tested. The expression in the non-induced state of the PGK-Tet.control declined to below 7%. After incorporation of the U630as, U630s and U670as into the vector, the expression showed the same low level compared to the PGK.Tet-control. However, incorporation of the U670s, U1.0s, U1.0as, U1.5s, U1.5as and CBX3 elements resulted in higher residual GFP expression (Figure 33A). This was also verified by the MFI as shown in Figure 33B. The MFI was highest with the vectors U670s and reached a MFI of 2.3×10^6 but also showed the highest background expression with a mean MFI of 2.8×10^5 . For better evaluation, the fold increase was determined and Figure 33C shows that the highest fold induction was observed in the cultures transduced with the Tet-vector U670s (270-fold, PGK.Tet-control vector 125-fold). This vector also showed the highest intensity of expression (MFI) which is increased 3.25-fold compared to PGK.Tet-control (Figure 33D). The coefficient of variegation (CV) determines the spread of the GFP signal within the positive population and is determined by the width of the fluorescent signal measured by flow cytometry. Here, the CV was highest in U1.0as transduced SC1 fibroblasts followed by U1.5as, indicating the influence of the elements on the variegation. The incorporation of U630as, U670as, U670s and CBX3 had no effects on the variegation and was within the range of the PGK.Tet-control (Figure 33E).

4.2.2 Anti-silencing potential of different A2UCOE-Tet vectors in P19 carcinoma cells

The different A2UCOE-Tet vectors were further characterized in terms of their anti-silencing potential. The murine embryonal carcinoma cell line P19 was used for the studies. P19 cells are embryonic carcinoma cells derived from teratomas in mice (He et al., 2005). P19 cells were transduced with the different A2UCOE-Tet-vectors to an efficiency of 25-55% and the vector copy number (VCN) ranged between 1 and 2. The GFP expression was followed up for 46 day and was analyzed every 3-4 days by flow cytometry. The results are plotted in Figure 34 where each bar represents one measurement at one time point. GFP expression was set to 100% at day 3 after transduction to compensate different transduction efficiencies.

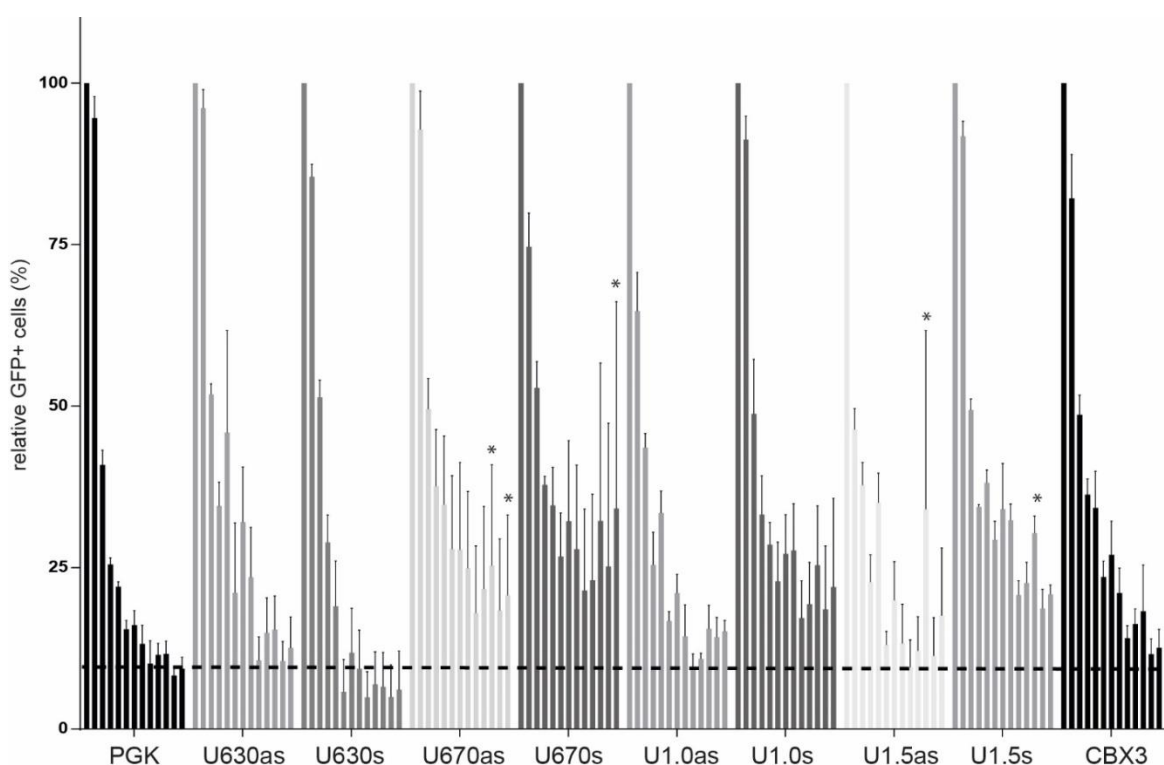


Figure 34 Stability of transgene expression on the embryonic carcinoma cell line P19 over a period of 46 days. P19 cells were transduced with viral vectors containing the different A2UCOE or with the PGK.Tet-control vector. The GFP expression was determined every 3-4 days by flow cytometry up to 46 days after transduction. Each column represents one measurement at the days 3, 7, 11, 14, 18, 21, 25, 28, 32, 35, 39, 42 and 46. The percent of GFP expression was normalized to 100% at day 3 after transduction. The horizontal dashed line indicates the endpoint value of the PGK.Tet-control (n=3, mean +/- SD, *p<0.05, 2-way ANOVA with Dunnett's multiple comparisons test).

Insertion of the A2UCOEs U670s, U670as, U1.0s and U1.5s upstream of the PGK promoter could maintain the GFP expression in more than 50% of the transduced cells after 14 days of cultivation, which persisted until the termination of the experiment at day 46. At this day, GFP expression from the A2UCOEs-Tet vectors U670s, U670as, U1.0s and U1.5s was still above 25%. In comparison, the PGK.Tet control was below 25% after 2 weeks. The anti-silencing effect after incorporation of U630as, U630s, U1.5as and U1.0as was less profound (in the range of 12%) compared to the other A2UCOE counterparts. Incorporation of the U630s resulted in the lowest residual percentage of GFP-expressing P19 cells (6%) (Figure 34, Figure 35A).

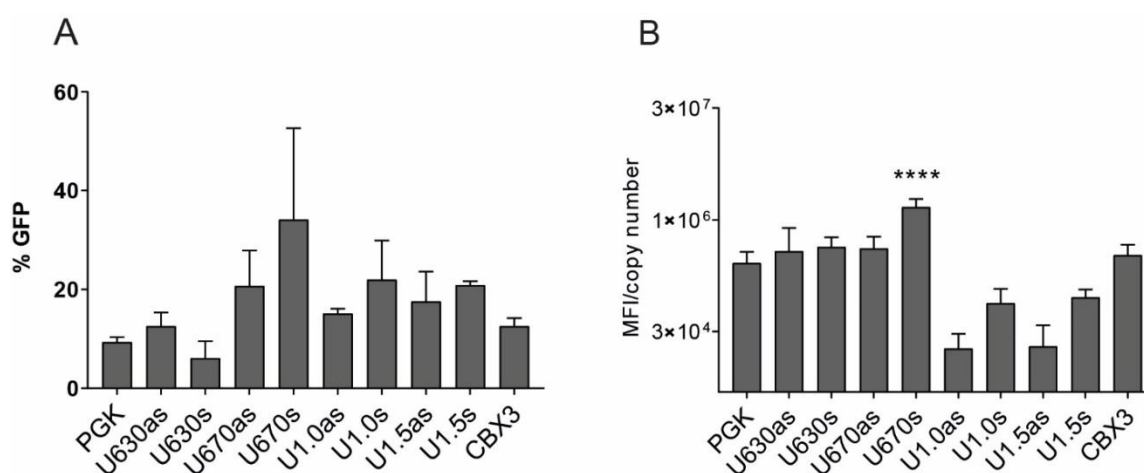


Figure 35 Evaluation of the anti-silencing capacity of different A2UCOE-vectors in P19 embryonic carcinoma cells. P19 cells were transduced with the respective vector and GFP expression was followed for 46 days. Differences in transduction efficiency were compensated by normalizing the percent GFP to 100% at day 3 after transduction. Bars show the residual GFP expression at termination of the experiment 46 days after transduction. (A) Percentage of expression at day 46 after transduction. (B) Intensity of GFP expression at day 46 correlated to the mean vector copy number (MFI/VCN, mean \pm SD, $n=3$, 1-way ANOVA with Dunnett's multiple comparisons test, **** $p<0.0001$).

The intensity of expression (MFI/VCN) was also strongest in U670s transduced P19 (5.7-fold higher than PGF, $p<0.001$) at day 46 when the experiment was terminated, indicating the best beneficial effect of U670s on the prevention of transgene silencing in Tet-inducible all-in-one gammaretroviral vectors. To investigate if the drop in the GFP expression was caused by silencing of the PGK promoter, another transduction experiment was performed using P19 cells that only expressed a residual GFP fluorescence after prolonged cultivation time. If silencing of the promoter was the reason for the drop in GFP expression, it should become reconstituted when a second external (rt)TA-M2 was introduced. To investigate this, the U670s-transduced P19 cells were transduced with a second gammaretroviral vector expressing the transactivator (rt)TA-M2. This vector was co-expressing M2 and a mCherry reporter signal. Percentages of GFP expression as well as fluorescent intensities within the M2.mCherry positive (M2 pos) and negative populations (M2 neg) were analyzed 7 days after the second transduction as shown in Figure 36A.

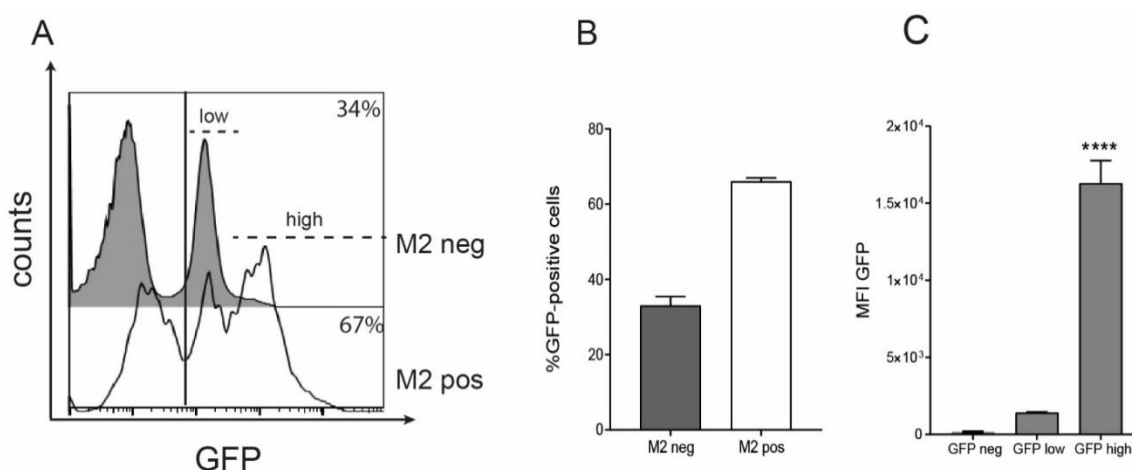


Figure 36 Re-expression of the transactivator rtTA-M2 in P19 cells by a second retroviral vector. U670s-transduced P19 cells were again transduced with a second gammaretroviral vector expressing the rtTA-M2 leading to a co-expression of the residual GFP and mCherry reporter signal at the same time. 7 days after the second transduction, GFP expression in the M2 positive population (mCherry positive) of U670s transduced P19 cells were analyzed by flow cytometry. GFP low and high populations are indicated. (A) Histogram plots of the flow cytometry results. (B) Percentage of GFP expression of M2neg and M2 pos cells (n=3, mean +/- SD, Student's t-test two tailed, **p=0.0023). (C) MFI of GFP expression in GFP^{low} versus GFP^{high} expressing P19 cells after restoring the GFP reporter expression after transduction of a second transactivator M2 (n=3, mean +/- SD, 1-way ANOVA with Dunnett's multiple comparisons test, ****p<0.0001).

Figure 36B summarizes the GFP expression within the M2.mCherry positive population which is restored to 67% GFP-expressing cells compared to the M2.mCherry-negative counterpart where only 34% express the GFP signal. This is especially prominent when analyzing the MFI. Due to the occurrence of the double-peak in Figure 36C, we therefore divided the population in GFP^{high} and GFP^{low} expressing populations. MFI of GFP-high population rises to more than 1.5×10^4 .

4.2.3 A2UCOE in Tet-inducible all-in-one vectors in murine iPSC

Since the incorporation of A2UCOE elements into Tet-inducible all-in-one vectors was designed to be used in pluripotent stem cells and their differentiated progeny, we next assessed their performance in the murine iPSC cell line CD45.1 published by A. Mucci et al (Mucci et al., 2018). We selected the most promising candidates U670s, U1.0s, U1.5s, and CBX3 from the data in SC1 and P19 cells (see Chapter 4.2.1 and 4.2.2) and transduced CD45.1 iPSC with an initial efficiency of 20-65% and cultivated for 2 weeks after transduction before the dox was withdrawn for the first time. GFP expression was analyzed. The results are plotted in Figure 37.

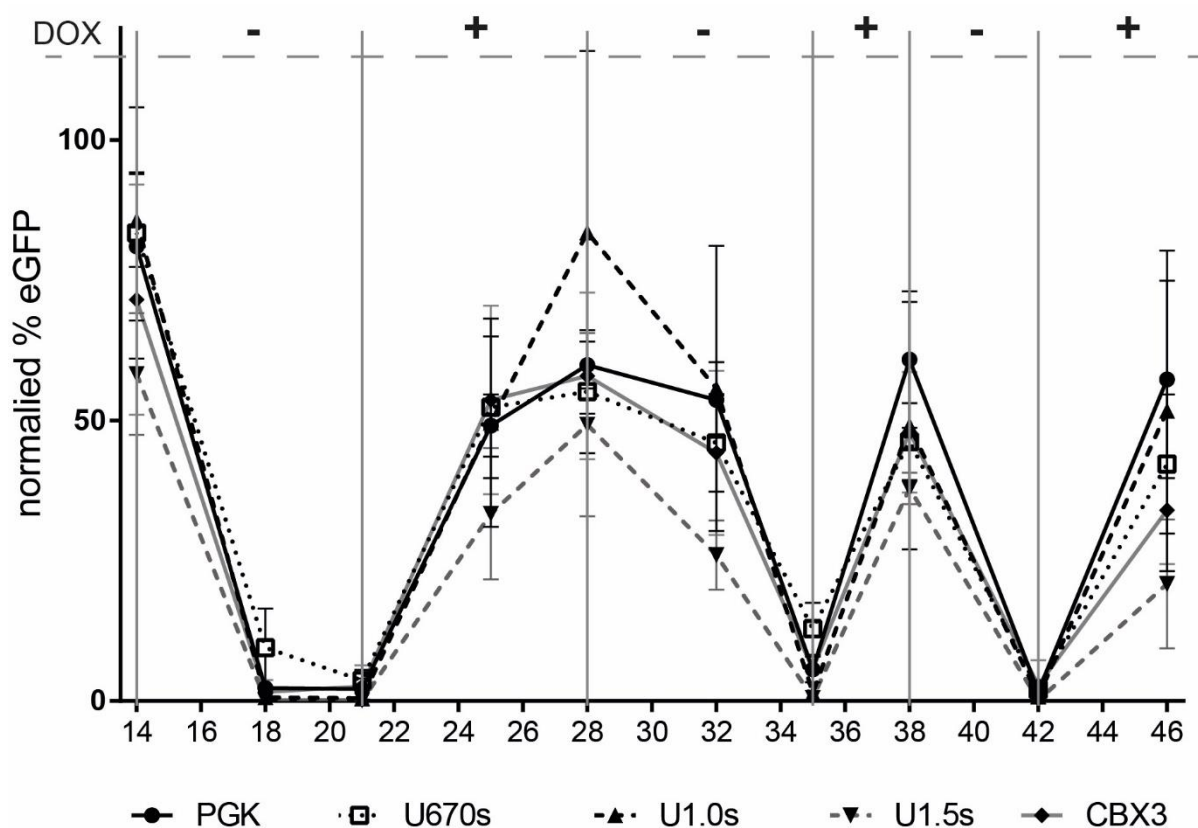


Figure 37 Regulation of expression from the A2UCOE Tet-inducible vectors in murine induced pluripotent stem cells. Murine iPSC were transduced with the respective A2UCOE Tet-vectors and GFP expression was analyzed during a course of repeated induction and withdrawal of dox over 46 days. Highest values of GFP positive cells were normalized to 100% GFP expression for each vector at day four after transduction. Dox was supplemented (+) and withdrawn (-) repetitively (n=3, mean +/-SD).

After withdrawal of dox, GFP expression was turned off efficiently to 1.2% of the initial expression when transducing with the U1.0s and U1.5s vectors. The GFP signal also declined to about 10% of the initial expression using the vectors U670s and CBX3. The GFP expression was continuously analyzed up to day 46 after transduction and the GFP expression was re-induced and turned off multiple times. The U1.0s, U670s and CBX3 vectors reached the percentage of their initial GFP expression after re-induction 7 days later and during 2 following repetitive cycles of dox withdrawal and re-application.

Despite the percentage of GFP expression, the MFI was of importance for evaluation of the performance. To compensate for different transduction efficiencies, the MFI was normalized to the corresponding VCN. Transduction of CD45.1 iPSC with the U670s resulted in the highest intensity of expression on day 14 after transduction compared to the PGK.Tet-control ($p < 0.02$) (Figure 38B). The significantly higher MFI of the U670s Tet-all-in-one vector compared to the PGK-Tet.control persisted until termination of the experiment in the induced state ($*p < 0.05$). Also, incorporation of the CBX3 element into the Tet-all-in-one vector resulted in an increase of the MFI at day 14 and 25 after transduction, but a significant difference could not be detected at later time points (Figure 38B, Figure 38C). At termination of the experiment at day 46, only the Tet-all-in-one vector U670s resulted in a significant

increase in MFI of GFP expression (1.8×10^5 , **** $p < 0.0001$). However, also background expression was higher when transduced with U670s and CBX3. In contrast, the MFI of the GFP expression dropped below the one of the PGK.Tet-control after incorporation of the U1.0s and U1.5s elements (Figure 38B+C). In addition, the U670s Tet-all-in-one vector also revealed the highest fold induction of the MFI (2.8-fold higher than from the PGK.Tet-control vector). The fold induction of the CBX3 vector was in the same range (100-fold) as the PGK.Tet-control and the fold induction of U1.0s (fold induction 31) and 1.5s (fold induction 25) was even below the PGK.Tet-control.

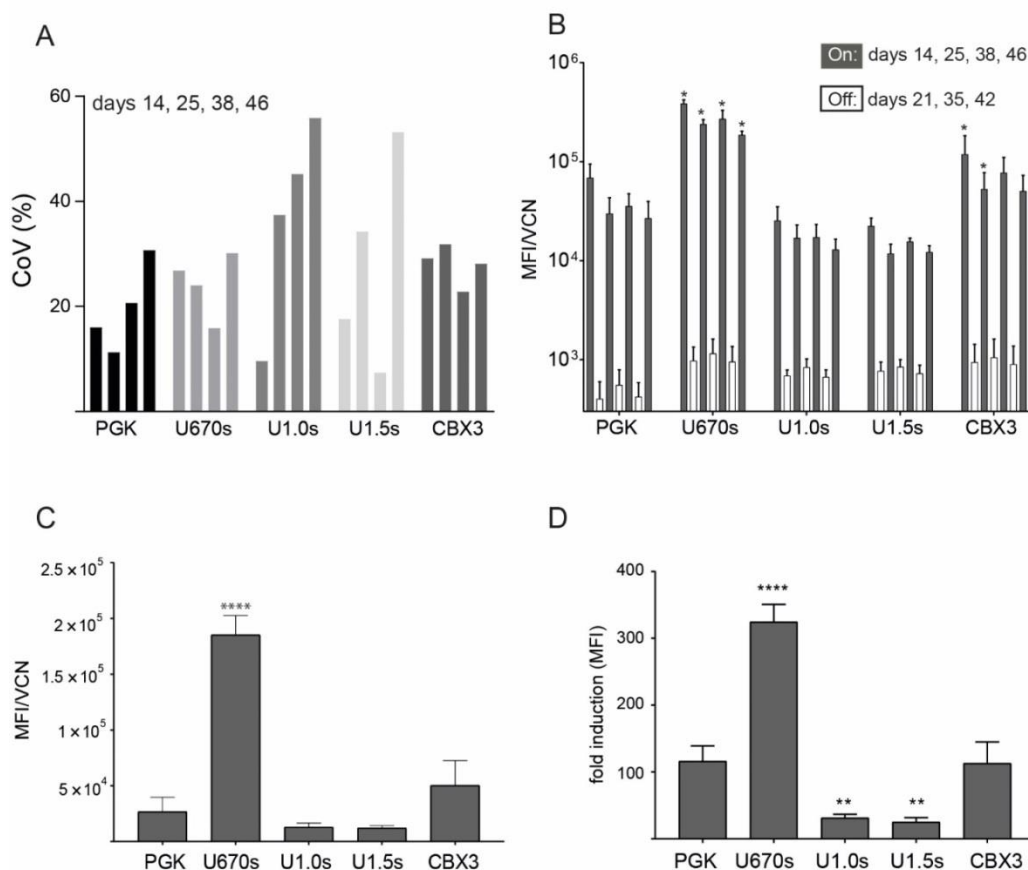


Figure 38 Summary of the regulation of expression from different A2UCOE Tet-inducible vectors in murine iPSC. (A) Coefficient of variegation (CoV) of the percentage GFP expression in murine iPSC. Mean and standard deviation were calculated from 3 individual transductions ($n=3$) at days 14, 25, 38 and 46. Coefficient of variation was calculated by the division of the standard deviation by the mean ($CoV=SD/mean$). Each bar represents the CoV at the respective days. (B) Intensity of GFP expression (MFI) normalized to the VCN. The analysis was performed at days 14, 25, 38, 46 (induced, grey bars) or after withdrawal of dox (days 21, 35, 42, white bars). Comparison of each data point with the corresponding data measured in the PGK.Tet-control group, 2-way ANOVA with Dunnett's multiple comparisons test, * $p < 0.05$). (C) Intensity of expression (MFI/VCN) at day 46 after transduction ($n=3$, mean \pm SD, 1-way ANOVA with Dunnett's multiple comparisons test, **** $p=0.0001$). (D) Mean fold induction MFI. Fold induction was calculated on the basis of 3 different induced and un-induced cultures at three time points, respectively ($n=9$, mean \pm SD, 1-way ANOVA with Dunnett's multiple comparisons test, **** $p < 0.0001$, ** $p < 0.01$).

With an overall culture period of 46 days in total, cultures were followed up for a relatively long culture period. We were interested whether the variance was also different between the beginning and termination of the experiment. To show this, the coefficient of variation (CoV, $SD/mean$) was determined of the induced states at days 14, 25, 38 and 46 after transduction

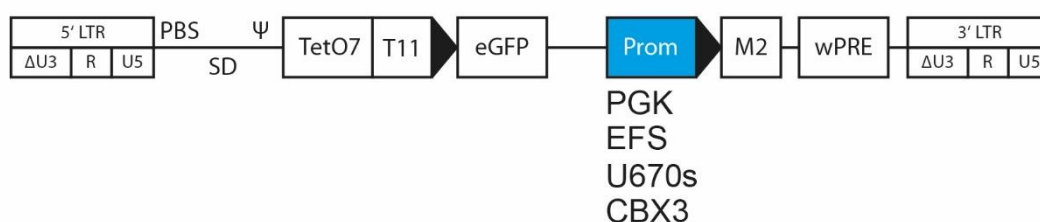
(Figure 38A). While the CoV stayed stable for the Tet-all-in-one vectors U670s and CBX3, the CoV increased after prolonged cultivation period for the U1.0s up to almost 56% (day 46) and U1.5s (up to 53% at day 46) and also slightly for the PGK.Tet-control (30.7%).

4.2.4 Vector performance after replacement of the PGK promoter by a U670s/CBX3 element

The PGK promoter is highly enriched in CpG islands (63 CpG) and was therefore speculated to be the sequence within the gammaretroviral vector which is most vulnerable to methylation and causes shutdown of the expression. The U670 element is located in close proximity to a transcriptional start site of the CBX3 gene and has been reported to have promoter activity itself (Müller-Kuller et al., 2015). It is therefore of interest if the PGK promoter can be excised from the vector and replaced by U670s or CBX3. Furthermore, the EFS promoter, which is already widely used in the field of genetic modification of iPSC with retroviral vectors, was also incorporated in our studies. In addition, lentiviral counterparts of the PGK.Tet-control and the 670s.M2 vectors were generated to compare the capability to sustain GFP expression of gammaretroviral and lentiviral vectors directly. The vector architecture of gamma-/lentiviral vectors with exchanged PGK promoters is shown in Figure 39A. After production of the viral vectors and subsequent titration on SC1 cells, it was shown that viral titers from lentiviral vectors were 30-fold lower compared to their gammaretroviral counterparts (titer gamma U670.M2: 3.7×10^6 IP/ml, titer lenti U670.M2: 1×10^6 IP/ml) (Figure 39B).

A

gammaretroviral/lentiviral vector



B

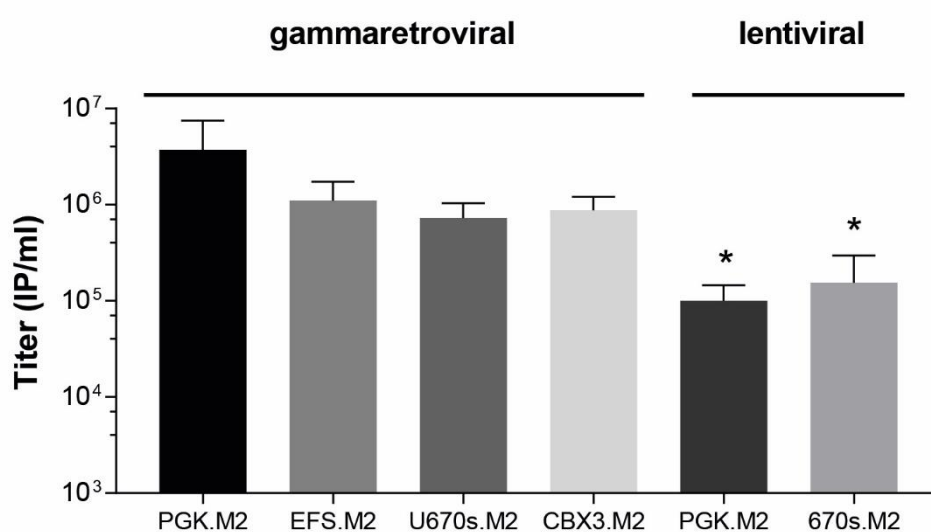


Figure 39 Gammaretroviral and lentiviral Tet-all-in-one vectors with replaced PGK promoter. (A) Vector architecture of the Tet-regulated, all-in-one vectors. The (rt)TAM2 was expressed from either the A2UCOE U670s/CBX3, EFS or PGK promoters (PGK.Tet-control vector). The U670s was also introduced in the lentiviral backbone and compared to the PGK.Tet-control lentiviral vector. (B) Titration of gammaretroviral and lentiviral vectors on SC1 cells. Murine fibroblasts (SC1) cell line was transduced with different volumes of viral vector. Transducing particles per ml were calculated based on the amount of GFP reporter positive cells ($n=3$, mean \pm SD). The titers of the two lentiviral vectors was significantly reduced ($*p=0.02$), Student's t-test.

Similar to the experiments performed in Chapter 4.2.1, the regulatory and anti-silencing potential of the different vectors was assessed by the transduction of the SC1 fibroblast cell line as well as P19 carcinoma cells and the results are included in Figure 40. In these experiments with P19 cells, the transduced and GFP expressing cells were enriched to 100% via FACS to exclude the possibility of competition and selective advantage between GFP⁺ and GFP⁻ cells. The GFP expression was followed over the next 45 days. In SC1 cells, the gammaretroviral vectors U670.M2 and CBX3.M2 expressed distinct GFP⁺ populations similar to the PGK.Tet-control and showed the highest relative intensity in GFP expression (Figure 40A+B). Furthermore, the dynamic range was significantly higher in case of gammaretroviral U670.M2 and CBX3.M2 vectors (~400-fold induction in intensity) compared to the expression in non-induced cells (Figure 40C). The EFS.M2 vector expressed lower intensities and lower-

fold induction compared to the PGK.Tet-control vector and the silencing of the GFP signal in P19 cells was most profound after transduction of the cells with the gammaretroviral EFS.M2 vector (Figure 40E). In contrast, transduction of the P19 cells with the gammaretroviral vectors U670.M2 and CBX3.M2 sustained GFP reporter gene expression to 41% and 37% respectively while the GFP reporter signal of the PGK.Tet-control decreased to 20% (Figure 40E). Exchange of the PGK promoter by the U670s element increased the coefficient of variegation (CV) in gamma-/and lentiviral vectors (Figure 40D).

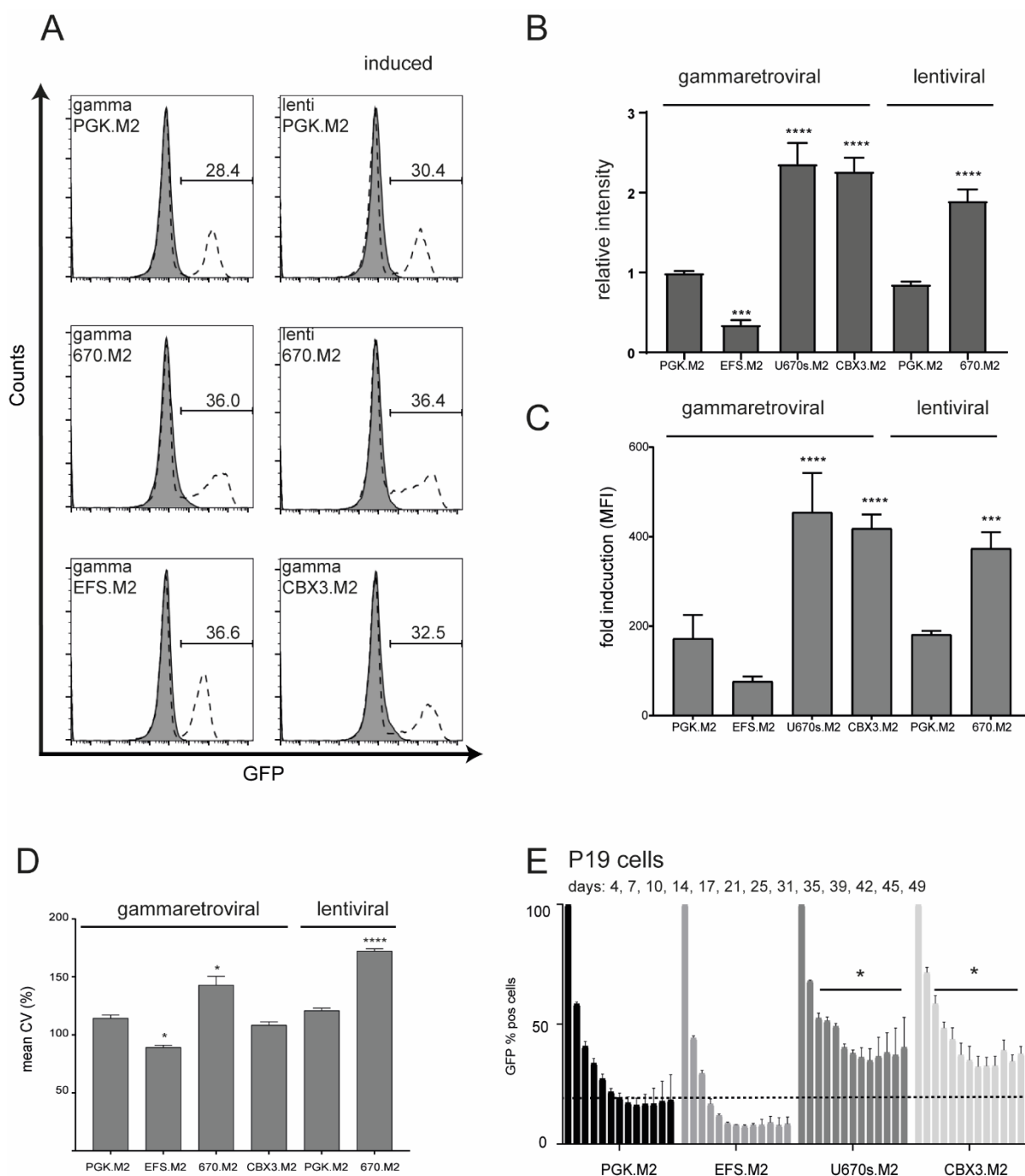


Figure 40 Tet-inducible vectors driving the transactivator by the A2UCOE. (A) Representative flow cytometry analysis of murine SC1 fibroblast cells transduced with the U670s.M2, CBX3.M2, EFS.M2 and PGK.Tet-control vector (PGK.M2) (gammaretroviral vectors) and U670s.M2 and PGK.M2 (lentiviral vectors). Induced: dashed line; non-induced: black line, grey filled area. (B) Relative intensity of GFP⁺ cells (MFI), expression of the PGK.M2 (PGK.Tet-control) is set to 1 (n=3, mean +/- SD, 1-way ANOVA with Dunnett's multiple comparisons test, ****p<0.0001, ***p=0.0005). (C) Fold induction of expression (MFI) from non-induced to induced state (1-way ANOVA with Dunnett's multiple comparisons test, ****p<0.0001, ***p=0.0004). (D) Mean coefficient of variation of SC1 cells transduced with the respective gammaretroviral and lentiviral vectors in the induced state. (1-way ANOVA with Dunnett's multiple comparisons test, ****p<0.0001). (E) GFP expression in P19 cells transduced with the U670s.M2, CBX3.M2, EFS.M2 and PGK.Tet-control vector (PGK.M2). Cells were sorted for GFP expression on day 4 after transduction, GFP expression was analyzed by flow cytometry every 3-4 days until day 49. Horizontal dashed line indicates the endpoint value of the PGK.Tet-control (n=3, mean +/- SD, comparison to PGK.Tet-control for both vectors *p<0.5, 2-way ANOVA with Dunnett's multiple comparisons test).

4.2.5 A2UCOE in Tet-all-in-one vectors in human induced pluripotent stem cells during differentiation

Silencing often occurs during differentiation of iPSC into the cell type of choice when they undergo massive chromatin remodeling. We also tested the above-mentioned candidates in differentiation experiments of human iPSC. The hiPSC line KOLF2 (Sanger Institute, Hinxton, UK) was transduced to an efficiency of 65-100% GFP expression and the functionality of the vectors was assessed using two different experimental designs. In the first approach, the GFP expression of the Tet-all-in-one gammaretroviral vectors U670s, U1.0s, U1.5s and CBX3 as well as the promoter-replaced versions 670s.M2 and CBX3.M2 was assessed during formation of EB by fluorescence microscopy and compared to the PGK.Tet-control. Fluorescent images of the EB are shown in Figure 41. As indicated by the fluorescent microscopy images, the GFP intensities of the U670s element and the promoter-replaced versions U670s.M2 and CBX3.M2 showed the strongest signal. This was verified by the determination of the fluorescent intensities of the fluorescence imaging using ImageJ and is summarized in Figure 41B. The intensities were normalized to the VCN to compensate for the difference in initial GFP expression. The GFP expression could be sustained from the U670s Tet-all-in-one vector (intensity/VCN U670s:3) which was increased 2-fold compared to the PGK.Tet-control (intensity/VCN U670s:1) after 5 days of EB formation. The intensity of GFP expression of U670s.M2 and CBX3.M2 was in a similar range (intensity/VCN 2.9 and 2.6, $p < 0.0001$). The intensity/VCN of the U1.5s and CBX3 Tet-all-in-one vectors in contrast was only slightly increased compared to the PGK.Tet-control (intensity/VCN 1.5, $*p = 0.0042/0.05$). Incorporation of the U1.0s upstream the PGK even decreased the intensity/VCN to 0.6, which is lower than the PGK-Tet.control.

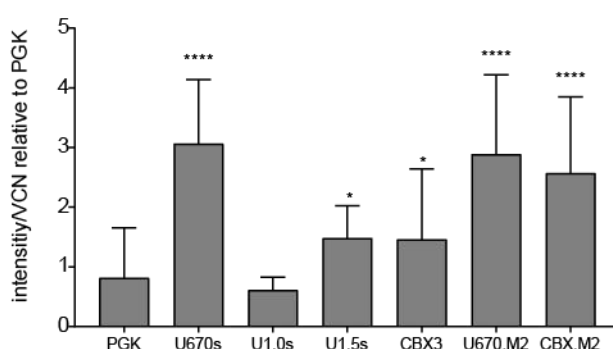
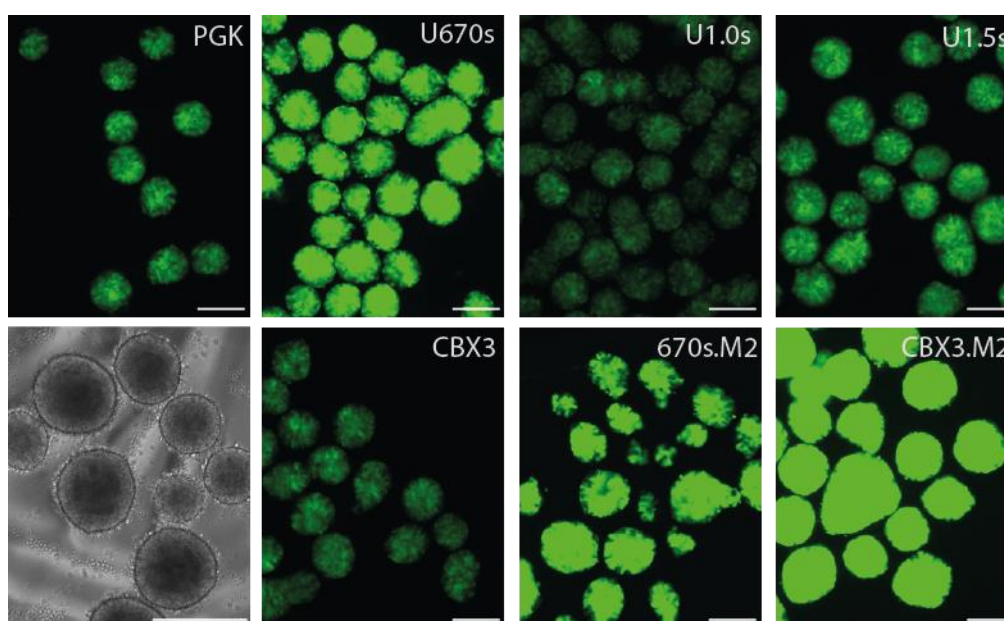
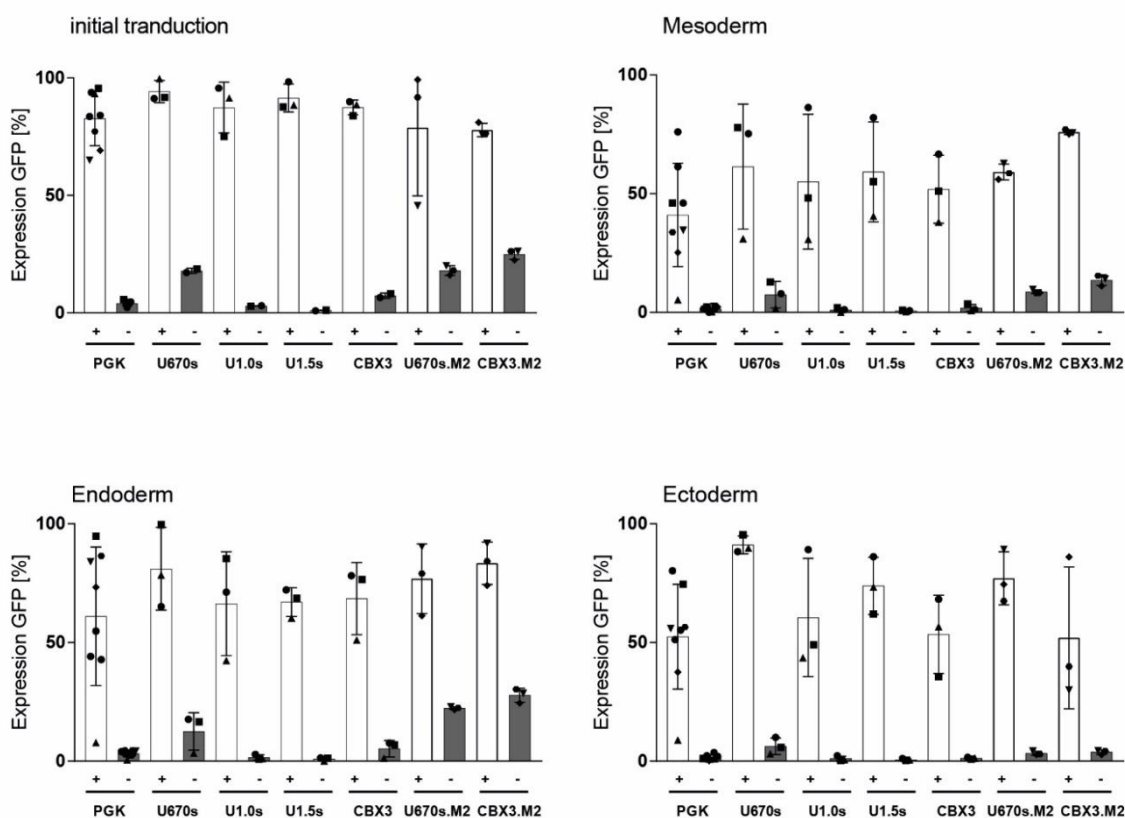


Figure 41 GFP reporter signal analyzed by fluorescent microscopy in EB. (A) Representative pictures of EB differentiated from human iPSC at day 5 of EB formation transduced with different A2UCOE vectors or the PGK.Tet-control. Left bottom: bright field image of EB. (B) Summary of the intensity of GFP expression in EB at day 4 of differentiation (n=3-8 independent transductions and differentiations in four independent fields each, mean +/- SD (1-way ANOVA with Dunnett's multiple comparisons test, ****p<0.00001, *p=0.0042/0.05). The scale bars indicate 200 μ m.

In the second approach, transduced hiPSC were subjected to monolayer differentiation into ectodermal, endodermal and mesodermal germ layers under defined conditions using the Stemdiff™ trilineage differentiation kit (Stemcell Technologies). The hiPSC were transduced to 66-100% GFP expression analyzed by flow cytometry. After completing differentiation into the respective germ layer, GFP expression was again evaluated by flow cytometry (Figure 42). In parallel to the doxycyclin-induced cultures, the respective un-induced cultures were analyzed. Here, the transgene expression has not been induced at any time. Interestingly, in contrast to the differentiations to the EB, the capability to sustain transgene expression after incorporation of the U670s element as well as the replacement of the PGK promoter by either U670s or CBX3 was less profound in all 3 germ layers. This was in part due to the high variability between independent experiments. The GFP expression from the PGK.Tet-control declined after differentiation to about 51 (mesoderm)-61% (endoderm) in meso-, ecto- and

endodermal differentiation. During ectodermal differentiation, GFP expression was most sustained from the U670s element (91% GFP expression). Furthermore, background expression in the non-induced state was highest from hiPSC transduced with U670s and CBX3, an effect that was further increased by the excision of the PGK promoter (U670s.M2 and CBX3.M2).

A



B

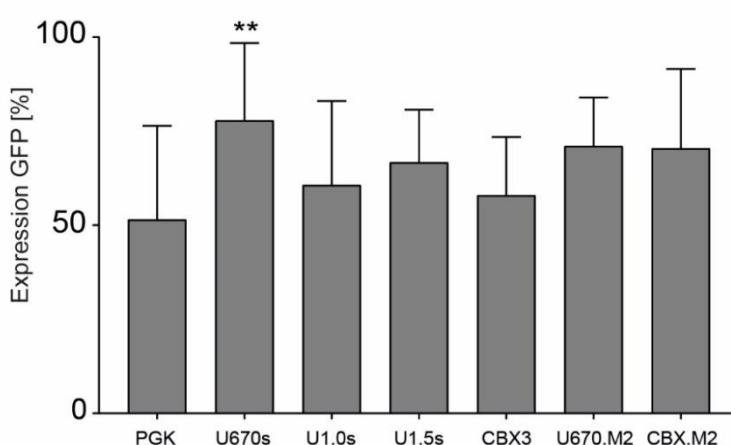


Figure 42 Evaluation of the GFP expression of different UCOE-Tet vectors during 3 germ layer differentiation of hiPSC. Human iPSC were transduced with the Tet-vectors containing the respective A2UCOE. Cells were differentiated into meso-, ecto, and endoderm using the StemDiff™ trilineage differentiation kit (STEMCELL Technologies) Initial GFP expression in human iPS cells four days after induction and their differentiated progeny are shown. (A) Dox-induced (+, white columns) and non-induced (-, grey columns) are plotted for each vector and germ layer respectively. Different symbols represent independent transductions (n=3-8, mean +/- SD). (B) Percentage of GFP positive cells after trilineage differentiation. Percentages in the germ

layers were combined (n=9, PGK N024 mean +/- SD, 1-way ANOVA with Dunnett's multiple comparisons test, **p=0.009).

4.2.5.1 Methylation state of the PGK promoter after differentiation of hiPSC into mesoderm

The PGK promoter driving the expression of the reverse transactivator (rt)TA-M2 in the Tet-all-in-one retroviral vectors is highly enriched in CpG sites (63 CpG in total) and therefore prone to be silenced by methylation of the cytosine residues. As it was shown in Chapter 4.2.2, the GFP expression in P19 cell was restored after introducing a second transactivator by a second viral vector transduction expressing the (rt)TA-M2-mCherry. DNA methylation is one of the major epigenetic silencing mechanisms. We were therefore interested whether the incorporation of the A2UCOE influenced the methylation status of the PGK promoter. Silencing of the PGK promoter could be one explanation because this could influence the generation of sufficient amounts of (rt)TA-M2. Since the U670s gammaretroviral vector showed the greatest potential of sustaining the expression of the GFP reporter signal and because MK and platelets derive from mesoderm, the hiPSC transduced with U670s and PGK differentiated into the mesodermal germ layer were chosen to be investigated. The methylation status was determined by bisulfite conversion of the whole genomic DNA. In this approach, methylated CpGs are protected from the conversion into uracil residues during the conversion whereas non-methylated CpGs are converted into uracil. After PCR amplification of a specific bisulfite-converted sequence, in this case a part of the PGK promoter which is spanning the majority of the 63 CpG sites, the PCR amplicons were subcloned into a TOPO TA cloning (pGEM™) vector and transformed into chemically competent *E.coli* (details see 3.2.1.6.). Different clones were then analyzed by Sanger sequencing and the methylated versus non-methylated CpGs were analyzed with the BiQ Analyzer software. The results of the different single clones as well as the percentages of the methylation state are shown in the diagram in Figure 43. The methylated CpGs are highlighted as black filled circles. The percentage of methylated CpGs increased after transduction with the PGK.Tet-control when hiPSC were differentiated into the mesodermal germ layer (from 19.1% to 36.6%). This effect could not be detected after incorporation of the A2UCOE U670s upstream the PGK promoter. Here, the methylation status was at the similar low level between 4.5% and 3.7% of the CpGs being methylated.

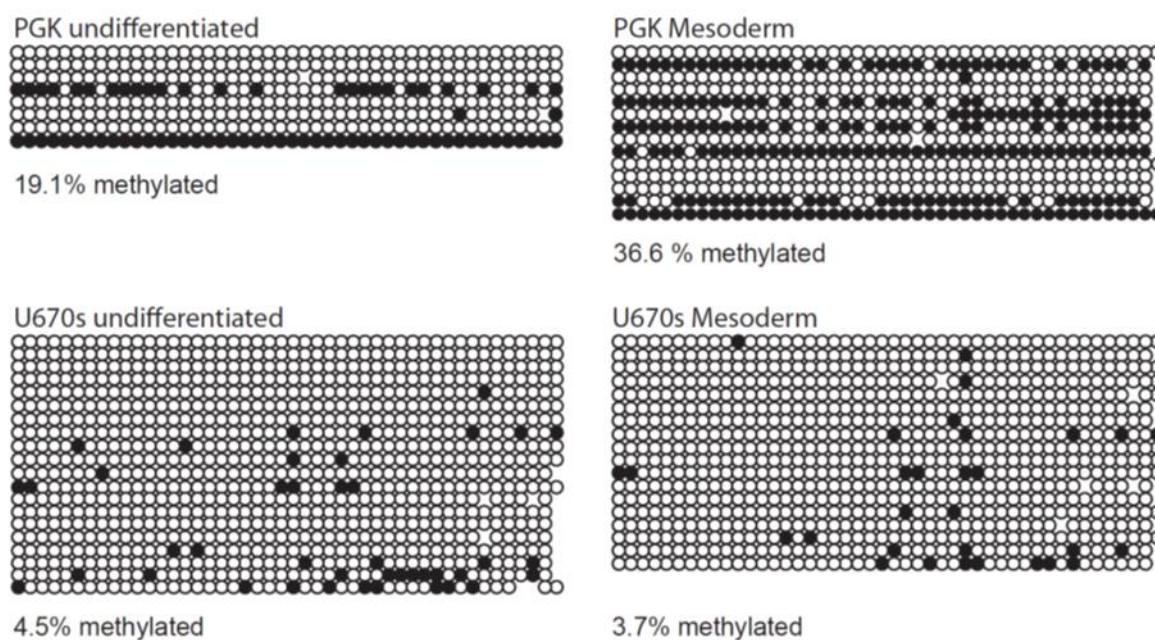


Figure 43 Methylation status of the PGK promoter after incorporation of the U670s element before and after mesodermal differentiation. DNA of human iPS cells at the pluripotent state and after mesodermal differentiation was purified from cultures transduced with the U670s vector or the PGK.Tet-control vector and analyzed by bisulfite conversion and PCR amplifying the PGK promoter. The amplicons were ligated into the pGEM vector and clones sequenced by Sanger sequencing. Methylated CpGs are indicated by the black filled circles.

4.2.6 Expression of Mpl from the UCOE-Tet gammaretroviral vectors

In all our previous studies, the UCOE-Tet vectors expressed the reporter protein GFP. It was therefore of interest whether the Tet-regulated all-in-one vector would also allow the controlled expression of a biologically active protein. To prove this, the Thpo receptor Mpl was incorporated into the Tet-all-in-one U670s vector termed Tet.U670s.Mpl. Mpl expression can be detected on the surface of the transduced cells via an incorporated hemagglutinin (HA) tag using an anti HA antibody by flow cytometry. The vector architecture of the Tet.U670s.Mpl gammaretroviral vector is depicted in Figure 44.



Figure 44 Vector architecture of the Tet.U670s.Mpl gammaretroviral vector. For controlled expression of the Thpo receptor Mpl from the UCOE-Tet vector, the coding sequence was incorporated downstream of the Tet-responsive promoter and upstream of the U670s element into the vector containing the U670s element..

For verification of the functionality of the Thpo receptor Mpl, the cytokine-dependent hematopoietic cell line 32D was transduced with the Tet.U670s.Mpl using two different MOIs

(10 and 20). In the untransduced state, survival and proliferation of 32D cells are dependent on stimulation with the cytokine mIL-3. However, after transduction with Mpl, this can be changed into Thpo-dependent growth of the cells. In this experiment, we used the Thpo/Mpl-dependent growth advantage of Mpl-transduced 32D cells to prove the biological functionality of the transgene delivered by the UCOE-vector. Mpl-transduced cells were selected by the supplementation of Thpo to almost 100% of Mpl expression as indicated by the dashed line in Figure 45A. Cell viability was analyzed by performing PrestoBlue® assays. In this fluorescence-based assay, the resazurin blue non-fluorescent dye is incorporated by the cells. Metabolically active cells quickly reduce resazurin to the fluorescent active metabolite resofurin which can be detected at an excitation wavelength of 530-570nm and an emission of 600nm with a spectrophotometer. 32D cells expressing Mpl were expected to have a higher viability and proliferation when incubated with Thpo compared to cells which do not express the Mpl receptor. Mpl negative cells will proliferate less and, therefore, a lower number of cells will be viable and can be measured in the viability test. As a control, 32D cells were transduced with the U670s.GFP vector. In our experiment, after enrichment of the cells, the cell viability was assessed 40h after Thpo re-stimulation and compared to non-induced cells. During the time of 40h, 32D cells are expected to divide at least once. By the application of PrestoBlue®, the measure of the cell viability will also reflect the increased number of viable cells due to increased cell proliferation in 32D.Mpl cells in contrast to 32D.GFP cells. Cell viability of 32D cells transduced with Tet.U670s.Mpl in the non-induced state was set to 1 (dashed line). 32D cells expressing the Mpl receptor on the surface in the induced state after application of dox showed a viability which was twice as high compared to the non-induced counterparts, indicating that the receptor which was transduced was functional after application of dox. In contrast, 32D cells expressing no functional transgene did not show differences in cell viability between the induced and uninduced state of the vector (Figure 45B).

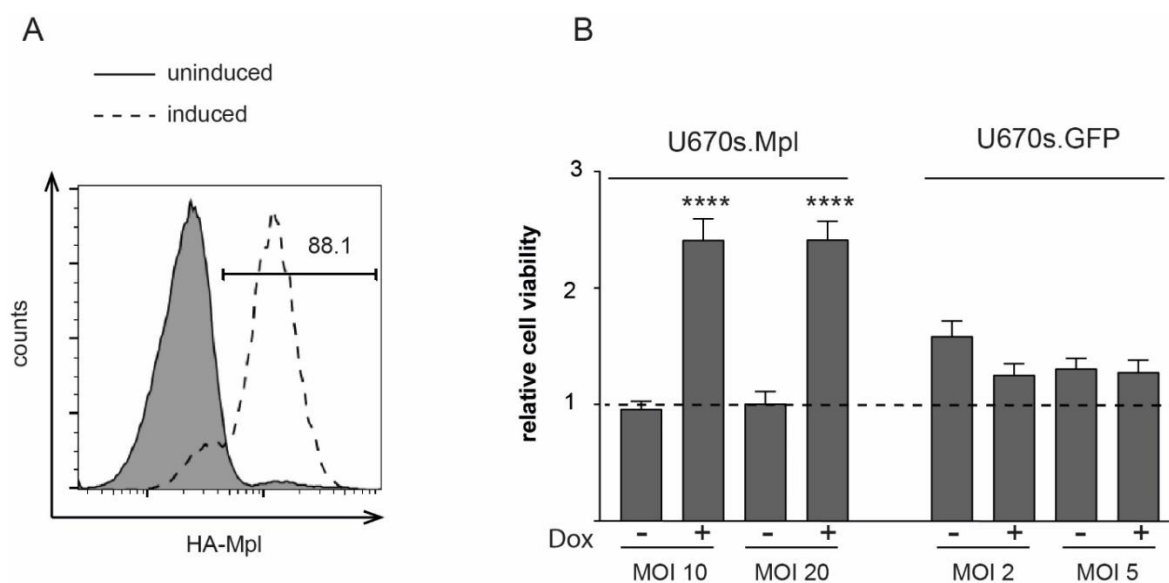


Figure 45 Determination of the functionality of the Tet.U670s.Mpl vector. For functionality tests, the murine hematopoietic cell line 32D was transduced and analyzed according to their expression of the transgene as well as viability as indicator for cell proliferation. (A) Representative flow cytometry plot of Mpl expression in 32D cells. After transduction of the cells with the Tet.U670s.Mpl vector, the Mpl expression was analyzed by detection of the incorporate HA tag via flow cytometry. (B) Viability of Mpl-expressing 32D cells. After Thpo-dependent enrichment of HA-Mpl-positive 32D cells, the cells were plated with 5ng/ml Thpo in the induced and non-induced state for 40h and cell viability was analyzed by the addition of the PrestoBlue®. Emission was detected after incubation for another 16h. Relative cell viability was determined by normalization to untransduced control (set to one, indicated by the dashed line). Cell viability of U670s.Mpl expressing cells was compared to transduced cells with the U670s.GFP (n=3, mean +/-SD, Students t-test ****p<0.0001).

5 DISCUSSION

5.1 Production of platelets and megakaryocytes *in vitro* from R26M2 iPSC

5.1.1 R26M2K2 iPSC for the generation of megakaryocytes and platelets *in vitro*

The production of functional platelets from pluripotent stem cells would provide an unlimited supply for patients of acute need for platelet transfusions. Furthermore, the use of murine iPSC would provide a powerful tool for disease modeling studies *in vivo*. Transfusion experiments of culture-derived platelets or MK could be performed in a syngeneic context. To date, the production of platelets in culture is still challenging due to limitations in platelet numbers and impaired functionality of the differentiated cells. Overexpression of supporting factors that either increase the numbers of generated MK or the release of platelets per MK and the functionality of the differentiated cells would provide a powerful tool towards future therapeutic applications of culture-derived platelets. In the first part of the study, we were aiming for the defined overexpression of the single supporting factors Gata1, Nfe2, Pbx1, Evi1, RhoAhc, and Cdc42hc via dox-inducible gammaretroviral vectors to support *in vitro* MK and platelet biogenesis from murine iPSC. The factors were transduced in the pluripotent state and induced in a dox-inducible manner to prevent unwanted effects during the course of differentiation. Another hurdle was the silencing of ectopic factors by iPSC especially during differentiation. In many Tet-all-in-one gammaretroviral vectors, the transactivator (rt)TA-M2 is expressed from the PGK promoter, which is highly enriched in CpG sites and therefore prone to be silenced. The generation of R26M2 iPSC from B6.Gt(ROSA)26Sor^{tm1(rtTA^{*}M2)Jae}/J mice, expressing the transactivator from the Rosa 26 safe harbor locus, allowed overexpression of the supporting factors independent of the PGK promoter. The R26M2 iPSC allowed stable expression of the tested transgenes. Pluripotency was verified on protein expression (flow cytometry experiments for SSEA-1 expression, detection of Oct3, Sox2 and Nanog by fluorescence microscopy, alkaline phosphatase activity) and mRNA levels (detection of Oct3, Sox2 and Nanog by qRT PCR). The study of A. Mucci et al., in which the same reprogramming vector was applied, also showed similar results, e.g. mRNA expression levels of the pluripotency markers Oct4, Sox2 and Nanog reaching the same expression levels as OG2 ESC (Mucci et al., 2018). Since the detection of the copy number identified R26M2K2 to be the clone having one integration only, further studies have been performed with this clone. To date, there are more sophisticated non-integrating reprogramming technologies available to generate footprint-free iPSC, e.g. non-integrating

viral vectors (sendai viral vectors, adenoviral vectors, adeno-associated viral vectors) based on reprogramming, plasmid transfection (including minicircles) and/or RNA delivery (Seo et al., 2017). Sendai virus-based viral vectors for example do not rely on the entrance to the nucleus and produce large amounts of protein. The reprogramming efficiency varies between 0.1 and 4%. However, it can take up to 25 passages until the residual viruses are diluted from the cells (Fusaki et al., 2009; Haridhasapavalan et al., 2019). Reprogramming efficiencies after plasmid transfection and with minicircle vectors are even lower due to their transient expression (Si-Tayeb et al., 2010; Haridhasapavalan et al., 2019). In our study, we were aiming for the generation of platelets as a final product from the differentiation. We were therefore not dependent on non-integrating reprogramming methods. However, incomplete silencing of the transgene cassette might also have influenced the differentiation efficiency as it has also been reported in several other studies (Haridhasapavalan et al., 2019). For example Kadari et al. have shown that Cre-mediated excision of the transgene cassette improved cardiac differentiation (Kadari et al., 2014). The reprogramming cassette of the vector used in this study is also flanked by FRT sites for potential Flp-mediated excision. It could be tested in future experiments whether this would also lead to improved differentiation efficiencies in our studies. After successful generation of the Tet-responsive gammaretroviral vectors containing Gata1, Nfe2, Pbx1, Evi1, RhoAhc, Cdc42hc, titration and transduction of R26M2K2 showed Evi1.iGFP to produce markedly lower titers compared to the other factors tested and efficient transduction could also not be achieved (Figure 10+11). Overexpression of Evi1 in the human BM cell line U2OS led to an arrest in the cell cycle in the G0/G1 phase and impaired proliferation (Karakaya et al., 2012). Similar results have been obtained in the study performed by Kustikova et al. Here, overexpression of Evi after transduction of Lin-BM cells led to an initial growth inhibition and cell cycle arrest (Kustikova et al., 2013). For these reasons, Evi1.iGFP-transduced cells in our study might not have been able to proliferate and were therefore not followed up.

5.1.2 Comparison of single supportive factors during MK differentiation and terminal maturation

After transduction of the R26M2K2 iPSC, the cells were subjected to differentiation into EB using the approach published by Pfaff et al. The protocol generated immature CD41⁺ hematopoietic stem and progenitor cells after 7 days of EB formation by the supplementation with mScf and mIL-3 (Figure 12) (Pfaff et al., 2012). According to what was published by A. Mucci et al., the protocol was modified in terms of generating EB via application of mechanic forces by orbital shaking (Mucci et al., 2018). Terminal

differentiation of MK and platelets occurred after co-cultivation on mitomycin C-treated OP9 feeder cells and supplementation of mScf and mThpo. With this protocol, MK and platelets were obtained after 2-3 weeks of starting the co-cultivation, which was delayed in comparison to the study by Lu et al. where fully mature MK were observed already 6 days after starting the co-culture from human ESC with similar cytokine conditions. In contrast to the differentiation protocol we used in the study, cells were differentiated into hemangioblast cells prior to co-cultivation (Lu et al., 2011). After harvesting the MK by day 21 of differentiation, the GFP expression from the transduced factors was detected by flow cytometry. The occurrence of a distinct GFP⁺ population was absent for all of the factors, indicating a high position effect variegation of the integrated vectors and thereby causing the distinct expression profiles (Figure 13). Differentiation of the R26M2K2 into cells of the MK lineage was possible, independent of the transduced factors as indicated by the apparent dark stain of the cytoplasm and the occurrence of the multilobulation of the nuclei (Figure 14). The morphology of the cells was similar to those of the differentiated MK from murine and human PSC cells in other studies (Noh et al., 2015). However, in our experiments, the occurrence of fully mature multilobulated nuclei was rare, if not completely absent. One explanation for this could be that iPSC-derived MK still resemble a fetal phenotype. It was observed that MK differentiated from human cord blood are generally smaller in size with lower ploidy compared to CD34⁺ derived MK isolated from adult blood or BM (Miyazaki et al., 2000; Mattia et al., 2002). Studies performed by Potts et al. also showed that platelets can be generated from yolk sac-derived, relatively small MK with only diploid nuclei (Potts et al., 2014). Since the branching of the MK could be detected in our *in vitro* differentiation (Figure 15), this would point to a more fetal phenotype which was differentiated in our cultures.

Furthermore, experiments performed in our own group have shown that the expression of the P-selectin marker in non-activated and activated platelets from the *in vitro* cultures was very low whereas the conformational change of the CD41/CD61, which also indicates platelet activation, could be detected by flow cytometry (Jahn, 2019). The low level of the expression of the P-selectin marker was also previously shown in fetal platelets and is another sign for platelets of a fetal phenotype.

In the next experiments the expression of the MK-specific surface receptors were evaluated by flow cytometry. In general, we observed a higher CD41 expression within the GFP⁺ population which was most distinct for MK harvested from Gata1-transduced cultures (Figure 17). Higher percentages of CD41 expression is also a sign that MK maturation has started. During the course of differentiation, endomitosis leads to an increased DNA content this in turn leads to the accumulation of GFP in cells that are more mature (CD41⁺). This is especially of importance for the expression of CD42d (Figure 18).

The analysis of the surface phenotype of differentiated MK showed that overexpression of Gata1 resulted in higher percentages of cells expressing the CD41 surface marker (about 70%) within the GFP⁺ population compared to the other candidate factors which were in the range between 19% (Cdc42.iGFP) and 40% (Pbx1.iGFP) (Figure 17). This indicates that Gata1 had a positive effect on the differentiation of the earlier MK progenitors. In contrast, an increase of CD42d expression could not be confirmed for the Gata1-overexpressing differentiations (Figure 19). In these cultures, the percentage of CD42d within the GFP⁺CD41⁺ population was lowest. Overexpression of Gata1 enhances differentiation of early CD41⁺ progenitors which are impaired in terminal maturation.

We have seen a spread in numbers of MK differentiated from Gata1-overexpressing cultures as indicated by the high error bars (Figure 20). Mutations in the *GATA1* gene occur in almost all of the cases of transient myeloproliferative disorder of Down syndrome-associated leukemia in neonates with trisomy 21 and are thought to be the founder mutations of the malignancies. The mutations are to date utilized as a diagnostic marker (Lee et al., 2018). These somatic mutations mostly occur in exon 2 of the gene leading a premature stop codon and forcing the start of the gene from the alternative start codon in exon 3 leading to an N-terminal truncation of GATA1 (GATA1s). Almost all of the blast cells in turn show the same mutation indicating a clonal dominance. The occurrence of the blast cells is also associated with a differentiation arrest (Gruber and Downing, 2015; Lee et al., 2018).

In mice, lineage-specific knockout of *Gata1* results in low platelet numbers associated with deregulated MK proliferation and impaired cytoplasmic maturation (Shivdasani et al., 1997). In addition, the knockout of *Gata1* influences platelet granule formation as well as release (see Chapter 1.4). Since these evidences pointed into the direction of Gata1, influencing megakaryopoiesis and platelet generation, we thought that overexpressing this factor may be sufficient for enhanced MK and platelet production *in vitro*. The impairment of MK maturation of Gata1-overexpressing MK in our experiments shows that the hypothesis of Gata1 overexpression alone leading to increased fully mature MK generation was not confirmed since the expression of CD42d as mature marker was impaired. Rescue experiments in *Gata1* knockout mice have shown that overexpression of Gata1 together with its co-factor Fog1 was able to restore MK formation and pro-platelet formation whereas Gata1 overexpression alone was not sufficient (Shimizu et al., 2004). Expression of Gata1 in combination with Fog1 could be another combination that could be tested in future experiments.

The size and ploidy of the differentiated MK in our experiments was rather low, pointing towards a more fetal phenotype. Fetal and neonatal MK proliferate faster, they are smaller and have a lower ploidy (Alarcon and Graeve, 1996; Ma et al., 1996; Mattia et al., 2002;

Sola-Visner, 2012). In contrast, fetal MK are more cytoplasmatically mature, as indicated by the increased expression of the CD42b receptor. It has been shown that the level of GATA1 expression is higher in cord blood- than in peripheral blood-derived MK (Liu et al., 2011). It could be that by overexpression of Gata1 in our experiments, we have shifted the phenotype of the differentiated MK towards a fetal state. Fetal and neonatal MK rapidly expand to populate the growing BM space and blood volume. To confirm the positive effect of Gata1 overexpression in our study, we could analyze Gata1 target genes such as VWF, GPIIb α and PF4 as it was shown in the study by Noh et al. In contrast to our study, Noh and colleagues regulated the Gata1 expression by dox-inducible knockdown. This approach generated fully mature MK (Noh et al., 2015).

In the study by T. Moreau and colleagues, a combination of the transcription factors GATA1, FLI1 and SCL1 were expressed in human pluripotent stem cells and led to the production of mature and cryopreservable MK (Moreau et al., 2016). Similar approaches by defined overexpression of MYC during differentiation and supplementation of the culture medium with the anti-apoptotic protein (drug) BCL-XL have led to increased expression of GATA1 and NFE2, indicating those to be key factors for *in vitro* differentiation of platelets leading to the generation of immortalized MK progenitor cells (Nakamura et al., 2014). In a similar manner, also in our experiments, only cultures overexpressing Gata1 could be expanded and allowed the generation of sufficient numbers of platelets to perform platelet activation experiments. In these cultures, Gata1 overexpression led to the differentiation of about 1.5×10^4 CD41⁺MK progenitors, which was a 15-fold higher number compared to the iGFP.control which only produced around 2000 CD41⁺ MK (Figure 20).

Nfe2 is a major regulator of platelet release as indicated by prenatal death in Nfe2 knockout mice due to hemorrhages or development of postnatal thrombocytopenia (Shivdasani 1995). Furthermore, loss of Nfe2 in zebrafish blocks thrombopoiesis and a secondary expansion of thrombocytic precursors (Rost et al., 2018), underlining the essential role of Nfe2 for platelet release. Based on these observations, we chose to overexpress Nfe2 as a single factor in our study. Interestingly, MK differentiated from Nfe2 overexpression showed the highest percentage of CD42d expression within the GFP⁺CD41⁺ population (78%), although this observation did not test significant, probably due to higher variance (Figure 19).

In addition to the transcription factors, also GTPases such as RhoA and Cdc42 are of importance in MK maturation and platelet release. Knockout of both RhoA and Cdc42 respectively in mice leads to the formation of severe macrothrombocytopenia. We wanted to investigate whether their overexpression during *in vitro* differentiation would also

increase platelet formation *in vitro*. Since GTPases are cycling between inactive (GDP-bound) and active (GTP-bound) state, hyperactive, fast cycling variants (hc) were overexpressed to guarantee their permanent activation (Dütting et al., 2017). Studies in MK differentiated from murine Lin- BM cells *in vitro* detected Cdc42 expression to be upregulated during DMS formation and polyploidization and knockout of Cdc42 reduced this. In this study it was observed that DMS formation as well as the formation of pro-platelets relies on F-actin polymerization and that this was regulated by active Cdc42 (Antkowiak et al., 2016). An increase in demarcation membrane formation by the overexpression of Cdc42 would therefore explain the higher percentages of CD41 expression and CD42d within the CD41 mature MK, indicating a more mature phenotype compared to the iGFP.control (Figure 17+19). The influence of Cdc42 overexpression on demarcation membrane formation and F-actin polymerization in *in vitro* cultures has to be further verified with electron microscopic imaging and immunofluorescence of the MK in future experiments. In addition, the GTPase RhoA has also been identified to be a major regulator of megakaryopoiesis and platelet release. Studies performed by A. Suzuki et al. have shown that it regulates cytokinesis during the pro-megakaryoblast stage, endomitosis, and migration of the MK within the BM matrix and these were impaired in mice with a conditional knockout (Suzuki et al., 2013). In the publication from S. Dütting et al., it was shown that there exists a regulatory circuit between Cdc42 and RhoA whereas RhoA functions more as a stop signal for pro-platelet production (Dütting et al., 2017). In our experiments, overexpression of RhoAhc did not lead to increase in numbers of differentiated MK that were harvested from the *in vitro* cultures and also the expression of the surface markers CD41 and CD42d were only slightly increased, indicating its influence on the MK only to a minor degree (Figure 17, 19, 20).

Studies performed in our own group have shown that overexpression of Pbx1 in a Mpl-deficient murine BM transplantation model generated increased numbers of MK (Kohlscheen, 2015). In our study, an increase in MK production by the overexpression of Pbx1 during the differentiation of murine MK and platelets could not be detected (Figure 17, 19, 20). The observations made by S. Kohlscheen were based on the Thpo/Mpl deficient model. In these experiments, Pbx1 overexpression might function as an alternative pathway since all signaling pathways in the iPSC differentiation are intact and therefore the effect of Pbx1 may be too weak to have a detectable influence on the MK differentiation *in vitro* from murine iPSC.

In conclusion, the expression of one transcription factor alone might not suffice for generating the greatest output of *in vitro* generated MK. Gata1 should be included in the panel because of its great influence on MK proliferation in early stages. Since the

overexpression of Nfe2 in our experiments resulted in the increased percentages of fully mature MK that also expressed CD42d, the combined overexpression of Gata1 and Nfe2 may provide another possibility to increase platelet generation from pluripotent stem cells *in vitro*. This has to be further verified in additional differentiations with overexpression of Gata1 and Nfe2, simultaneously. For this purpose, we have generated 2 different clones of Gata1-transduced R26M2K2 which could be transduced with Nfe2 in an additional step. Furthermore, it would be possible to generate a gammaretroviral vector expressing Gata1 and Nfe2 from the same vector.

5.1.3 Comparison of candidate factors on platelet generation from R26R2K2 iPSC

In addition to the MK, also platelets were analyzed. As indicated in Figure 23, the ultrastructure of the platelets was similar to that of freshly isolated platelets as shown in several publications (White and Rao, 1982; Chang et al., 2007). Even though they could not all be detected within one platelet, all different ultrastructural features were present, such as the different types of granules, mostly α -granules and δ -granules as well as OCN and mitochondria. The size of the cells (approximately 2-7 μ m) was, however, increased compared to platelets freshly isolated from mouse blood. This has also already been detected in other *in vitro* platelet differentiation studies and is a phenomenon that is also known from fetal platelets (Saving et al., 1994; Feng et al., 2014). Most likely, the lack of the shear force would explain the increased size of the platelets, but in addition it is another hint for the generation of more a fetal-like phenotype of platelets that were differentiated from our cultures.

Discrimination between GFP⁺ and GFP⁻ populations was not performed in platelets since GFP expression could not be detected by flow cytometry. The reason for the GFP expression not being propagated to the platelets remains unclear. Studies on transduction of HSPC by viral vectors expressing GFP from different lineage-specific promoters by our own group have shown that *in vivo*, the transgenes were detected in platelets descending from the modified HSC in transplantation experiments, however, this was highly dependent on the internal promoter. In this study, promoter fragments of lineage-specific genes were analyzed for their expression in MK and platelets. It was shown that the promoter descending from the platelet factor 4 (*PF4*) gene had the strongest activity in MK and platelets (Latorre-Rey et al., 2017). It could be the case that the T11 minimal promoter used for the expression of the transgenes in this study did not generate sufficient amounts of protein that could be propagated to the platelets. Significant differences in either CD41 expression or CD42d within the CD41⁻ population were not detected, indicating a similar equipment of surface receptors on the platelets released

(Figure 22). The percentage of CD42d⁺ cells within the CD41⁺ population of the platelets differentiated *in vitro* was in general very low and varied between 7% (iGFP.control) and 25% (RhoAhc.iGFP). This may also be due to the expression of the CD42d. The GPIb-IX-V receptor mostly interacts with the VWF and thereby mediates platelet activation. The GPIb-IX (CD42a, CD42b, CD42c) subunit of the complex is highly integrated into the membrane whereas the GPV (CD42d) is only loosely associated (Modderman et al., 1992). The expression of the receptor on the plasma membrane only requires the association of the GPIb α , GPIb β and GPIX subunits of the receptor and the subunits interact with and stabilize each other (López et al., 1992; Li and Emsley, 2013). The deletion of the GPV in mice has shown that expression and functionality of the residual receptor components was still present (Kahn et al., 1999; Ramakrishnan et al., 1999). In turn, after deletion of the GPIb α , GPIb β and GPIX, GPV was not expressed on the surface of transfected cells (Strassel et al., 2004). Furthermore, the bleeding disorder Bernard-Soulier syndrome is only associated with mutations within the GPIb α , GPIb β and GPIX subunits but not GPV (Li and Emsley, 2013). PSC-derived platelets from other studies with human iPSC have generated higher percentages of CD41/CD42 double-positive cells up to almost 60% (Börger et al., 2016; Moreau et al., 2016). In these studies, antibodies against the CD42a (GPIX) were utilized for detection of the GPIb-IX-V multiprotein complex. In contrast, we utilized the CD42d (GPV) for detection of the receptor complex. Even though GPV is a late marker for MK and platelets, taking into account that the GPV is only loosely associated with the receptor and that it is not necessary for the assembly and receptor expression on the surface and is also shed faster after activation, we should include other markers (eg.CD42a) into our analysis to prove the full expression of the receptor on the surface. This should also be adapted for the analysis of MK in future experiments. Detecting only CD42d may not have been sufficient. Additionally, we have shown that platelets released from the Gata1-overexpressing clone were pre-activated in the cultures (Jahn, 2019). During platelet activation, shedding of GPV occurs after addition of agonists like thrombin, matrix-metallo-proteinases (ADAM10, ADAM17) and stress-induced reactive oxygen species (Au and Josefsson, 2017). Taking this into consideration, it could be that in pre-activated culture-derived platelets the detection of CD42d expression was reduced.

5.1.4 Platelets differentiated from Gata1-overexpressing R26M2K2 iPSC were functional

Functional analysis of *in vitro* differentiated platelets by platelet spreading assays was only performed in case of Gata1-overexpressing iPSC since they were expandable, as indicated by the higher cell numbers of CD41⁺ cells (Chapter 4.1.5.3). Platelets were identified using confocal microscopy according to their expression of GPVI, CD41/CD61 and β 1-tubulin. As seen in the platelets isolated from whole blood as control, platelets undergo a shape change losing their discoid shape (resting state, β 1-tubulin ring distinct) and become spherical, followed by formation of filopodia and lamellipodia (β 1-tubulin ring disintegrated) (Figure 27+28) (Bearer et al., 2002). We could verify the expression of the CD41/CD61 on the culture-derived platelets by confocal microscopy. Additionally, the expression of GPVI and the distinct ring structure of β 1-tubulin were detectable in the resting state on Poly-L-Lysine-coated cover slips. The spreading on CRP and fibrinogen indicates that the platelet receptors, responsible for the attachment to the matrices, were functional. This goes in line with the results by Moreau and colleagues showing attachment of *in vitro* generated platelets from human iPSC on fibrinogen (Moreau et al., 2016), who also could visualize the β 1-tubulin ring at the cortex of the *in vitro* differentiated platelets as well as their spreading. During activation platelets lose the discoid shape and become spherical and extend filopodia which are long (0.1-0.3 μ m), finger-like membrane protrusions which contain tight bundles of F-actin. Formation of filopodia increases the contact between the extracellular matrix or juxtaposed other platelets (Goggs et al., 2015). Subsequently, lamellipodia, which are also F-actin filaments, fill the gaps between the filopodia, leading to the final platelet spreading and thereby persistent cellular protrusions (Mejillano et al., 2004; Paknikar et al., 2019). Formation of filopodia and lamellipodia relies on cytoskeletal rearrangements controlled by GTPases such as RhoA, Cdc42 and Rac1 (Goggs et al., 2015). In contrast to our observations, Moreau et al. observed lamellipodia formation (Moreau et al., 2016). Spreading of the *in vitro* generated platelets in our experiments resulted in the formation of filopodia, however, the formation of lamellipodia and thereby the endpoint of platelet spreading was absent. The platelet spreading on fibrinogen in our study was, therefore, similar to results observed from studies which lack the expression of Rac1, another very important GTPase involved in cytoskeleton reorganization (Hall et al., 2003). Rac1 stimulates actin polymerization via suppressor of cyclic AMP receptor (SCAR)/WASP family verprolin-homologous protein (WAVE) (Rac binding proteins). The SCAR/WAVE complex in turn activates the Arp2/3 complex which leads to the forming of branching actin-filaments and absence in Rac1 also implicates lack of lamellipodia formation in platelets (McCarty et al., 2005). The reason for the impairment of lamellipodia formation of

our *in vitro* generated platelets has to be further investigated, but in addition to RhoAhc and Cdc42hc, we could include Rac1 in future overexpressing experiments. The inducible overexpression MK still might indeed improve the platelet functionality. This absence of lamellipodia formation was independent from the matrices and agonists applied. In a very recently published article by Y. Schurr et al., it was shown that lamellipodia formation was not required for thrombus formation and stability, indicating that culture-derived platelets, even though their spreading is impaired, still can be utilized for clinical application (Schurr et al., 2019). This has to be further verified in *in vivo* studies with the *in vitro* differentiated platelets.

5.1.5 Overexpression of Nfe2 during differentiation increased the platelet production per megakaryocyte

The general number of platelets produced was highest from Gata1-overexpressing differentiations with 5×10^5 CD41⁺ platelets and 6.5×10^4 CD42d⁺ within the CD41⁺ population (shown in Figure 25). This might also be due to the overall higher numbers of CD41 positive progenitors that were also differentiated from Gata1-overexpressing cells. However, the highest numbers of platelets per MK were generated from Nfe2-overexpressing cells (Figure 25). Here, 101 CD41⁺ platelets and 22 CD42d⁺ (within the CD41 positive population) were generated per MK (Figure 25B). In case of the CD41⁺ platelets, this is about 5 times higher than the number of CD41⁺ platelets that were generated from the iGFP.control-overexpressing cells. This is also markedly higher than the numbers of platelets per MK that were generated in other studies which are in the range between 3 and 10 platelets per MK (Moreau et al., 2016; Sugimoto and Eto, 2017). The results for platelet counts received from these studies were based on the expression of the two surface antigens CD41 (GPIIb) and CD42d (GPV). Again, the detection of the CD42d (GPV) on the surface of differentiated platelets could be misleading since it can be shed during platelet activation. Taken into consideration that the receptor is shed, the actual amount of platelets generated by MK with the overexpression of Nfe2 might be even higher, making it an ideal candidate for combined-regulated overexpression in future experiments. However, *in vivo* MK are capable of releasing up to 1000-2000 platelets per MK (Sugimoto and Eto, 2017). To date, these amounts are still not achieved with any of the differentiation studies *in vitro*. It might be possible that due to the embryonic/iPSC background of the cells, also the differentiated MK may resemble more a fetal phenotype. Fetal MK differentiated from human cord-blood-derived CD34⁺ cells form fewer pro-platelets compared to those isolated from adult blood (Mattia et al., 2002; Elagib et al., 2018). Since the platelets isolated from our *in vitro* differentiations were also larger in size (up to 6µm) compared to murine platelets *in vivo* (0.5µm), another explanation for the low

cell numbers could be the lack of the shear force which *in vivo* leads to the shedding of the platelets into the circulation. Several groups have been working on the development of bioreactors to mimic these shear forces and could escalate the platelet yield (Thon et al., 2014; Blin et al., 2016). Based on the observation that turbulence is a critical factor for platelet release *in vivo*, Y. Ito et al. generated a bioreactor mimicking the turbulence *in vitro* and resulting in a yield of 70-80 platelets per MK (Ito et al., 2018). Although this approach still is nowhere close to the 1000-2000 platelets per MK produced *in vivo*, a combined approach of Nfe2 overexpression and application of a platelet bioreactor would lead to a faster generation of *in vitro* platelets to generate the tremendous amount of 4-5 x 10¹¹ platelets needed for one transfusion unit.

5.2 Incorporation of A2UCOE to prevent silencing of Tet-all-in-one gammaretroviral vectors

5.2.1 Incorporation of some of the A2UCOE lowers titers and interferes with regulation of Tet-all-in-one gammaretroviral vectors

After incorporation of the different elements upstream of the PGK promoter in either sense or antisense orientation, it turned out that elements of larger sizes lowered viral vector titers of about 7-fold. This was most profound after incorporation of the U1.5s element which only reached a titer of about 1 x 10⁴IP/ml and is about 70-fold lower compared to the PGK.Tet-control (Figure 31). Most likely, bi-directionality of the promoter interfered with efficient transcription during packaging and after integration, thereby impairing the function of the vector. Not only the titers, but also the regulation of the Tet-all-in-one vectors was altered after incorporation of some of the elements. Transduction of the fibroblast cell line SC1 with U630s, U1.0s, U1.0as and U1.5as resulted in less distinct GFP⁺ populations in the dox-induced state (Figure 32) accompanied by low dynamic ranges and fold inductions (MFI) in GFP expression (Figure 33B+C). In contrast, regulation of dox induction was similar to that of the PGK.Tet-control after incorporation of the elements U630as, U670as, U670s and U1.5s and CBX3 (Figure 32). The dynamic range and fold induction of vectors with the U670s incorporated was highest, but at the cost of an elevated background expression and coefficient of variegation (Figure 33E). Promoter activity of the A2UCOE was also verified in other studies and it was decided to replace the promoter by the CBX3 and U670s element (Müller-Kuller et al., 2015; Kunkiel et al., 2017). Replacement of the PGK promoter by the U670s and CBX3 elements resulted in similar regulation in SC1 cells without impairment of the viral vector titers (Figure 39+40). The relative intensity of GFP expression and fold induction were even doubled from these vectors, which was a very interesting observation indicating that the

(rt)TA-M2 expression levels from the CBX3 promoter were sufficient. In studies performed with constitutively expressing retroviral vectors in pluripotent stem cells, the EFS promoter in combination with the U1.5s element is a popular strategy for sustained vector expression (Ackermann et al., 2014; Hoffmann et al., 2017). We therefore decided to replace the PGK promoter also by the EFS in Tet-all-in-one gammaretroviral vectors. Titers in the range of the PGK.Tet-control were also obtained from gammaretroviral vectors containing the EFS promoter to drive the expression of the (rt)TA-M2 (1×10^6 IP/ml) and regulation was also similar as indicated by the distinct GFP positive population in SC1 cells (Figure 39+40A), but relative intensity of GFP expression in the same cell line as well as fold induction were impaired (Figure 40B+C). Comparison of the lentiviral Tet-all-in-one with U670s.M2 and PGK.Tet-control showed that titers of were about 30-fold lower than those of their gammaretroviral counterparts (Figure 39). For this reason and because of high percentage of mean CV indicating higher variegation, the lentiviral vectors were not followed up in further experiments.

5.2.2 Anti-silencing efficiency in P19 cells

Incorporation of the elements U670s, U670as, U1.0s, and U1.5s was shown to protect expression of GFP in the P19 cell line. At the termination of the experiment on day 46, the U670s element performed best as indicated by the overall GFP expression which was more than twice as high (34% residual GFP expression at day 46) compared to the PGK.Tet-control (10% residual GFP expression at day 46) (see Figure 34). But the GFP expression could also be sustained from the U1.0s (21% residual GFP expression at day 46) and U1.5s elements (21% residual GFP expression at day 46). This is consistent with other studies in which the incorporation of the U1.5s element into lentiviral vectors sustained GFP expression in human and murine iPSC including their differentiated progeny (Ackermann et al., 2014). Interestingly, after incorporation of the CBX3, silencing of the GFP expression was not sustained, which is surprising since results from U. Müller-Kuller et al. showed that incorporation of the element into constitutive lentiviral vectors could prevent the silencing in P19 cells very efficiently (Müller-Kuller et al., 2015). It could be possible that the absence of the splice sites and the presence of the downstream transcription start site might reduce efficient transcription of the (rt)TA-M2. When replacing the PGK promoter in the gammaretroviral Tet-all-in-one vectors by CBX3, GFP expression in P19 cells was sustained probably because in this configuration potential promoter interference could not impair expression. The major effect on chromatin opening by A2UCOEs seems to be dependent on the CBX3 part of the region (Müller-Kuller et al., 2015). Efforts made in tracking down the minimal required region in the A2UCOE have

shown that the 455pb 3' to exon1 or U670s/CBX3 element mediated most of the protective effects (Zhang et al., 2017). An additional study by Kunkiel et al. showed that most of the promoter activity of the CBX3 region resides in a core region of 500bp upstream and exon1 of the CBX3 sequence (Kunkiel et al., 2017). The drop in GFP expression from the U670s.M2 and CBX3.M2 vectors was less pronounced (42% and 37% residual GFP expression) than from the PGK.Tet-control which declined below 20% after 42 days. In case of these experiments, cells were sorted by fluorescent activated cell sorting to 100% of GFP expression to compensate for different expression levels. Interestingly, in contrast to the results observed in PGK-containing candidates, GFP expression was sustained from U670s and CBX3 to a similar level. In addition to the lower intensity of GFP expression obtained in SC1 cells, the EFS.M2 also did not prevent silencing of GFP expression in P19 cells and was therefore also not followed up in further experiments (Figure 40 B, C, E). The incorporation of the U630 element per se did not contribute to anti-silencing, independent of the orientation. A2UCOEs devoid the CBX3 part also has been shown to have lower anti-silencing activity (Antoniou et al., 2003).

5.2.3 Expression of Mpl from the Tet-all-in-one vectors confers growth advantage to cytokine dependent cells

To detect an effect of a functional protein expressed from Tet-all-in-one gammaretroviral vectors, we incorporated the Mpl coding sequence (containing an HA Tag for easier flow cytometric analysis), the receptor for the cytokine Thpo, into our U670s containing gammaretroviral vectors. The survival and proliferation of 32D cells is dependent on IL-3. Proliferation of the cells can be shifted towards Thpo-dependent growth after transduction of the cells with the respective receptor. In our experiments, the HA-Mpl expressing cells were selected by the supplementation of Thpo and thereby enriched to almost 100%, demonstrating the functionality of the transgene (Figure 45). Further characterization of the functionality was demonstrated by determining whether the expression of Mpl confers growth advantage to 32D cells under Thpo stimulation. For these experiments, the PrestoBlue® viability assay was utilized (see Chapter 4.2.6). The viability assays were performed 40h after Thpo re-stimulation and compared to the non-induced state. During this time, 32D cells can be expected to divide and therefore, the determination of viable cells was also an indirect measure of proliferation. The fold increase in cell viability was 2.5-fold higher in HA-expressing cells compared to their non-expressing, non-induced counterparts. With this experiment, we have been able to demonstrate that Mpl was efficiently expressed and that the Tet.inducible vector was effectively shut off in the absence of dox.

Similar to our observations, lentiviral vectors containing the U1.5 element upstream the PGK promoter allowed sustained expression of the drug resistance gene MGMT. After transduction and transplantation of Lin⁻ BM cells with the lentiviral vector containing the UCOE to protect MGMT expression, treatment with chemotherapeutics (O6-benzylguanine, 3-bis(2-chloroethyl)-1-nitrosourea) in the mice was better tolerated (Phaltane et al., 2014). Also functional tests of differentiated iPSC with gene correction for Chronic Granulomatous Disease have shown that ROS levels and functionality of the neutrophils differentiated from patient-derived iPSC could only be satisfactorily restored after incorporation of a 1600bp element in the vector (similar to the U1.5 in our study) (Haenseler et al., 2018).

5.2.4 Anti-silencing effects of A2UCOE in pluripotent stem cells

The phenomenon of silencing of Tet-regulated vectors in pluripotent stem cells has been observed also in earlier studies. This does not only hold true for Tet-inducible vectors but also for constitutively vectors and is independent from the species that needs to be transduced (Hong et al., 2007; Xia et al., 2007; Stewart et al., 2008). In our case, the gammaretroviral vectors which were most promising in terms of anti-silencing in P19 cells and maintained the regulatory potential were analyzed in murine and human iPSC. Due to the fact of the lower viral vector titer achieved, lentiviral Tet-all-in-one vectors were not followed up further. Murine CD45.1 iPSC were transduced and subjected to several rounds of dox-induction and withdrawal (Figure 37). In these cells, the regulation of the gene expression by application and withdrawal of dox was confirmed (Figure 37, 38B). The incorporation of the U670s element again showed the highest fold induction (fold induction MFI: ~300) in the pluripotent state (two-fold induction compared to PGK.Tet-control). In contrast, the incorporation of the elements U1.0s and U1.5s showed even lower-fold inductions in GFP expression than the PGK.Tet-control (Figure 33C). This is consistent with the findings of the latest studies focusing on different A2UCOE elements. Incorporation of a U1.5 into vectors expressing cytidine deaminase restored gene expression after differentiation of murine iPSC (Pfaff et al., 2013). Similar results were obtained in human iPSC using the same approach (Ackermann et al., 2014). Furthermore, GFP expression from the vectors with the U670s incorporated showed the highest intensity of expression (MFI/VCN 1.8×10^6) at day 46 when the experiment was terminated compared to the PGK.Tet-control (MFI/VCN 2.7×10^4), making this a potent candidate for the usage in pluripotent stem cells. Results obtained in the study by Müller-Kuller et al. that compared different A2UCOE elements incorporated in constitutive

lentiviral vectors were similar to what we have shown with the A2UCOE-Tet-vectors in hiPSC. In the study by Müller-Kuller, hiPSC were transduced with lentiviral vectors containing the CBX3 element and the U1.5 element and differentiated into myeloid cells. They could demonstrate that the anti-silencing potential after incorporation of CBX3 was increased compared to the U1.5 part (Müller-Kuller et al., 2015). However, in addition, the background expression from all of the vectors tested in our study was also relatively high (up to an MFI/copy number of 1150 for the U670s element) and all within a similar range. Even though in our study we analyzed polyclonal cultures where a position effect should be no major bias, the variegation of the expression was increased during prolonged cultivation periods. This could be problematic in future applications when a tight regulation of the expression is indispensable. The increase on CoV was highest for the U1.0s and U1.5s vectors. The CoV of the U670s in contrast was stable (Figure 38A). A strategy to overcome position effects in pluripotent stem cell is the integration of the Tet-regulated all-in-one expression cassette into the AAVS1 locus in human iPSC by gene editing. Results by Ordovas et al. have shown that also the AAVS1 site did not in all cases protect the accessibility of the Tet-regulated cassette during differentiation (Ordovás et al., 2015). Another reported strategy to prevent transgene silencing in Tet-all-in-one vectors is the incorporation of insulators in the LTRs allowing a tight regulation of the Tet-vectors achieved with only one integration. Insulators are derived from naturally occurring DNA sequences known to shield gene expression of one gene from other adjacent located genes to form functional boundaries and thereby prevent uncontrolled gene expression (Benabdellah et al., 2016). Incorporation of insulators into the LTR might also prevent expression of genes in close proximity and thereby contribute to the vector safety for the usage in gene therapy approaches. On the other hand, as shown by Benabdellah et al., incorporation of the insulator did also lead to lower viral vector titers (Benabdellah et al., 2016). To compensate for variations in copy number, the intensities were normalized to the VCN in our study.

The promoter-replaced candidates U670s.M2 expressed GFP with higher fluorescent intensities (Intensity/MFI: 2.9) and CBX3.M2 (Intensity/MFI 2.6) like the PGK.control in SC1 cells, making them potent candidates for the usage in iPSC. In a second approach, the transduced iPSC were subjected to ecto-, endo- and mesodermal differentiation, respectively. These experiments showed that the silencing of the vectors was most distinct during mesodermal differentiation in general (Figure 42A). In this case, the anti-silencing effect from all elements tested was in a similar range (between 61% and 51% residual GFP expression) and therefore only slightly sustained (residual expression PGK.Tet-control: 41%). Interestingly, the differentiation into mesoderm resulted in the highest percentage of GFP expression of the U670s.M2 vector which showed almost 80%

residual expression and the lowest spread in the individual experiments. Unfortunately, the results could not be confirmed in the endo- and ectodermal differentiation experiments. The overall spread between single measurements was in general very high in all vectors tested. One problem might be the high (almost 100%) transduction efficiency which was achieved during initial transduction. Percentages of GFP expression of more than 30% are associated with multiple vector integrations in different integration sites. Due to the different locations of the integrated vector in the genome and the fact that there was more than one integration present, silencing might not be as strong as it would be after single vector integration only. Furthermore, as it is known from other differentiation studies with human iPSC, some lines have a preference in differentiation to a specific cell type, which can be related to an epigenetic memory of the cells (Kim et al., 2010; Vaskova et al., 2013). The iPSC line utilized in our study was originally generated to identify host factors of *Chlamydia trachomatis* pathogenesis after infection of iPSC-derived macrophages, also originating from the mesodermal germ layer (Yeung et al., 2017). It could be the case that the KOLF2 iPSC line used in this study is more efficient in differentiation into mesodermal origin and since the differentiation into the ectodermal and endodermal layer is reduced, also the silencing is less pronounced due to the lack of chromatin modifications. We could test the differentiated germ layers from the iPSC for the differentiation efficiency for example by the expression of germ-layer specific mRNAs in gene expression analysis by real time PCR in the next experiments. Nonetheless, the combination of the data from each of the germ layers again resulted in a significantly higher residual GFP expression after incorporation of the U670s element (Figure 42B).

The methylation status of the PGK promoter after incorporation of the U670s element was therefore examined before and after mesodermal differentiation and compared to the methylation of the promoter of the PGK.Tet-control. As indicated in Figure 43, incorporation of the U670s resulted in lower PGK promoter methylation in the pluripotent state of the cells which could be maintained also during mesodermal differentiation. Another element vulnerable to silencing could be the Tet-responsive promoter T11. It has been reported from experiments in murine ES cell that promoter methylation was observed even though incorporation into the Rosa26 locus occurred (Gödecke et al., 2017). The minimal promoter utilized in this study was derived from the CMV promoter making it per se more susceptible for silencing. In contrast the promoter used in our study is a chimera of the promoter-sequences of LTRs of mouse mammary tumor virus sequence (MMTV) and Human Immunodeficiency Virus 1 (HIV1) in combination with sequences from the transcription factor IIB (TFIIB) and therefore mostly synthetic and less prone to be silenced (Loew et al., 2010; Heinz et al., 2011; Heinz et al., 2013).

This again highlights the beneficial effect of the U670s after incorporation into Tet-inducible-all-in one gammaretroviral vectors and makes them a promising tool to apply the beneficial effects of Gata1 overexpression on the proliferation of MK progenitors from *in vitro* cultures which was obtained from the approach in murine iPSC also to the human system.

6 CONCLUSION

Taken together, we have successfully developed an approach for the increased production of platelets *in vitro* by the expansion of progenitor cells. This approach can be used for disease modeling studies of MK and platelets. Especially the murine systems are beneficial to better understand rare hematological platelet disorders and improve their treatment opportunities. The final goal of all the *in vitro* platelet differentiation strategies is to transfuse the culture-derived platelets into a living organism to actually mimic a patient situation. The huge benefit of the murine differentiation approach is that in the end we could investigate the actual patient situation in syngeneic preclinical transplantation studies. In contrast, human iPSC-derived platelets rely on humanized mouse models to test for actual functionality, which does not fully resemble a patient situation. The generation of Tet-inducible-all-in one gammaretroviral vectors with the incorporated U670s was most efficient in terms of anti-silencing and regulation with the lowest background. This vector therefore is a very promising tool to apply the strategy also to human iPSC to increase platelet numbers. After successful demonstration of functionality of the *in vitro* generated platelets and completion of clinical trials with safe and efficient *in vitro* differentiated platelets, this would be a powerful strategy for donor-independent platelet transfusion into patients of acute need. To date, there are three major concerns about platelet transfusion. First of all, the risk of bacterial contamination within the transfusion units could be minimized utilizing *in vitro* derived platelets for cellular therapies. Due to the manufacturing under sterile conditions, the potential contamination hazard is minimized and the storage at room temperature would no longer be a problem. This would in turn lead to extended dates of expiry of the transfusion units and thereby to a reduction of waste and minimization of the costs to the healthcare system. In the long run, it provides a cost minimization due to increased manufacturing of batches. Another obstacle of today's platelet transfusion is the development of platelet autoimmune reactions refractoriness as a result of repetitive transfusions. To date, the most promising approaches of T. Mureau et al and Y. Ito et al. rely on the huge expansion of MK progenitors to achieve a sufficient amount of platelets while still the amount of platelets released per MK is very low. Our strategy of Tet-inducible overexpression of GATA1 and NFE2 as a second factor in the human context would provide a strategy to also increase production of culture-derived HLA-compatible platelets from a master bank. This would help to overcome the difficulties of finding HLA-compatible or crossmatch-negative donors. A knockdown of the HLA in iPSC has already been performed, however, the generated numbers of MK and platelets also were not very efficient (Börger et al., 2016).

The donor dependence is another issue which is widely discussed in the field because of the increasing demands of platelet transfusion but static donor pool. Pluripotent stem cells as basis of *in vitro* differentiated platelets provide an infinite source which ensures the generation of high numbers of transfusion units and could help to contribute to therapies being also available to more patients worldwide.

REFERENCES

- Ackermann, M., Kuhn, A., Kunkiel, J., Merkert, S., Martin, U., Moritz, T., and Lachmann, N. (2017). Ex vivo Generation of Genetically Modified Macrophages from Human Induced Pluripotent Stem Cells. *Transfusion medicine and hemotherapy : offizielles Organ der Deutschen Gesellschaft fur Transfusionsmedizin und Immunhamatologie* 44, 135-142.
- Ackermann, M., Lachmann, N., Hartung, S., Eggenschwiler, R., Pfaff, N., Happle, C., Mucci, A., Göhring, G., Niemann, H., and Hansen, G., et al. (2014). Promoter and lineage independent anti-silencing activity of the A2 ubiquitous chromatin opening element for optimized human pluripotent stem cell-based gene therapy. *Biomaterials* 35, 1531-1542.
- Agarwal, M., Austin, T.W., Morel, F., Chen, J., Böhnlein, E., and Plavec, I. (1998). Scaffold attachment region-mediated enhancement of retroviral vector expression in primary T cells. *Journal of virology* 72, 3720-3728.
- Alarcon, P.A. de, and Graeve, J.L. (1996). Analysis of megakaryocyte ploidy in fetal bone marrow biopsies using a new adaptation of the feulgen technique to measure DNA content and estimate megakaryocyte ploidy from biopsy specimens. *Pediatric research* 39, 166-170.
- Ali, R.A., Wuescher, L.M., and Worth, R.G. (2015). Platelets: essential components of the immune system. *Current trends in immunology* 16, 65-78.
- Amit, M., Margulets, V., Segev, H., Shariki, K., Laevsky, I., Coleman, R., and Itskovitz-Eldor, J. (2003). Human feeder layers for human embryonic stem cells. *Biology of reproduction* 68, 2150-2156.
- Andrews, N.C. (1998). The NF-E2 transcription factor. *The international journal of biochemistry & cell biology* 30, 429-432.
- Andrews, R.K., Arthur, J.F., and Gardiner, E.E. (2014). Targeting GPVI as a novel antithrombotic strategy. *Journal of blood medicine* 5, 59-68.
- Antkowiak, A., Viaud, J., Severin, S., Zanoun, M., Ceccato, L., Chicanne, G., Strassel, C., Eckly, A., Leon, C., and Gachet, C., et al. (2016). Cdc42-dependent F-actin dynamics drive structuration of the demarcation membrane system in megakaryocytes. *Journal of thrombosis and haemostasis : JTH* 14, 1268-1284.
- Antoniou, M., Harland, L., Mustoe, T., Williams, S., Holdstock, J., Yague, E., Mulcahy, T., Griffiths, M., Edwards, S., and Ioannou, P.A., et al. (2003). Transgenes encompassing dual-promoter CpG islands from the human TBP and HNRPA2B1 loci are resistant to heterochromatin-mediated silencing. *Genomics* 82, 269-279.
- Arthur, J.F., Shen, Y., Kahn, M.L., Berndt, M.C., Andrews, R.K., and Gardiner, E.E. (2007). Ligand binding rapidly induces disulfide-dependent dimerization of glycoprotein VI on the platelet plasma membrane. *The Journal of biological chemistry* 282, 30434-30441.
- Aslan, J.E., Itakura, A., Gertz, J.M., and McCarty, O.J.T. (2012). Platelet shape change and spreading. *Methods in molecular biology (Clifton, N.J.)* 788, 91-100.
- Aslan, J.E., and McCarty, O.J.T. (2013). Rho GTPases in platelet function. *Journal of thrombosis and haemostasis : JTH* 11, 35-46.

- Asou, N. (2003). The role of a Runt domain transcription factor AML1/RUNX1 in leukemogenesis and its clinical implications. *Critical Reviews in Oncology/Hematology* 45, 129-150.
- Au, A.E., and Josefsson, E.C. (2017). Regulation of platelet membrane protein shedding in health and disease. *Platelets* 28, 342-353.
- Avraham, H., Vannier, E., Cowley, S., Jiang, S.X., Chi, S., Dinarello, C.A., Zsebo, K.M., and Groopman, J.E. (1992). Effects of the stem cell factor, c-kit ligand, on human megakaryocytic cells. *Blood* 79, 365-371.
- Baum, C., Hegewisch-Becker, S., Eckert, H.G., Stocking, C., and Ostertag, W. (1995). Novel retroviral vectors for efficient expression of the multidrug resistance (mdr-1) gene in early hematopoietic cells. *Journal of virology* 69, 7541-7547.
- Bearer, E.L., Prakash, J.M., and Li, Z. (2002). Actin Dynamics in Platelets. *International Review of Cytology* 217, 137-182.
- Begley, C.G., and Green, A.R. (1999). The SCL gene: from case report to critical hematopoietic regulator. *Blood* 93, 2760-2770.
- Behrens, K., and Alexander, W.S. (2018). Cytokine control of megakaryopoiesis. *Growth factors (Chur, Switzerland)*, 1-15.
- Benabdellah, K., Cobo, M., Muñoz, P., Toscano, M.G., and Martin, F. (2011). Development of an all-in-one lentiviral vector system based on the original TetR for the easy generation of Tet-ON cell lines. *PloS one* 6, e23734.
- Benabdellah, K., Muñoz, P., Cobo, M., Gutierrez-Guerrero, A., Sánchez-Hernández, S., Garcia-Perez, A., Anderson, P., Carrillo-Gálvez, A.B., Toscano, M.G., and Martin, F. (2016). Lent-On-Plus Lentiviral vectors for conditional expression in human stem cells. *Scientific reports* 6.
- Bennett, J.S. (2005). Structure and function of the platelet integrin $\alpha\text{IIb}\beta\text{3}$. *The Journal of clinical investigation* 115, 3363-3369.
- Blin, A., Le Goff, A., Magniez, A., Poirault-Chassac, S., Teste, B., Sicot, G., Nguyen, K.A., Hamdi, F.S., Reyssat, M., and Baruch, D. (2016). Microfluidic model of the platelet-generating organ: beyond bone marrow biomimetics. *Scientific reports* 6, 21700.
- Börger, A.-K., Eicke, D., Wolf, C., Gras, C., Aufderbeck, S., Schulze, K., Engels, L., Eiz-Vesper, B., Schambach, A., and Guzman, C.A., et al. (2016). Generation of HLA-Universal iPSC-Derived Megakaryocytes and Platelets for Survival Under Refractoriness Conditions. *Molecular medicine (Cambridge, Mass.)* 22, 274-285.
- Broudy, V.C., and Kaushansky, K. (1995). Thrombopoietin, the c-mpl ligand, is a major regulator of platelet production. *Journal of leukocyte biology* 57, 719-725.
- Broudy, V.C., Lin, N.L., and Kaushansky, K. (1995). Thrombopoietin (c-mpl ligand) acts synergistically with erythropoietin, stem cell factor, and interleukin-11 to enhance murine megakaryocyte colony growth and increases megakaryocyte ploidy in vitro. *Blood* 85, 1719-1726.
- Brown, E., Carlin, L.M., Nerlov, C., Lo Celso, C., and Poole, A.W. (2018). Multiple membrane extrusion sites drive megakaryocyte migration into bone marrow blood vessels. *Life science alliance* 1.

- Buecker, C., Chen, H.-H., Polo, J.M., Daheron, L., Bu, L., Barakat, T.S., Okwieka, P., Porter, A., Gribnau, J., and Hochedlinger, K., et al. (2010). A murine ESC-like state facilitates transgenesis and homologous recombination in human pluripotent stem cells. *Cell stem cell* 6, 535-546.
- Burnouf, T., Strunk, D., Koh, M.B.C., and Schallmoser, K. (2016). Human platelet lysate: Replacing fetal bovine serum as a gold standard for human cell propagation? *Biomaterials* 76, 371-387.
- Burns, J.C., Friedmann, T., Driever, W., Burrascano, M., and Yee, J.K. (1993). Vesicular stomatitis virus G glycoprotein pseudotyped retroviral vectors. Concentration to very high titer and efficient gene transfer into mammalian and nonmammalian cells. *Proceedings of the National Academy of Sciences of the United States of America* 90, 8033-8037.
- Burstein, S.A., Mei, R.L., Henthorn, J., Friese, P., and Turner, K. (1992). Leukemia inhibitory factor and interleukin-11 promote maturation of murine and human megakaryocytes in vitro. *Journal of cellular physiology* 153, 305-312.
- Carver-Moore, K., Broxmeyer, H.E., Luoh, S.M., Cooper, S., Peng, J., Burstein, S.A., Moore, M.W., and Sauvage, F.J. de (1996). Low levels of erythroid and myeloid progenitors in thrombopoietin-and c-mpl-deficient mice. *Blood* 88, 803-808.
- Challita, P.M., and Kohn, D.B. (1994). Lack of expression from a retroviral vector after transduction of murine hematopoietic stem cells is associated with methylation in vivo. *Proceedings of the National Academy of Sciences of the United States of America* 91, 2567-2571.
- Chang, Y., Auradé, F., Larbret, F., Zhang, Y., Le Couedic, J.-P., Momeux, L., Larghero, J., Bertoglio, J., Louache, F., and Cramer, E., et al. (2007). Proplatelet formation is regulated by the Rho/ROCK pathway. *Blood* 109, 4229-4236.
- Chen, I.-P., Fukuda, K., Fusaki, N., Iida, A., Hasegawa, M., Lichtler, A., and Reichenberger, E.J. (2013). Induced pluripotent stem cell reprogramming by integration-free Sendai virus vectors from peripheral blood of patients with craniometaphyseal dysplasia. *Cellular reprogramming* 15, 503-513.
- Choi, E.S., Nichol, J.L., Hokom, M.M., Hornkohl, A.C., and Hunt, P. (1995). Platelets generated in vitro from proplatelet-displaying human megakaryocytes are functional. *Blood* 85, 402-413.
- Christensen, J.L., Wright, D.E., Wagers, A.J., and Weissman, I.L. (2004). Circulation and chemotaxis of fetal hematopoietic stem cells. *PLoS biology* 2, E75.
- Ciau-Uitz, A., Monteiro, R., Kirmizitas, A., and Patient, R. (2014). Developmental hematopoiesis. Ontogeny, genetic programming and conservation. *Experimental hematology* 42, 669-683.
- Cortegano, I., Serrano, N., Ruiz, C., Rodríguez, M., Prado, C., Alía, M., Hidalgo, A., Cano, E., Andrés, B. de, and Gaspar, M.-L. (2018). CD45 expression discriminates waves of embryonic megakaryocytes in the mouse. *Haematologica*.
- Coughlin, S.R. (2000). Thrombin signalling and protease-activated receptors. *Nature* 407, 258-264.
- Coughlin, S.R. (2005). Protease-activated receptors in hemostasis, thrombosis and vascular biology. *Journal of thrombosis and haemostasis : JTH* 3, 1800-1814.

- Cullmann, K., Blokland, K.E.C., Sebe, A., Schenk, F., Ivics, Z., Heinz, N., and Modlich, U. (2019). Sustained and regulated gene expression by Tet-inducible "all-in-one" retroviral vectors containing the HNRPA2B1-CBX3 UCOE®. *Biomaterials* 192, 486-499.
- Debili, N., Coulombel, L., Croisille, L., Katz, A., Guichard, J., Breton-Gorius, J., and Vainchenker, W. (1996). Characterization of a bipotent erythro-megakaryocytic progenitor in human bone marrow. *Blood* 88, 1284-1296.
- Debili, N., Wendling, F., Katz, A., Guichard, J., Breton-Gorius, J., Hunt, P., and Vainchenker, W. (1995). The Mpl-ligand or thrombopoietin or megakaryocyte growth and differentiative factor has both direct proliferative and differentiative activities on human megakaryocyte progenitors. *Blood* 86, 2516-2525.
- Deng, W., Xu, Y., Chen, W., Paul, D.S., Syed, A.K., Dragovich, M.A., Liang, X., Zakas, P., Berndt, M.C., and Di Paola, J., et al. (2016). Platelet clearance via shear-induced unfolding of a membrane mechanoreceptor. *Nature communications* 7, 12863.
- Di Buduo, C.A., Wray, L.S., Tozzi, L., Malara, A., Chen, Y., Ghezzi, C.E., Smoot, D., Sfara, C., Antonelli, A., and Spedden, E., et al. (2015). Programmable 3D silk bone marrow niche for platelet generation ex vivo and modeling of megakaryopoiesis pathologies. *Blood* 125, 2254-2264.
- DiMartino, J.F., Selleri, L., Traver, D., Firpo, M.T., Rhee, J., Warnke, R., O'Gorman, S., Weissman, I.L., and Cleary, M.L. (2001). The Hox cofactor and proto-oncogene Pbx1 is required for maintenance of definitive hematopoiesis in the fetal liver. *Blood* 98, 618-626.
- Drachman, J.G., Sabath, D.F., Fox, N.E., and Kaushansky, K. (1997). Thrombopoietin signal transduction in purified murine megakaryocytes. *Blood* 89, 483-492.
- Dull, T., Zufferey, R., Kelly, M., Mandel, R.J., Nguyen, M., Trono, D., and Naldini, L. (1998). A third-generation lentivirus vector with a conditional packaging system. *Journal of virology* 72, 8463-8471.
- Durrant, T.N., van den Bosch, M.T., and Hers, I. (2017). Integrin $\alpha\text{IIb}\beta\text{3}$ outside-in signaling. *Blood* 130, 1607-1619.
- Dütting, S., Gaits-Iacovoni, F., Stegner, D., Popp, M., Antkowiak, A., van Eeuwijk, J.M.M., Nurden, P., Stritt, S., Heib, T., and Aurbach, K., et al. (2017). A Cdc42/RhoA regulatory circuit downstream of glycoprotein Ib guides transendothelial platelet biogenesis. *Nature communications* 8, 15838.
- Ebbe, S., Phalen, E., D'Amore, P., and Howard, D. (1978). Megakaryocytic responses to thrombocytopenia and thrombocytosis in SI/SId mice. *Experimental hematology* 6, 201-212.
- Eckly, A., Heijnen, H., Pertuy, F., Geerts, W., Proamer, F., Rinckel, J.-Y., Léon, C., Lanza, F., and Gachet, C. (2014). Biogenesis of the demarcation membrane system (DMS) in megakaryocytes. *Blood* 123, 921-930.
- Elagib, K.E., Brock, A.T., and Goldfarb, A.N. (2018). Megakaryocyte ontogeny: Clinical and molecular significance. *Experimental hematology* 61, 1-9.
- Emery, D.W., Yannaki, E., Tubb, J., and Stamatoyannopoulos, G. (2000). A chromatin insulator protects retrovirus vectors from chromosomal position effects. *Proceedings of the National Academy of Sciences of the United States of America* 97, 9150-9155.

- Emi N. (1991). Pseudotype formation of murine leukemia virus with the G protein of vesicular stomatitis virus. *J Virol* 1991.
- Escolar, G., Lopez-Vilchez, I., Diaz-Ricart, M., White, J.G., and Galan, A.M. (2008). Internalization of tissue factor by platelets. *Thrombosis research* 122 Suppl 1, S37-41.
- Etienne-Manneville, S., and Hall, A. (2002). Rho GTPases in cell biology. *Nature* 420, 629-635.
- Feng, Q., Shabrani, N., Thon, J.N., Huo, H., Thiel, A., Machlus, K.R., Kim, K., Brooks, J., Li, F., and Luo, C., et al. (2014). Scalable generation of universal platelets from human induced pluripotent stem cells. *Stem cell reports* 3, 817-831.
- Ferkowicz, M.J., Starr, M., Xie, X., Li, W., Johnson, S.A., Shelley, W.C., Morrison, P.R., and Yoder, M.C. (2003). CD41 expression defines the onset of primitive and definitive hematopoiesis in the murine embryo. *Development (Cambridge, England)* 130, 4393-4403.
- Fox, N., Priestley, G., Papayannopoulou, T., and Kaushansky, K. (2002). Thrombopoietin expands hematopoietic stem cells after transplantation. *The Journal of clinical investigation* 110, 389-394.
- French, D.L., and Seligsohn, U. (2000). Platelet glycoprotein IIb/IIIa receptors and Glanzmann's thrombasthenia. *Arteriosclerosis, thrombosis, and vascular biology* 20, 607-610.
- Fujiwara, Y., Browne, C.P., Cunniff, K., Goff, S.C., and Orkin, S.H. (1996). Arrested development of embryonic red cell precursors in mouse embryos lacking transcription factor GATA-1. *Proceedings of the National Academy of Sciences of the United States of America* 93, 12355-12358.
- Fusaki, N., Ban, H., Nishiyama, A., Saeki, K., and Hasegawa, M. (2009). Efficient induction of transgene-free human pluripotent stem cells using a vector based on Sendai virus, an RNA virus that does not integrate into the host genome. *Proceedings of the Japan Academy. Series B, Physical and Biological Sciences* 85, 348-362.
- Gaertner, F., Ahmad, Z., Rosenberger, G., Fan, S., Nicolai, L., Busch, B., Yavuz, G., Luckner, M., Ishikawa-Ankerhold, H., and Hennel, R., et al. (2017). Migrating Platelets Are Mechano-scavengers that Collect and Bundle Bacteria. *Cell* 171, 1368-1382.e23.
- Gardiner-Garden, M., and Frommer, M. (1987). CpG islands in vertebrate genomes. *Journal of molecular biology* 196, 261-282.
- Gerrard, J.M., White, J.G., and Peterson, D.A. (1978). The platelet dense tubular system. Its relationship to prostaglandin synthesis and calcium flux. *Thrombosis and haemostasis* 40, 224-231.
- Gilboa, E., Kolbe, M., Noonan, K., and Kucherlapati, R. (1982). Construction of a mammalian transducing vector from the genome of Moloney murine leukemia virus. *Journal of virology* 44, 845-851.
- Gödecke, N., Zha, L., Spencer, S., Behme, S., Riemer, P., Rehli, M., Hauser, H., and Wirth, D. (2017). Controlled re-activation of epigenetically silenced Tet promoter-driven transgene expression by targeted demethylation. *Nucleic acids research* 45, e147.
- Goggs, R., Williams, C.M., Mellor, H., and Poole, A.W. (2015). Platelet Rho GTPases—a focus on novel players, roles and relationships. *The Biochemical journal* 466, 431-442.

- Gossen, M., and Bujard, H. (1992). Tight control of gene expression in mammalian cells by tetracycline-responsive promoters. *Proceedings of the National Academy of Sciences of the United States of America* *89*, 5547-5551.
- Goyama, S., Yamamoto, G., Shimabe, M., Sato, T., Ichikawa, M., Ogawa, S., Chiba, S., and Kurokawa, M. (2008). Evi-1 is a critical regulator for hematopoietic stem cells and transformed leukemic cells. *Cell stem cell* *3*, 207-220.
- Greenberger, J.S., Eckner, R.J., Sakakeeny, M., Marks, P., Reid, D., Nabel, G., Hapel, A., Ihle, J.N., and Humphries, K.C. (1983). Interleukin 3-dependent hematopoietic progenitor cell lines. *Federation proceedings* *42*, 2762-2771.
- Growney, J.D., Shigematsu, H., Li, Z., Lee, B.H., Adelsperger, J., Rowan, R., Curley, D.P., Kutok, J.L., Akashi, K., and Williams, I.R., et al. (2005). Loss of Runx1 perturbs adult hematopoiesis and is associated with a myeloproliferative phenotype. *Blood* *106*, 494-504.
- Gruber, T.A., and Downing, J.R. (2015). The biology of pediatric acute megakaryoblastic leukemia. *Blood* *126*, 943-949.
- Gurney, A.L., Carver-Moore, K., Sauvage, F.J. de, and Moore, M.W. (1994). Thrombocytopenia in c-mpl-deficient mice. *Science (New York, N.Y.)* *265*, 1445-1447.
- Haenseler, W., Kuzmenko, E., Smalls-Mantey, A., Browne, C., Seger, R., James, W.S., Cowley, S.A., Reichenbach, J., and Siler, U. (2018). Lentiviral gene therapy vector with UCOE stably restores function in iPSC-derived neutrophils of a CDG patient. *Matters* *2018*.
- Hall, M.A., Curtis, D.J., Metcalf, D., Elefanty, A.G., Sourris, K., Robb, L., Gothert, J.R., Jane, S.M., and Begley, C.G. (2003). The critical regulator of embryonic hematopoiesis, SCL, is vital in the adult for megakaryopoiesis, erythropoiesis, and lineage choice in CFU-S12. *Proceedings of the National Academy of Sciences of the United States of America* *100*, 992-997.
- Haridhasapavalan, K.K., Borgohain, M.P., Dey, C., Saha, B., Narayan, G., Kumar, S., and Thummer, R.P. (2019). An insight into non-integrative gene delivery approaches to generate transgene-free induced pluripotent stem cells. *Gene* *686*, 146-159.
- Harrison, P., Wilbourn, B., Debili, N., Vainchenker, W., Breton-Gorius, J., Lawrie, A.S., Masse, J.M., Savidge, G.F., and Cramer, E.M. (1989). Uptake of plasma fibrinogen into the alpha granules of human megakaryocytes and platelets. *The Journal of clinical investigation* *84*, 1320-1324.
- Hartley, J.W., and Rowe, W.P. (1975). Clonal cell lines from a feral mouse embryo which lack host-range restrictions for murine leukemia viruses. *Virology* *65*, 128-134.
- He, J., Yang, Q., and Chang, L.-J. (2005). Dynamic DNA Methylation and Histone Modifications Contribute to Lentiviral Transgene Silencing in Murine Embryonic Carcinoma Cells. *Journal of virology* *79*, 13497-13508.
- Hechler, B., and Gachet, C. (2011). P2 receptors and platelet function. *Purinergic signalling* *7*, 293-303.
- Heijnen, H., and van der Sluijs, P. (2015). Platelet secretory behaviour: as diverse as the granules ... or not? *Journal of thrombosis and haemostasis : JTH* *13*, 2141-2151.

- Heinz, N., Hennig, K., and Loew, R. (2013). Graded or threshold response of the tet-controlled gene expression: all depends on the concentration of the transactivator. *BMC Biotechnology* 13, 5.
- Heinz, N., Schambach, A., Galla, M., Maetzig, T., Baum, C., Loew, R., and Schiedlmeier, B. (2011). Retroviral and transposon-based tet-regulated all-in-one vectors with reduced background expression and improved dynamic range. *Human gene therapy* 22, 166-176.
- Hindmarsh, P., and Leis, J. (1999). Retroviral DNA integration. *Microbiology and molecular biology reviews* : MMBR 63, 836-43, table of contents.
- Ho, R., Chronis, C., and Plath, K. (2011). Mechanistic Insights into Reprogramming to Induced Pluripotency. *Journal of cellular physiology* 226, 868-878.
- Hochedlinger, K., Yamada, Y., Beard, C., and Jaenisch, R. (2005). Ectopic expression of Oct-4 blocks progenitor-cell differentiation and causes dysplasia in epithelial tissues. *Cell* 121, 465-477.
- Hoffmann, D., Schott, J.W., Geis, F.K., Lange, L., Müller, F.-J., Lenz, D., Zychlinski, D., Steinemann, D., Morgan, M., and Moritz, T., et al. (2017). Detailed comparison of retroviral vectors and promoter configurations for stable and high transgene expression in human induced pluripotent stem cells. *Gene therapy* 24, 298-307.
- Hong, S., Hwang, D.-Y., Yoon, S., Isacson, O., Ramezani, A., Hawley, R.G., and Kim, K.-S. (2007). Functional analysis of various promoters in lentiviral vectors at different stages of in vitro differentiation of mouse embryonic stem cells. *Molecular therapy : the journal of the American Society of Gene Therapy* 15, 1630-1639.
- Hotta, A., and Ellis, J. (2008). Retroviral vector silencing during iPS cell induction. An epigenetic beacon that signals distinct pluripotent states. *Journal of cellular biochemistry* 105, 940-948.
- Huang, H., and Cantor, A.B. (2009). Common features of megakaryocytes and hematopoietic stem cells. What's the connection? *Journal of cellular biochemistry* 107, 857-864.
- Ichikawa, M., Asai, T., Saito, T., Seo, S., Yamazaki, I., Yamagata, T., Mitani, K., Chiba, S., Ogawa, S., and Kurokawa, M., et al. (2004). AML-1 is required for megakaryocytic maturation and lymphocytic differentiation, but not for maintenance of hematopoietic stem cells in adult hematopoiesis. *Nature medicine* 10, 299-304.
- Inoue, O., Suzuki-Inoue, K., McCarty, O.J.T., Moroi, M., Ruggeri, Z.M., Kunicki, T.J., Ozaki, Y., and Watson, S.P. (2006). Laminin stimulates spreading of platelets through integrin alpha6beta1-dependent activation of GPVI. *Blood* 107, 1405-1412.
- Ishibashi, T., Kimura, H., Uchida, T., Kariyone, S., Friese, P., and Burstein, S.A. (1989). Human interleukin 6 is a direct promoter of maturation of megakaryocytes in vitro. *Proceedings of the National Academy of Sciences of the United States of America* 86, 5953-5957.
- Italiano, J.E., Patel-Hett, S., and Hartwig, J.H. (2007). Mechanics of proplatelet elaboration. *Journal of thrombosis and haemostasis* : JTH 5 Suppl 1, 18-23.
- Ito, Y., Nakamura, S., Sugimoto, N., Shigemori, T., Kato, Y., Ohno, M., Sakuma, S., Ito, K., Kumon, H., and Hirose, H., et al. (2018). Turbulence Activates Platelet Biogenesis to Enable Clinical Scale Ex Vivo Production. *Cell* 174, 636-648.e18.

- Jaffredo, T., Nottingham, W., Liddiard, K., Bollerot, K., Pouget, C., and Bruijn, M. de (2005). From hemangioblast to hematopoietic stem cell: an endothelial connection? *Experimental hematology* 33, 1029-1040.
- Jahn, M. (2019). Platelet production from genetically modified murine induced pluripotent stem cells. Masterarbeit.
- Jähner, D., Stuhlmann, H., Stewart, C.L., Harbers, K., Löhler, J., Simon, I., and Jaenisch, R. (1982). De novo methylation and expression of retroviral genomes during mouse embryogenesis. *Nature* 298, 623-628.
- Jennings, L.K., and Phillips, D.R. (1982). Purification of glycoproteins IIb and III from human platelet plasma membranes and characterization of a calcium-dependent glycoprotein IIb-III complex. *The Journal of biological chemistry* 257, 10458-10466.
- Jia, F., Wilson, K.D., Sun, N., Gupta, D.M., Huang, M., Li, Z., Panetta, N.J., Chen, Z.Y., Robbins, R.C., and Kay, M.A., et al. (2010). A nonviral minicircle vector for deriving human iPS cells. *Nature methods* 7, 197-199.
- Kadari, A., Lu, M., Li, M., Sekaran, T., Thummer, R.P., Guyette, N., Chu, V., and Edenhofer, F. (2014). Excision of viral reprogramming cassettes by Cre protein transduction enables rapid, robust and efficient derivation of transgene-free human induced pluripotent stem cells. *Stem cell research & therapy* 5, 47.
- Kahn, M.L., Diacovo, T.G., Bainton, D.F., Lanza, F., Trejo, J., and Coughlin, S.R. (1999). Glycoprotein V-deficient platelets have undiminished thrombin responsiveness and Do not exhibit a Bernard-Soulier phenotype. *Blood* 94, 4112-4121.
- Karakaya, K., Herbst, F., Ball, C., Glimm, H., Krämer, A., and Löffler, H. (2012). Overexpression of EVI1 interferes with cytokinesis and leads to accumulation of cells with supernumerary centrosomes in G0/1 phase. *Cell cycle (Georgetown, Tex.)* 11, 3492-3503.
- Kasirer-Friede, A., Kahn, M.L., and Shattil, S.J. (2007). Platelet integrins and immunoreceptors. *Immunological reviews* 218, 247-264.
- Kato, T., Ogami, K., Shimada, Y., Iwamatsu, A., Sohma, Y., Akahori, H., Horie, K., Kokubo, A., Kudo, Y., and Maeda, E. (1995). Purification and characterization of thrombopoietin. *Journal of biochemistry* 118, 229-236.
- Kaushansky, K. (2009). Determinants of platelet number and regulation of thrombopoiesis. *Hematology. American Society of Hematology. Education Program*, 147-152.
- Kim, D., Kim, C.-H., Moon, J.-I., Chung, Y.-G., Chang, M.-Y., Han, B.-S., Ko, S., Yang, E., Cha, K.Y., and Lanza, R., et al. (2009). Generation of human induced pluripotent stem cells by direct delivery of reprogramming proteins. *Cell stem cell* 4, 472-476.
- Kim, K., Doi, A., Wen, B., Ng, K., Zhao, R., Cahan, P., Kim, J., Aryee, M.J., Ji, H., and Ehrlich, L.I.R., et al. (2010). Epigenetic memory in induced pluripotent stem cells. *Nature* 467, 285-290.
- Kimura, S., Roberts, A.W., Metcalf, D., and Alexander, W.S. (1998). Hematopoietic stem cell deficiencies in mice lacking c-Mpl, the receptor for thrombopoietin. *Proceedings of the National Academy of Sciences of the United States of America* 95, 1195-1200.

- Kirito, K., Osawa, M., Morita, H., Shimizu, R., Yamamoto, M., Oda, A., Fujita, H., Tanaka, M., Nakajima, K., and Miura, Y., et al. (2002). A functional role of Stat3 in in vivo megakaryopoiesis. *Blood* 99, 3220-3227.
- Kohlscheen, S. (2015). Screening for hematopoietic stem cell regeneration in the Mpl-deficient mouse model. Dissertation.
- Kohlscheen, S., Schenk, F., Rommel, M.G.E., Cullmann, K., and Modlich, U. (2019). Endothelial protein C receptor supports hematopoietic stem cell engraftment and expansion in Mpl-deficient mice. *Blood*.
- Kunkiel, J., Gödecke, N., Ackermann, M., Hoffmann, D., Schambach, A., Lachmann, N., Wirth, D., and Moritz, T. (2017). The CpG-sites of the CBX3 ubiquitous chromatin opening element are critical structural determinants for the anti-silencing function. *Scientific reports* 7, 7919.
- Kustikova, O.S., Schwarzer, A., Stahlhut, M., Brugman, M.H., Neumann, T., Yang, M., Li, Z., Schambach, A., Heinz, N., and Gerdes, S., et al. (2013). Activation of Evi1 inhibits cell cycle progression and differentiation of hematopoietic progenitor cells. *Leukemia* 27, 1127-1138.
- Kuter, D.J. (2014). Milestones in understanding platelet production. A historical overview. *British journal of haematology* 165, 248-258.
- Kuter, D.J., Beeler, D.L., and Rosenberg, R.D. (1994). The purification of megapoeitin: a physiological regulator of megakaryocyte growth and platelet production. *Proceedings of the National Academy of Sciences of the United States of America* 91, 11104-11108.
- Latorre-Rey, L.J., Wintterle, S., Dütting, S., Kohlscheen, S., Abel, T., Schenk, F., Wingert, S., Rieger, M.A., Nieswandt, B., and Heinz, N., et al. (2017). Targeting expression to megakaryocytes and platelets by lineage-specific lentiviral vectors. *Journal of thrombosis and haemostasis : JTH* 15, 341-355.
- Lecine, P., Villeval, J.L., Vyas, P., Swencki, B., Xu, Y., and Shivdasani, R.A. (1998). Mice lacking transcription factor NF-E2 provide in vivo validation of the proplatelet model of thrombocytopoiesis and show a platelet production defect that is intrinsic to megakaryocytes. *Blood* 92, 1608-1616.
- Lee, D., Fong, K.P., King, M.R., Brass, L.F., and Hammer, D.A. (2012). Differential dynamics of platelet contact and spreading. *Biophysical journal* 102, 472-482.
- Lee, W.Y., Weinberg, O.K., Evans, A.G., and Pinkus, G.S. (2018). Loss of Full-Length GATA1 Expression in Megakaryocytes Is a Sensitive and Specific Immunohistochemical Marker for the Diagnosis of Myeloid Proliferative Disorder Related to Down Syndrome. *American journal of clinical pathology* 149, 300-309.
- Lepage, A., Leboeuf, M., Cazenave, J.P., La Salle, C. de, Lanza, F., and Uzan, G. (2000). The alpha(IIb)beta(3) integrin and GPIb-V-IX complex identify distinct stages in the maturation of CD34(+) cord blood cells to megakaryocytes. *Blood* 96, 4169-4177.
- Li, J.L., Zarbock, A., and Hidalgo, A. (2017). Platelets as autonomous drones for hemostatic and immune surveillance. *The Journal of experimental medicine*.
- Li, R., and Emsley, J. (2013). The organizing principle of the platelet glycoprotein Ib-IX-V complex. *Journal of thrombosis and haemostasis : JTH* 11, 605-614.

- Lin, R., Cerione, R.A., and Manor, D. (1999). Specific Contributions of the Small GTPases Rho, Rac, and Cdc42 to Dbl Transformation. *The Journal of biological chemistry* 274, 23633-23641.
- Lindahl Allen, M., Koch, C.M., Clelland, G.K., Dunham, I., and Antoniou, M. (2009). DNA methylation-histone modification relationships across the desmin locus in human primary cells. *BMC molecular biology* 10, 51.
- Liu, Z.-J., Italiano, J., Ferrer-Marin, F., Gutti, R., Bailey, M., Poterjoy, B., Rimsza, L., and Sola-Visner, M. (2011). Developmental differences in megakaryocytopoiesis are associated with up-regulated TPO signaling through mTOR and elevated GATA-1 levels in neonatal megakaryocytes. *Blood* 117, 4106-4117.
- Loew, R., Heinz, N., Hampf, M., Bujard, H., and Gossen, M. (2010). Improved Tet-responsive promoters with minimized background expression. *BMC Biotechnology* 10, 81.
- López, J.A., Leung, B., Reynolds, C.C., Li, C.Q., and Fox, J.E. (1992). Efficient plasma membrane expression of a functional platelet glycoprotein Ib-IX complex requires the presence of its three subunits. *The Journal of biological chemistry* 267, 12851-12859.
- Lowe, K.L., Navarro-Nunez, L., and Watson, S.P. (2012). Platelet CLEC-2 and podoplanin in cancer metastasis. *Thrombosis research* 129, S30-S37.
- Lu, S.-J., Li, F., Yin, H., Feng, Q., Kimbrel, E.A., Hahm, E., Thon, J.N., Wang, W., Italiano, J.E., and Cho, J., et al. (2011). Platelets generated from human embryonic stem cells are functional in vitro and in the microcirculation of living mice. *Cell research* 21, 530-545.
- Ma, D.C., Sun, Y.H., Chang, K.Z., and Zuo, W. (1996). Developmental change of megakaryocyte maturation and DNA ploidy in human fetus. *European journal of haematology* 57, 121-127.
- Maetzig, T., Galla, M., Baum, C., and Schambach, A. (2011). Gammaretroviral vectors. *Biology, technology and application. Viruses* 3, 677-713.
- Magnusson, M., Brun, A.C.M., Miyake, N., Larsson, J., Ehinger, M., Bjornsson, J.M., Wutz, A., Sigvardsson, M., and Karlsson, S. (2007). HOXA10 is a critical regulator for hematopoietic stem cells and erythroid/megakaryocyte development. *Blood* 109, 3687-3696.
- Matsumura, G., and Sasaki, K. (1988). The ultrastructure of megakaryopoietic cells of the yolk sac and liver in mouse embryo. *The Anatomical record* 222, 164-169.
- Mattia, G., Vulcano, F., Milazzo, L., Barca, A., Macioce, G., Giampaolo, A., and Hassan, H.J. (2002). Different ploidy levels of megakaryocytes generated from peripheral or cord blood CD34+ cells are correlated with different levels of platelet release. *Blood* 99, 888-897.
- McBurney, M.W., Jones-Villeneuve, E.M., Edwards, M.K., and Anderson, P.J. (1982). Control of muscle and neuronal differentiation in a cultured embryonal carcinoma cell line. *Nature* 299, 165-167.
- McCarty, O.J.T., Larson, M.K., Auger, J.M., Kalia, N., Atkinson, B.T., Pearce, A.C., Ruf, S., Henderson, R.B., Tybulewicz, V.L.J., and Machesky, L.M., et al. (2005). Rac1 Is Essential for Platelet Lamellipodia Formation and Aggregate Stability under Flow*unk. *The Journal of biological chemistry* 280, 39474-39484.

- McCormack, M.P., Hall, M.A., Schoenwaelder, S.M., Zhao, Q., Ellis, S., Prentice, J.A., Clarke, A.J., Slater, N.J., Salmon, J.M., and Jackson, S.P., et al. (2006). A critical role for the transcription factor Scl in platelet production during stress thrombopoiesis. *Blood* 108, 2248-2256.
- McInerney, J.M., Nawrocki, J.R., and Lowrey, C.H. (2000). Long-term silencing of retroviral vectors is resistant to reversal by trichostatin A and 5-azacytidine. *Gene therapy* 7, 653-663.
- Mejillano, M.R., Kojima, S.-i., Applewhite, D.A., Gertler, F.B., Svitkina, T.M., and Borisy, G.G. (2004). Lamellipodial versus filopodial mode of the actin nanomachinery: pivotal role of the filament barbed end. *Cell* 118, 363-373.
- Miller, A.D. (1990). Retrovirus packaging cells. *Human gene therapy* 1, 5-14.
- Minoguchi, S., and Iba, H. (2008). Instability of retroviral DNA methylation in embryonic stem cells. *Stem cells (Dayton, Ohio)* 26, 1166-1173.
- Mitjavila-Garcia, M.T., Cailleret, M., Godin, I., Nogueira, M.M., Cohen-Solal, K., Schiavon, V., Lecluse, Y., Le Pesteur, F., Lagrue, A.H., and Vainchenker, W. (2002). Expression of CD41 on hematopoietic progenitors derived from embryonic hematopoietic cells. *Development (Cambridge, England)* 129, 2003-2013.
- Miyazaki, R., Ogata, H., Iguchi, T., Sogo, S., Kushida, T., Ito, T., Inaba, M., Ikehara, S., and Kobayashi, Y. (2000). Comparative analyses of megakaryocytes derived from cord blood and bone marrow. *British journal of haematology* 108, 602-609.
- Modderman, P.W., Admiraal, L.G., Sonnenberg, A., and Borne, A.E. von dem (1992). Glycoproteins V and Ib-IX form a noncovalent complex in the platelet membrane. *The Journal of biological chemistry* 267, 364-369.
- Moreau, T., Evans, A.L., Vasquez, L., Tijssen, M.R., Yan, Y., Trotter, M.W., Howard, D., Colzani, M., Arumugam, M., and Wu, W.H., et al. (2016). Large-scale production of megakaryocytes from human pluripotent stem cells by chemically defined forward programming. *Nature communications* 7, 11208.
- Mucci, A., Lopez-Rodriguez, E., Hetzel, M., Liu, S., Suzuki, T., Happle, C., Ackermann, M., Kempf, H., Hillje, R., and Kunkiel, J., et al. (2018). iPSC-Derived Macrophages Effectively Treat Pulmonary Alveolar Proteinosis in Csf2rb-Deficient Mice. *Stem cell reports* 11, 696-710.
- Müller-Kuller, U., Ackermann, M., Kolodziej, S., Brendel, C., Fritsch, J., Lachmann, N., Kunkel, H., Lausen, J., Schambach, A., and Moritz, T., et al. (2015). A minimal ubiquitous chromatin opening element (UCOE) effectively prevents silencing of juxtaposed heterologous promoters by epigenetic remodeling in multipotent and pluripotent stem cells. *Nucleic acids research* 43, 1577-1592.
- Mulligan, R.C. (1993). The basic science of gene therapy. *Science (New York, N.Y.)* 260, 926-932.
- Muntean, A.G., Pang, L., Poncz, M., Dowdy, S.F., Blobel, G.A., and Crispino, J.D. (2007). Cyclin D-Cdk4 is regulated by GATA-1 and required for megakaryocyte growth and polyploidization. *Blood* 109, 5199-5207.

- N Debili, L Coulombel, L Croisille, A Katz, J Guichard, J Breton-Gorius and W Vainchenker (1996). Characterization of a bipotent erythro-megakaryocytic progenitor in human bone marrow. *Blood* 88(4), 1284-1296.
- Nakamura, S., Takayama, N., Hirata, S., Seo, H., Endo, H., Ochi, K., Fujita, K.-i., Koike, T., Harimoto, K.-i., and Dohda, T., et al. (2014). Expandable megakaryocyte cell lines enable clinically applicable generation of platelets from human induced pluripotent stem cells. *Cell stem cell* 14, 535-548.
- Nakano, T., Kodama, H., and Honjo, T. (1994). Generation of lymphohematopoietic cells from embryonic stem cells in culture. *Science (New York, N.Y.)* 265, 1098-1101.
- Naldini, L., Blömer, U., Gallay, P., Ory, D., Mulligan, R., Gage, F.H., Verma, I.M., and Trono, D. (1996). In vivo gene delivery and stable transduction of nondividing cells by a lentiviral vector. *Science (New York, N.Y.)* 272, 263-267.
- Neville, J.J., Orlando, J., Mann, K., McCloskey, B., and Antoniou, M.N. (2017). Ubiquitous Chromatin-opening Elements (UCOEs). Applications in biomanufacturing and gene therapy. *Biotechnology advances* 35, 557-564.
- Nieman, M.T., and Schmaier, A.H. (2007). Interaction of thrombin with PAR1 and PAR4 at the thrombin cleavage site. *Biochemistry* 46, 8603-8610.
- Nobes, C.D., and Hall, A. (1995). Rho, rac, and cdc42 GTPases regulate the assembly of multimolecular focal complexes associated with actin stress fibers, lamellipodia, and filopodia. *Cell* 81, 53-62.
- Noh, J.-Y., Gandre-Babbe, S., Wang, Y., Hayes, V., Yao, Y., Gadue, P., Sullivan, S.K., Chou, S.T., Machlus, K.R., and Italiano, J.E., et al. (2015). Inducible Gata1 suppression expands megakaryocyte-erythroid progenitors from embryonic stem cells. *The Journal of clinical investigation* 125, 2369-2374.
- Ordovás, L., Boon, R., Pistoni, M., Chen, Y., Wolfs, E., Guo, W., Sambathkumar, R., Bobis-Wozowicz, S., Helsen, N., and Vanhove, J., et al. (2015). Efficient Recombinase-Mediated Cassette Exchange in hPSCs to Study the Hepatocyte Lineage Reveals AAVS1 Locus-Mediated Transgene Inhibition. *Stem cell reports* 5, 918-931.
- Paknikar, A.K., Eltzner, B., and Köster, S. (2019). Direct characterization of cytoskeletal reorganization during blood platelet spreading. *Progress in biophysics and molecular biology* 144, 166-176.
- Palis, J., Robertson, S., Kennedy, M., Wall, C., and Keller, G. (1999). Development of erythroid and myeloid progenitors in the yolk sac and embryo proper of the mouse. *Development (Cambridge, England)* 126, 5073-5084.
- Pang, L., Weiss, M.J., and Poncz, M. (2005). Megakaryocyte biology and related disorders. *The Journal of clinical investigation* 115, 3332-3338.
- Patel, S.R., Richardson, J.L., Schulze, H., Kahle, E., Galjart, N., Drabek, K., Shivdasani, R.A., Hartwig, J.H., and Italiano, J.E. (2005). Differential roles of microtubule assembly and sliding in proplatelet formation by megakaryocytes. *Blood* 106, 4076-4085.
- Patel-Hett, S., Richardson, J.L., Schulze, H., Drabek, K., Isaac, N.A., Hoffmeister, K., Shivdasani, R.A., Bulinski, J.C., Galjart, N., and Hartwig, J.H., et al. (2008). Visualization of microtubule growth in living platelets reveals a dynamic marginal band with multiple microtubules. *Blood* 111, 4605-4616.

Pfaff, N., Lachmann, N., Ackermann, M., Kohlscheen, S., Brendel, C., Maetzig, T., Niemann, H., Antoniou, M.N., Grez, M., and Schambach, A., et al. (2013). A ubiquitous chromatin opening element prevents transgene silencing in pluripotent stem cells and their differentiated progeny. *Stem cells (Dayton, Ohio)* 31, 488-499.

Pfaff, N., Lachmann, N., Kohlscheen, S., Sgodda, M., Araúzo-Bravo, M.J., Greber, B., Kues, W., Glage, S., Baum, C., and Niemann, H., et al. (2012). Efficient hematopoietic redifferentiation of induced pluripotent stem cells derived from primitive murine bone marrow cells. *Stem cells and development* 21, 689-701.

Phaltane, R., Lachmann, N., Brenning, S., Ackermann, M., Modlich, U., and Moritz, T. (2014). Lentiviral MGMT(P140K)-mediated in vivo selection employing a ubiquitous chromatin opening element (A2UCOE) linked to a cellular promoter. *Biomaterials* 35, 7204-7213.

Pleines, I., Eckly, A., Elvers, M., Hagedorn, I., Eliautou, S., Bender, M., Wu, X., Lanza, F., Gachet, C., and Brakebusch, C., et al. (2010). Multiple alterations of platelet functions dominated by increased secretion in mice lacking Cdc42 in platelets. *Blood* 115, 3364-3373.

Pleines, I., Hagedorn, I., Gupta, S., May, F., Chakarova, L., van Hengel, J., Offermanns, S., Krohne, G., Kleinschnitz, C., and Brakebusch, C., et al. (2012). Megakaryocyte-specific RhoA deficiency causes macrothrombocytopenia and defective platelet activation in hemostasis and thrombosis. *Blood* 119, 1054-1063.

Potts, K.S., Sargeant, T.J., Markham, J.F., Shi, W., Biben, C., Josefsson, E.C., Whitehead, L.W., Rogers, K.L., Liakhovitskaia, A., and Smyth, G.K., et al. (2014). A lineage of diploid platelet-forming cells precedes polyploid megakaryocyte formation in the mouse embryo. *Blood* 124, 2725-2729.

Pulikkan, J.A., Madera, D., Xue, L., Bradley, P., Landrette, S.F., Kuo, Y.-H., Abbas, S., Zhu, L.J., Valk, P., and Castilla, L.H. (2012). Thrombopoietin/MPL participates in initiating and maintaining RUNX1-ETO acute myeloid leukemia via PI3K/AKT signaling. *Blood* 120, 868-879.

Ramadan A. Ali, Leah M. Wuescher, and Randall G. Worth. Platelets: essential components of the immune system.

Ramakrishnan, V., Reeves, P.S., DeGuzman, F., Deshpande, U., Ministri-Madrid, K., DuBridge, R.B., and Phillips, D.R. (1999). Increased thrombin responsiveness in platelets from mice lacking glycoprotein V. *Proceedings of the National Academy of Sciences of the United States of America* 96, 13336-13341.

Rost, M.S., Shestopalov, I., Liu, Y., Vo, A.H., Richter, C.E., Emly, S.M., Barrett, F.G., Stachura, D.L., Holinstat, M., and Zon, L.I., et al. (2018). Nfe2 is dispensable for early but required for adult thrombocyte formation and function in zebrafish. *Blood advances* 2, 3418-3427.

Rucker, D., and Dharmoon, A.S. (2019). StatPearls. Physiology, Thromboxane A2 (Treasure Island (FL)).

Sadoul, K. (2015). New explanations for old observations: marginal band coiling during platelet activation. *Journal of thrombosis and haemostasis : JTH* 13, 333-346.

- Sanada, C., Xavier-Ferrucio, J., Lu, Y.-C., Min, E., Zhang, P.-X., Zou, S., Kang, E., Zhang, M., Zerafati, G., and Gallagher, P.G., et al. (2016). Adult human megakaryocyte-erythroid progenitors are in the CD34+CD38mid fraction. *Blood* 128, 923-933.
- Sauvage, F.J. de, Carver-Moore, K., Luoh, S.M., Ryan, A., Dowd, M., Eaton, D.L., and Moore, M.W. (1996). Physiological regulation of early and late stages of megakaryocytopoiesis by thrombopoietin. *The Journal of experimental medicine* 183, 651-656.
- Saving, K.L., Jennings, D.E., Aldag, J.C., and Caughey, R.C. (1994). Platelet ultrastructure of high-risk premature infants. *Thrombosis research* 73, 371-384.
- Schambach, A., Mueller, D., Galla, M., Verstegen, M.M.A., Wagemaker, G., Loew, R., Baum, C., and Bohne, J. (2006). Overcoming promoter competition in packaging cells improves production of self-inactivating retroviral vectors. *Gene therapy* 13, 1524-1533.
- Schambach, A., Zychlinski, D., Ehrnstroem, B., and Baum, C. (2013). Biosafety features of lentiviral vectors. *Human gene therapy* 24, 132-142.
- Schurr, Y., Sperr, A., Beck, S., Volz, J., Nieswandt, B., Machesky, L., and Bender, M. (2019). Platelet Lamellipodia Formation is not Required for Thrombus Formation and Stability. In *Science meets clinical practice* (Georg Thieme Verlag KG).
- Selvadurai, M.V., and Hamilton, J.R. (2018). Structure and function of the open canalicular system - the platelet's specialized internal membrane network. *Platelets* 29, 319-325.
- Seo, B.J., Hong, Y.J., and Do, J.T. (2017). Cellular Reprogramming Using Protein and Cell-Penetrating Peptides. *International journal of molecular sciences* 18.
- Sharda, A., and Flaumenhaft, R. (2018). The life cycle of platelet granules. *F1000Research* 7, 236.
- Shimizu, R., Ohneda, K., Engel, J.D., Trainor, C.D., and Yamamoto, M. (2004). Transgenic rescue of GATA-1-deficient mice with GATA-1 lacking a FOG-1 association site phenocopies patients with X-linked thrombocytopenia. *Blood* 103, 2560-2567.
- Shimizu, S., Nagasawa, T., Katoh, O., Komatsu, N., Yokota, J., and Morishita, K. (2002). EVI1 is expressed in megakaryocyte cell lineage and enforced expression of EVI1 in UT-7/GM cells induces megakaryocyte differentiation. *Biochemical and biophysical research communications* 292, 609-616.
- Shin, E.-K., Park, H., Noh, J.-Y., Lim, K.-M., and Chung, J.-H. (2017). Platelet Shape Changes and Cytoskeleton Dynamics as Novel Therapeutic Targets for Anti-Thrombotic Drugs. *Biomolecules & therapeutics* 25, 223-230.
- Shivdasani, R.A., Fujiwara, Y., McDevitt, M.A., and Orkin, S.H. (1997). A lineage-selective knockout establishes the critical role of transcription factor GATA-1 in megakaryocyte growth and platelet development. *The EMBO journal* 16, 3965-3973.
- Shivdasani, R.A., Rosenblatt, M.F., Zucker-Franklin, D., Jackson, C.W., Hunt, P., Saris, C.J., and Orkin, S.H. (1995). Transcription factor NF-E2 is required for platelet formation independent of the actions of thrombopoietin/MGDF in megakaryocyte development. *Cell* 81, 695-704.

- Sim, X., Poncz, M., Gadue, P., and French, D.L. (2016). Understanding platelet generation from megakaryocytes: implications for in vitro-derived platelets. *Blood* 127, 1227-1233.
- Si-Tayeb, K., Noto, F.K., Sepac, A., Sedlic, F., Bosnjak, Z.J., Lough, J.W., and Duncan, S.A. (2010). Generation of human induced pluripotent stem cells by simple transient transfection of plasmid DNA encoding reprogramming factors. *BMC developmental biology* 10, 81.
- Solar, G.P., Kerr, W.G., Zeigler, F.C., Hess, D., Donahue, C., Sauvage, F.J. de, and Eaton, D.L. (1998). Role of c-mpl in early hematopoiesis. *Blood* 92, 4-10.
- Sola-Visner, M. (2012). Platelets in the neonatal period: developmental differences in platelet production, function, and hemostasis and the potential impact of therapies. *Hematology. American Society of Hematology. Education Program 2012*, 506-511.
- Stadtfeld, M., Nagaya, M., Utikal, J., Weir, G., and Hochedlinger, K. (2008). Induced pluripotent stem cells generated without viral integration. *Science (New York, N.Y.)* 322, 945-949.
- Stanton, M.M., Tzatzalos, E., Donne, M., Kolundzic, N., Helgason, I., and Ilic, D. (2019). Prospects for the Use of Induced Pluripotent Stem Cells in Animal Conservation and Environmental Protection. *Stem cells translational medicine* 8, 7-13.
- Štefková, K., Procházková, J., and Pacherník, J. (2015). Alkaline phosphatase in stem cells. *Stem cells international* 2015, 628368.
- Stewart, R., Yang, C., Anyfantis, G., Przyborski, S., Hole, N., Strachan, T., Stojkovic, M., Keith, W.N., Armstrong, L., and Lako, M. (2008). Silencing of the expression of pluripotent driven-reporter genes stably transfected into human pluripotent cells. *Regenerative medicine* 3, 505-522.
- Strassel, C., Brouard, N., Mallo, L., Receveur, N., Mangin, P., Eckly, A., Bieche, I., Tarte, K., Gachet, C., and Lanza, F. (2016). Aryl hydrocarbon receptor-dependent enrichment of a megakaryocytic precursor with a high potential to produce proplatelets. *Blood* 127, 2231-2240.
- Strassel, C., Moog, S., Baas, M.-J., Cazenave, J.-P., and Lanza, F. (2004). Biosynthesis of platelet glycoprotein V expressed as a single subunit or in association with GPIb-IX. *European journal of biochemistry* 271, 3671-3677.
- Sugimoto, N., and Eto, K. (2017). Platelet production from induced pluripotent stem cells. *Journal of thrombosis and haemostasis : JTH* 15, 1717-1727.
- Suzuki, A., Shin, J.-W., Wang, Y., Min, S.H., Poncz, M., Choi, J.K., Discher, D.E., Carpenter, C.L., Lian, L., and Zhao, L., et al. (2013). RhoA is essential for maintaining normal megakaryocyte ploidy and platelet generation. *PloS one* 8, e69315.
- Szalai, G., LaRue, A.C., and Watson, D.K. (2006). Molecular mechanisms of megakaryopoiesis. *Cellular and molecular life sciences : CMLS* 63, 2460-2476.
- Takahashi, K., Tanabe, K., Ohnuki, M., Narita, M., Ichisaka, T., Tomoda, K., and Yamanaka, S. (2007). Induction of pluripotent stem cells from adult human fibroblasts by defined factors. *Cell* 131, 861-872.
- Takahashi, K., and Yamanaka, S. (2006). Induction of pluripotent stem cells from mouse embryonic and adult fibroblast cultures by defined factors. *Cell* 126, 663-676.

- Teramura, M., Kobayashi, S., Hoshino, S., Oshimi, K., and Mizoguchi, H. (1992). Interleukin-11 enhances human megakaryocytopoiesis in vitro. *Blood* 79, 327-331.
- Thon, J.N., Mazutis, L., Wu, S., Sylman, J.L., Ehrlicher, A., Machlus, K.R., Feng, Q., Lu, S., Lanza, R., and Neeves, K.B., et al. (2014). Platelet bioreactor-on-a-chip. *Blood* 124, 1857-1867.
- Tijssen, M.R., and Ghevaert, C. (2013). Transcription factors in late megakaryopoiesis and related platelet disorders. *Journal of thrombosis and haemostasis : JTH* 11, 593-604.
- Tober, J., Koniski, A., McGrath, K.E., Vemishetti, R., Emerson, R., Mesy-Bentley, K.K.L. de, Waugh, R., and Palis, J. (2007). The megakaryocyte lineage originates from hemangioblast precursors and is an integral component both of primitive and of definitive hematopoiesis. *Blood* 109, 1433-1441.
- Tozawa, K., Ono-Uruga, Y., and Matsubara, Y. (2014). Megakaryopoiesis. *Clin Exp Thromb Hemost* 1, 54-58.
- Tsang, A.P., Visvader, J.E., Turner, C.A., Fujiwara, Y., Yu, C., Weiss, M.J., Crossley, M., and Orkin, S.H. (1997). FOG, a multitype zinc finger protein, acts as a cofactor for transcription factor GATA-1 in erythroid and megakaryocytic differentiation. *Cell* 90, 109-119.
- Tubman, V.N., Levine, J.E., Campagna, D.R., Monahan-Earley, R., Dvorak, A.M., Neufeld, E.J., and Fleming, M.D. (2007). X-linked gray platelet syndrome due to a GATA1 Arg216Gln mutation. *Blood* 109, 3297-3299.
- van Nispen tot Pannerden, H., Haas, F. de, Geerts, W., Posthuma, G., van Dijk, S., and Heijnen, H.F.G. (2010). The platelet interior revisited. Electron tomography reveals tubular alpha-granule subtypes. *Blood* 116, 1147-1156.
- Vannucci, L., Lai, M., Chiappesi, F., Ceccherini-Nelli, L., and Pistello, M. (2013). Viral vectors. A look back and ahead on gene transfer technology. *The new microbiologica* 36, 1-22.
- Varga-Szabo, D., Pleines, I., and Nieswandt, B. (2008). Cell adhesion mechanisms in platelets. *Arteriosclerosis, thrombosis, and vascular biology* 28, 403-412.
- Vaskova, E.A., Stekleneva, A.E., Medvedev, S.P., and Zakian, S.M. (2013). "Epigenetic Memory" Phenomenon in Induced Pluripotent Stem Cells. *Acta Naturae* 5, 15-21.
- Vigna, E., Cavalieri, S., Ailles, L., Geuna, M., Loew, R., Bujard, H., and Naldini, L. (2002). Robust and efficient regulation of transgene expression in vivo by improved tetracycline-dependent lentiviral vectors. *Molecular therapy : the journal of the American Society of Gene Therapy* 5, 252-261.
- Wagner, C.L., Mascelli, M.A., Neblock, D.S., Weisman, H.F., Coller, B.S., and Jordan, R.E. (1996). Analysis of GPIIb/IIIa receptor number by quantification of 7E3 binding to human platelets. *Blood* 88, 907-914.
- Walsh, T.G., Metharom, P., and Berndt, M.C. (2015). The functional role of platelets in the regulation of angiogenesis. *Platelets* 26, 199-211.
- Warren, L., Manos, P.D., Ahfeldt, T., Loh, Y.-H., Li, H., Lau, F., Ebina, W., Mandal, P.K., Smith, Z.D., and Meissner, A., et al. (2010). Highly efficient reprogramming to pluripotency and directed differentiation of human cells with synthetic modified mRNA. *Cell stem cell* 7, 618-630.

- White, J.G., and Rao, G.H. (1982). Effects of a microtubule stabilizing agent on the response of platelets to vincristine. *Blood* 60, 474-483.
- Whiteheart, S.W. (2011). Platelet granules. Surprise packages. *Blood* 118, 1190-1191.
- Williams, D.A., Lemischka, I.R., Nathan, D.G., and Mulligan, R.C. (1984). Introduction of new genetic material into pluripotent haematopoietic stem cells of the mouse. *Nature* 310, 476-480.
- Xia, X., Zhang, Y., Zieth, C.R., and Zhang, S.-C. (2007). Transgenes delivered by lentiviral vector are suppressed in human embryonic stem cells in a promoter-dependent manner. *Stem cells and development* 16, 167-176.
- Xie, Q.W., Leung, M., Fuortes, M., Sassa, S., and Nathan, C. (1996). Complementation analysis of mutants of nitric oxide synthase reveals that the active site requires two hemes. *Proceedings of the National Academy of Sciences of the United States of America* 93, 4891-4896.
- Xu M, J., Matsuoka, S., Yang, F.C., Ebihara, Y., Manabe, A., Tanaka, R., Eguchi, M., Asano, S., Nakahata, T., and Tsuji, K. (2001). Evidence for the presence of murine primitive megakaryocytopoiesis in the early yolk sac. *Blood* 97, 2016-2022.
- Yeaman, M.R. (2014). Platelets: at the nexus of antimicrobial defence. *Nature reviews. Microbiology* 12, 426-437.
- Yeung, A.T.Y., Hale, C., Lee, A.H., Gill, E.E., Bushell, W., Parry-Smith, D., Goulding, D., Pickard, D., Roumeliotis, T., and Choudhary, J., et al. (2017). Exploiting induced pluripotent stem cell-derived macrophages to unravel host factors influencing *Chlamydia trachomatis* pathogenesis. *Nature communications* 8, 15013.
- Yu, J., Vodyanik, M.A., Smuga-Otto, K., Antosiewicz-Bourget, J., Frane, J.L., Tian, S., Nie, J., Jonsdottir, G.A., Ruotti, V., and Stewart, R., et al. (2007). Induced pluripotent stem cell lines derived from human somatic cells. *Science (New York, N.Y.)* 318, 1917-1920.
- Yu, S.F., Rüdén, T. von, Kantoff, P.W., Garber, C., Seiberg, M., Rütther, U., Anderson, W.F., Wagner, E.F., and Gilboa, E. (1986). Self-inactivating retroviral vectors designed for transfer of whole genes into mammalian cells. *Proceedings of the National Academy of Sciences of the United States of America* 83, 3194-3198.
- Zapata, J.C., Cox, D., and Salvato, M.S. (2014). The role of platelets in the pathogenesis of viral hemorrhagic fevers. *PLoS neglected tropical diseases* 8, e2858.
- Zhang, F., Santilli, G., and Thrasher, A.J. (2017). Characterization of a core region in the A2UCOE that confers effective anti-silencing activity. *Scientific reports* 7, 10213.

ABBREVIATIONS

°C	degree Celsius
(rt)TA-M2	transactivator
μ	micro
μm	micrometer
Ψ	packaging signal
ADP	adenosin diphosphate
AGM	aorta-gonad-mesonephros region
ALL	acute lymphoblastic leukemia
AML	acute myeloid leukemia
amp	ampicillin
APC	Allophycocyanin
BFU MK	burst-forming unit-megakaryocytes
BM	bone marrow
bp	base pair
BSA	bovine serum albumin
CBX3	Chromobox 3
CD	cluster of differentiation
Cdc42(hc)	Cell division control protein 42 homolog (hyperactive variant)
CFU MK	colony-forming unit-megakaryocytes
Clec2	C-type-lectin-like-2
CLP	common lymphoid progenitor
CMP	common myeloid progenitor
cMyc	myelocytomatosis viral oncogene homolog
CpG	cytosine-guanosintriphosphate
CpG island	sequence of non-methylated cytosine-guanosintriphosphate
d	day(s)
DAPI	4',6-Diamin-2-phylinol
ddH ₂ O	double distilled water
DMEM	Dulbecco's modified eagle medium
DMS	demacration membrane system
DNA	desoxyribonucleic acid
dox	doxycycline
DTS	dense tubular system
DTS	dense tubular system
<i>E. coli</i>	Escherichia coli
EB	embryoid body
EDTA	Ethylenediaminetetraacetic acid
env	envelope

ESC	embryonic stem cell
et al.	und andere
EtOH	ethanol
Evi1	Ectopic viral integration site 1
FACS	fluorescence-activated cell sorting
Fc	Fragment, crystallizable
FL	fetal liver
Fog1	friend of Gata1, transcription factor
g	gram
gag	group associated antigen
gDNA	genomic DNA
GFP	enhanced green fluorescent protein
GMP	granulocyte macrophage progenitor
GOI	gene of interest
GP	glycoprotein
GTPase	Guanosin triphosphate hydrolyzing enzyme
h	hour
HA	Hemagglutinin-Tag
HeBS	HEPES buffered-saline
HEK	human embryonic kidney
HLA	Human leukocyte antigen
HNRPA2B1	Heterogeneous nuclear ribonucleoproteins A2/B1
HOX	homeobox genes
HPP-CFU-MK	high proliferative potential-colony forming unit-megakaryocytes
HSC	hematopoietic stem cell
HSV	herpes simplex virus
ICM	inner cell mass
Ig	Immunoglobulin
IRES	internal ribosomal entry site
IL	Interleukin
IMDM	Iscove's Modified Dulbecco's Medium
IN	integrase
IP	PGI2 receptor
iPSC	induced pluripotent stem cell
IPTG	Isopropyl- β -D-thiogalactopyranosid
kb	kilobase
l	litre
LacZ	beta-galactosidase
LB	Luria Bertani lysogeny broth
LB ^{Amp}	Luria Bertani lysogeny broth containing ampicillin

LIF	leukemia inhibitory factor
LT-HSC	long-term hematopoietic stem cell
LTR	long terminal repeats
m	milli
M	Molar
MACS	Magnetic associated cell sorting
MafG	bZip Maf transcription factor protein G
mafK	bZip Maf transcription factor protein K
MAPK	mitogen-activated protein kinase
MEF	murine embryonic fibroblast
MEM	Minimal essential medium
MEP	Megakaryocyte-Erythrocyte progenitor
mGATA1	murine GATA binding factor 1
min	minute
MK	megakaryocyte
MLV	murine leukemia virus
MMP	matrix-metalloproteinase
MOI	multiplicity of infection
Mpl	Myeloproliferative leukemia protein, Thpo receptor
MPP	multipotent progenitor
mRNA	messenger RNA
n	nano
N	haploid number
Nanog	homeobox protein NANOG
Nfe2	nuclear factor erythroid 2
nm	nanometer
OCS	open canalicular system
Oct4	Octamer binding transcription factor 4
P	promoter
p45	hematopoietic specific protein p45
PAR	Protease-activated receptors
PAS-AGM	para-aortic splanchnopleura/aorta-gonad-mesonephros region
PBS	phosphate buffered saline
Pbx1	Pre-B-cell leukemia transcription factor 1
PE	Phycoerythrin
Pen/Strep	Penicillin/Streptomycin
PerCP-Cy5.5	Peridinin-Chlorophyll-Protein-Cyanin5.5(tandemkonjugate)
PF4	platelet factor 4
PGI2	Prostacycline
PGK	phosphoglycerate promoter
pol	open reading frame for replication
Pol	Polymerase

pos	positive
PPT	polypurine tract
qPCR	quantitative PCR
RANTES	Regulated And Normal T cell Expressed and Secreted
rev	regulator of viral gene expression
RhoA(hc)	Ras Homolog Gene Family, Member A (hyperactive variant)
RNA	ribonucleic acid
Rosa26	Reverse Oriented Splice Acceptor, Clone 26
RRE	rev responsive element
RT	room temperature
rt	reverse transcribed
Runx1	Runt-related transcription factor 1
SA	splice acceptor
Scf	Stem cell factor
Scl1	Stem cell leukemia factor 1
SD	splice donor
sec	second
SIN	self-inactivating vector
Sox2	sex determining region Y-2
Ssea-1	stage specific embryonic antigen-1
STAT3	Signal transducer and activator of transcription 3
ST-HSC	short term self-renewing hematopoietic stem cell
SU	surface
T11	Tet-responsive minimal promoter
TAE	tris-acetat-EDTA
Tal1	T-cell acute lymphoblastic leukemia
Taq	Termus aquaticus
tet	tetracycline
TetO	tet-operon
TetR	Tetracycline repressor
TF	tissue factor
Thpo	Thrombopoietin
TLR	Toll-like-receptor
TM	transmembrane domain
TNF	tumor necrosis factor
TP	thromboxane receptor
TXA	thromboxane
U	units
UCOE	ubiquitous chromatin opening element
UTR	untranslated region
V	Volt
VCN	vector copy number

VEGF	Vascular Endothelial Growth Factor
Vif	Viral infectivity factor
VP16	viral protein 16 herpes simplex virus
Vpr	viral protein R
Vpu	viral protein U
Vsvg	Vesicular stomatitis virus g glycoprotein
VWF	Von-Willebrand-Factor
wPre	Woodchuk hepatitis virus post transcriptional element
wt	wildtype
xg	multiplied gravity
Xgal	5-Brom-4-chlor-3-indoxyl- β -D-galactopyranosid

CONTRIBUTIONS

Dr. Attila Sebe	Culture and differentiation of hiPSC (Figure 41+42, Chapter 4.2.5)
Dr. Niels Heinz	Plasmid generation for the vectors tested in Chapter 4.2
Franziska Schenk	<ul style="list-style-type: none"> • Plasmid generation for the vectors SERS11.T11-RhoAhc-iGFP.pre, SERS11.T11-Cdc42-iGFP.pre, pSERS11.T11-HA-Mpl-U670s-GFP.pre • Gene expression analysis of pluripotency marker (Figure 7C, Chapter 4.1.2) • Methylation analysis of the PGK promoter (Figure 43, Chapter 4.2.5.1) • Cell viability assay (Figure 45, Chapter 4.2.6)
Kaj Blokland	<ul style="list-style-type: none"> • Plasmid generation for the vectors tested in Chapter 4.2 • Evaluation of the Tet-all-in-one vectors in P19 cells (Figure 34+45, Chapter 4.2.2) • Titration of the gammaretroviral Tet-all-in-one vectors (Figure 31, Chapter 4.2) • Evaluation of the performance of gammaretroviral Tet-all-in-one vectors in SC1 cells (Figure 32, Chapter 4.2.1)
Markus Spindler/Markus Bender	Platelet spreading assays (Figure 25-27, Chapter 4.4.1.4)
Sofia Lorke	Plasmid generation for SERS11.T11-Evi1-iGFP.pre

LIST OF FIGURES

Figure 1 Mammalian megakaryopoiesis and platelet biogenesis.	10
Figure 2 Schematic overview of platelet structure and surface markers.	14
Figure 3 Genome of gammaretroviruses and lentiviruses and the corresponding designed expression vectors with helper plasmids and the split packaging design.	20
Figure 4 Generation of retroviral vectors.	21
Figure 5 Self-inactivating retroviral vectors.	22
Figure 6 Ubiquitous chromatin opening elements and their location.	25
Figure 7 Generation of R26M2 iPSC.	56
Figure 8 Characterization of pluripotency of R26M2K2 and R26M2K3.	58
Figure 9 Rosa26 locus expressing (rt)TA-M2 and the design of the SIN gammaretroviral vector expressing the supporting factors to support megakaryopoiesis and platelet generation.	60
Figure 10 Titration of the Tet-inducible gammaretroviral vectors expressing the MK supporting genes.	61
Figure 11 Transduction of R26 rTAM2 iPSC with candidate vectors and induction of transgene expression in the pluripotent state.	62
Figure 12 Differentiation scheme and workflow for transduction of R26M2K2 iPSC and differentiation into MK and platelets.	63
Figure 13 Detection of GFP reporter gene expression of the candidate factors at day 21 of differentiation in the MK.	64
Figure 14 Differentiation of transduced R26M2K2 iPSC produced progenitors from the MK/erythrocyte lineage.	65
Figure 15 Gata1.iGFP overexpressing MK extending cellular protrusions.	66
Figure 16 Expression of CD41 on the surface of MK differentiated from iGFP.control and Gata1.iGFP overexpressing cells in the GFP+ versus GFP- populations.	67
Figure 17 Summary of CD41 expression on differentiated MK at day 21 of differentiation.	68
Figure 18 Expression of the surface marker CD42d within CD41+ for GFP+ and GFP- populations of differentiated MK.	69
Figure 19 Summary of CD42d expression on differentiated MK at day 21 of differentiation.	70
Figure 20 Quantification of MK differentiated from R26M2K2 iPSC at day 21 of differentiation.	71
Figure 21 Expression of CD41 and CD42d on the surface of differentiated platelets.	73
Figure 22 Summary of CD41 and CD42d surface marker expression on <i>in vitro</i> differentiated platelets.	74
Figure 23 Transmission electron microscopy of platelets.	75
Figure 24 Quantification of platelets differentiated from R26M2K2 iPSC.	77
Figure 25 Quantification of platelets released per MK during <i>in vitro</i> differentiations.	78
Figure 26 Resting platelets on poly-L-lysine-coated cover slips.	80
Figure 27 Platelets spread on fibrinogen-coated cover slips.	81
Figure 28 Platelets spread on CRP-coated cover slips.	82
Figure 29 Tet-inducible all in one gammaretroviral vectors containing A2UCOE of different sizes.	83

Figure 30 Different A2UCOES are inserted into the Tet-all-in-one gammaretroviral vector in different orientations.	84
Figure 31 Titers of non-concentrated viral vector preparations.	84
Figure 32 Regulation of A2UCOE-containing Tet-vectors by dox in SC1 fibroblasts.	85
Figure 33 Regulation of A2UCOE-containing Tet-vectors by dox in SC1 fibroblasts.	86
Figure 34 Stability of transgene expression on the embryonic carcinoma cell line P19 over a period of 46 days.	88
Figure 35 Evaluation of the anti-silencing capacity of different A2UCOE-vectors in P19 embryonic carcinoma cells.	89
Figure 36 Re-expression of the transactivator rtTA-M2 in P19 cells by a second retroviral vector.	90
Figure 37 Regulation of expression from the A2UCOE Tet-inducible vectors in murine induced pluripotent stem cells.	91
Figure 38 Summary of the regulation of expression from different A2UCOE Tet-inducible vectors in murine iPSC.	92
Figure 39 Gammaretroviral and lentiviral Tet-all-in-one vectors with replaced PGK promoter.	94
Figure 40 Tet-inducible vectors driving the transactivator by the A2UCOE.	96
Figure 41 GFP reporter signal analyzed by fluorescent microscopy in EB.	98
Figure 42 Evaluation of the GFP expression of different UCOE-Tet vectors during 3 germ layer differentiation of hiPSC.	99
Figure 43 Methylation status of the PGK promoter after incorporation of the U670s element before and after mesodermal differentiation.	101
Figure 44 Vector architecture of the Tet.U670s.Mpl gammaretroviral vector.	101
Figure 45 Determination of the functionality of the Tet.U670s.Mpl vector.	103

CURRICULUM VITAE

PERSÖNLICHE INFORMATIONEN

Name: Katharina Cullmann
Geburtsdatum: 31.10.1984
Geburtsort: Idar-Oberstein

WISSENSCHAFTLICHER WERDEGANG

07/2019 Abgabe der Doktorarbeit am Fachbereich Biologie der Technischen Universität Darmstadt
Titel: Doxycycline-inducible viral vector systems for selective overexpression of supportive factors to enhance in vitro megakaryocyte and platelet production

04/2015-07/2019 Promotionsstudentin in der Arbeitsgruppe „Gene Modificaton in Stem Cells“ am Paul-Ehrlich-Institut in Langen

10/2013-04/2015 Master of Science in Biologie
Paris-Lodron-Universität in Salzburg

11/2010-09/2012 Bachelor of Science in Biologie

Paris-Lodron-Universität in Salzburg

10/2005-10/2010 Diplomstudiengang Biotechnologie

Fachhochschule Bingen in Bingen am Rhein

DANKSAGUNG

Zunächst einmal möchte ich mich bei Frau Prof. Dr. Ute Modlich bedanken, die es mir ermöglicht hat, meine Promotion in ihrer Arbeitsgruppe „Gene Modification in Stem Cells“ am Paul-Ehrlich-Institut und unter ihrer Leitung durchzuführen. Danke, Ute, für die vielen Ideen, Ratschläge, wissenschaftliche Anleitung und immer wieder aufbauenden Worte während der ganzen Zeit und manchmal auch für deine Geduld.

Frau Prof. Dr. Beatrix Süß danke ich für die nette und unkomplizierte Betreuung seitens der TU Darmstadt. Ich bedanke mich bei Frau Prof. Dr. Ulrike Nuber für die Bereitschaft, die Aufgabe als Zweitgutachterin für meine Arbeit zu übernehmen.

Ich möchte mich bei Herrn Prof. Dr. Thomas Moritz und bei Dr. Adele Mucci bedanken, die es mir ermöglicht haben, die murinen iPSC in der Arbeitsgruppe „iPS based Hematopoietic Regeneration“ an der Medizinischen Hochschule Hannover herzustellen.

Prof. Dr. Zoltán Ivics und Dr. Attila Sebe danke ich für die Hilfe bei den Experimenten mit den humanen iPSC.

Dr. Markus Bender und Markus Spindler von der Universität Würzburg danke ich für die „schönen Bilder“, die wir noch ganz am Ende meiner Zeit von den Plättchen machen konnten.

Auch bei meinen aktuellen und ehemaligen Kollegen in der Arbeitsgruppe möchte ich mich für zahlreiche Diskussionen und die perfekte Teamarbeit bedanken. Niels Heinz, von dem ich alle möglichen (und unmöglichen) Laborgrundlagen gelernt habe. Saskia Kohlscheen, danke, dass ich alle meine „dummen“ Fragen an dich stellen durfte und du trotzdem noch bereit warst, mit mir auch den einen oder anderen Abend zu verbringen. Franziska Schenk, vielen Dank für die tolle Zusammenarbeit im Labor. Das war für mich unendlich wertvoll. Marcel Rommel und Christian Milde, ohne euch wäre ich an der Formatierung verzweifelt.

Besonderer Dank gilt meiner Familie und meinen Eltern Thomas und Regina. Danke, dass ihr nicht aufgehört habt an mich zu glauben und dass ihr mich immer bedingungslos unterstützt habt!

EHRENWÖRTLICHE ERKLÄRUNG

Ich erkläre hiermit ehrenwörtlich, dass ich die vorliegende Arbeit entsprechend den Regeln guter wissenschaftlicher Praxis selbstständig und ohne unzulässige Hilfe Dritter angefertigt habe.

Sämtliche aus fremden Quellen direkt oder indirekt übernommenen Gedanken sowie sämtliche von Anderen direkt oder indirekt übernommenen Daten, Techniken und Materialien sind als solche kenntlich gemacht. Die Arbeit wurde bisher bei keiner anderen Hochschule zu Prüfungszwecken eingereicht.

Darmstadt,

.....

Katharina Cullmann